

**Functional Group Transposition of Bicyclo[5.3.0]decadienones Afforded by the Allenic
Pauson-Khand Reaction. An Approach Toward the Total Synthesis of (-)-
Dehydroleucodine**

by

Joseph Eugene Burchick Jr.

Bachelor of Science, Allegheny College, 2013

Submitted to the Graduate Faculty of
The Kenneth P. Dietrich School of Arts and Sciences in partial fulfillment
of the requirements for the degree of
Doctor of Philosophy

University of Pittsburgh

2020

UNIVERSITY OF PITTSBURGH
DIETRICH SCHOOL OF ARTS AND SCIENCES

This dissertation was presented

by

Joseph Eugene Burchick Jr.

It was defended on

November 5, 2020

and approved by

Paul Floreancig, PhD, Professor, Department of Chemistry

Peng Liu, PhD, Associate Professor, Department of Chemistry

Lee A. McDermott, PhD, Assistant Professor, Department of Pharmaceutical Sciences

Dissertation Director: Kay M. Brummond, PhD, Professor, Department of Chemistry

Copyright © by Joseph Eugene Burchick Jr.

2020

Functional Group Transposition of Bicyclo[5.3.0]decadienones Afforded by the Allenic Pauson-Khand Reaction. An Approach Toward the Total Synthesis of (-)-Dehydroleucodine

Joseph Eugene Burchick Jr., PhD

University of Pittsburgh, 2020

The allenic Pauson-Khand reaction (APKR) has proven to be a powerful method for the construction of seven-membered rings. Despite this, only a few reports of this methodology being employed in total syntheses exist. Reported herein are synthetic studies targeted towards the elaboration of APKR adducts via the functionalization of the resulting enone motif. In addition, a rapid synthetic route towards the core 5,7,5-framework of biologically active 6,12-gaianolides was developed in an enantioselective fashion, utilizing the APKR as they key ring-forming step. The successful APKR adduct functionalization studies were combined with this novel synthetic route in an effort towards the first total synthesis of (-)-dehydroleucodine.

Table of Contents

List of Tables	viii
List of Figures.....	ix
List of Schemes.....	x
List of Abbreviations	xv
Preface.....	xvi
1.0 Introduction.....	1
1.1 Guaianolides and Strategies Towards the Rapid Construction of the 5,7-Ring System.....	1
1.2 The Allenic Pauson-Khand Reaction.....	4
1.2.1 History and mechanistic details	4
1.2.2 Applications of the allenic Pauson-Khand reaction in total synthesis	7
1.3 Functional Group Interconversions of the APKR Adduct.....	9
2.0 Allylic Diazene Rearrangement and Base-Mediated Isomerization of APKR Adducts	12
2.1 Introduction	12
2.1.1 Proposed strategies for the reductive transposition of the C3-C5 enone.....	13
2.2 Synthesis of Model Bicyclo[5.3.0]decadienone 2.2.....	16
2.2.1 Synthesis of alkynyl ketone 2.7	16
2.2.2 Synthesis of allene-yne 2.1	19
2.2.3 Application and optimization of the APKR to allene-yne 2.1	22
2.3 ¹H NMR Studies of Tosylhydrazone Reduction with Catecholborane	25

2.4 ADR on C1-C10 Hydrogenated APKR Adduct.....	31
2.5 ADR on Bicyclo[5.3.0]decadienone Tosylhydrazone Model System 2.6.....	40
2.6 Conclusions for ADR Studies	45
2.7 Base-Induced Transposition of α -Hydroxy Enone	46
2.7.1 Introduction and background.....	46
2.7.2 Synthesis of α -hydroxy enone 2.53.....	49
2.7.3 Base-induced isomerization of α -hydroxy enone 2.53.....	51
2.8 Conclusions for the Base-Induced Enone Isomerization	58
3.0 Studies Towards the First Total Synthesis of (-)-Dehydroleucodine.....	60
3.1 Introduction	60
3.2 Ring Closing Metathesis and Claisen Rearrangement of (<i>R</i>)-linalool.....	67
3.3 Conversion of γ,δ -unsaturated Amide to γ,δ -unsaturated Ester.....	73
3.4 Oxidative Cleavage.....	74
3.4.1 Ozonolysis	74
3.4.2 OsO ₄ -Catalyzed oxidative cleavage	80
3.5 Diastereoselective 1,2-Addition/Lactonization to 3.40 and 3.52.....	84
3.6 Conversion of Ketone 3.51 to Allenes	93
3.6.1 Formation of propargyl carbonate	93
3.6.2 Synthesis of allenyl carboxyesters	95
3.7 Allenic Pauson-Khand Reactions of 3.57a, 3.60a, and 3.60b.....	98
3.7.1 APKR of 3,3-disubstituted allene 3.57a	98
3.7.2 APKR of allenyl carboxyesters 3.60a and 3.60b	100
3.8 Hydrolysis of β -Keto Esters.....	102

3.9 Base-Mediated Isomerization of α-Hydroxy Enone	104
3.10 Conclusions Towards the Total Synthesis of (-)-Dehydroleucodine (<i>ent</i>-3.1)	106
Appendix A : Experimental Information for Chapter Two	107
Appendix B : Experimental Information for Chapter Three	144
Appendix C : NMR Spectra	172
Bibliography	266

List of Tables

Table 1.1. Reaxys search of 6,12- and 8,12-guaianolides.	2
Table 2.1. Reaxys search for 6,12-guaianolide frameworks possessing discrete double bond at C4-C5 position and C3-C4 position.....	12
Table 2.2. Optimization of allenic Pauson-Khand reaction of allene-yne 2.1.....	24
Table 2.3. Screening of catecholborane reduction conditions for ADR of tosylhydrazone 2.6. ..	28
Table 2.4. Alternative reduction conditions and ADR of 2.36.	35
Table 2.5. Conditions for the ADR of bicyclo[5.3.0]decadienone tosylhydrazone 2.6.....	41
Table 2.6. Reaxys search for 6,12-guaianolide frameworks possessing discrete double bond at C4-C5 position and oxygen at C3 position, and discrete double bond at C3-C4 position and oxygen at C2 position.	47
Table 2.7. Conditions for the attempted base-induced isomerization of epoxide 2.61.....	58
Table 3.1. Conditions to effect RCM and Johnson-Claisen rearrangement fo (<i>R</i>)-linalool (3.34).	70
Table 3.2. Conditions for the diastereoselective 1,2-addition of propynylmagnesium bromide to β -formyl amide 3.52.....	90

List of Figures

Figure 1.1. Desired C3-C5 enone functionalization in the presence of C1-C10 alkene.....	11
Figure 2.1. A) Reference spectrum, no catecholborane. B) 3 equiv HBcat after 1 h at 0 °C. C) after 1 h at rt. D) After addition of 3 equiv sodium acetate trihydrate and reacting at 60 °C for 1 h....	28
Figure 2.2. Structural confirmation of Wolff-Kishner reduction product 2.43.	43
Figure 3.1. Determination of 3.40 enantiomeric ratio by reaction of chiral amine 3.49, and ¹ H NMR integration of imine 3.50 proton H ^a	78
Figure 3.2. OsO ₄ and PhI(OAc) ₂ -mediated oxidative cleavage of ester 3.36 with retention of C1 stereochemistry.	81
Figure 3.3. Chemical shift assignments for APKR C2 diastereomers.....	101

List of Schemes

Scheme 1.1. Selected examples of the construction of the 5,7-ring system of guaianolides.....	3
Scheme 1.2. Brummond's strategy towards the 5,7-ring system of guaianolides.....	4
Scheme 1.3. Co-mediated Pauson-Khand reaction.....	5
Scheme 1.4. Rh- and Mo-catalyzed APKR and corresponding double bond selectivity of cyclopentenones.....	6
Scheme 1.5. Natural product total syntheses which employed an APKR as the key ring forming step.....	8
Scheme 1.6. Precedent for the functional group interconversion of APKR adducts.....	10
Scheme 2.1. Proposed reductive transposition of C3-C5 enone of APKR adduct 2.2 to C3-C4 alkene 2.3.....	13
Scheme 2.2. Potential strategies for the reductive transposition of bicyclo[5.3.0]decadienone 2.2.....	14
Scheme 2.3. Retrosynthetic analysis of bicyclo[5.3.0]decadienone 2.2.....	16
Scheme 2.4. Initial synthetic route of alkynyl ketone 2.7.....	17
Scheme 2.5. Acetone homologation of alkynyl iodide 2.8 using <i>tert</i> -butyl acetoacetate.....	18
Scheme 2.6. Attempted direct allenation of ketone 2.7 with alkenylidene titanocene.....	19
Scheme 2.7. Optimization of 1,2-addition of ethynylmagnesium bromide to ketone 2.7 via transmetallation with CeCl ₃	20
Scheme 2.8. Palladium-catalyzed hydrogenolysis of propargyl carbonate 2.16.....	21
Scheme 2.9. Palladium-catalyzed hydrogenolysis catalytic cycle and potential elimination of η^1 -palladium.....	22

Scheme 2.10. Inverse addition of allene-yne 2.1 to Rh(I) solution.	23
Scheme 2.11. Attempted ADR of bicyclo[5.3.0]decadienone tosylhydrazone 2.6.	26
Scheme 2.12. Synthesis and crystal structure of <i>E</i> -tosylhydrazone of bicyclo[5.3.0]decadienone 2.2.....	27
Scheme 2.13. Precedent for ADRs performed on bicyclo[5.3.0]decenones.....	30
Scheme 2.14. Hydrogenation of C1-C10 double bond of 2.2.....	32
Scheme 2.15. Formation of tosylhydrazone 2.36 from C1-C10 hydrogenated APKR adduct 2.35.	33
Scheme 2.16. HBCat reduction of C1-C10 hydrogenated tosylhydrazone 2.36 and ADR.	34
Scheme 2.17. (BzO) ₂ BH reduction of tosylhydrazone 2.36 and ADR.....	38
Scheme 2.18. Mechanism of the ADR of tosylhydrazone 2.6.....	42
Scheme 2.19. Proposed divergent retro-ene and radical decomposition pathways of diazene intermediate 2.45.....	44
Scheme 2.20. Previous precedent for base-induced isomerization of α -hydroxy enone motif. ...	48
Scheme 2.21. Proposed conversion of α -hydroxy enone 2.53 to α -keto enol 2.54 and subsequent deoxygenation to enone 2.55.	48
Scheme 2.22. A) Potential routes to hydroxy enone 2.53. B) Synthesis of allenyl esters 2.56a-b and Rh(I)-catalyzed APKR.	49
Scheme 2.23. Rh(II)-catalyzed formal 3,3-sigmatropic rearrangement of propargyl esters to allenyl carboxyesters 2.56.....	50
Scheme 2.24. Base induced isomerization of α -hydroxy enone 2.53 to α -keto enol 2.54 and ¹ H NMR structural confirmation.....	51

Scheme 2.25. Two-step, one-pot deprotection/isomerization of α -acyloxy enones 2.58a and 2.58b.	52
Scheme 2.26. Two-step one-pot deprotection/isomerization of chloroacetate 2.58b and C3 deoxygenation of α -keto enol 2.54.	54
Scheme 2.27. A) Biologically active guaiane stelleraguaianone B (2.60). B) Proposed route to stelleraguaianone B analog 2.62.	54
Scheme 2.28. <i>m</i> CPBA epoxidation of α -hydroxy ketone 2.53.	55
Scheme 2.29. Diastereoselective epoxidation of C1-C10 double bond of 2.53.	56
Scheme 3.1. Retrosynthetic analysis of (+)-dehydroleucodine (3.1), employing an APKR as the key ring forming step, followed by isomerization.	61
Scheme 3.2. Proposed access to allenyl carboxyester 4 from β -formyl ester 3.6.	62
Scheme 3.3. Potential retrosynthetic approaches for the enantioselective construction of β -formyl ester 3.6.	63
Scheme 3.4. Proposed Diels-Alder approach to β -formyl ester 3.6.	63
Scheme 3.5. A) Diphenylprolinol methyl ester-catylyzed 1,4-conjugate additions of aldehydes to enones. B) Imidazolidinone-catalyzed 1,4-conjugate addition of aldehydes to enones.	64
Scheme 3.6. Proposed route to γ,δ -unsaturated ester 3.12 via chiral cyclopentenol 3.25.	65
Scheme 3.7. Retrosynthetic analysis of β -formyl ester 3.6.	66
Scheme 3.8. Reported synthetic route to (<i>S</i>)-linalool (3.24).	67
Scheme 3.9. Reported RCM of (\pm)-linalool (3.29), and dehydration of cyclopentenol 3.30 in the presence of H-GII at elevated temperature.	68
Scheme 3.10. Attempted two-step-one-pot RCM/Johnson-Claisen rearrangement of (<i>R</i>)-linalool (3.34).	69

Scheme 3.11. Successful RCM/Eschenmoser-Claisen rearrangement of (R)-linalool (3.34) to generate γ,δ -unsaturated amide 3.37.....	72
Scheme 3.12. Tf ₂ O-mediated esterification of amide 3.37 via imidate 3.38.....	73
Scheme 3.13. Proposed oxidative cleavage of γ,δ -unsaturated ester 3.36.....	74
Scheme 3.14. Ozonolysis of γ,δ -unsaturated ester 3.39 in CH ₂ Cl ₂ with Me ₂ S as the terminal reductant.....	75
Scheme 3.15. Mechanism of ozonolysis, leading to isolated secondary ozonide 3.45.....	76
Scheme 3.16. Ozonolysis of γ,δ -unsaturated ester 3.36 in CH ₂ Cl ₂ /MeOH with Me ₂ S as the terminal reductant.....	77
Scheme 3.17. Ozonolysis of γ,δ -unsaturated ester 3.36 in CH ₂ Cl ₂ /MeOH with Me ₂ S as the terminal reductant.....	79
Scheme 3.18. Oxidative cleavage of γ,δ -unsaturated ester 3.36 and γ,δ -unsaturated amide 3.37, and use of the resulting β -formyl ester 3.40 and β -formyl amide 3.52 to generate lactone 3.51. .	82
Scheme 3.19. Ozonolysis of γ,δ -unsaturated amide 3.37 in CH ₂ Cl ₂ with PPh ₃ as the terminal reductant.....	82
Scheme 3.20. Relative rates of racemization of β -formyl ester 3.40 and β -formyl amide 3.52 while standing in the freezer.....	83
Scheme 3.21. OsO ₄ and PhI(OAc) ₂ -mediated oxidative cleavage of β -formyl amide 3.37 with retention of C1 stereochemistry.....	84
Scheme 3.22. Proposed diastereoselective 1,2-addition/lactonization of β -formyl ester 3.40.	84
Scheme 3.23. Precedent for the diastereoselective 1,2-addition/lactonization of β -formyl esters.	85

Scheme 3.24. Reissig's proposed transition states leading to the diastereoselective 1,2-addition of nucleophiles to β -formyl esters.....	86
Scheme 3.25. Addition of ethynylmagnesium bromide to β -formyl ester 3.40.....	87
Scheme 3.26. Chlorotitaniumtriisopropoxide-mediated 1,2-addition of ethynylmagnesium bromide to β -formyl ester 3.40.	88
Scheme 3.27. Titanium tetrachloride-mediated 1,2-addition of propynylmagnesium bromide to β -formyl ester 3.40.	89
Scheme 3.28. Proposed conversion of ketone 3.51 to allenes 3.57a and 3.57b.....	93
Scheme 3.29. Synthesis of propargyl carbonate 3.58.	94
Scheme 3.30. Synthesis of 3,3-disubstituted allene 3.57a.	95
Scheme 3.31. Synthesis of propargyl esters 3.59a and 3.59b.	96
Scheme 3.32. Rh(II)-catalyzed formal 3,3-sigmatropic rearrangement of allenyl carboxyesters 3.60a and 3.60b.	97
Scheme 3.33. APKR of 3,3-disubstituted allene-yne 3.57a.....	99
Scheme 3.34. APKR of allenyl carboxyesters 3.60a and 3.60b.	100
Scheme 3.35. Proposed hydrolysis of α -acyloxy enone 3.62a or 3.62b to access α -hydroxy enone 3.63.....	103
Scheme 3.36. Proposed base-mediated isomerization of α -hydroxy enone 3.63 to α -keto enol 3.64.	104
Scheme 3.37. Base-mediated isomerization/eliminative lactone opening of <i>trans</i> -3.63 and 3.62b.	105

List of Abbreviations

APKR	Allenic Pauson-Khand Reaction
ADR	Allylic Diazene Rearrangement
WK	Wolff-Kishner
HBcat	Catecholborane
EtOAc	Ethyl acetate
DCM	Dichloromethane
THF	Tetrahydrofuran
DMF	<i>N,N</i> -Dimethylformamide
DMSO	Dimethyl sulfoxide
<i>m</i> CPBA	meta-Chloroperoxybenzoic acid
TBHP	<i>tert</i> -Butyl hydroperoxide

Preface

I would like to thank Professor Kay Brummond for her excellent mentorship in developing my skills as a scientist. Her consistent encouragement inspired me and gave me the confidence to pursue my own lines of scientific inquiry. To all current and previous Brummond group members which I have had the privilege of spending the past six years with, you have proven to be knowledgeable and entertaining colleagues, as well as great friends.

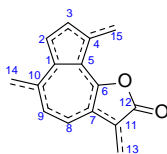
I would also like to thank my family for their unwavering support, without which I would not have made it to this point. I dedicate this document to all of you.

1.0 Introduction

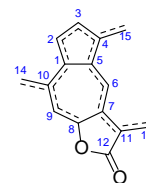
1.1 Guaianolides and Strategies Towards the Rapid Construction of the 5,7-Ring System

The guaianolides are a large class of naturally-occurring sesquiterpene lactones (SLs). Defined by a fused 5,7,5-ring system, these SLs present a difficult and exciting challenge for the synthetic chemist. Utilizing the Reaxys database, two searches were performed—one for 6,12-guaianolides and one for 8,12-guaianolides. The structures were variable at every position, with the dotted lines indicating either a single or double bond. The search returned 5351 6,12-guaianolides and 838 8,12-guaianolides. The results were further filtered to identify the compounds which showed biological activity (pharmacological data), those which have been isolated from natural sources (natural source), and those which show biological activity and have also been isolated from a natural source (natural source + pharm. data). As can be seen from these search results, there are a vast number of both 6,12- and 8,12-guaianolides which are biologically active. In addition to their biological activity, the structural diversity of these compounds presents an interesting challenge from the perspective of a synthetic chemist. For these reasons the rapid and efficient construction of the core 5,7,5-ring system of guaianolides has been the topic of many synthetic studies.^{1,2}

Table 1.1. Reaxys search of 6,12- and 8,12-guaianolides.



6,12-guaianolide



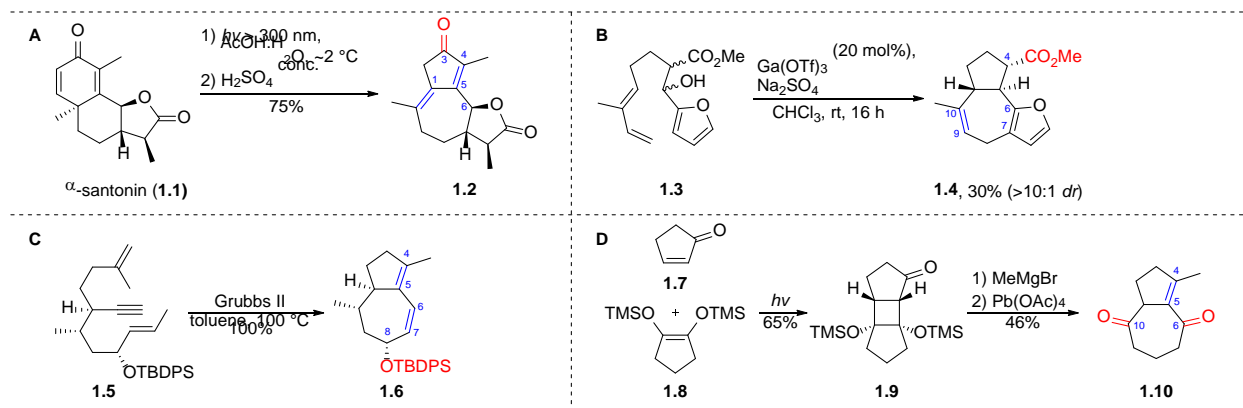
8,12-guaianolide

Total hits	5351	838
Pharmacological data	1787	251
Natural source	2163	484
Natural source + pharm. data	653	199

Data obtained via Reaxys search using structures shown (9/28/2020). Search parameters were limited to 'as substructure' variable 'on all atoms', 'stereo', and 'additional ring closures'. Filtered by 'pharmacological data available' and 'isolated from natural product + pharmacological data available'.

Many diverse methods have been adopted to access the core 5,7-ring system of guaianolides; however, a handful have been most commonly employed to access the 5,7-ring system of guaianolides in a single step. The most common method for the construction of the 5,7-ring system of the 6,12-guaianolides is the photoisomerization of α -santonin (**1.1**) (Scheme 1.1A). This method is often used in the semisynthesis of 6,12-guaianolides.³ While typically low-yielding, Macias and coworkers found that maintaining the reaction at low temperature (~ 2 °C) while using a $\text{Ni}(\text{SO}_4)_2/\text{Co}(\text{SO}_4)_2$ salt solution to filter wavelengths below 300 nm afforded the photoisomerized product in 75% yield.⁴ Use of this methodology grants access to 6,12-guaianolide cores with an enone at the C3-C5 position, and an acetoxy group at the C10 position; which can be eliminated under acidic conditions to install an alkene at the C1-C10 position. While α -santonin (**1.1**) is relatively cheap, toxicity is a concern for larger scale reactions.⁵ In addition, access to more functionally complex 6,12-guaianolides, or different stereochemistry difficult. Baran and

coworkers have showcased this photoisomerization process on a cross-conjugated dienone derived from dihydrocarvone in their total synthesis of thapsigargin.⁶



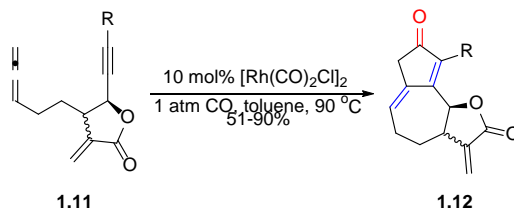
Scheme 1.1. Selected examples of the construction of the 5,7-ring system of guaianolides.

Winne and coworkers have employed a Lewis acid-catalyzed [4+3] cycloaddition of furfuryl alcohol **1.3** to access the core 5,7-ring system **1.4** with a furan at the C6-C7 position, an alkene at the C9-C10 position, and a methyl ester at the C4 position (Scheme 1.1B).⁷ While good diastereoselectivity is achieved, the authors report modest to low yields for this transformation.

Wissinger and coworkers were able to access the 5,7-ring system via a tandem ring-closing metathesis of acyclic precursor **1.5** (Scheme 1.1C).⁸ The resulting bicyclic system **1.6** possesses alkenes at the C4-C5 and C6-C7 position, as well as a silyl ether at the C8 position. The reaction is performed in excellent yields with complete retention of stereochemistry.

Photoinduced [2+2] cyclization of cyclopentenone **1.7** with the vicinal silyl enol ether **1.8** has been shown to afford the 5,4,5-tricyclic system **1.9** (Scheme 1.1D).⁹ Oxidative cleavage of the corresponding vicinal diol afforded the desired 5,7-ring system **1.10** in modest yields. Application of this strategy affords access to ketones at the C10 and C6 positions, as well as an alkene at the C4-C5 position.

The Brummond group has developed a complementary methodology to access the 5,7-ring system **1.12** of guaianolides by employing an allenic Pauson-Khand reaction (APKR) of allene-yne precursors similar to **1.11** (Scheme 1.2). Application of this methodology grants access to alkenes at the C1-C10 and C4-C5 position, as well as a ketone at the C3 position.¹⁰ While the functional group array generated via the APKR is similar to that of the photoisomerization of α -santonin, the allene-yne precursor of the APKR can be functionalized in a variety of ways; granting access to functionalities which are unachievable via the photoisomerization of α -santonin.¹¹ This methodology could thus enable access to not only more functionally complex guaianolides, but also unnatural guaianolide analogs.



Scheme 1.2. Brummond's strategy towards the 5,7-ring system of guaianolides.

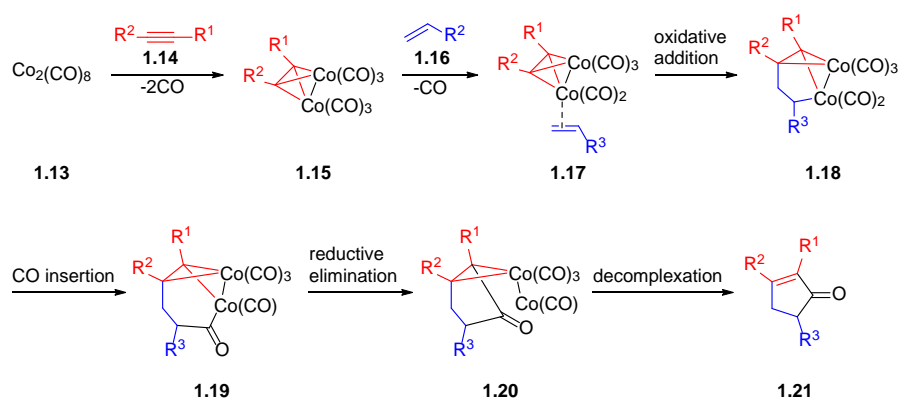
1.2 The Allenic Pauson-Khand Reaction

1.2.1 History and mechanistic details

The Pauson-Khand reaction is a formal $[2+2+1]$ cyclocarbonylation reaction between an alkene, alkyne, and carbon monoxide, affording cyclopentenone products. First reported by Pauson and Khand in 1971, the reaction typically employs $\text{Co}_2(\text{CO})_8$ as a promoter and source of CO .¹² Initial complexation of an alkyne **1.14** with $\text{Co}_2(\text{CO})_8$ affords derivative **1.15**. Loss of CO ,

complexation of alkene **1.16**, followed by oxidative addition generates the metallocycle **1.18**. Upon CO insertion, reductive elimination, then decomplexation, cyclopentenone **1.21** is produced. While initial application of this methodology for the generation of cyclopentenones was limited in substrate scope, many improvements have been made since its first report to make the PKR a broadly applied strategy for the synthesis of cyclopentenones.^{13–20}

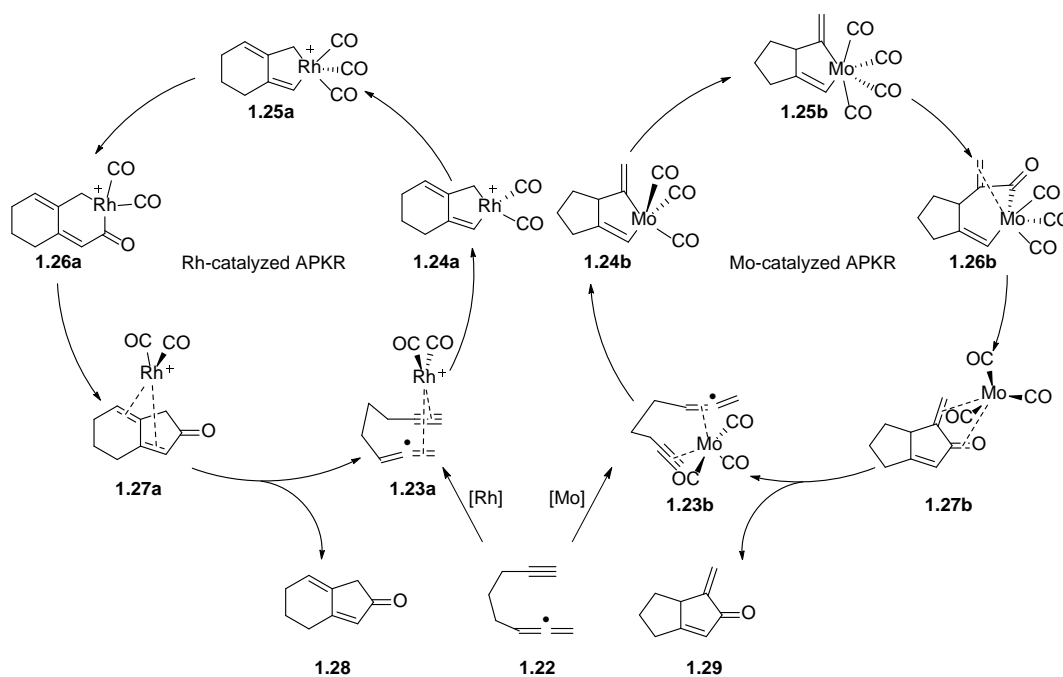
Narasaka and Brummond were the first to replace the alkene moiety with an allene, developing the first intramolecular allenic Pauson-Khand reactions in 1994 and 1995,



Scheme 1.3. Co-mediated Pauson-Khand reaction.

respectively.^{21,22} Brummond later showed that the identity of the transition metal catalyst could be used to double bond selectivity of the cyclopentenone product; with molybdenum selectively affording α -alkylidene cyclopentenones similar to **1.29**, and rhodium selectively forming 4-alkylidene cyclopentenones similar to **1.28** (Scheme 1.4).²³ These results were explained computationally by differences in the transition state structures for the oxidative cyclization between the two metals.²⁴ The lowest energy transition state structure of the Rh(I)-catalyzed APKR shows the distal double bond of the allene complexed to the rhodium metal, generating complex **1.23a** with a distorted square planar geometry. This complex undergoes an oxidative

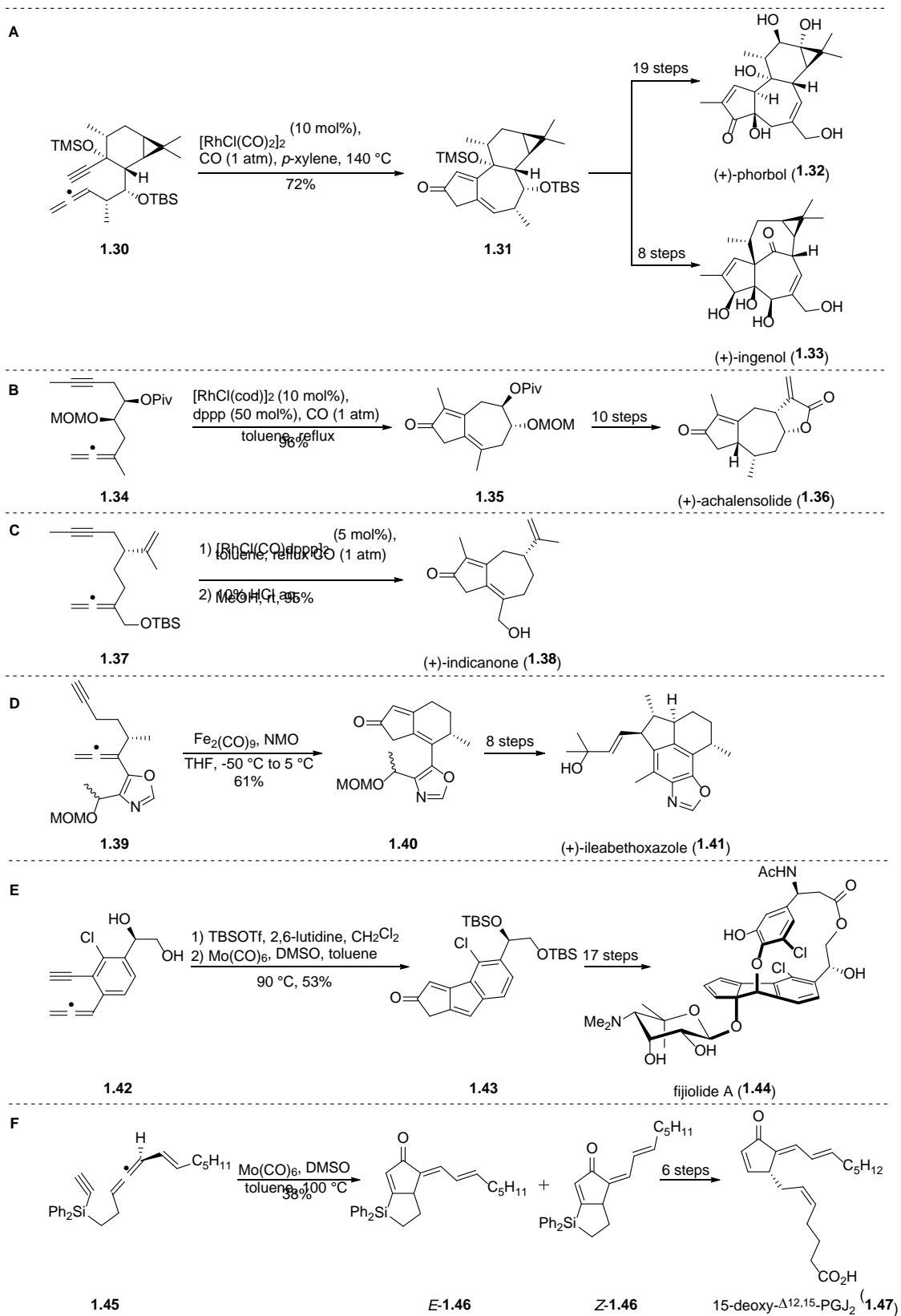
cyclization step leading to metallocycle **1.24a**. The Mo-catalyzed APKR, on the other hand shows the lowest energy transition state structure complexed with the proximal double bond of the allene affording complex **1.23b**, which adopts a trigonal bipyramidal geometry. Oxidative cyclization of this complex affords metallocycle **1.24b**. The catalytic cycle between the two metals is similar from this point forward. Association of CO affords Rh(III) complex **1.25a** or Mo(II) complex **1.25b**. Both complexes undergo migratory CO insertion to afford the Rh(III) complex **1.26a** or the Mo(II) complex **1.26b**. This is followed by reductive elimination, regenerating the Rh(I) or Mo(0) catalyst, as well as forming the respective 4-alkylidene **1.28** and α -alkylidene **1.29** products.



Scheme 1.4. Rh- and Mo-catalyzed APKR and corresponding double bond selectivity of cyclopentenones.

1.2.2 Applications of the allenic Pauson-Khand reaction in total synthesis

Despite its clear synthetic potential for the rapid construction of bicyclic systems, the APKR has only been applied to seven natural product total syntheses to date. Baran and coworkers employed the APKR as the key ring-forming step to generate bicyclo[5.3.0]decadienone intermediate **1.31** (Scheme 1.4A).²⁵ They used this intermediate in their total syntheses of both (+)-phorbol (**1.32**) and (+)-ingenol (**1.33**).^{26,27} Mukai and coworkers showcased the application of the APKR in their total syntheses of (+)-achalensolide (**1.36**) and (+)-indicanone (**1.38**) (Scheme 1.4B and 1.4C).^{28,29} Williams and coworkers employed an iron-mediated APKR in their total synthesis of (+)-ileabethoxazole (**1.41**) (Scheme 1.4D).³⁰ Cramer and coworkers completed their total synthesis of fijiolide A (**1.44**) by employing an APKR to access the 5,5,6 ring system of intermediate **1.43** (Scheme 1.4E).³¹ Finally, Brummond and coworkers applied an APKR to silicon-tethered allene-yne **1.51** in their total synthesis of 15-deoxy- $\Delta^{12,14}$ -prostaglandin J_2 .³² While four of these total syntheses take advantage of the APKR's capability to generate medium-sized seven-membered rings in good yield, there is a dearth of information on the synthetic potential of the bicyclo[5.3.0]decadienone systems generated via the APKR.

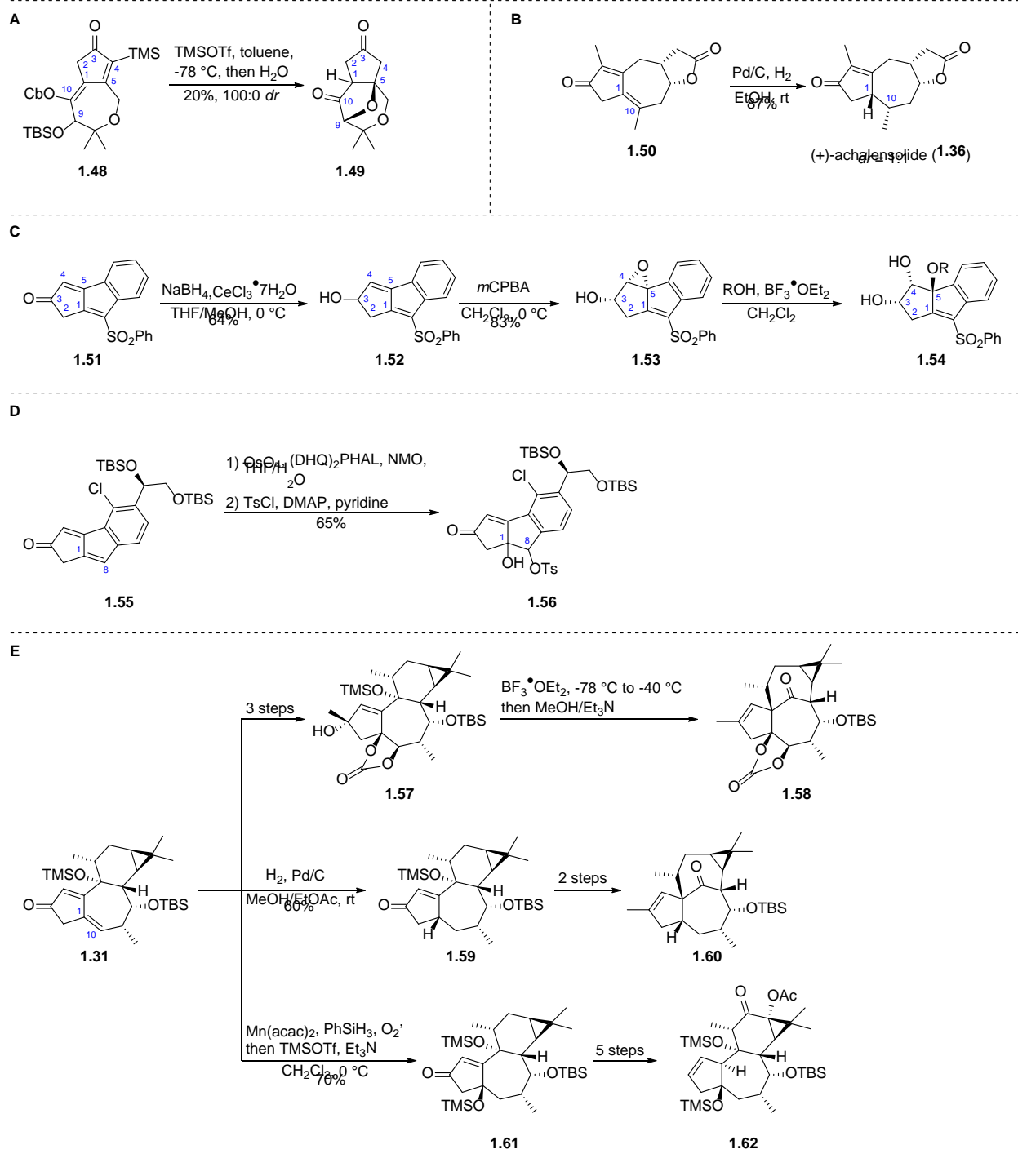


Scheme 1.5. Natural product total syntheses which employed an APKR as the key ring forming step.

1.3 Functional Group Interconversions of the APKR Adduct

The relatively rare application of the APKR to the synthesis of bicyclic natural products prompted us to perform a systematic literature search for reported strategies to functionalize the bicyclo[x.3.0]dienone system. This search produced only a handful of transformations with all involving the functionalization of the double bond at the C1 position, or the ketone at the C3 position. There have been no reports on functionalizing of the C3-C5 enone with the double bond at the C1 position maintained. For example, Sorin and Lannou reported an intramolecular conjugate addition of a C9 hydroxyl group to the C3-C5 enone of **1.48**, affording tricycle **1.49** in low yields (Scheme 1.6A).³³ This transformation first involved the deprotection and tautomerization of the C10 benzyl carbonate protected enol to the corresponding ketone. Thus, the C1-C10 alkene did not remain intact during this transformation.

Hydrogenation of the C1-C10 double bond is also common, as showcased by Mukai and coworkers in their total synthesis of (+)-achalensolide (**1.36**) (Scheme 1.6B).²⁸ Reduction of the C3 ketone of the 5,5,6-ring system **1.51** followed by *m*CPBA-mediated epoxidation of the C4-C5 alkene has been reported by Mukai and coworkers, as part of their studies towards the synthesis of the core carbon framework of cyanosporasides A and B (Scheme 1.6C).³⁴ Alcoholysis of epoxide **1.53** proceeded smoothly in the presence of $\text{BF}_3 \cdot \text{OEt}_2$, affording vicinal diol **1.54**. Cramer was able to dehydroxylate the C1-C8 double bond of tricycle **1.55** in the presence of OsO_4 , affording derivative **1.56** towards their total synthesis of fijiolide A (**1.44**) (Scheme 1.4D).³¹



Scheme 1.6. Precedent for the functional group interconversion of APKR adducts.

Perhaps the most extensive studies on the further elaboration of APKR adducts has been performed by Baran and coworkers. With access to bicyclo[5.3.0]decadienone **1.31**, they have been able to successfully functionalize the C1-C10 double bond via dihydroxylation, hydrogenation, and hydration (Scheme 1.6E).^{25,26,35} They were then able to further elaborate the enone via a Lewis acid-mediated pinacol-type rearrangement to access the 5,7,8 ring systems **1.58** and **1.60**. These intermediates were used in their total synthesis of (+)-ingenol (**1.33**) as well as their selective C-H oxidation studies of ingenanes, respectively.^{25,35} In addition, they were able to effect an allylic diazene rearrangement on cyclopentenone **1.61** as part of their total synthesis of (+)-phorbol (**1.32**).²⁶

With the lack of strategies for the selective functionalization of the C3-C5 enone in the presence of the C1-C10 alkene of bicyclo[5.3.0]decadienones arising from the APKR, we reasoned that this would be the most impactful area of study to increase the synthetic utility of the APKR. We thus turned to the literature to develop strategies which could be applied directly to the C3-C5 enone of the bicyclo[5.3.0]decadienone APKR adducts, without prior functionalization of the C1-C10 double bond. Furthermore, we wanted to narrow the scope of these strategies to be directly applicable to the guaianolide family of natural products. Thus, we set out to determine the most common motifs observed in the guaianolide class which could be accessed via direct functionalization of the C3-C5 enone.

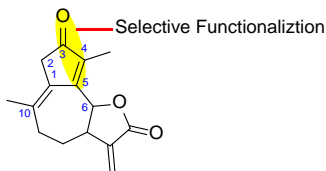


Figure 1.1. Desired C3-C5 enone functionalization in the presence of C1-C10 alkene.

2.0 Allylic Diazene Rearrangement and Base-Mediated Isomerization of APKR Adducts

2.1 Introduction

Within the guaianolide family of natural products, many different functional group patterns are represented. With the application of the allenic Pauson-Khand reaction to the construction of the 5,7-ring system, we can access guaianolides with a double bond at the C4-C5 position and an oxygen at the C3 position. However, transposition of the C4-C5 double bond to the C3-C4 position grants access to a much larger number of guaianolide frameworks. Shown in Table 1 below is a Reaxys search performed for 6,12-guaianolide frameworks with double bonds at the C4-C5 position, as well as the C3-C4 position. There has been a total of 771 6,12-guaianolide structures reported with an explicit double bond at the C4-C5 position; 319 are biologically active, 106 have been isolated from a natural product, and 26 are both biologically

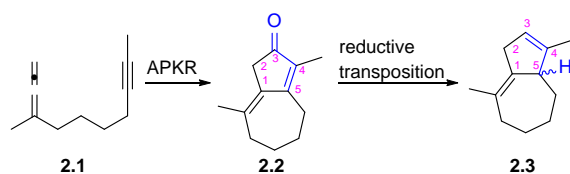
Table 2.1. Reaxys search for 6,12-guaianolide frameworks possessing discrete double bond at C4-C5 position and C3-C4 position.



Total hits	771	1053
Pharmacological data	319	308
Natural source	106	647
Natural source + pharm. data	26	174

Data obtained via Reaxys search using structures shown (7/20/2020). Search parameters were limited to 'as substructure' variable 'on all atoms', 'stereo', and 'additional ring closures'. Filtered by 'pharmacological data available' and 'isolated from natural product + pharmacological data available'.

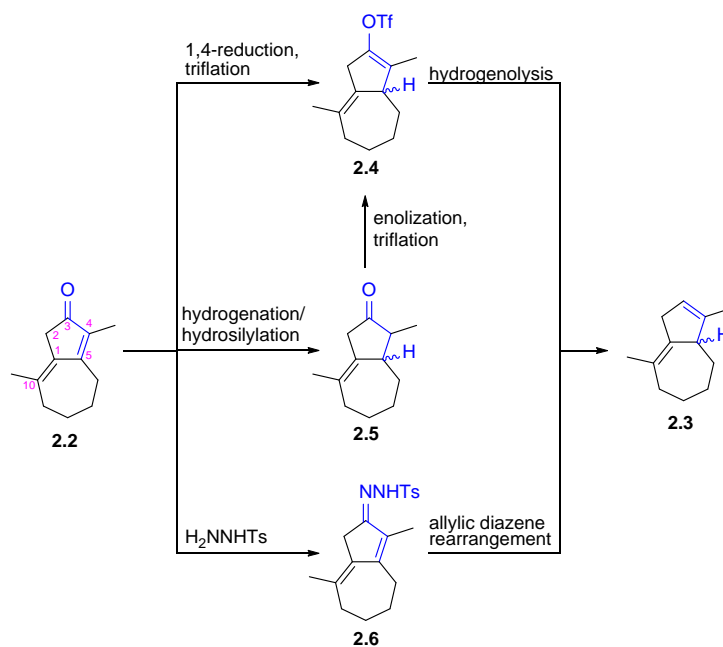
active and naturally occurring. The same Reaxys search performed on the regioisomeric 6,12-guaianolide framework, with an explicit double bond at the C3-C4 position, returns a total of 1053 unique compounds. Of these, 308 are biologically active, 647 have been isolated from natural sources, and 174 are both biologically active and naturally occurring. Successful transposition of the C4-C5 double bond to the C3-C4 position would grant us the means to access both guaianolide cores from a common APK intermediate. To this end, we proposed to study the feasibility of leveraging the inherent functional group array generated via the APKR of allene-yne **2.1** to access the C3-C4 alkene **2.3** by reductive transposition of the C3-C5 enone **2.2** (Scheme 2.1).



Scheme 2.1. Proposed reductive transposition of C3-C5 enone of APKR adduct **2.2** to C3-C4 alkene **2.3**.

2.1.1 Proposed strategies for the reductive transposition of the C3-C5 enone

The first strategy we considered for the reductive transposition of the C3-C5 enone was a 1,4-reduction followed by triflation to generate the vinyl triflate **2.4** (Scheme 2.2). Hydrogenolysis of the vinyl triflate would then afford the desired deoxygenated product **2.3**.³⁶ While this procedure is relatively straightforward, two obstacles were potentially problematic. Due to steric environment at the C5 position, hydride delivery from a bulky hydride source such as L-



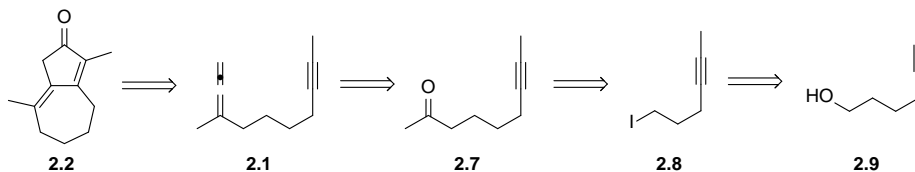
Scheme 2.2. Potential strategies for the reductive transposition of bicyclo[5.3.0]decadienone 2.2.

Selectride would most likely occur in a 1,2-fashion, at the less sterically congested C3 carbonyl carbon. Chemoselectivity was also a concern, with potential competitive reduction of other reactive functional groups on more functionally complex bicyclo[5.3.0]decadienones, required for the preparation of bioactives. The next strategy we considered was hydrogenation of the C4-C5 double bond to access cyclopentanone **2.5**, followed by enolization, triflation, and hydrogenolysis of vinyl triflate **2.4**. This strategy alleviated the concern of 1,2-reduction; however, there was a high likelihood that hydrogenation of C1-C10 double bond would occur under standard hydrogenation conditions.³⁷ To circumvent this potential chemoselectivity issue, we reasoned that we could use a transition metal-catalyzed 1,4-hydrosilylation strategy.³⁸⁻⁴¹ Hydrolysis of the corresponding silyl enol ether to cyclopentanone **2.5**, followed by enolization, triflation, then hydrogenolysis of vinyl triflate **2.4** would afford the desired reductive transposition product **2.3**. While hydrogenation or hydrosilylation conditions could work for the selective reduction of the

C3-C4 double bond, our primary concern was the enolization/triflation step. Because deprotonation could occur at either the C4 position, giving the desired trisubstituted enolate, or the C2 position, we had to be mindful of regioselectivity. In the case of bicyclo[5.3.0]decadienone **2.2**, we reasoned that the thermodynamic enolate would most likely be generated via deprotonation at the C2 position, to generate an extended enolate in conjugation with the C1-C10 double bond. Thus, even if we were able to effect selective hydrogenation or hydrosilylation at the C4-C5 double bond, generating the desired C3-C4 enolate under either thermodynamic or kinetic conditions would be difficult. Hence, we proposed a third strategy which would mitigate both chemo- and regioselectivity issues.

The final strategy that we proposed was an allylic diazene rearrangement (ADR). Condensation of enone **2.2** with tosyl hydrazide to generate tosyl hydrazone **2.6**, followed by borane reduction and subsequent ADR would afford the desired reductive transposition product **2.3**.⁴²⁻⁴⁴ A major benefit of this strategy is the chemoselectivity of the reduction. We felt confident that the borane reduction would be selective for the reduction of the tosyl hydrazone in a 1,2-fashion, leaving both the C1-C10 and C4-C5 double bond intact.⁴⁵⁻⁴⁷ In addition, conditions for the tosyl hydrazone formation are mild and functional group tolerant.⁴⁸ Because the ADR proceeds via a concerted, 1,5-sigmatropic rearrangement, the stereochemical determining step is the initial 1,2-reduction of the tosyl hydrazone, not the reduction of the alkene. Thus, due to its operational simplicity, chemoselectivity, and mild reaction conditions, we decided to first explore the allylic diazene rearrangement as our preferred strategy towards the reductive transposition of the C3-C5 enone. While this strategy has been well documented in the literature, to the best of our knowledge, this would be the first example of an allylic diazene rearrangement being performed on a conjugated bicyclic system, where both double bonds are at the ring fusion positions.

With a suitable strategy in hand, we set out to first develop a model bicyclo[5.3.0]decadienone system with minimal functionality, thus preventing any undesired side reactions that could potentially occur in the presence of other reactive functional groups. We reasoned that we could synthesize bicyclo[5.3.0]decadienone **2.2** in a reasonable number of steps via APKR of allene-yne **2.1**, which could in turn be accessed via alkynyl ketone **2.7** (Scheme 2.3). Unfortunately, alkynyl ketone **2.7** is not commercially available; however, we reasoned that it could be synthesized via alkynyl iodide **2.8**, which has been prepared starting with commercially available 5-hexyn-1-ol **2.9**.⁴⁹ With a feasible route to bicyclo[5.3.0]decadienone **2.2** in hand, we set out to first synthesize alkynyl ketone **2.7**.



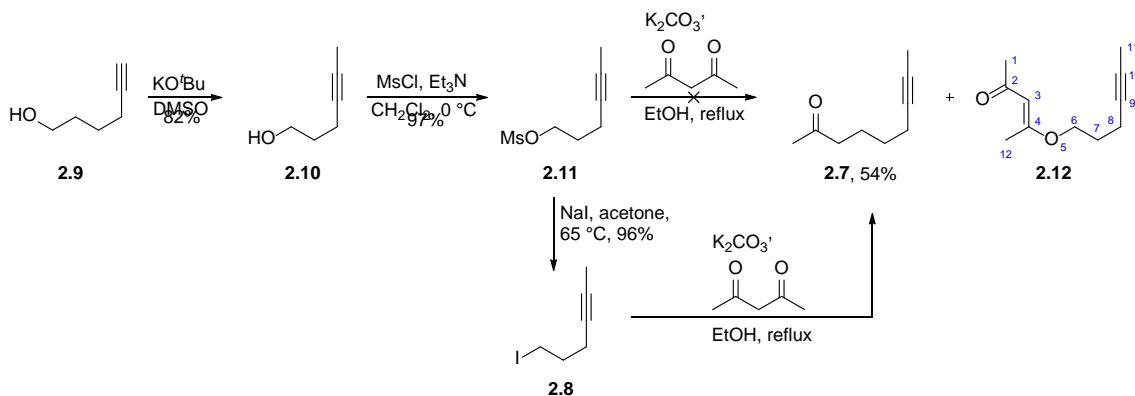
Scheme 2.3. Retrosynthetic analysis of bicyclo[5.3.0]decadienone 2.2.

2.2 Synthesis of Model Bicyclo[5.3.0]decadienone 2.2

2.2.1 Synthesis of alkynyl ketone 2.7

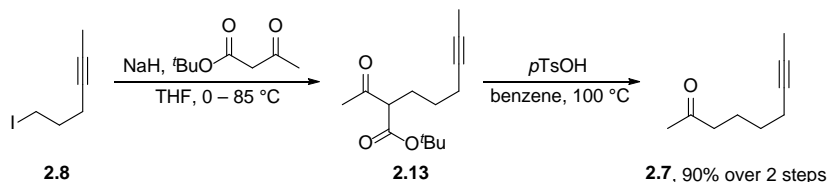
Synthesis of alkynyl ketone **2.7** began with commercially available hexyn-1-ol **2.9** (Scheme 2.4). Following a literature procedure for the synthesis of 4-hexyn-1-ol **2.10**, potassium *tert*-butoxide mediated isomerization of the terminal alkyne **2.9** to the thermodynamically favored internal alkyne **2.10** proceeded in DMSO at room temperature in 82% yield.⁴⁹ The hydroxyl group

was converted to the corresponding mesylate **2.11** in 97% yield in the presence of methanesulfonyl chloride and triethylamine in dichloromethane at 0 °C. Attempts to convert mesylate **2.11** to ketone **2.7** via addition of acetylacetone in the presence of K₂CO₃ in refluxing ethanol afforded none of the desired product.⁵⁰ Mesylate **2.11** as well as alcohol **2.10** were both detected via ¹H NMR of the crude reaction mixture after 42 h, suggesting that alcoholysis of the methanesulfonate group was the predominant reaction pathway. For this reason, mesylate **2.11** was converted to iodide **2.8** via reaction of sodium iodide in acetone at 65 °C (oil bath temperature) in 96% yield. Alkynyl iodide **2.8** was then reacted with acetylacetone in the presence of potassium carbonate in refluxing ethanol to afford the desired ketone **2.7** in 54% yield, while recovering 19% of the alkynyl iodide **2.8**. In addition to this reaction not going to completion vinyl ether **2.12**, the product of *O*-alkylation, was isolated as a single stereoisomer; the structure of which was confirmed by ¹H and ¹³C NMR. Defining spectroscopic features of vinyl ether **2.12** include resonances at 2.26 (s, 3H) ppm, and 2.15 (s, 3H) ppm corresponding to the C1 and C12 methyl protons, respectively, as well as resonances at 5.47 (s, 1H) ppm and 3.85 (t, 2H) ppm, corresponding to the C3 methine proton the C6 methylene protons, respectively. While isolated as a single stereoisomer, we did not confirm the geometry of **2.12**.



Scheme 2.4. Initial synthetic route of alkynyl ketone 2.7.

The modest yield, due to incomplete conversion of starting material and competing *O*-alkylation, led us to consider a two-step, two-pot procedure involving the alkylation of *tert*-butyl acetoacetate followed by decarboxylation to effect the desired acetone homologation of alkynyl iodide **2.8** (Scheme 2.5). Deprotonation of *tert*-butyl acetoacetate with sodium hydride in THF at 0 °C followed by addition of alkynyl iodide **2.8** afforded acetoacetate **2.13**. The crude residue was taken up in benzene and heated to 100 °C in the presence of *p*-toluenesulfonic acid (0.2 equiv), effecting decarboxylation to generate the desired alkynyl ketone **2.7** in 90% yield over two steps. With the high yield and clean TLC reaction profile of this procedure, we reasoned that we could apply the same conditions to alkynyl mesylate **2.11**, thus eliminating the need to convert the mesylate to alkynyl iodide **2.8**. We thus applied the same reaction conditions

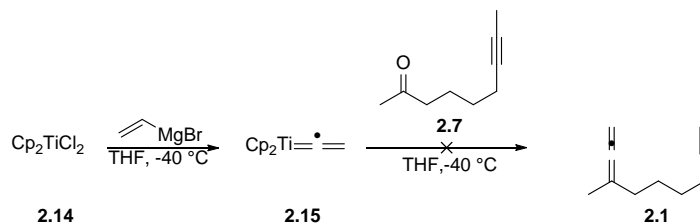


Scheme 2.5. Acetone homologation of alkynyl iodide 2.8 using *tert*-butyl acetoacetate.

reported above, with addition of alkynyl mesylate **2.11** instead of alkynyl iodide **2.8** after reaction of *tert*-butyl acetoacetate with sodium hydride. While the reaction profile showed a single spot by TLC, suggesting no *O*-alkylation product, slow reaction times were observed (> 48 h) as well as incomplete conversion of starting material. Because conversion of the mesylate **2.11** to iodide **2.8** was so rapid and high yielding, and the product required no further purification, we decided not to optimize the alkylation with alkynyl mesylate **2.11** and instead continue using alkynyl iodide **2.8**. With a rapid, high yielding route to alkynyl ketone **2.7** in hand, we next sought to convert the ketone functionality to the desired 3,3-disubstituted allene **2.1**.

2.2.2 Synthesis of allene-yne **2.1**

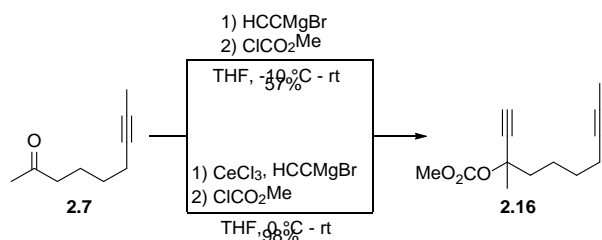
When examining potential procedures for the conversion of a ketone to a 3,3-disubstituted allene, we first explored the most direct, step-economical routes. Takeda has reported the direct conversion of carbonyl compounds to 3,3-disubstituted allenes via reaction of titanium alkenylidene **2.15**, generated *in situ* via addition of two equiv of vinylmagnesium bromide to titanocene dichloride **2.14** (Scheme 2.6).⁵¹ We reasoned that this procedure would offer the most direct access to the desired 3,3-disubstituted allene-yne **2.1**. Thus, vinylmagnesium bromide (2 equiv) was added to titanocene dichloride **2.14** in THF at -40 °C. This solution was then cannulated



Scheme 2.6. Attempted direct allenation of ketone **2.7** with alkenylidene titanocene.

into a solution alkynyl ketone **2.7**, which had been dissolved in THF and cooled to -40 °C. Upon complete consumption of **2.7**, as visualized by TLC, an aliquot of the reaction mixture was worked up and subjected to ¹H NMR, which revealed mostly uncharacterizable decomposition products. It was not immediately evident why this reaction failed on our system; however, it should be noted that the substrate scope reported by Takeda and coworkers was mostly limited to at least one aromatic ring adjacent to the carbonyl group, or α,β -unsaturated carbonyls. Due to the level of apparent decomposition, we chose not to pursue this route any further, but instead examine alternative, less direct routes to generate the desired 3,3-disubstituted allene **2.1**.

Tsuji and coworkers have reported a palladium-catalyzed hydrogenolysis of propargyl carbonates to generate 3,3-disubstituted allenes.⁵² To apply these conditions to our substrate, alkynyl ketone **2.7** had to first be converted to propargyl carbonate **2.16** via addition of ethynylmagnesium bromide, followed by addition chloromethylformate (Scheme 2.7). Thus, ketone **2.7** was dissolved in THF and cooled to -10 °C. Ethynylmagnesium bromide (1.5 equiv) was added and, after complete consumption of **2.7** was observed by TLC, methyl chloroformate (1.6 equiv) was added. Upon workup and purification via SiO₂ flash column chromatography, propargyl carbonate **2.16** was isolated in 57% yield.

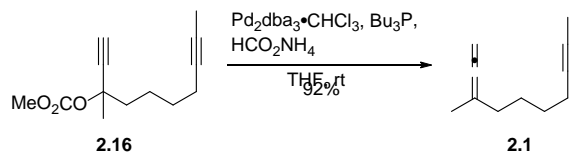


Scheme 2.7. Optimization of 1,2-addition of ethynylmagnesium bromide to ketone 2.7 via transmetalation with CeCl₃.

With these promising initial results in hand, we sought to improve the overall yield of this two-step, one-pot procedure. Cerium trichloride is known to render Grignard reagents simultaneously more nucleophilic, less basic, and less susceptible to participation in single-electron transfer reactions.⁵³ To our delight, initial transmetalation of ethynylmagnesium bromide with cerium trichloride followed by addition of alkynyl ketone **2.7**, then trapping with methyl chloroformate afforded propargyl carbonate **2.16** in 98% yield.

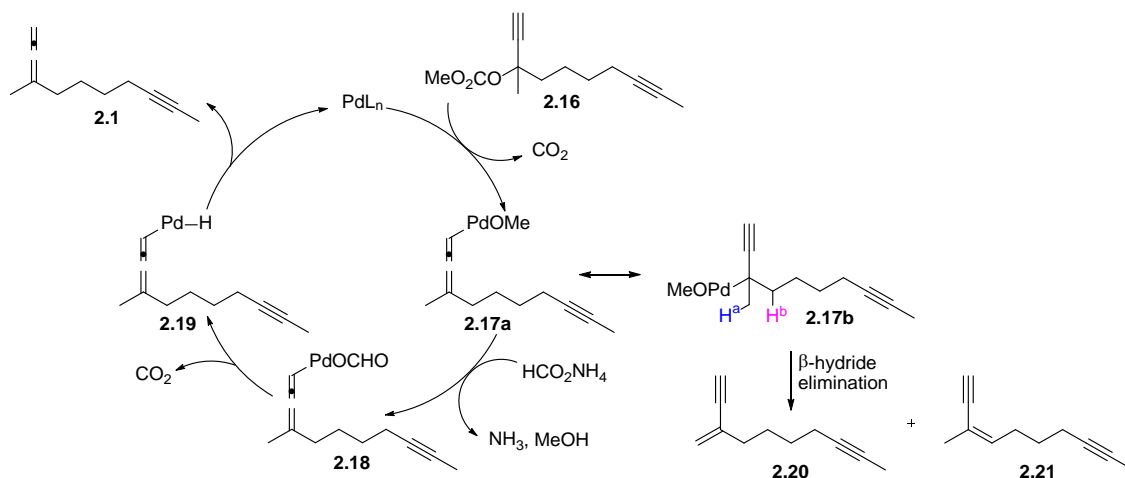
With propargyl carbonate **2.16** in hand, we were poised to apply Tsuji's palladium-catalyzed hydrogenolysis conditions.⁵² Thus Pd₂dba₃•CHCl₃ (0.025 equiv) and tri-*n*-

butylphosphine (0.1 equiv) were dissolved in THF, followed by addition of ammonium formate (2 equiv) (Scheme 2.8). Propargyl carbonate **2.16** was added and the mixture reacted at room temperature for 24 h. Upon concentration and purification, the desired allene **2.1** was obtained in 92% yield. It must be noted that this reaction was extremely sensitive to catalyst and ligand purity.



Scheme 2.8. Palladium-catalyzed hydrogenolysis of propargyl carbonate 2.16.

While this reaction was consistently high-yielding, there was a single case where agitation of the reaction was interrupted overnight, resulting in a 3:1:1 ratio of allene **2.1**, enyne **2.20** and enyne **2.21**, respectively (Scheme 2.9). Analysis of the proposed catalytic cycle for the palladium-catalyzed hydrogenolysis reveals a potential pathway to both enyne byproducts. As proposed by Tsuji and coworkers, oxidative insertion of Pd(0) followed by elimination of carbon dioxide affords palladium(II) methoxide species **2.17a**.⁵² Exchange of the methoxide ligand with formate affords palladium(II) formate **2.18**. The formate ligand undergoes a β -hydride elimination to generate palladium(II) hydride **2.19** and CO₂. Reductive elimination affords allene **2.1** and regenerates the Pd(0) catalyst.



Scheme 2.9. Palladium-catalyzed hydrogenolysis catalytic cycle and potential elimination of η^1 -palladium.

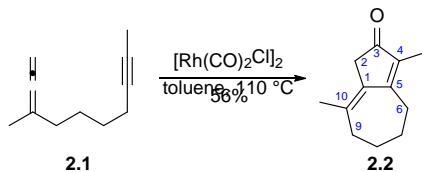
Due to the limited solubility of ammonium formate in THF, we propose that loss of agitation starves palladium(II) methoxide **2.17a** of the formate necessary to generate **2.18**. As the concentration of **2.17a** increases, the palladium center could undergo a haptotropic shift, most likely through an η^3 -allylpalladium intermediate, to generate palladium(II) intermediate **2.17b**. Ensuing β -hydride elimination of H^a or H^b then generates the observed enyne products **2.20** and **2.21**, respectively; a process that has been reported by Tsuji and coworkers.⁵⁴ Thus, it is crucial to maintain the limited solubility of ammonium formate throughout the entire course of the reaction.

With the success of the palladium-catalyzed hydrogenolysis to afford allene-yne **2.1**, we were poised to complete the synthesis of the desired bicyclo[5.3.0]decadieneone **2.2** via application of the allenic Pauson-Khand reaction.

2.2.3 Application and optimization of the APKR to allene-yne **2.1**

With allene-yne **2.1** in hand, we set out to test the feasibility of the allenic Pauson-Khand reaction (APKR) as a way to access bicyclo[5.3.0]decadienone **2.2**. We opted to begin with

conditions previously shown by our group to be optimal for methyl substituted alkynes.⁵⁵ Addition of allene-yne **2.1** to a dilute solution (0.025 M) of $[\text{Rh}(\text{CO})_2\text{Cl}]_2$ (5 mol%) in toluene at 110 °C (oil bath temperature) afforded bicyclo[5.3.0]decadienone **2.2** in a modest yield of 56% in 2 h (Scheme 2.10).



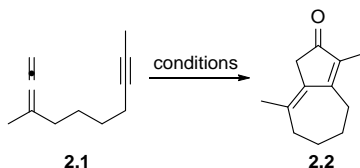
Scheme 2.10. Inverse addition of allene-yne 2.1 to Rh(I) solution.

Diagnostic ^1H NMR resonances were observed at 2.91(s) ppm corresponding to the C2 methylene protons, 2.69 (t, $J = 6.4$ Hz, 2H) ppm and 2.39 (t, $J = 6.0$ Hz, 2H) ppm corresponding to the allylic protons at C6 and C9, respectively, and 1.84(s) ppm and 1.75(s) ppm, corresponding to the C10 and C4 methyl protons, respectively. In addition to the ^1H NMR data, ^{13}C NMR resonances at 205 ppm confirmed the presence of a ketone, and resonances at 169 ppm, 138 ppm, 137 ppm, and 132 ppm confirmed the presence of four sp^2 carbons. While the initial conditions for the conversion of **2.1** to **2.2** were successful, the modest yield prompted us to further optimize the reaction conditions for this substrate.

Because the APKR required only 2 h to reach completion when using 5 mol% $[\text{Rh}(\text{CO})_2\text{Cl}]_2$ (Table 2.2, entry 1), we reasoned that we could decrease the catalyst loading in an effort to increase overall efficiency, while maintaining an acceptable reaction time and yield. Reducing the catalyst loading to 2 mol% afforded **2.2** in a comparable yield of 53%, but a slightly extended reaction time of 3 h (Table 2.2, entry 2). While the reaction times were reasonable using $[\text{Rh}(\text{CO})_2\text{Cl}]_2$, we wanted to examine an alternative Rh(I) catalyst, in an effort to increase the yield of the APKR.

Cationic $\text{Rh}(\text{cod})_2\text{BF}_4$ in the presence of a phosphine ligand has been successfully employed in the APKR by previous group members, often with good results.⁵⁶ While computational studies have suggested that the rate determining step for the Rh(I)-catalyzed APKR is the initial oxidative cyclization of the Rh(I)-allene-yne complex in the case of a ligand-free catalyst, we proposed that this could also be the case for rhodium catalysts in the presence of phosphine ligands. It follows that the strongly σ -donating character of trialkyl and triaryl phosphine ligands would render the cationic Rh(I) catalyst sufficiently electron-rich to facilitate the oxidative cyclization, even at reduced reaction temperatures.²⁴ Thus, we decided to first screen $\text{Rh}(\text{cod})_2\text{BF}_4$ in the presence of triphenylphosphine as the next catalyst for the APKR. $\text{Rh}(\text{cod})_2\text{BF}_4$

Table 2.2. Optimization of allenic Pauson-Khand reaction of allene-yne 2.1.



Entry	Catalyst	Catalyst Loading (mol %)	Solvent	Substrate concentration (M)	Temp (°C)	Time (h)	Yield (%)
1	$[\text{Rh}(\text{CO})_2\text{Cl}]_2$	5	Toluene	0.025	110	2	56
2	$[\text{Rh}(\text{CO})_2\text{Cl}]_2$	2	Toluene	0.025	110	3	53
3	$\text{Rh}(\text{cod})_2\text{BF}_4$	10	DCE	0.02	70	24	85
4	$\text{Rh}(\text{cod})_2\text{BF}_4$	5	DCE	0.02	70	24	90
5	$\text{Rh}(\text{cod})_2\text{BF}_4$	2.5	DCE	0.02	70	24	88
6	$\text{Rh}(\text{cod})_2\text{BF}_4$	2.5	DCE	0.1	70	20	86

(10 mol%) and PPh_3 (15 mol%) were dissolved in dichloroethane (Table 2.2, entry 3). The reaction flask was evacuated and refilled with carbon monoxide using a CO-filled balloon, and allene-yne **2.1** was added. After 24 h, complete conversion of **2.1** was observed, and bicyclo[5.3.0]decadienone **2.2** was isolated in 85% yield.

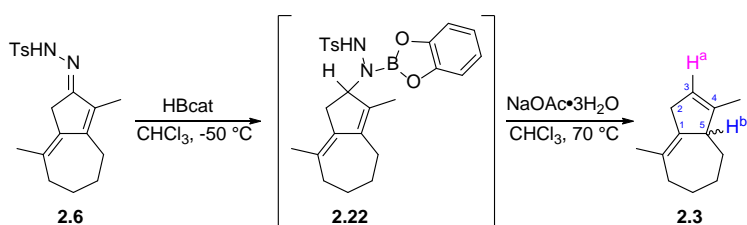
With a marked increase in reaction yield, we again decided to lower the catalyst loading to determine what effect, if any, this would have on reaction time and yield. The catalyst loading was reduced to 5 mol% with no appreciable impact on time or yield (Table 2.2, entry 4). The loading was further decreased to 2.5 mol%, again with no appreciable impact on time or yield (Table 2.2, entry 5). With this optimal catalyst system in hand, we next wanted to explore the effect of substrate concentration. Previous reports using $[\text{Rh}(\text{CO})_2\text{Cl}]_2$ suggest the formation of a dimeric byproduct when substrate concentrations exceed 0.025M.⁵⁵ We did not see any evidence of byproducts when using $\text{Rh}(\text{cod})_2\text{BF}_4$ with a substrate concentration of 0.025M, so we decided to increase the substrate concentration to 0.1 M, in an effort to consume less halogenated solvent (Table 2.2, entry 6). Gratifyingly, we saw no appreciable impact on reaction yield, and reaction time was decreased by 4 h. With these optimized conditions in hand, we had rapid access to the bicyclo[5.3.0]decadienone model system **2.2** in high yield. We were thus poised to explore the feasibility of reductive transposition of the C3-C5 enone.

2.3 ¹H NMR Studies of Tosylhydrazone Reduction with Catecholborane

The strategy we chose to pursue for the reductive transposition of bicyclo[5.3.0]decadienone **2** was an allylic diazene rearrangement (ADR), for the reasons enumerated above. We reasoned that catecholborane (HBcat) reduction of tosylhydrazone **2.6** would occur chemoselectively at the hydrazone, leaving the double bonds intact.⁵⁷ In addition, the allylic diazene rearrangement (ADR) of α,β -unsaturated hydrazones has been shown to selectively form the product of alkene migration, even in cases where that product is thermodynamically disfavored.^{44,58} We thus felt confident that application of the ADR to tosylhydrazone **2.6** would

afford the desired 1,4-alkene **2.3**, despite the fact that double bond conjugation would be broken (Scheme 2.12).

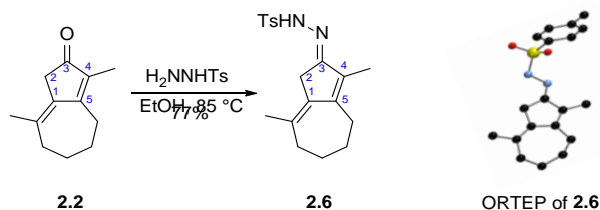
First, we had to convert bicyclo[5.3.0]decadienone **2.2** to the tosylhydrazone derivative **2.6** (Scheme 2.12). This was accomplished in 77% yield via reaction of **2.2** with tosylhydrazide (1.2 equiv) in ethanol at 85 °C for 18 h. Diagnostic ^1H resonances at 2.89(s) ppm corresponding to the C2 protons, 1.77(s) ppm and 1.75(s) ppm corresponding to the protons on the methyl groups at the C4 and C10 positions, respectively, and 2.53(t) ppm and 2.29(t) ppm, corresponding to the protons at the C9 and C6 positions, respectively, confirmed the formation of **2.6**. We also observed that, under the reaction conditions, a single stereoisomer of the hydrazone was formed. We predicted that the *E*-hydrazone would be the thermodynamically preferred isomer, owing to the presence of an unfavorable steric between the tosyl group of the hydrazone and the methyl group at the C4 position of the *Z*-isomer. The *E*-hydrazone stereochemistry was confirmed via single crystal X-ray of **2.6**, a crystal of which was obtained via dissolution in ethyl acetate and slow evaporation of the solvent.



Scheme 2.11. Attempted ADR of bicyclo[5.3.0]decadienone tosylhydrazone 2.6.

With hydrazone **2.6** in hand, initial conditions for the allylic diazene rearrangement were investigated (Scheme 2.12). The first step is reduction of the tosylhydrazone **2.6** to the corresponding tosylhydrazine derivative **2.22**. The most common reagent employed for this

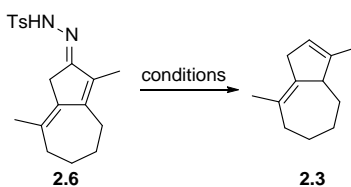
reduction is catecholborane, as it is highly selective for the reduction of tosylhydrazones in the presence of other reactive functional groups, and the reaction conditions are very mild.⁶ Thus, tosylhydrazone **2.6** was reacted with catecholborane (neat, 3 equiv) in chloroform at -50 °C (Table 3, entry 1). After 1 h, sodium acetate trihydrate (3 equiv) was added and the reaction was warmed to room temperature and stirred for 1 h. It was then brought to 70 °C for an additional 1 h. Upon workup, ¹H NMR of the crude residue revealed none of the desired ADR product **2.3**, as evidenced by the lack of the expected C3 olefinic proton H^a between 5-6 ppm. The progress of the reaction was unable to be followed by TLC, due to the large excess of catecholborane overlapping with tosylhydrazone **2.6** on the TLC plate. Thus, we were not certain whether **2.6** was undergoing catecholborane reduction.



Scheme 2.12. Synthesis and crystal structure of *E*-tosylhydrazone of bicyclo[5.3.0]decadienone **2.2**.

To overcome this issue and accurately monitor the progress of the reduction step, we decided to perform the reaction in CDCl₃, and periodically take aliquots for analysis by ¹H NMR. Thus, tosylhydrazone **2.6** was dissolved in CDCl₃, cooled to 0 °C and allowed to react with catecholborane (neat, 3 equiv) (Table 2.3, entry 2). A reference spectrum was taken before the addition of catecholborane (Figure 2.1A). After stirring for 1 h with catecholborane at 0 °C, an aliquot was taken and subjected to ¹H NMR analysis (Figure 2.1B). The mixture was warmed to

Table 2.3. Screening of catecholborane reduction conditions for ADR of tosylhydrazone 2.6.



Entry	Reducing Agent (equiv)	Solvent	Additive (equiv)	Time (h)	Temp (°C)	Result
1	HBcat neat (3)	CDCl ₃	-	2	-40	2.6 by NMR
2	HBcat neat (3)	CDCl ₃	-	1	0 - rt	2.6 by NMR
3	HBcat neat (3)	CDCl ₃	SiO ₂ (2 wt. equiv)	1	0 - rt	2.6 by NMR
4	HBcat neat (3)	CDCl ₃	AcOH (2)	1	rt	2.6 by NMR
5	HBcat neat (6)	CDCl ₃	-	24	0	2.6 by NMR

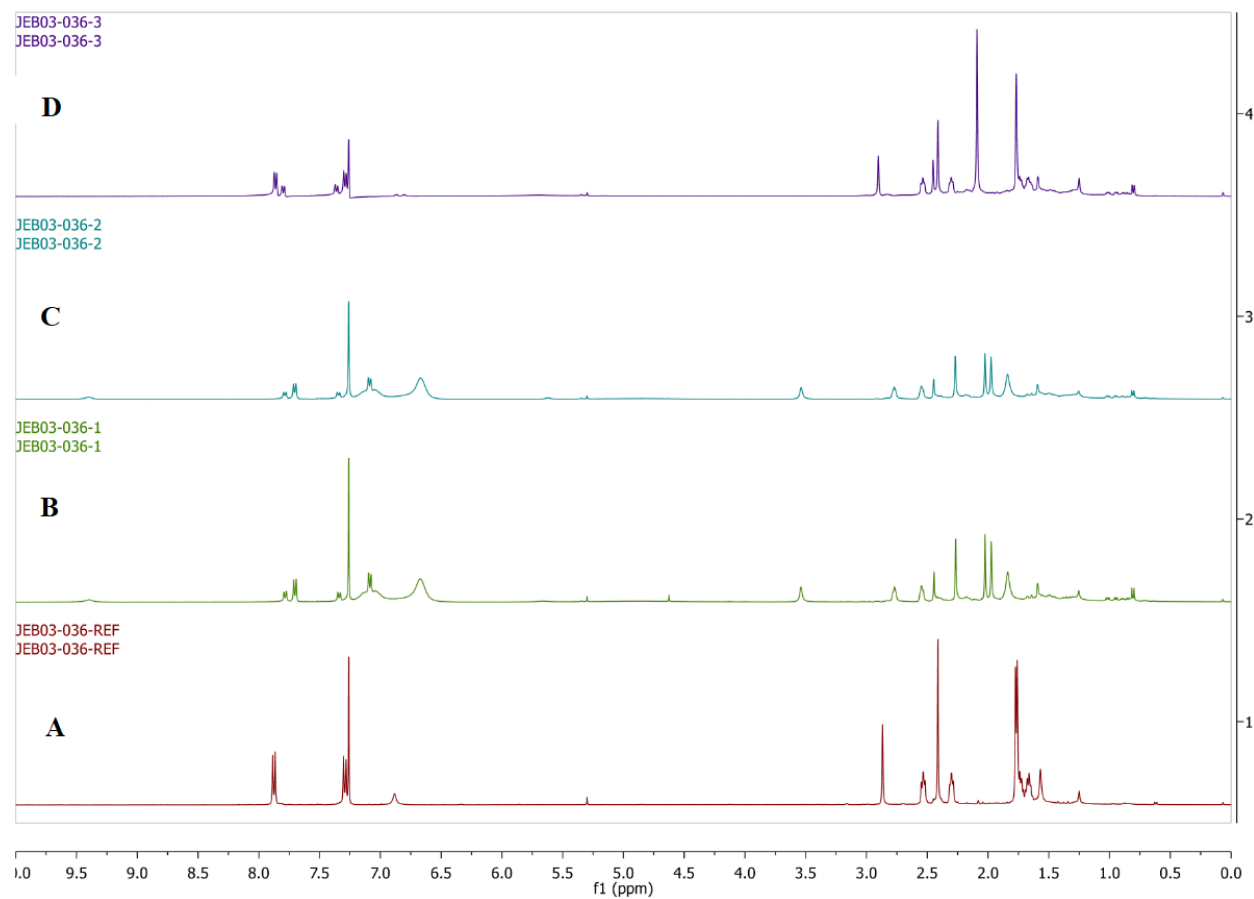


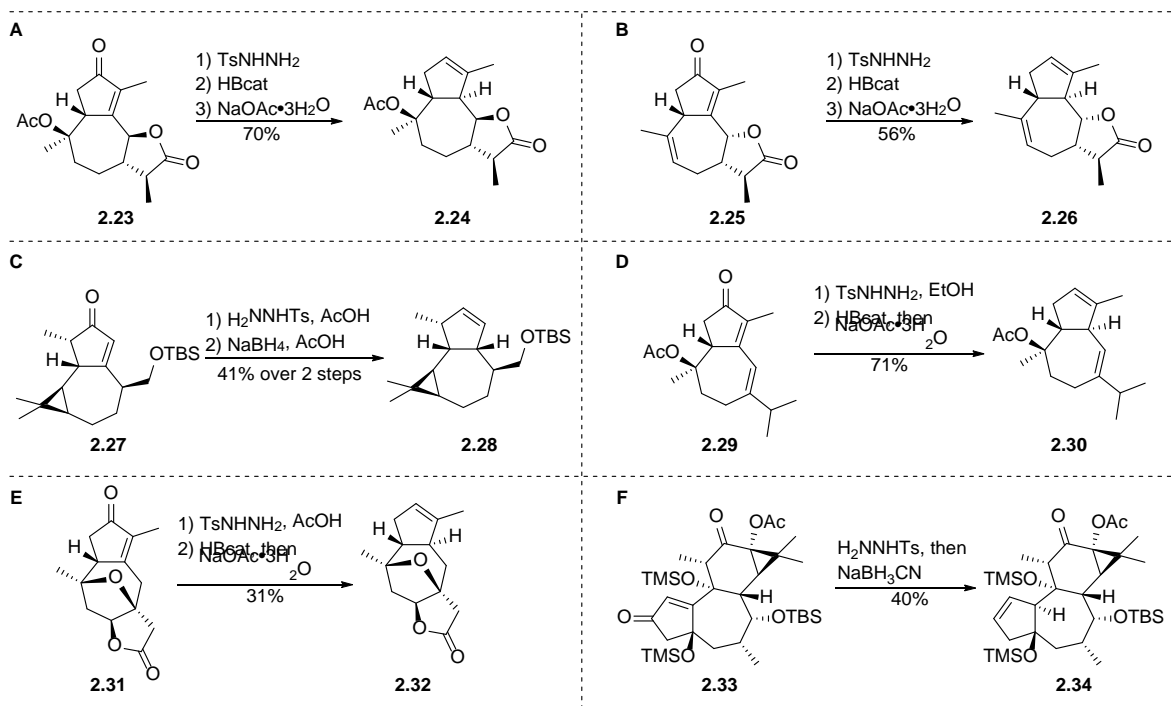
Figure 2.1. A) Reference spectrum, no catecholborane. B) 3 equiv HBcat after 1 h at 0 °C. C) after 1 h at rt. D) After addition of 3 equiv sodium acetate trihydrate and reacting at 60 °C for 1 h.

room temperature and stirred for an additional 1 h and a second aliquot was taken (Figure 2.1C). Sodium acetate trihydrate (3 equiv) was added to the reaction mixture, and it was brought to 70 °C for 1 h. A third aliquot was taken at this time (Figure 2.1D).

After initial addition of the catecholborane, no starting material was detected, as evidenced by the disappearance of the resonances at 2.87 (s) ppm corresponding to the C2 methylene protons of **2.6**, 2.41 (s) ppm corresponding to the tosyl methyl protons of **2.6**, 1.77 (s) ppm, and 1.76 (s) ppm (compare Figures 2.1A and 2.1B). Warming the reaction and stirring for an additional hour appeared to have no effect as evidenced by the similarities between the spectra of Figure 2.1B and 2.1C. After addition of sodium acetate trihydrate followed by heating, ¹H NMR analysis of the crude reaction mixture revealed a substantial amount of tosylhydrazone **2.6**, as evidenced by the reappearance of resonances at 2.90(s) ppm, 2.41(s) ppm, and 1.77(s) ppm (Figure 2.1D). The observation of predominately **2.6** after addition of NaOAc·3H₂O strongly suggested that reduction of the hydrazone was not occurring under these reaction conditions.

With data suggesting that hydrazone reduction is not occurring, we turned to the literature in an effort to find alternative conditions for the catecholborane reduction of tosylhydrazones. McIntosh has shown that the reaction time of the catecholborane reduction of tosylhydrazones, followed by ADR, is reduced in the presence of SiO₂ or acetic acid.⁵⁹ Thus, we repeated the reaction using the previous conditions, this time with the introduction of SiO₂ into the reaction mixture (two times the mass of **2.6**) (Table 2.3 entry 3). The reaction was performed at 0 °C, and after 1 h we saw no discernable difference between the spectrum of this reaction to that of the reaction performed without SiO₂. The reaction was allowed to warm to room temperature and maintained for an additional hour. Again, there was no discernable change in the ¹H NMR of the reaction mixture. We concluded that addition of SiO₂ did not impact the reduction of

tosylhydrazone **2.6**. We next wanted to screen the effect of acetic acid, as McIntosh had also shown it to be effective for the ADR. Thus, tosylhydrazone **2.6** was dissolved in CDCl_3 and AcOH (2 equiv) was added. Catecholborane (3 equiv) was added at room temperature and aliquots of the reaction mixture were subjected to ^1H NMR (Table 2.3, entry 4). No reduction of **2.6** occurred under these reaction conditions as evidenced by ^1H NMR of the crude reaction mixture. Finally, a large excess of catecholborane (6 equiv) was employed in an effort to force the reduction (Table 2.3, entry 5). After reacting at room temperature for 24 h, none of the desired ADR product **2.3** was observed by ^1H NMR; providing further evidence that tosylhydrazone **2.6** was not undergoing



Scheme 2.13. Precedent for ADRs performed on bicyclo[5.3.0]decenones.

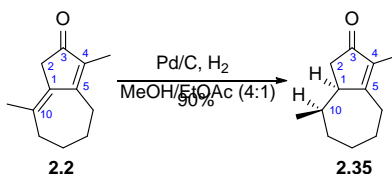
reduction. It was unclear why tosylhydrazone **2.6** was so resistant to catecholborane reduction; however, an exhaustive literature search for ADRs performed on 5,7-ring systems revealed six such reports.

Greene applied an ADR to bicyclo[5.3.0]decenones **2.23** and **2.25** in his total syntheses of (+)-pachydictoyl A and (-)-dicytolene, and oxoisodehydroleucodin in 1980 and 1989, respectively (Scheme 2.13A and B).^{45,60} Iwata successfully employed an ADR on bicyclo[5.3.0]decenone **2.27** towards the total synthesis of (+)-aromadendrene and (-)-alloaromadendrene in 1996 (Scheme 2.13C).⁶¹ The ADR of **2.29** was a key step in Pedro's synthesis of (+)-alismoxide in 2006 (Scheme 2.13D).⁶² Sun was able to employ an ADR on tricycle **2.31** in his total synthesis of hedyosumin E aglycon (Scheme 2.13E).⁶³ Recently, Baran showcased the use of an ADR of bicyclo[5.3.0]decenone **2.33** towards the total synthesis of (+)-phorbol (Scheme 2.13F).²⁶ While most of the above examples of this transformation were performed on an enone motif, Pedro's showed that this transformation can indeed be performed on a conjugated dienone of a 5,7-ring system. However, unlike Pedro's dienone **2.33**, both ring-fused carbons (C1 and C5) of APKR adduct **2.2** are sp^2 hybridized. To the best of our knowledge, there have been no reported applications of an ADR on such systems. We sought to understand the effect of the C1-C10 double bond on the catecholborane reduction of **2.6**, and hypothesized that hydrogenation of the C1-C10 double bond of **2.2** would serve to simplify the 5,7-ring system and offer a direct comparison between the dienone **2.2** and the analogous enone. It should be noted that none of the above reports of the ADR performed on 5,7-ring systems resulted in high yields; suggesting that we may not observe high yields for our system either.

2.4 ADR on C1-C10 Hydrogenated APKR Adduct

In order to test the impact of the C1-C10 double on the ADR, we reasoned that a Pd-catalyzed hydrogenation could be employed to chemoselectively reduce the C1-C10 double bond,

in the presence of the C3-C5 enone.³⁷ Thus, dienone **2.2** was reacted with Pd/C (10 mol%) under a H₂ atmosphere (1 atm, balloon), in a 4:1 mixture of MeOH/EtOAc at room temperature (Scheme 2.14). Dienone **2.2** and enone **2.35** were inseparable by TLC, thus the reaction was monitored via ¹H NMR.

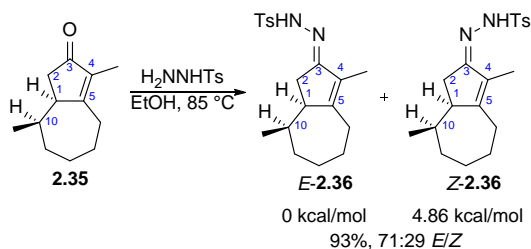


Scheme 2.14. Hydrogenation of C1-C10 double bond of 2.2.

A resonance at 2.91 (s) ppm corresponding to the C2 methylene protons of **2.2** was chosen to monitor the progress of the hydrogenation. Disappearance of this resonance was an indication that the reaction had gone to completion. The reaction was rapid, affording enone **2.35** in 90% yield after 10 mins. The reaction proceeded in a diastereoselective fashion, affording a single diastereomer of **2.35**, as evidenced by the presence of a resonance at 1.66 (s) ppm corresponding to the protons on the C4 methyl group, and a resonance at 0.69 (d, $J = 8.0$ Hz) ppm, corresponding to the protons on the C10 methyl group of **2.35**. It must be noted that careful monitoring of the reaction progress was crucial. Extended reaction times (>45 min) resulted in a complex mixture of products; presumably due to further reduction of **2.35**.

With the C1-C10 hydrogenated APKR adduct **2.35** in hand, we sought to prepare the tosylhydrazone derivative **2.36** (Scheme 2.15). Ketone **2.35** was dissolved in ethanol and tosylhydrazide (1.2 equiv) added. The reaction mixture was maintained at 85 °C for 18 h, affording tosylhydrazone **2.36** in 93% yield. Both the *E*-**2.36** and *Z*-**2.36** isomers were formed in a 71:29 ratio, as evidenced by the presence of a resonance at 0.99 (d, $J = 6.4$ Hz, 1.2H) ppm in the ¹H NMR, corresponding to the protons on the C10 methyl group of the minor *Z*-isomer, and a

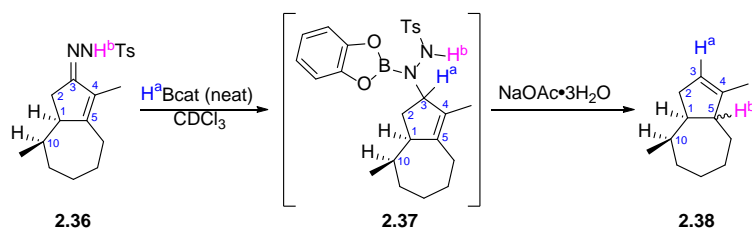
resonance at 0.64 (d, $J = 7.2$ Hz, 3H) ppm corresponding to the protons on the C10 methyl group of the major *E*-isomer. Other resonances diagnostic of tosylhydrazone **2.36**, but appearing as overlapping peaks for the individual isomers at 2.44 (s) ppm corresponding to the tosyl methyl



Scheme 2.15. Formation of tosylhydrazone **2.36** from C1-C10 hydrogenated APKR adduct **2.35**.

protons, as well as a resonance at 1.68 (s) ppm, corresponding to the protons on the C4 methyl group were also present. The two isomers were inseparable by SiO₂ flash column chromatography, however *in silico* geometry optimization of *E*-**2.36** and *Z*-**2.36** using B3LYP with a 6-31G* basis set *in vacuo* predicted *Z*-**2.36** to be 4.86 kcal/mol higher in energy than *E*-**2.36**. We thus predict *E*-**2.40** to be the major isomer; however, both isomers were used as a mixture for all subsequent transformations.

With tosylhydrazone **2.36** in hand, the feasibility of the ADR was tested on the C1-C10 hydrogenated 5,7-ring system and reaction progress of the catecholborane reduction monitored by ¹H NMR. Tosylhydrazone **2.36** was dissolved in CDCl₃ and the mixture cooled to -40 °C.



Scheme 2.16. HBcat reduction of C1-C10 hydrogenated tosylhydrazone **2.36** and ADR.

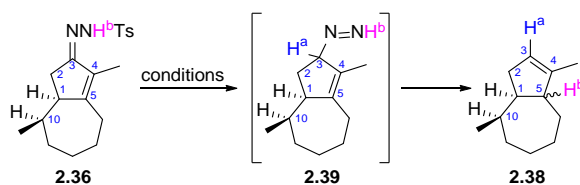
Catecholborane (3 equiv, neat) was added and aliquots were taken for ^1H NMR analysis every hour (Table 2.4, entry 1). We did not observe a resonance between 3-4 ppm corresponding to H^a of tosylhydrazone intermediate **2.37**, suggesting that hydrazone **2.36** was not reduced with catecholborane (Scheme 2.16). Upon SiO_2 chromatographic purification of the crude reaction mixture, ^1H NMR of the major reaction component revealed that it was indeed tosylhydrazone **2.36**, thus confirming that reduction of the tosylhydrazone under these conditions did not take place. Because of this, we sought to screen alternative conditions for the reduction of the hydrazone.

We reasoned that increasing the reaction temperature from $-40\text{ }^\circ\text{C}$ to $0\text{ }^\circ\text{C}$ could facilitate the catecholborane reduction of the tosylhydrazone moiety (Table 2.4, entry 2). Thus, tosylhydrazone **2.36** was dissolved in CDCl_3 and the solution cooled to $0\text{ }^\circ\text{C}$. Catecholborane was added (3 equiv, neat) and the mixture stirred at $0\text{ }^\circ\text{C}$. An aliquot of the reaction mixture was taken after 45 min and analyzed via ^1H NMR. The resulting spectrum was nearly identical to the spectrum obtained from the previous reaction, and thus was inferred that tosylhydrazone **2.36** was unaffected by catecholborane under these conditions, so we decided to further increase the temperature to room temperature. After reacting for 45 min at room temperature, another aliquot of the reaction mixture was taken and analyzed by ^1H NMR. The spectrum was very similar the

spectra previously taken at the lower temperature, indicating that tosylhydrazone **2.36** remained unreacted.

We next examined the effect of 10 equiv of catecholborane, hoping to force the reduction of **2.36**. Thus, tosylhydrazone **2.36** was dissolved in CDCl_3 and cooled to $-40\text{ }^\circ\text{C}$. Catecholborane (10 equiv, neat) was added and the mixture stirred for 1 h before an aliquot of the reaction mixture was taken for ^1H NMR analysis (Table 2.4, entry 3). The spectrum was, again, nearly identical to those of the previously reported conditions. It became apparent from varying the reaction

Table 2.4. Alternative reduction conditions and ADR of 2.36.



Entry	Reducing Agent (equiv)	Solvent	Additive (equiv)	Time (h)	Temp ($^\circ\text{C}$)	Result
1 ^a	HBcat neat (3)	CHCl_3	-	4	-40	No reduction, mostly 2.36 by ^1H NMR
2 ^a	HBcat neat (3)	CHCl_3	-	1.5	0-rt	No reduction, mostly 2.36 by ^1H NMR
3 ^a	HBcat neat (10)	CHCl_3	-	4	-40	No reduction, mostly 2.36 by ^1H NMR
4 ^b	NaCNBH_3 (4)	THF	pTsOH	5	rt	No reduction, mostly 2.36 by ^1H NMR
5 ^b	NaCNBH_3 (4)	THF	pTsOH	18	rt - 70	Trace 2.38
6 ^b	NaCNBH_3 (10)	MeOH	AcOH (6)	4	70	Trace 2.38
7	$(\text{BzO})_2\text{BH}$ (3)	THF/ CHCl_3	-	3	0 - rt	40% 2.38 , 59:41 dr
8	HBcat (1M in THF) (3)	CHCl_3	-	3	0	48% 2.38 , 60:40 dr

^aReaction progress monitored by ^1H NMR. ^bReaction progress monitored by TLC.

temperature and equiv of catecholborane that the reduction of the tosylhydrazone moiety would not proceed under these commonly employed conditions. To continue our studies on the feasibility of applying the ADR to the C1-C10 hydrogenated tosylhydrazone **2.36**, we turned to the literature in search of alternative conditions for the reduction, and subsequent ADR.

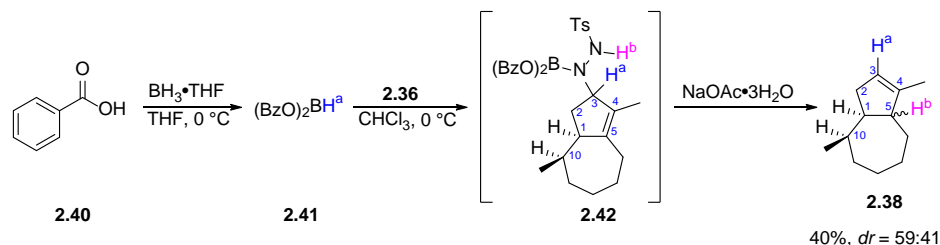
Sodium cyanoborohydride (NaBH_3CN) in the presence of stoichiometric amounts of acid has been used to successfully effect allylic diazene rearrangements.⁶⁴ Though the reaction conditions are less mild than the catecholborane conditions, due to the structural simplicity of tosylhydrazone **2.36**, we felt confident that the substrate would survive the acidic medium at the elevated temperature required to effect the reduction in the presence of sodium cyanoborohydride. Thus, we set out to apply these conditions to our system. Tosylhydrazone **2.36** was dissolved in THF and *p*-toluenesulfonic acid (*p*TsOH) was added. Sodium cyanoborohydride was then added portion-wise until 4 equiv were reached (Table 2.4, entry 4). The mixture was reacted at room temperature for 5 h, during which time tosylhydrazone **2.36** remained unreacted, as evidenced by TLC, and confirmed by the presence of resonances corresponding to **2.36** in the ^1H NMR of the crude reaction mixture. This result led us to conclude that, while the tosylhydrazone moiety was not reduced, the substrate did survive the acidic reaction conditions, and we could proceed by increasing the reaction temperature in an effort to force the reduction. Thus, the reaction was repeated at elevated temperature (70 °C) for an extended period of time (18 h) (Table 2.4, entry 5). Tosylhydrazone **2.36** was fully consumed over this time, as evidenced by TLC. Upon workup, ^1H NMR analysis of the crude residue confirmed the complete consumption of **2.36**. In addition, we observed a resonance at 5.25 ppm which we hypothesized could correspond to H^a of ADR product **2.38**; however, the integral value of this resonance was small relative to the other unassigned

resonances. With these promising preliminary results in hand, we sought to optimize the conditions for the formation of ADR product **2.38**.

Baran has reported the use of sodium cyanoborohydride in methanol, in the presence of acetic acid, as effective conditions for the reduction of a tosylhydrazone, and subsequent ADR.²⁶ Tosylhydrazone **2.36** was dissolved in methanol and acetic acid was added, followed by sodium cyanoborohydride portion-wise (Table 2.4, entry 6). The mixture was stirred at 70 °C for 4 h. TLC indicated complete consumption of **2.36**, and upon ¹H NMR analysis of the crude reaction mixture, we observed the diagnostic resonance of H^a at 5.25 ppm. However, as in the previous case, there were substantial uncharacterizable resonances present in the ¹H NMR. It was because of these suboptimal reaction profiles, low conversions to the presumed ADR product **2.38**, and a large amount of uncharacterizable products in the aliphatic region of the ¹H NMR that we again decided to shift our focus to alternative borane hydride sources.

Kabalka and coworkers reported to use of bis(benzoyloxy)borane as an effective alternative to catecholborane for the ADR.⁶⁵ Bis(benzoyloxy)borane (**2.41**) was prepared *in situ* via addition of BH₃·THF (1 M solution) to 2 equiv of benzoic acid (**2.40**) in CDCl₃ (Scheme 2.17). Tosylhydrazone **2.36** was dissolved in CDCl₃ and added to this solution at 0 °C (Table 2.4, entry 7). After reacting for 3 h while warming to room temperature, complete consumption of **2.36** was observed via TLC. A benefit of using bis(benzoyloxy)borane was that the reduction progress could be monitored via TLC, as the borane reagent remained on the baseline and stained less intensely than its catecholborane analog. NaOAc·3H₂O was then added and the mixture stirred at 70 °C in a sealed reaction vessel for 1 h, during which time a large fast-moving spot was observed by TLC. The borane reagent was removed from the reaction mixture via mild aqueous base workup (sat. aq. NaHCO₃), an additional benefit of using bis(benzoyloxy)borane rather than catecholborane.

Upon purification of the resulting crude residue via SiO₂ flash column chromatography, this fast-moving reaction component was isolated in 40% yield and confirmed to be the desired ADR product **2.38**. The key alkenyl resonances at 5.28 (m) ppm and 5.24 (m) ppm, corresponding to H^a of each C5 epimer of **2.38**, were shown to have a *J*¹ correlation with the ¹³C alkenyl resonances at



Scheme 2.17. (BzO)₂BH reduction of tosylhydrazone **2.36** and ADR.

123.5 ppm and 123.3 ppm (C3) via HSQC, thus providing evidence for the presence of alkenyl proton H^a. In addition, resonances at 0.91 (d, *J* = 6.4 Hz, 2.2 H) and 0.83 (d, *J* = 6.8, 3H) provided evidence for the presence of the C10 methyl group, as well as further evidence in support of the ADR generating two diastereomers at C5. Finally, a ¹H resonance at 1.62 (m, 5.2H) ppm showed a *J*² correlation with the ¹³C alkenyl resonances at 143.7 ppm and 143.3 ppm (C4), and a *J*³ correlation with the ¹³C alkenyl resonances at 123.5 ppm and 123.3 ppm (C3), providing support for the presence of a methyl group at C4. Based on the integral values of the methyl proton resonances at 0.91 ppm and 0.83 ppm, the ADR was shown to occur with a diastereomeric ratio of 59:41.

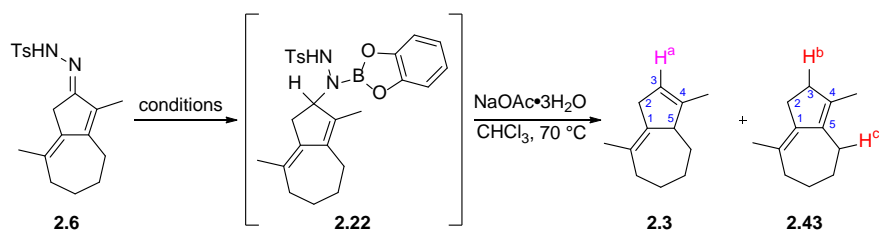
The reaction conditions differed from those of the catecholborane reaction conditions in both the borane used, as well as the solvent system. In Kabalka's initial report for the use of bis(benzoyloxy)borane, it was noted that the reactivity was very similar to that of catecholborane. Given this observation, we reasoned that the reducing capability of bis(benzoyloxy)borane was

similar to that of catecholborane, and tosylhydrazone **2.36** most likely could be reduced with either. The only other significant difference with these new reaction conditions was the solvent. The successful ADR was performed in the presence of a Lewis basic cosolvent (THF). We thus decided to reexamine the catecholborane conditions for the reduction of tosylhydrazone **2.36**, with the addition of THF as a cosolvent. Tosylhydrazone **2.36** was dissolved in CHCl_3 and the mixture cooled to 0 °C. Catecholborane (1 M in THF) was added and the mixture stirred for 3 h (Table 2.4, entry 8). After addition of $\text{NaOAc}\cdot 3\text{H}_2\text{O}$ and heating to 70 °C, we observed the formation of a fast-moving reaction component via TLC. Upon workup and purification, ADR product **2.38** was isolated in 48% yield with a diastereomeric ratio of 60:40, as confirmed by ^1H and ^{13}C NMR. This experiment confirmed the necessity for THF as a cosolvent for the reduction of the tosylhydrazone to take place. It was not evident what role the cosolvent was playing in the reduction of the tosylhydrazone, as, to the best of our knowledge, there have been no reports of THF necessary for the catecholborane reduction and subsequent ADR of tosylhydrazones. However, Brown and coworkers have reported a significant rate increase for the hydroboration of simple alkenes with 9-borabicyclo[3.3.1]nonane dimer (9-BBN)₂ in the presence of THF, as opposed to carbon tetrachloride.⁶⁶ The authors propose that the active hydroborating agent is the 9-BBN monomer. THF complexes with the dimer to form two $9\text{-BBN}\cdot\text{THF}$ complexes. These complexes in turn dissociate into the 9-BBN monomers more rapidly than (9-BBN)₂ dissociates into the corresponding monomers. We propose that a similar effect could be operative in our case with the catecholborane reduction of tosylhydrazones.

2.5 ADR on Bicyclo[5.3.0]decadienone Tosylhydrazone Model System 2.6

With the discovery that THF is necessary as a cosolvent for the successful catecholborane reduction and subsequent ADR of C1-C10 hydrogenated tosylhydrazone **2.36**, we sought to apply this finding to the ADR of bicyclo[5.3.0]decadienone tosylhydrazone **2.6**. Thus, **2.6** was dissolved in CHCl₃ and cooled to 0 °C (Table 2.5, Entry 1). Catecholborane (3 equiv, 1 M in THF) was added and the mixture reacted for 3 h. NaOAc·3H₂O (3 equiv) was added and the mixture heated to 70 °C for 1 h. Upon filtration and purification, we isolated a colorless oil in 49% yield. ¹H NMR of this residue revealed a mixture of two major products. The presence of an olefinic resonance at 5.35 (s) ppm, presumably corresponding to H^a of ADR product **2.3**, suggesting that one component was indeed the desired product. ¹³C NMR of the crude residue provided further evidence of the presence of two major products, each containing four *sp*² carbons and eight *sp*³ carbons. Given this NMR data, the two products were tentatively assigned as ADR product **2.3**, as well as the Wolff-Kishner-type (WK) reduction product **2.43**. Based upon the integral value of H^a of **2.3** relative to that of an allylic resonance corresponding to the four allylic protons H^b and H^c of **2.43** (see Figure 2.2 below), the ratio was determined to be 43:57 **2.3** to **2.43**. The formula used to calculate the abundance of each component is $2.3 = \frac{H^a}{(H^{b+c}/4) + H^a}$.

Table 2.5. Conditions for the ADR of bicyclo[5.3.0]decadienone tosylhydrazone **2.6.**

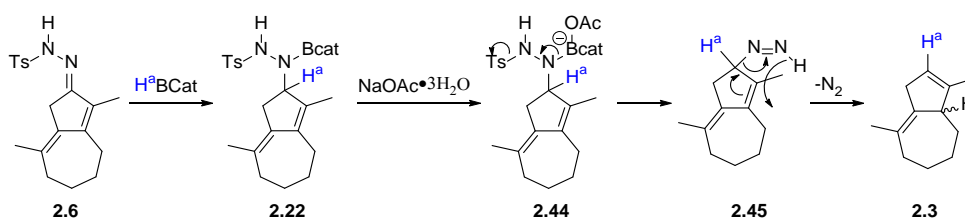


Entry	Reducing Agent (equiv)	Solvent	Additive (equiv)	Time (h)	Temp (°C)	Yield	Ratio (2.3:2.43)
1	HBcat (1 M in THF) (3)	CHCl ₃	-	3	0	49	43:57
2	HBcat (1 M in THF) (5)	THF	-	3	0	30	79:21
3	(BzO) ₂ BH (5)	CHCl ₃ / THF	-	3	0	38	4:96
4	NaBH ₄ (10)	AcOH	-	1	100	Trace 2.3	-
5	NaCNBH ₃ (3)	MeOH	AcOH (10)	1	70	Trace 2.3	-
6	NaCNBH ₃ (3)	AcOH	-	4	70	Trace 2.3	-

*Yield of crude reaction residue after passing through a silica plug

To this point, all of the successful ADRs had been performed in a solvent mixture of CHCl₃/THF. With the discovery that THF was necessary for the ADR to proceed on tosylhydrazone **2.6**, we reasoned that we could entirely remove the CHCl₃ from the reaction mixture. Thus, tosylhydrazone **2.6** was dissolved in THF and cooled to 0 °C (Table 2.5, entry 2). Catecholborane (3 equiv, 1 M in THF) was added and the mixture reacted for 3 h. NaOAc·3H₂O (3 equiv) was added and the mixture heated to 70 °C for 1 h. Upon filtration and purification, 30% of a colorless oil was isolated. Analysis of this residue by ¹H NMR revealed the same product mixture that we had previously observed; however, the product ratio was now 79:21 **2.3** to **2.43**. Thus, we were able to show that solvent not only affects the progress of the reaction, but it also plays a critical role in ratio of reaction products, though we did not have an explanation for this phenomenon at the time.

To the best of our knowledge, no reports of an allylic diazene intermediate, similar to **2.49** (Scheme 2.18), preferentially decomposing to the Wolff-Kishner product **2.47** rather than undergoing the retro-ene process under catecholborane reduction conditions exist; however, Djerassi and coworkers have reported similar outcomes in the presence of sodium cyanoborohydride.⁶⁴ Houk and coworkers have shown that the concerted retro-ene decomposition of cyclohexene diazene is exergonic by -51.2 kcal/mol.⁶⁷ With this information in hand, we reasoned that if allylic diazene intermediate **2.49** is being formed, it would most likely rapidly



Scheme 2.18. Mechanism of the ADR of tosylhydrazone 2.6.

decompose to the desired rearrangement product **2.3**. We thus shifted our focus to alternative reaction conditions to effect this transformation, as the data collected to this point strongly indicated that the product ratio is dependent on the reaction conditions. We next wanted to probe the effect of different hydride sources, beginning with bis(benzoyloxy)borane.

Thus, benzoic acid (10 equiv) was dissolved in THF and cooled to 0 °C. Borane (1 M in THF) was added and the mixture reacted for 1 h (Table 2.5, entry 4). Tosylhydrazone **2.6** was dissolved in a minimal amount of CHCl_3 was added and allowed to react for 3 h. After complete consumption of starting material was observed by TLC, $\text{NaOAc}\cdot 3\text{H}_2\text{O}$ (5 equiv) was added and the mixture heated to 70 °C and reacted for 1 h. Upon workup and purification via SiO_2 flash column chromatography, we isolated 30% of the product mixture, but were surprised to find a ratio

of 4:96 **2.3** to **2.43**. Due to the highly selective nature of these reaction conditions for the Wolff-Kishner product, we were able to unequivocally confirm that we were indeed generating this product by employing 2-D NMR techniques (Figure 2.2).

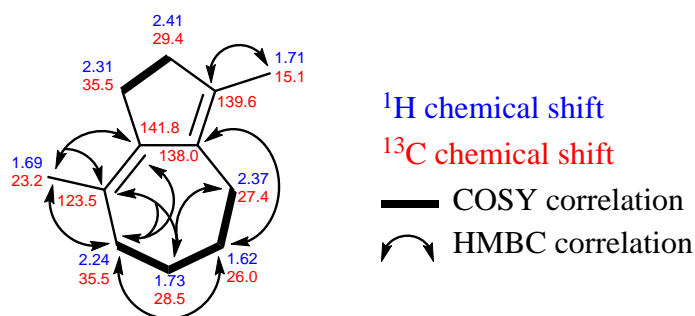
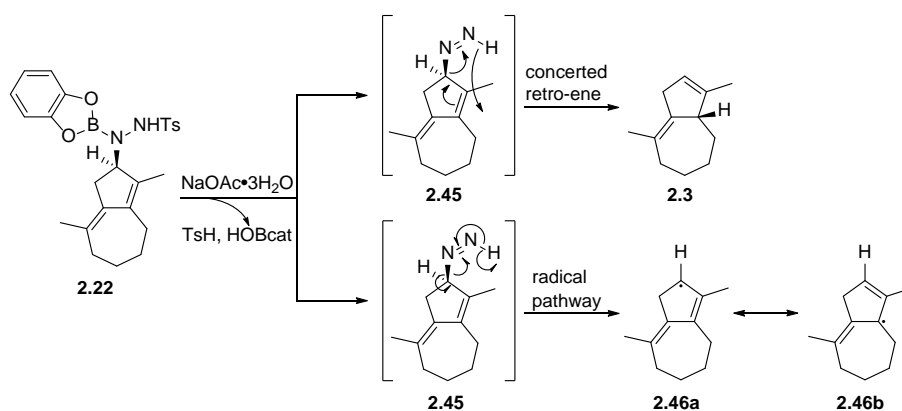


Figure 2.2. Structural confirmation of Wolff-Kishner reduction product 2.43.

We proposed that the Wolff-Kishner product could be generated via a radical decomposition pathway of diazene intermediate **2.45**, a process that is known to occur, but has yet to be reported for α,β -unsaturated hydrazones (Scheme 2.19).^{68,69} To test this hypothesis, we proposed two experiments. The first involved meticulously degassing, then the constant bubbling of argon through the reaction mixture as the reaction proceeded. We reasoned this would prevent any adventitious oxygen from entering the reaction system. Thus, a two-necked flask was equipped with a balloon of argon with a needle inserted through a septum, and a solid addition funnel preloaded with NaOAc \cdot 3H₂O. Benzoic acid (10.2 equiv) was added to the flask, followed by THF which had been degassed by the freeze-pump-thaw method (x 3), and cooled to 0 °C. At this point, a valve between the argon balloon and needle was opened and argon began bubbling through the reaction mixture. BH₃ (5.1 equiv, 1 M in THF) was added dropwise and the mixture reacted for 1 h. Tosylhydrazone **2.6** was dissolved in degassed CHCl₃ (freeze-pump-thaw x 3) and added to the



Scheme 2.19. Proposed divergent retro-ene and radical decomposition pathways of diazene intermediate **2.45**.

reaction mixture. After reacting for 3 h, $\text{NaOAc}\cdot 3\text{H}_2\text{O}$ (7 equiv) was added via the solid addition funnel, thus avoid the need to open the reaction system to oxygen. The mixture warmed to 70 °C and reacted for 2 h. An aliquot of the reaction mixture was taken and analyzed via ^1H NMR, which revealed a Wolff-Kishner product **2.43** to ADR product **2.3** in a 94:6 ratio and 38% yield. Interestingly, the reaction had not gone to completion, and after purification 8% of tosylhydrazone **2.6** was recovered.

Next, we proposed to run the reaction in the presence of a radical inhibitor, such as butylated hydroxytoluene (BHT). We reasoned that this would serve to eliminate any radical processes that were being initiated by any reagents or solvents. Thus, benzoic acid (1 M in THF, 20 equiv) was added dropwise to borane in THF (1 M, 10 equiv) and reacted at 0 °C for 1 h. Tosylhydrazone **2.6** along with BHT (2 equiv) were dissolved in THF and added dropwise to the reaction vessel. The reaction was maintained at 0 °C for 3 h, then $\text{NaOAc}\cdot 3\text{H}_2\text{O}$ (15 equiv) added. The vessel was lowered into an oil bath (70 °C) where it was maintained for 1 h. Upon aqueous workup with Na_2CO_3 , ^1H NMR of the crude residue revealed a 17:83 ADR **2.3**/WK **2.43** ratio; a slight improvement over the use of no radical inhibitor. While the results of these experiments provide

some evidence that a radical decomposition mechanism may not be operative, they cannot be used to definitively rule out this mechanism.

2.6 Conclusions for ADR Studies

The development of an efficient, high-yielding synthesis to an all-carbon model bicyclo[5.3.0]decadienone system with methyl groups at the C4 and C10 position was accomplished via application of the APKR. Initial ¹H NMR experiments revealed that the tosylhydrazone **2.6** was highly resistant to catecholborane reduction. The system was further simplified via hydrogenation of the C1-C10 double bond, and it was found that the presence of THF in the reaction mixture was necessary to effect catecholborane reduction of **2.36**. These conditions were applied to tosylhydrazone **2.6**, where it was discovered that a mixture of ADR product **2.3** and Wolff-Kishner product **2.43** was obtained. The ratio was mostly dependent on the nature of the borane reducing agent, suggesting two competing mechanisms. We were able to rule out a radical decomposition pathway via inclusion of BHT in the reaction mixture; however, the mechanism giving rise to the Wolff-Kishner product is still unclear. Due to the low yields and poor ADR selectivity, we shifted our focus to alternative strategies for the transposition of the C4-C5 double bond of systems similar to **2.2**.

2.7 Base-Induced Transposition of α -Hydroxy Enone

2.7.1 Introduction and background

We again turned to Reaxys to perform a comprehensive literature search for the most common motifs present in 6,12-guaianolides. We decided to search for compounds more similar to those generated via the APKR, possessing an oxygen at the C3 position and an explicit double bond at the C4-C5 position. Instead of a reductive transposition of the C3-C5 enone, we decided to examine a formal transposition of this motif to the C2-C4 position. The resulting Reaxys searches for these two regioisomers are presented in Table 2.6. In the case of the 6,12-guaianolides with an oxygen at the C3 position and an explicit double bond at the C4-C5 position, there were 674 total hits; 290 of which are biologically active, 59 have been isolated from a natural source, and 12 are both biologically active and naturally occurring. Transposition of the C3 oxygen to the C2 position and the C4-C5 double bond to the C3-C4 position returned 710 total hits. Of these, 216 are biologically active, 452 are naturally occurring, and 131 are both naturally occurring and biologically active. With these search results in hand, we reasoned that transposition of the C3-C5 enone to the C2-C4 position would greatly expand the synthetic utility of the APKR towards the rapid access of biologically active 6,12-guaianolides.

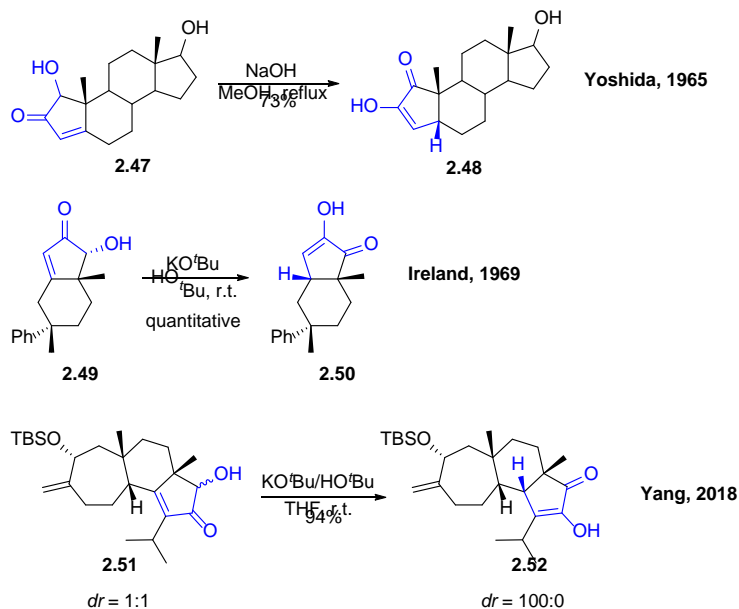
Table 2.6. Reaxys search for 6,12-gaianolide frameworks possessing discrete double bond at C4-C5 position and oxygen at C3 position, and discrete double bond at C3-C4 position and oxygen at C2 position.



Total hits	674	710
Pharmacological data	290	216
Natural source	59	452
Natural source + pharm. data	12	131

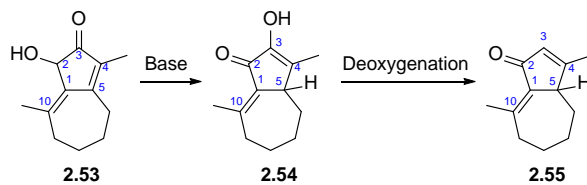
Data obtained via Reaxys search using structures shown (7/20/2020). Search parameters were limited to 'as substructure' variable 'on all atoms', 'stereo', and 'additional ring closures'. Filtered by 'pharmacological data available' and 'isolated from natural product + pharmacological data available'.

We next shifted our focus to strategies to effect such a transposition. To the best of our knowledge, such a direct transposition has yet to be reported in the literature; however, there have been three reports of a base-induced isomerization of α -hydroxy enones, affording α -keto enols. The exhaustive literature precedent for this transformation is presented in Scheme 2.20. The first report of this transformation was made by Yoshida and coworkers in 1965.⁷⁰ Ireland further explored this transformation in 1970, and most recently, Yang applied this transformation to his total synthesis of cyanthiwigin I.^{71,72} All three examples result in the *cis*-fused 5,6-ring systems single diastereomers. Ireland reports this to be the thermodynamically favored product; however, there has been no experimental evidence provided to definitively rule out the possibility that this process is under kinetic control.⁷¹ To complete their total synthesis of cyanthiwigin I, Yang and coworkers



Scheme 2.20. Previous precedent for base-induced isomerization of α -hydroxy enone motif.

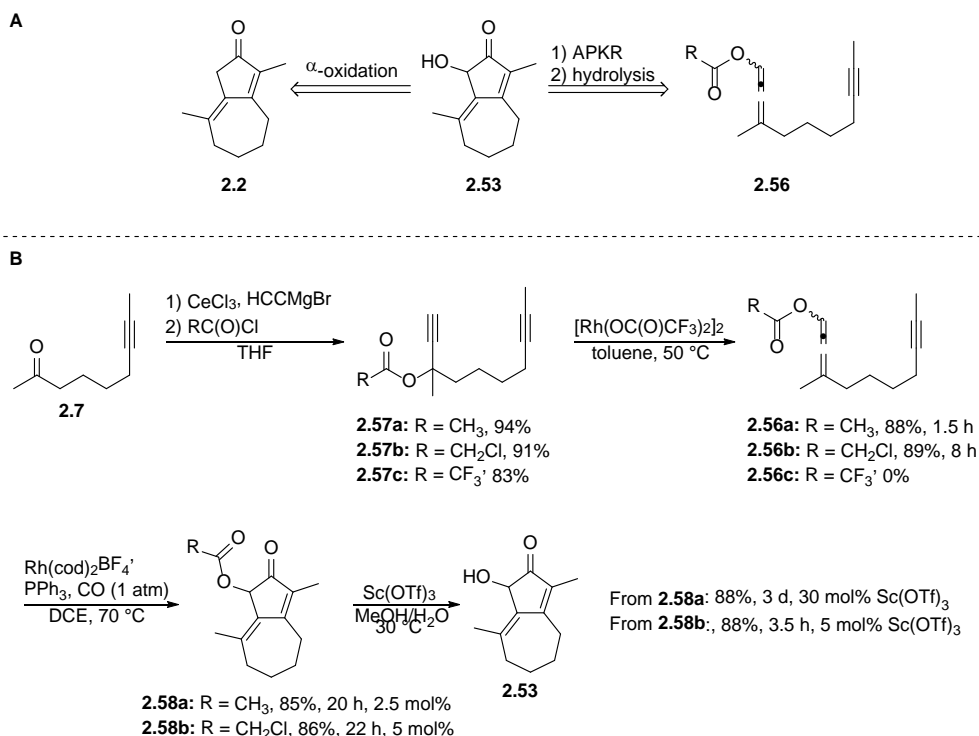
were able to deoxygenate enol **2.52** via triflation and Pd-catalyzed hydrogenolysis of the resulting vinyl triflate. We reasoned that we could apply this methodology to α -hydroxy enone **2.53** to generate α -keto enol **2.54**. From there, deoxygenation would afford the desired C3-C5 transposed product **2.55** (Scheme 2.21).



Scheme 2.21. Proposed conversion of α -hydroxy enone **2.53** to α -keto enol **2.54** and subsequent deoxygenation to enone **2.55**.

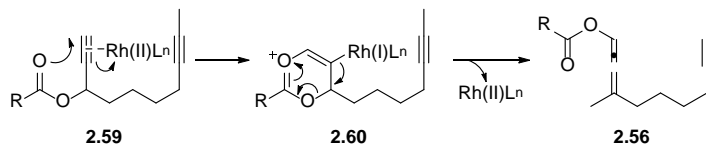
2.7.2 Synthesis of α -hydroxy enone 2.53

With a feasible method to access **2.55** in hand, we turned our attention to the synthesis of α -hydroxy enone **2.53**. Retrosynthetically, we reasoned that we could install a hydroxyl group at the C2 position in two ways; oxidation of bicyclo[5.3.0]decadienone **2.2**, or APKR of allenyl carboxyester **2.56**, followed by hydrolysis (Scheme 2.22A). We opted to pursue the APKR of allenyl carboxyester **2.56**, as there is more precedent within our group for the synthesis of allenyl carboxyesters and subsequent APKR than there is for α -hydroxylations of APKR adducts.⁷³ In addition, we could use alkynyl ketone **2.7** as the starting material to access the desired allenyl carboxyesters (see Section 2.2.1).



Scheme 2.22. A) Potential routes to hydroxy enone **2.53**. B) Synthesis of allenyl esters **2.56a-b** and Rh(I)-catalyzed APKR.

Thus, we proceeded with the synthesis of a series of allenyl carboxyesters, beginning with alkynyl ketone **2.7**. Cerium-mediated addition of ethynylmagnesium bromide, followed by addition of acetyl chloride afforded the desired propargyl acetate **2.57a** in 94% yield. Rh(II)-catalyzed formal 3,3-sigmatropic rearrangement of **2.57a** generated allenyl acetate **2.56a** in 88% yield. The Rh(I)-catalyzed allenic Pauson-Khand reaction was then employed to access bicyclo[5.3.0]decadienone **2.58a** in 85% yield. Scandium triflate mediated hydrolysis afforded the desired α -hydroxy ketone **2.53** in 88% yield; however, this reaction required high $\text{Sc}(\text{OTf})_3$ loadings, as well as long reaction times (3 d).⁷⁴ It was reasoned that substitution of the acetyl group at the C2 position with a more hydrolytically labile ester would increase the rate of hydrolysis.⁷⁵ To test this hypothesis, ketone **2.7** was converted to propargyl trifluoroacetate **2.57c** in 83% yield. The Rh(II)-catalyzed formal 3,3-sigmatropic rearrangement of **2.57c** to generate allenyl ester **2.56c** was not successful, most likely due to the highly electron-withdrawing nature of the trifluoromethyl group rendering the ester carbonyl oxygen non-nucleophilic towards the Rh(II)-alkyne complex **2.59** (Scheme 2.23).⁷⁶ With these results in hand, an ester with electronic properties between those of an acetyl and a trifluoroacetyl group was selected. Thus, ketone **2.7** was converted to propargyl chloroacetate **2.57b** in 91% yield. The Rh(II)-catalyzed formal 3,3-sigmatropic rearrangement of **2.57b** proceeded in good yield, affording allenyl chloroacetate **2.56b** in 89% yield, comparable to that of propargyl acetate **2.56a**. Rh(I)-catalyzed APKR of

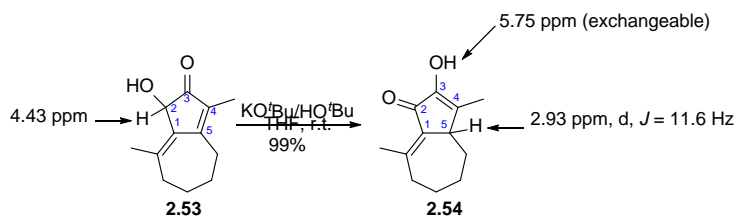


Scheme 2.23. Rh(II)-catalyzed formal 3,3-sigmatropic rearrangement of propargyl esters to allenyl carboxyesters **2.56**.

2.56b afforded bicyclo[5.3.0]decadienone **2.58b** in 86% yield. It should be noted that the APKR time for **2.56b** was also extended, requiring 5 mol% Rh(cod)₂BF₄ to achieve comparable reaction times relative to that of **2.56a**. With a more hydrolytically reactive ester installed at the C2 position, **2.58b** was subjected to the Sc(OTf)₃ mediated hydrolysis conditions. To our delight hydrolysis of **2.58b** proceeded very rapidly with respect to the hydrolysis of **2.58a**, achieving complete conversion to **2.53** in 1 h with 30 mol% Sc(OTf)₃ loading. With conditions for the rapid hydrolysis of **2.58b** in hand, we next sought to render the process catalytic in Sc(OTf)₃. We found that we were able to decrease the Sc(OTf)₃ loading to as low as 5 mol%, and still achieve complete hydrolysis in 3.5 h.

2.7.3 Base-induced isomerization of α -hydroxy enone **2.53**

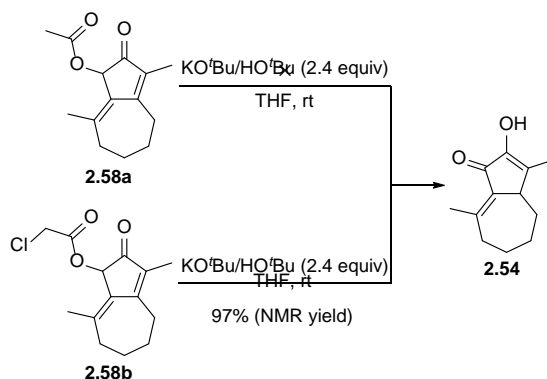
With α -hydroxy enone **2.53** in hand, efforts began to test the feasibility of the proposed isomerization of the C2-C5 α -hydroxy enone motif to the α -keto enol motif present in **2.54** (Scheme 2.24). Reaction of **2.53** with potassium *tert*-butoxide (KO^tBu) in THF at room temperature afforded α -keto enol **2.54** in 99% yield after 5 min. To confirm the structure of **2.54**, one- and two-dimensional NMR techniques were employed. Disappearance of the C2 proton of **2.53** at 4.43 ppm confirmed that the starting material was fully consumed. Appearance of a



Scheme 2.24. Base induced isomerization of α -hydroxy enone **2.53 to α -keto enol **2.54** and ¹H NMR structural confirmation.**

resonance at 2.93 (d, 11.6 Hz, 1H) ppm provided evidence of the bis-allylic C5 proton of **2.54**; the chemical shift, splitting pattern, and coupling constant of which is in accordance with similar structures.⁷⁷ A deuterium exchange experiment confirmed the proton at 5.75 ppm in product **2.54** was exchangeable, lending support for the presence of a hydroxyl group in the compound. In addition to the NMR data, mass spectrometry confirmed the predicted mass of **2.54**. This evidence was used to unambiguously confirm the successful conversion of **2.53** to **2.54**.

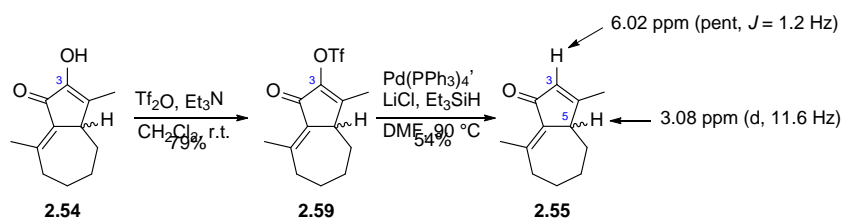
With the initial success of the isomerization of **2.53** to **2.54**, we next wanted to test the feasibility of performing a two-step one-pot deprotection/isomerization of carboxyesters **2.58a** and **2.58b** to α -keto enol **2.54**, thus eliminating the need for the independent Sc(OTf)₃-catalyzed hydrolysis. Thus acetate **2.58a** was dissolved in THF and KO^tBu (2.4 equiv of a 0.5 M solution in HO^tBu) added (Scheme 2.25). Complete disappearance of starting material was observed by TLC after 10 min; however, upon working with sat. aq. NH₄Cl, only starting material **2.58a** was recovered. We reasoned that the disappearance of the starting material was most likely due to enolization of the α -acetoxy enone, which was converted back to the starting material after workup.



Scheme 2.25. Two-step, one-pot deprotection/isomerization of α -acyloxy enones **2.58a** and **2.58b**.

We next subjected the more reactive chloroacetate **2.58b** to the same reaction conditions, and to our delight observed complete conversion to α -keto enol **2.54** in 15 min. While this reaction was only performed on an exploratory scale, we observed spot to spot conversion on TLC, and the ^1H NMR of the crude residue was very clean with only trace amounts of *tert*-butanol. We were able to integrate the *tert*-butanol relative to **2.54** to determine that **2.54** was formed in approximately 97% yield, though we did not purify this material. With these results in hand, we were able to show that a high-yielding, two-step, one-pot deprotection/isomerization process is indeed possible with **2.64b**. We next shifted our focus to the deoxygenation of **2.54** at the C3 position.

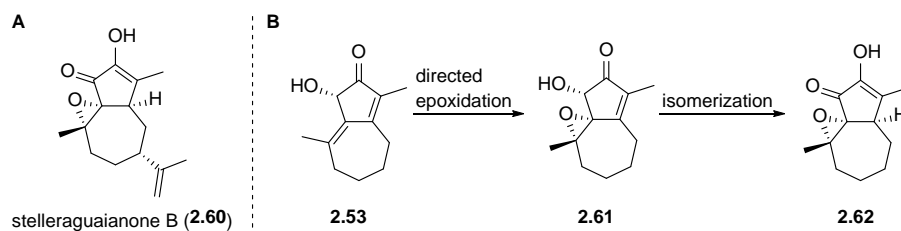
To this end, of α -keto enol **2.54** was reacted with triflic anhydride (1.2 equiv) in the presence of triethylamine (1.3 equiv) in CH_2Cl_2 . The reaction was complete in 30 min, and vinyl triflate **2.59** was isolated in 79% yield (Scheme 2.26). Triflate **2.59** was then reacted with tetrakis(triphenylphosphine)palladium(0) (0.5 equiv), lithium chloride (8.75 equiv), and triethylsilane (20 equiv) in degassed DMF. After 1 h, the reaction had gone to completion and enone **2.55** was isolated in 54% yield. Diagnostic ^1H NMR resonances were observed at 6.02 ppm (pent, $J = 1.2$ Hz, 1H) corresponding the C3 alkenyl proton, and 3.08 ppm (d, $J = 11.6$ Hz) corresponding to the bis-allylic C5 proton. In addition, a ^{13}C resonance at 197 ppm confirmed the presence of a carbonyl group, and resonances at 172, 151, 137, and 133 ppm confirmed the presence of four olefinic carbons. While we were able to show that C3 deoxygenation of **2.54** is possible, we did not optimize the reaction conditions in an effort to achieve a higher yield with lower tetrakis(triphenylphosphine)palladium(0) or triethylsilane loading.



Scheme 2.26. Two-step one-pot deprotection/isomerization of chloroacetate **2.58b and C3 deoxygenation of α -keto enol **2.54**.**

With conditions for the rapid isomerization of both **2.53** and **2.58b** to **2.54**, and subsequent C3 deoxygenation in hand, we wanted to further probe the scope and functional group compatibility of this reaction. We decided to first apply these conditions to a substrate with a more reactive functional group at the C1-C10 position.

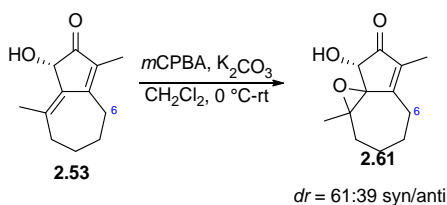
Hao and coworkers have reported the isolation of the naturally occurring guaiane stelleraguaianone B (**2.60**); which has been shown to be cytotoxic against the A549 cell line with an IC_{50} of 8.52 μ M (Scheme 2.27A).⁷⁸ We thus sought to leverage the C2 hydroxyl group of **2.53** to effect a stereocontrolled, directed epoxidation at the C1-C10 position (Scheme 2.27B). If successful, the base-mediated isomerization of the resulting epoxide **2.61** would grant rapid access the α -keto enol **2.62**, a stelleraguaianone B analog. Literature precedent offers several methodologies in which a hydroxyl-directed epoxidation of an alkene can be performed.^{79,80} The most common method for cyclic allylic alcohols is the use of *tert*-butyl hydroperoxide (TBHP) in



Scheme 2.27. A) Biologically active guaiane stelleraguaianone B (2.60**). B) Proposed route to stelleraguaianone B analog **2.62**.**

the presence of catalytic vanadyl acetylacetonate (VO(acac)₂); however, in some cases meta-chloroperoxybenzoic acid (*m*CPBA) has been shown to effect hydroxyl-directed epoxidation of cyclic allylic alcohols.⁸¹ Because of the operational simplicity of *m*CPBA epoxidation, we chose first apply this methodology.

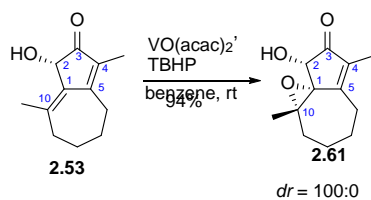
α -Hydroxy ketone **2.53** was dissolved in CH₂Cl₂ and cooled to 0 °C (Scheme 2.28). To this solution was added K₂CO₃ (3 equiv) followed by *m*-chloroperoxybenzoic acid (*m*CPBA) (1.5 equiv). After reacting for 3 h TLC indicated complete consumption of starting material, and a solution of saturated aq. Na₂S₂O₃ was added. ¹H NMR of the crude reaction mixture revealed a relatively clean reaction profile; however, poor diastereoselectivity was achieved under these conditions. Two sets of resonances, one at 2.91 ppm corresponding to one of the C6 diastereotopic allylic protons of the *syn*-epoxidation product, and one at 2.81 ppm corresponding to the same proton of the *anti*-epoxidation product were observed. With these encouraging results in hand, we moved to apply different epoxidation conditions in an effort to increase diastereoselectivity.



Scheme 2.28. *m*CPBA epoxidation of α -hydroxy ketone **2.53**.

Tert-butyl hydroperoxide (TBHP) in the presence of VO(acac)₂ has been commonly applied to the directed epoxidation of cyclic allylic alcohols.⁸² Having observed a mixture of diastereomers with the application of *m*CPBA, we turned to VO(acac)₂ to effect the directed epoxidation. To a solution of **2.53** and VO(acac)₂ (1 mol%) in benzene was added *tert*-butyl

hydroperoxide at room temperature (Scheme 2.29). This was allowed to react for 30 min, at which point it was complete, as evidenced by TLC. The reaction was quenched with sat. aq. Na₂S₂O₃ affording epoxide **2.61** in high yield without the need for further purification; however, in one experiment, an uncharacterized byproduct was formed upon addition of Na₂S₂O₃. It is unclear how this byproduct was generated; however, Na₂S₂O₃ has been shown to act as a nucleophile under



Scheme 2.29. Diastereoselective epoxidation of C1-C10 double bond of 2.53.

certain conditions.⁸³ Addition of Na₂S₂O₃ was circumvented by concentration of the reaction mixture without workup, followed by purification via SiO₂ column chromatography, again affording **2.61** in 94% yield.

In addition to generating **2.69** in high yield, only a single diastereomer was formed as evidenced by ¹H and ¹³C NMR. Diagnostic ¹H NMR resonances appear at 3.88 ppm (d, *J* = 3.6 Hz) corresponding to the proton on C2, 1.48 ppm (s) corresponding to the protons on the C4 methyl group, and 1.82 (d, *J* = 0.8 Hz) ppm corresponding to the protons on the C10 methyl group. In addition, ¹³C NMR resonances at 204 ppm corresponding to the C3 carbonyl carbon, 168 ppm and 141 ppm, corresponding to the C5 and C4 alkenyl carbons, respectively, and 71 ppm, 68.3 ppm, and 67.9 ppm, corresponding to the C1, C2, C10 carbons, confirmed the presence of only one diastereomer. The downfield ¹³C resonance at 168 ppm confirmed that the C4-C5 double bond had not undergone epoxidation. Based on literature precedent for the *syn*-selective epoxidation of

allylic alcohols under these conditions, we propose that the relative stereochemistry of **2.61** is *syn*.⁸² With a single diastereomer of **2.61** in hand, we could now test the isomerization conditions that were successful for the conversion of **2.53** to **2.54** on a substrate with a C1-C10 epoxide to probe the functional group tolerance of this reaction.

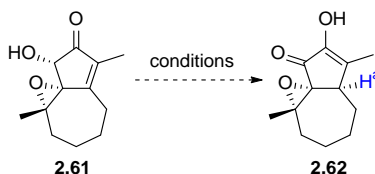
Epoxide **2.61** was dissolved in THF. To this was added a solution of KO^tBu in ^tBuOH (2 equiv, 0.5 M). The mixture was stirred for 10 min at room temp during which period it turned dark yellow. Under these strongly basic conditions, only decomposition of **2.61** and no desired isomerization product **2.62** was detected via either TLC, which showed only baseline material, or ¹H NMR of the crude reaction mixture, which showed predominately aliphatic resonances, and nothing in the region of 3 ppm, which is where we expect H^a to be (Table 2.8, entry 1).

With preliminary results in hand, we decided to alter the reaction conditions in an effort to mitigate decomposition and generate isomerization product **2.62**. The first variable we chose to alter was the solvent, as this type of isomerization has been performed in both THF as well as ^tBuOH.^{71,72} Thus, **2.61** was dissolved in ^tBuOH and KO^tBu in ^tBuOH (2 equiv, 0.5 M) was added. The rate of consumption of **2.61** was markedly slower when performed in ^tBuOH as opposed to THF, however only decomposition was observed, as evidenced by TLC and ¹H NMR of the crude reaction mixture (Table 2.8, entry 2). Based upon the rapid rate of decomposition, we decided to run the reaction at a depressed temperature. Epoxide **2.61** was dissolved in THF and cooled to -78 °C. A solution of KO^tBu in ^tBuOH (2 equiv, 0.5 M) was added. The mixture was slowly warmed and **2.61** did not start being consumed to any appreciable extent until the temperature reached about -10 °C. Again, only decomposition of **2.61** was observed (Table 2.8, entry 3).

It became evident that the epoxide at the C1-C10 position was incompatible with the strongly basic conditions required to effect the isomerization. These results suggested that the

base-mediated isomerization conditions were incompatible with a reactive functional group at the C1-C10 position.

Table 2.7. Conditions for the attempted base-induced isomerization of epoxide 2.61.



Entry	Solvent	Temp (°C)	Time (min)	Result
1	THF	rt	10	decomposition
2	^t BuOH	rt	30	decomposition
3	THF	-78 - rt	60	decomposition

2.8 Conclusions for the Base-Induced Enone Isomerization

A rapid, high-yielding route to multiple allenyl carboxyesters was developed. It was found that the Sc(OTf)₃-catalyzed hydrolysis to reveal the 2-hydroxy bicyclo[5.3.0]decadienone **2.53** could be accelerated via replacement of the acetoxy group with a chloroacetoxy group. In addition, catalyst loading was reduced from 30 mol% to 5 mol%. The potassium *tert*-butoxide-mediated isomerization of 2-hydroxy bicyclo[5.3.0]decadienone **2.53** was a rapid, facile process affording the α -keto enol **2.54** in quantitative yields. It was found that a two-step, one-pot protocol could be applied for the hydrolysis/isomerization of the 2-chloroacetoxy bicyclo[5.3.0]decadienone **2.58b**, affording **2.54** in cleanly and in high yields. α -Keto enol **2.54** was successfully deoxygenated to afford enone **2.55**; validating this base-mediated isomerization process as a valid strategy to access the C2-C4 enone motif observed in many 6,12-guaianolide frameworks. When these base-

mediated isomerization conditions were applied to a substrate bearing an epoxide at the C1-C10 position, complete decomposition of the starting material was observed. This suggests that this method is not applicable to substrates with leaving groups at the allylic C1-C10 position. With these successful results in hand, we shifted our focus to the application of this methodology to a more complex system. We felt that it would be of interest to the synthetic community to take on a total synthesis project where we could showcase the base-mediated isomerization of a lactone-containing allenic Pauson-Khand adduct towards the synthesis of a biologically active 6,12-guaianolide.

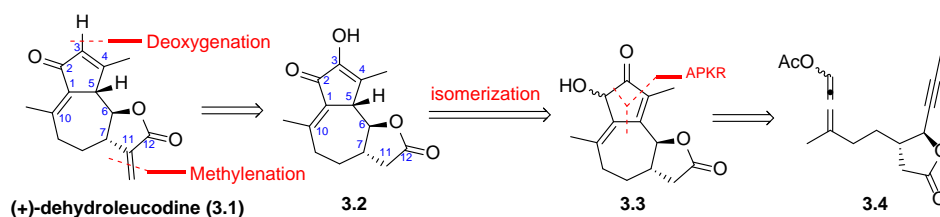
3.0 Studies Towards the First Total Synthesis of (-)-Dehydroleucodine

3.1 Introduction

With a method to further functionalize the α -hydroxy ketones afforded by the APKR, we sought to apply this methodology to the total synthesis of a naturally occurring 6,12-guaianolide. Few reports of the use of the APKR to generate the core 5,7-ring system of guaianolides exist.⁸⁴⁻⁸⁷ We sought to leverage what we had learned about the functionalization of the APKR adduct to further expand the utility of the APKR, thus showcasing its application for the rapid synthesis of 6,12-guaianolides.

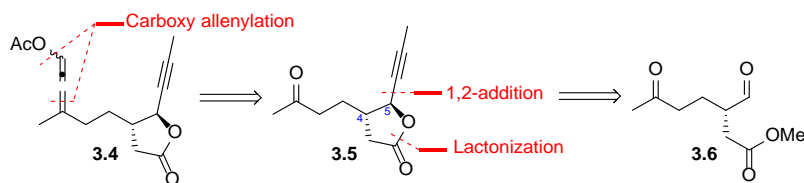
(+)-Dehydroleucodine (**3.1**) is a 6,12-guaianolide first isolated from *Lidbeckia pectinata* in 1972 by Bohlmann and Zdero (Scheme 3.1).⁸⁸ It has been shown to be cytotoxic towards the human astrocytoma D384 cell line, eight different acute myeloid leukemia cell lines, and human glioblastoma cells.⁸⁹⁻⁹¹ It is believed that (+)-dehydroleucodine (**3.1**) induces phosphorylation of tumor protein TP73, inducing apoptosis.⁸⁹ In addition, (+)-dehydroleucodine (**3.1**) has been shown to inhibit adipogenesis; making it a compound of interest for the potential treatment of obesity.⁹² With an enone at the C2-C4 position and a double bond at the C1-C10 position, we reasoned that this biologically active 6,12-guaianolide would be an ideal candidate for a total synthesis study. It would give us the opportunity to develop the first enantioselective synthetic route to the 6,12-guaianolide framework within our group, as well as test the feasibility of applying the previously reported base-mediated enone isomerization to a system with a potentially reactive functionality at the C6 position.

Our desire was to develop a synthetic route to access both enantiomers of dehydroleucodine (**3.1**) in a selective manner. Our first retrosynthetic disconnections were methylenation at the C11 position of the lactone of **3.2**, and deoxygenation at the C3 position of **3.2** (Scheme 3.1). Though previous group members have shown that the C11 methylene unit could be installed during the lactonization step via tandem allylboration/lactonization to afford a mixture of the *trans*- and *cis*-lactones, the methodology has yet to be rendered enantioselective, and with the strongly electrophilic nature of the exocyclic α,β -unsaturated lactone, we were concerned that it would be incompatible with the conditions applied for the isomerization of **3.3** and deoxygenation of **3.2**. We reasoned that **3.2** could be accessed via isomerization of α -hydroxy ketone **3.3**, which could in turn be accessed via APKR of allenyl carboxyester **3.4**, followed by deacetylation of the corresponding ester. With a direct route from allenyl carboxyester **3.4** to (+)-dehydroleucodine (**3.1**) in hand, we set out to devise a route to **3.4** in an enantio- and diastereoselective fashion.



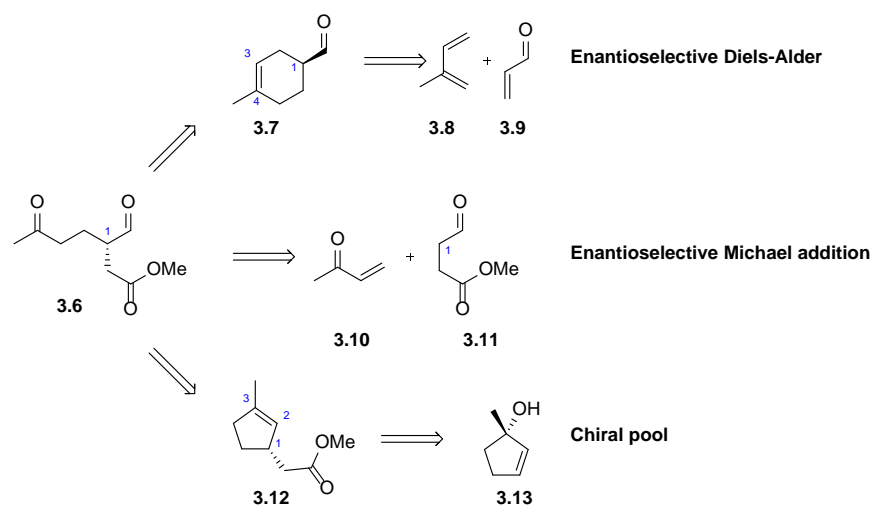
Scheme 3.1. Retrosynthetic analysis of (+)-dehydroleucodine (3.1**), employing an APKR as the key ring forming step, followed by isomerization.**

Installation of the allenyl carboxyester of **3.4**, we reasoned, could be performed via 1,2-addition of an ethynyl unit to ketone **3.5**, followed by acetylation of the resulting propargyl alcohol, then Lewis acid-mediated formal 3,3-sigmatropic rearrangement of the corresponding propargyl carboxyester, as our group has previously shown (Scheme 3.2).⁹³ Ketone **3.5** could in turn be



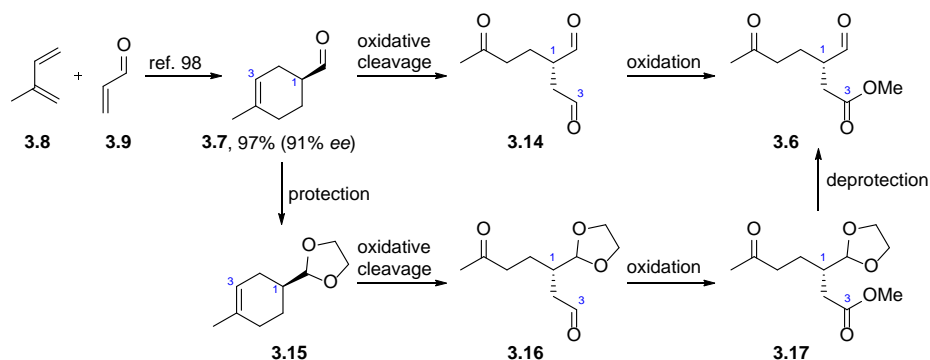
Scheme 3.2. Proposed access to allenyl carboxyester **4 from β -formyl ester **3.6**.**

generated via 1,2-addition of a propynyl unit to β -formyl ester **3.6**, followed by lactonization of resulting propargyl alcohol. This key step must be performed in a diastereoselective manner to afford the *trans*-lactone. Reissig has reported the diastereoselective addition of Grignard reagents and organocuprates to β -formyl esters, affording the *trans*-lactones in good to excellent diastereomeric ratios.⁹⁴ Another criterion for this key step is the chemoselectivity of the 1,2-addition. We would expect that 1,2-addition could occur carbonyl carbon of the ketone, ester, or aldehyde. While we would expect the ester to be substantially less electrophilic than either the ketone or the aldehyde, we needed a reagent that selectively adds to aldehydes in the presence of ketones in a 1,2-fashion. Reetz has shown that both organolithium and Grignard reagents, when transmetalated with TiCl_4 , add to aldehydes in the presence of ketones with complete chemoselectivity.⁹⁵ Later, Reissig showed that they were able to achieve diastereoselective addition of organotitanium reagents to β -formyl esters, affording *trans*-lactones.⁹⁶ We reasoned that we could use an organotitanium nucleophile to achieve both chemo- and diastereoselective 1,2-addition to the aldehyde, affording *trans*-lactone **3.5**, while leaving the ketone intact. Using this chemoselective methodology would also circumvent the need mask the ketone with a protecting group. With a feasible route allenyl carboxyester **3.4** in hand, we shifted our analysis to synthesis of β -formyl ester **3.6** in an enantioselective fashion.



Scheme 3.3. Potential retrosynthetic approaches for the enantioselective construction of β -formyl ester **3.6.**

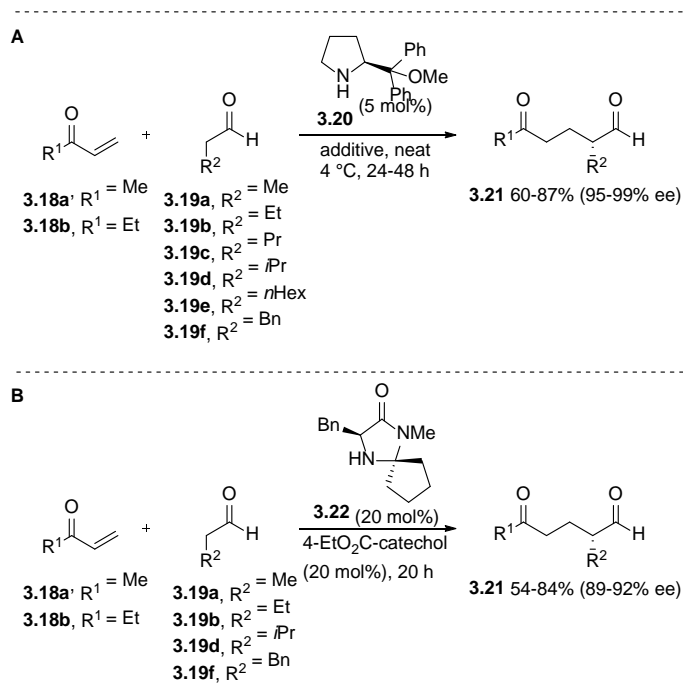
Retrosynthetically, we devised three feasible routes to β -formyl ester **3.6** in an enantioselective fashion (Scheme 3.3). The first proposed route involved the oxidative cleavage of cyclohexene **3.7**. Nino and Maiuolo have reported the use of a chiral imidazolidinone catalyst supported on an ionic liquid in water as an efficient way to access **3.7** via the enantioselective Diels-Alder reaction of isoprene (**3.8**) and acrolein (**3.9**) in 97% yield and 91% ee (Scheme 3.4).⁹⁷ Oxidative cleavage of **3.7** would afford aldehyde **3.14**, which would then need to be selectively oxidized to generate β -formyl ester **3.6**. To ensure regioselective oxidation at the C3 position,



Scheme 3.4. Proposed Diels-Alder approach to β -formyl ester **3.6.**

Diels-Alder adduct **3.7** would most likely need to be protected as acetal **3.15**, followed by oxidative cleavage, oxidation, then deprotection. Benefits of this route include the low cost, commercial availability of the starting materials, and either enantiomer of **3.6** could theoretically be accessed. The acetal protection/deprotection step, however, not only impacts step and atom economy, but the mildly acidic conditions required for the acetal protection and deprotection could cause epimerization of the C1 stereocenter. While feasible, alternative routes to β -formyl ester **3.6** that would not require a protection/deprotection sequence were examined.

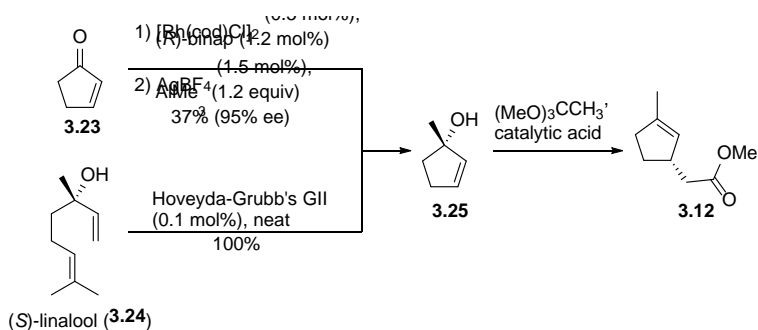
The second route to β -formyl ester **3.6** that was considered was the enantioselective 1,4-addition of aldehyde **3.11** to methyl vinyl ketone **3.10** (Scheme 3.3). Gellman and coworkers have reported the use of diphenylprolinol methyl ether **3.20** and chiral imidazolidinone **3.22** as effective organocatalysts for the enantioselective 1,4-conjugate additions of simple aldehydes to enones



Scheme 3.5. A) Diphenylprolinol methyl ester-catalyzed 1,4-conjugate additions of aldehydes to enones. B) Imidazolidinone-catalyzed 1,4-conjugate addition of aldehydes to enones.

(Scheme 3.5).^{98,99} This methodology benefits from low catalyst loadings, cheap and commercially available starting materials, good yields, and high enantiomeric excesses. While this method offers the most direct route to β -formyl ester **3.6**, the reported substrate scope is fairly limited, with no reports of this methodology being applied to aldehydes or enones that possess additional heteroatoms. While not disqualifying, we nonetheless chose to examine the feasibility of the third proposed route; oxidative cleavage of γ,δ -unsaturated ester **3.12** (Scheme 3.3).

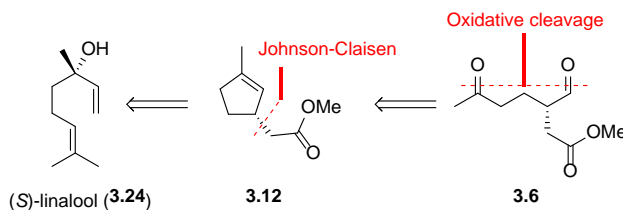
While not as step-economical as the direct enantioselective conjugate addition of aldehyde **3.11** to methyl vinyl ketone **3.10**, the oxidative cleavage of γ,δ -unsaturated ester **3.12** offered an alternative way to set the stereochemistry at the C1 position. Both the enantioselective Diels-Alder reaction and the enantioselective 1,4-addition rely on a chiral catalyst to set the stereochemistry of the aldehyde at the C1 position. In the case of γ,δ -unsaturated ester **3.12**, we propose the stereochemistry can be set in a previous step, then retained in a 3,3-sigmatropic rearrangement; in this case a Johnson-Claisen rearrangement of allylic alcohol **3.25** to install the desired methyl ester (Scheme 3.6). Unlike the enantioselective 1,4-addition of aldehyde **3.11** to methyl vinyl ketone **10**, there is literature precedent for the preparation of allylic alcohol **3.25** in an enantioselective fashion. Zezschwitz and coworkers have reported a Rh(I)-catalyzed enantioselective 1,2-addition



Scheme 3.6. Proposed route to γ,δ -unsaturated ester **3.12** via chiral cyclopentenol **3.25**.

of AlMe_3 to cyclic enones to afford the corresponding allylic alcohols (Scheme 3.6).¹⁰⁰ While yields were typically good for 6- and 7-membered rings (72-90%), the yields for the analogous 5-membered rings were relatively low (37-58%); however, the enantiomeric excess for all examples was very high (95-99% ee).

An alternative route to access allylic alcohol **3.25** is the ring-closing metathesis of (*S*)-linalool (**3.24**). Harvey and coworkers have shown the quantitative, solvent-free conversion of (\pm)-linalool to (\pm)-**3.25** in the presence of 0.1 mol% Hoveyda-Grubb's 2nd generation catalyst (H-GII).¹⁰¹ Though Harvey did not report the results of the reaction performed on an enantioenriched substrate, Minnaard and coworkers have performed ring-closing metatheses on similar substrates using H-GII to generate enantioenriched **3.25**, and reported complete retention of stereochemistry under the reaction conditions.¹⁰² We thus predict that the stereochemistry of (*S*)-linalool (**3.24**) should be retained during the metathesis. Due to the high yield, stereoretention of the starting material, low catalyst loading, and solvent-free reaction conditions, we opted to pursue ring-closing metathesis of (*S*)-linalool (**3.24**) followed by Johnson-Claisen rearrangement to afford γ,δ -unsaturated ester **3.12**, then oxidative cleavage to afford β -formyl ester **3.6** (Scheme 3.7).



Scheme 3.7. Retrosynthetic analysis of β -formyl ester **3.6.**

With a feasible route to (+)-dehydroleucodine (**3.1**) in hand, we set out to begin our studies towards its total synthesis. To our surprise, (*S*)-linalool (**3.24**) was not commercially available;

however, (*R*)-linalool (**3.34**) (90% ee) is commercially available at a cost of \$0.11 per gram. While it is recognized that only the (*R*)- enantiomer of linalool is cheap and commercially available, the (*S*)- enantiomer has been accessed via Sharpless asymmetric epoxidation of geraniol (**3.26**), followed by mesylation of the terminal hydroxyl group (Scheme 3.8).^{103,104} Reductive elimination of epoxy mesylate **3.28** with lithium naphthalenide affords (*S*)-linalool (**2.24**) in good yield, with retention of stereochemistry.¹⁰⁵ Though this short synthetic route to (*S*)-linalool (**2.24**) has been reported, we reasoned that it would be of interest to develop a synthetic route to the unnatural (–)-dehydroleucodine, as there is little available information on the biological activity of the unnatural enantiomers of guaianolides. Thus, we commenced our synthetic studies towards (–)-dehydroleucodine, starting with (*R*)-linalool (**3.34**).

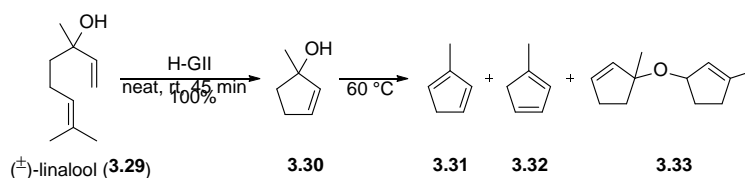


Scheme 3.8. Reported synthetic route to (*S*)-linalool (**3.24**).

3.2 Ring Closing Metathesis and Claisen Rearrangement of (*R*)-linalool

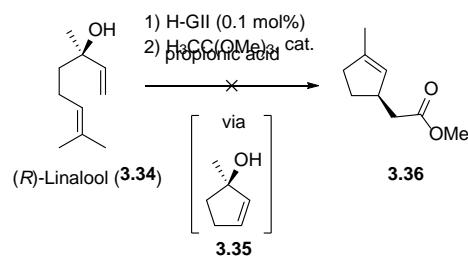
As mentioned above, Harvey and coworkers were able to convert (\pm)-linalool (**3.29**) to the corresponding allylic cyclopentenol **3.30** via H-GII under solvent-free conditions at ambient temperature (Scheme 3.9). They then purified the product via vacuum distillation at room temperature, confirming the highly volatile nature of cyclopentenol **3.30**. The authors also report the dehydration of cyclopentenol **3.30** to a mixture of cyclopentadienes **3.31** and **3.32**, ether **3.33**, as well as cyclopentadiene dimers, at elevated

temperatures, in the presence of H-GII. The authors noted that oxidation of the H-GII catalyst by bubbling air through the reaction mixture mitigated the dehydration pathway completely. We proposed moving forward by leveraging Harvey's conditions to effect the ring-closing metathesis, then rendering the catalyst inactive via oxidation. Application of the Johnson-Claisen rearrangement conditions would afford the desired γ,δ -unsaturated methyl ester **3.36** directly in a two-step-one-pot process.



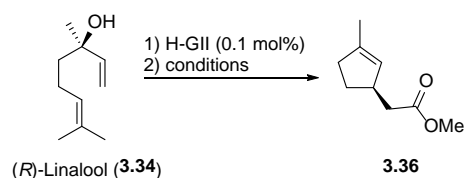
Scheme 3.9. Reported RCM of (±)-linalool (**3.29**), and dehydration of cyclopentenol **3.30** in the presence of H-GII at elevated temperature.

Thus, Hoveyda-Grubb's 2nd generation catalyst (H-GII, 0.001 equiv) was added to a flask equipped with a nitrogen inlet adapter and a second outlet adapter attached to an oil bubbler. To the flask was added neat (*R*)-linalool (**3.34**) at room temperature (Scheme 3.10). After approximately 10 min, the green solution began violently bubbling due to the release of isobutylene gas. The bubbling diminished over the course of 1 h, at which point complete consumption of starting material was observed by TLC. A needle attached to an airline was inserted into the reaction vessel, and air bubbled through the solution for 45 min. During this time the color of the solution changed from green to dark brown, indicating oxidation of the H-GII catalyst, as reported by Harvey. A small aliquot of the reaction mixture was taken at this point, and ¹H NMR was employed to confirm that (*R*)-linalool (**3.34**) had been fully converted to cyclopentenol **3.35**. The needle attached to the airline was removed and trimethyl orthoacetate (3



Scheme 3.10. Attempted two-step-one-pot RCM/Johnson-Claisen rearrangement of (R)-linalool (**3.34**).

equiv) was added followed by propionic acid (0.1 equiv). The solution was lowered into a preheated oil bath set to 130 °C and cyclopentenol **3.35** was fully consumed within 30 min. ¹H NMR of the crude reaction mixture revealed complete dehydration of cyclopentenol **3.35**, affording a mixture of methyl cyclopentadiene isomers and dimers, as evidenced by multiple olefinic resonances in the 6-5 ppm region (Table 3.1 entry 1). We reasoned that the acidic conditions required for the Johnson-Claisen rearrangement were causing dehydration of cyclopentenol **3.35**. Because of this, we decided to try the Johnson-Claisen with no acid catalyst. The RCM procedure was repeated, as reported above, and trimethyl orthoacetate (3 equiv) added to the crude reaction mixture. The mixture was heated to 140 °C for 2 h, during which time no consumption of cyclopentenol **3.35** was observed by TLC (Table 3.1 entry 2). Thus, the mixture was transferred to a microwave vial and heated to 140 °C for 30 min in a microwave reactor, as described by others.¹⁰⁶ However, no reaction was observed. It was clear that we would need an acid catalyst, but due to the lability of the tertiary hydroxyl group of cyclopentenol **3.35**, we reasoned that we would have to use a weak acid. We turned to the literature to seek conditions for which a Johnson-Claisen rearrangement was performed on an acid-sensitive, tertiary allylic cyclic alcohol.

Table 3.1. Conditions to effect RCM and Johnson-Claisen rearrangement fo (*R*)-linalool (3.34).

Entry	Additive (equiv)	Temp (°C)	Result
1	Propionic acid	140 °C	Dehydration
2	None	140 °C	No reaction
3	Hünig's base, 4Å mol. sieves	180 °C	No reaction
4	Hydroquinone	160 °C	No desired product

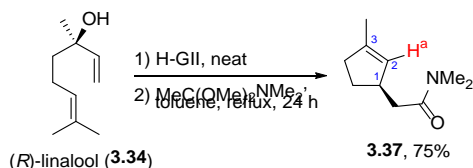
Brimble and Zhu have both used phenol to catalyze a Johnson-Claisen rearrangement in the synthetic studies towards oleocanthal, and total synthesis of (+)-peganumine A, respectively.^{107,108} Iwata and Bach reported the use of hydroquinone as a suitable, weak Brønsted acid for the Johnson-Claisen rearrangement used in their total syntheses of (±)-descarboxyquadrone and meloscine, respectively.^{109,110} In addition to the use of phenol and phenol derivatives, Tokuyama and coworkers reported the use of 4 Å molecular sieves in Hünig's base as a basic set of conditions to effect the Johnson-Claisen in their total synthesis of (-)-isoschizogamine.¹¹¹ With multiple sets of conditions in hand, we set out to apply a some of these catalysts to our system. The pK_a of phenol is 9.98 while the pK_a of hydroquinone is 9.96.¹¹² Due to the marginal pK_a difference between the two acids, we reasoned that if the reaction failed in the presence of hydroquinone it would be unlikely to succeed in the presence of phenol. Thus, we chose to screen only hydroquinone as a potential phenolic acid catalyst. H-GII (0.001 equiv) was added to (*R*)-linalool (**3.34**) and the mixture reacted at room temperature for 1 h. Upon complete consumption of starting material, as evidenced by TLC, air was bubbled through the reaction mixture for 1 h. Trimethyl orthoacetate (12 equiv) and benzoquinone (white crystals, 1 equiv) were

added and the mixture placed in a microwave reactor at 130 °C for 1 h. No reaction occurred during this period, as evidenced by TLC, so the mixture was resubjected to the microwave at 130 °C for 4 h. Again, no appreciable reaction had occurred. The temperature was increased to 160 °C, and the mixture reacted at this temperature for 4 h. No appreciable reaction had taken place based on TLC (Table 3.1 entry 4). It seemed unlikely that phenolic acid catalysts would be sufficient to catalyze the Johnson-Claisen rearrangement on our system, though we saw no dehydration of **3.35** under these conditions. With these results in hand, we set out to test the effect of 4 Å molecular sieves in Hünig's base on the Johnson-Claisen rearrangement.

After the standard RCM procedure was applied to (*R*)-linalool (**3.34**), Hünig's base (3 equiv) was added followed by 4 Å molecular sieves (~1:1 wt/wt of (*R*)-linalool). The mixture was reacted in the microwave reactor at 140 °C for 1 h, during which period no reaction had occurred, as evidenced by TLC. The temperature was increased to 180 °C for 1 h, with no effect (Table 3.1 entry 3). With limited success for the two-step-one pot conversion of (*R*)-linalool (**3.34**) to γ,δ -unsaturated ester **3.36** via RCM followed by Johnson-Claisen, we decided to pursue an alternative route. While we still wanted to use this sequence of reactions to set the stereochemistry at the C1 position of **3.36**, it was apparent that the Johnson-Claisen rearrangement was incompatible with our system. We thus turned to the Eschenmoser-Claisen rearrangement, which requires no acid additives and affords γ,δ -unsaturated amides.^{113,114}

Thus H-GII (0.001 equiv) was added to (*R*)-linalool (**3.34**) (Scheme 3.11). The green mixture was reacted at room temperature for 1 h at which point complete consumption of starting material was evidenced by TLC. Air was bubbled through the reaction mixture for 1 h, followed by addition of toluene (0.2 M) then dimethylacetamide dimethyl acetal (3 equiv). The mixture was refluxed for 24 h, at which point complete consumption of allylic alcohol **3.35** was observed by

TLC. The mixture was concentrated and purified via SiO₂ flash column chromatograph, affording the desired γ,δ -unsaturated amide **3.37** in 75% yield over two steps. ¹H NMR and ¹³C NMR were utilized to confirm the structure of **3.37**.

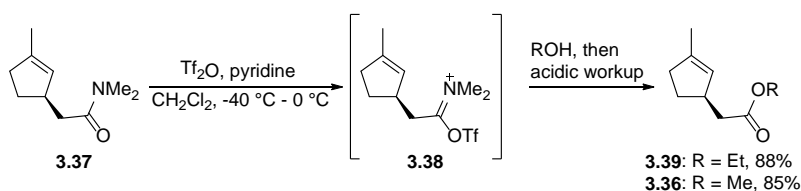


Scheme 3.11. Successful RCM/Eschenmoser-Claisen rearrangement of (R)-linalool (3.34) to generate γ,δ -unsaturated amide 3.37.

A ¹H resonance at 5.31–5.27 ppm (m, 1H) corresponding to alkenyl proton H^a provided evidence for a trisubstituted alkene. Two methyl singlets at 2.99 and 2.94 ppm corresponded to the methyl groups of the amide, and a third, broadened methyl resonance at 1.70 ppm corresponded to the protons on the C3 methyl group. The broadening of this signal most likely suggested allylic coupling to H^a, however the splitting pattern was not well defined, and a coupling constant could not be discerned. ¹³C NMR revealed a resonance at 172.7, corresponding to the amide carbonyl carbon, and two alkenyl carbons at 141.1 and 128.4 ppm, corresponding to C2 and C3, respectively. It was later found that the RCM proceeds in toluene in comparable yields to when performed neat, though the reaction time had to be extended to 3 h. By running the initial RCM in toluene, the process was converted to a true two-step-one-pot procedure which did not require the transfer of cyclopentenol **3.35** to a larger reaction vessel before application of the Eschenmoser-Claisen conditions. With γ,δ -unsaturated amide **3.37** in hand, our next goal was to convert the dimethyl amide moiety to an ester.

3.3 Conversion of γ,δ -unsaturated Amide to γ,δ -unsaturated Ester

Tertiary amides can be exceedingly difficult to convert to the corresponding esters, often requiring strongly acidic or basic reaction conditions and elevated temperatures.¹¹⁵ We wanted to avoid the harsh reaction conditions required for standard alcoholysis, so we turned to the literature for guidance. McClure and coworkers have shown the use of trimethyl- and triethyloxonium tetrafluoroborates in acidic solution for the conversion of tertiary amides to the corresponding esters.¹¹⁶ The authors report the operative mechanism involving the formation of an imidate ester,



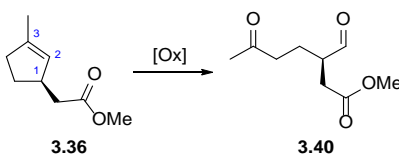
Scheme 3.12. Tf₂O-mediated esterification of amide **3.37** via imidate **3.38**.

similar to **3.38** (Scheme 3.12). A milder set of conditions was reported by Charette and coworkers, where imidate intermediates, similar to **3.38**, are generated via reaction of triflic anhydride with the amide.¹¹⁷ Addition of alcohol, followed by acidic workup afforded the esters in good to excellent yields. We decided to apply these conditions to amide **3.37**. Thus, amide **3.37** was dissolved in CH₂Cl₂ and pyridine (3 equiv) added. The mixture was cooled to -40 °C and Tf₂O added dropwise over the course of a few mins. The mixture was reacted at -40 °C for 1 h, then slowly warmed to 0 °C over the course of 2 h. The mixture was reacted at this temperature for 1 h, at which point EtOH (30 equiv) was added. The mixture was warmed to room temperature and reacted for 16 h. It was then diluted with Et₂O and 1 N aq. HCl added (approximately equal volume to solvent). Upon extractive workup and purification via SiO₂ flash column chromatography, ethyl

ester **3.39** was obtained in 65% yield. While not reported by Charette, it was found that after addition of 1 N aq. HCl, the reaction must be allowed to stir for at least 1 h for optimal conversion. Doing this led to ethyl ester **3.39** being formed in 88% yield. While the authors reported the conversion of amides to the corresponding ethyl esters, we found that replacement of EtOH with MeOH afforded methyl ester **3.36** in comparable yields. With successful access to ester **3.36** in an enantioselective fashion, we were poised to execute the next step towards the total synthesis of (–)-dehydroleucodine; oxidative cleavage of the C2-C3 double bond (Scheme 3.13).

3.4 Oxidative Cleavage

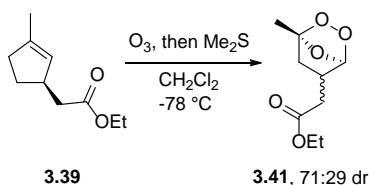
3.4.1 Ozonolysis



Scheme 3.13. Proposed oxidative cleavage of γ,δ -unsaturated ester **3.36**.

When searching the literature for suitable methods for the oxidative cleavage of **3.36**, there were myriad conditions that seemed appropriate to generate **3.40**.¹¹⁸ Ozonolysis conditions looked especially appealing, as they are mild, rapid, generate few byproducts, and do not use toxic metals. The first substrate we applied ozonolysis conditions to was ethyl ester **3.39**. Thus, γ,δ -unsaturated ester **3.39** was dissolved in CH_2Cl_2 and the solution cooled to $-78\text{ }^\circ\text{C}$. A stream of O_3/O_2 was bubbled through the solution until a blue color was observed (~ 15 min) (Scheme 3.14). At this point, Me_2S was added and the mixture reacted while warming to room temperature for 24 h. We

could visualize the disappearance of starting material **3.39** by TLC (KMnO₄ stain); however, we were unable to visualize any other component of the reaction mixture, regardless of the stain used. KMnO₄, *p*-anisaldehyde, ceric molybdate, and even 2,4-dinitrophenylhydrazone all failed at visualizing any reaction component. The crude reaction mixture was concentrated via rotary evaporation and the residue subjected to ¹H NMR and ¹³C NMR analysis. A ¹H signal at 5.71 and 5.67 ppm suggested the presence of an alkene, though this was not likely given the reaction conditions and the fact that this compound did not stain on TLC. In addition, the integral

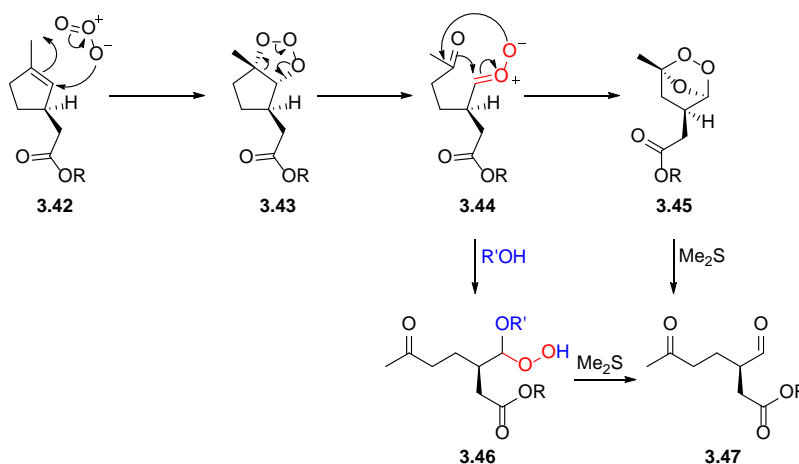


Scheme 3.14. Ozonolysis of γ,δ -unsaturated ester **3.39** in CH₂Cl₂ with Me₂S as the terminal reductant.

values of these resonances seemed to suggest a single compound was present as two diastereomers. Indeed, every major resonance was associated with a corresponding minor resonance. Using the integral values of the signal at 5.71 and 5.67, the diastereomeric ratio was determined to be 71:29, respectively. In addition to this resonance, triplets corresponding to each diastereomer were observed at 1.30-1.23 ppm, and quartets at 4.18-4.10 ppm, providing strong evidence for the presence of an ethyl ester. Singlets at 1.53 and 1.51 ppm corresponded to the methyl group of each diastereomer. Groups of signals at 2.61-2.54 ppm integrating for 1 H, 2.45-2.35 ppm integrating for 2H, and 2.31-2.19 ppm integrating for 1 H, suggested the presence of relatively deshielded protons, though no coupling constants could be ascertained from these groups. ¹³C signals at 172.1 and 171.8 confirmed the presence of an ester carbonyl carbon for each diastereomer. Interestingly, resonances at 108.1 and 104.5 ppm, corresponding to the major diastereomer, and 107.7 and 104.4

ppm, corresponding to the minor diastereomer, were observed. Based on the reaction mechanism of ozonolysis and these diagnostic resonances, we determined that the compound isolated was secondary ozonide **3.41** (Scheme 3.14). We reasoned that the isolation of secondary ozonide **3.41** was a result of incomplete reduction of this species with the terminal reductant, in this case, Me₂S.

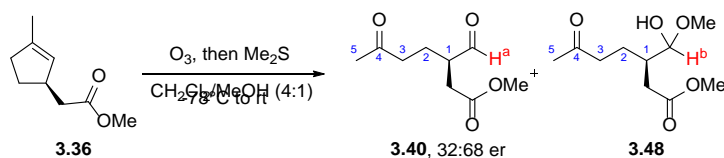
A common solution to this problem is the use of MeOH as a cosolvent, which is reported to act as a nucleophile towards carbonyl *O*-oxide intermediate **3.44**, affording hydroperoxyl acetal **3.46** (Scheme 3.15).¹¹⁹ This is then reduced to the carbonyl compound **3.47** via terminal reductant.



Scheme 3.15. Mechanism of ozonolysis, leading to isolated secondary ozonide 3.45.

With this information in hand, we repeated the above reaction, this time on methyl ester **3.36** using a 4:1 CH₂Cl₂/MeOH solvent system (Scheme 3.16). The products of this reaction were unable to be visualized by TLC; however, upon concentration of the reaction mixture and ¹H NMR of the crude residue, we noticed the presence of two distinct products. A ¹H resonance at 9.67 ppm (d, *J* = 0.8 Hz) corresponding to H^a provided evidence for the presence of aldehyde **3.40**; however, the signal was a part of the minor reaction component based on the integral value. Another key diagnostic resonance was observed at 4.16 ppm (d, *J* = 5.2 Hz), and corresponded a single proton

of the major reaction component. Two methyl singlets at 3.65 ppm (3 H) and 2.12 ppm (3 H) provided evidence for the presence of a methyl ester and a methyl ketone on the major reaction component. Similarly, methyl singlets at 3.67 ppm (1 H) and 2.13 ppm (1 H) confirmed the presence of a methyl ester and methyl ketone on aldehyde **3.40**. A diagnostic methyl singlet at 3.33 (3 H) ppm suggested the presence of a methyl ether on the major reaction component. Based upon this methyl singlet, as well as the downfield doublet at 4.16 ppm, we reasoned that the major reaction component was most likely hemiacetal **3.48**, where the signal at 4.16 ppm corresponded



Scheme 3.16. Ozonolysis of γ,δ -unsaturated ester **3.36** in $\text{CH}_2\text{Cl}_2/\text{MeOH}$ with Me_2S as the terminal reductant.

to H^b . In addition to these data, a large singlet at 2.61 ppm (8H) corresponding to a dimethyl sulfoxide impurity suggested that the dimethyl sulfide had indeed been oxidized. For this reason, we propose a hydroperoxy acetal intermediate similar to **3.48** was formed, then reduced via action of dimethyl sulfide (Scheme 3.15). This result led us to the conclusion that dimethyl sulfide was not the optimal reducing agent for use on our system.

We again turned to the literature for alternative reducing agents that could be used for the oxidative cleavage of β -formyl ester **3.36**. In the meantime, with the 1:3 mixture of **3.40/3.48** in hand, we wanted to determine the enantiomeric ratio of β -formyl ester **3.40** to ensure that no epimerization of the C1 stereocenter had occurred during the oxidative cleavage. We were concerned with the configurational stability of the C1 aldehyde under acidic conditions and for this reason were reluctant to subject the mixture to silica-based chiral resolution. We searched for

alternative methods to determine the enantiomeric ratio of α -chiral aldehydes and came across a methodology developed by Gellman and coworkers.¹²⁰ By reacting β -formyl ester **3.40** with the commercially available chiral amine (*S*)-1-methoxypropan-2-amine **3.49** in CDCl₃ in an NMR tube, ¹H NMR can be used to ascertain the diastereomeric ratio of the resulting imine **3.50** based on the relative integral values of H^a for each imine diastereomer (Figure 3.1). The diastereomeric ratio of imine **3.50** is equivalent to the enantiomeric ratio of β -formyl ester **3.40**. Using this protocol, the enantiomeric ratio of β -formyl ester **3.40** was determined to be 32:68. This was

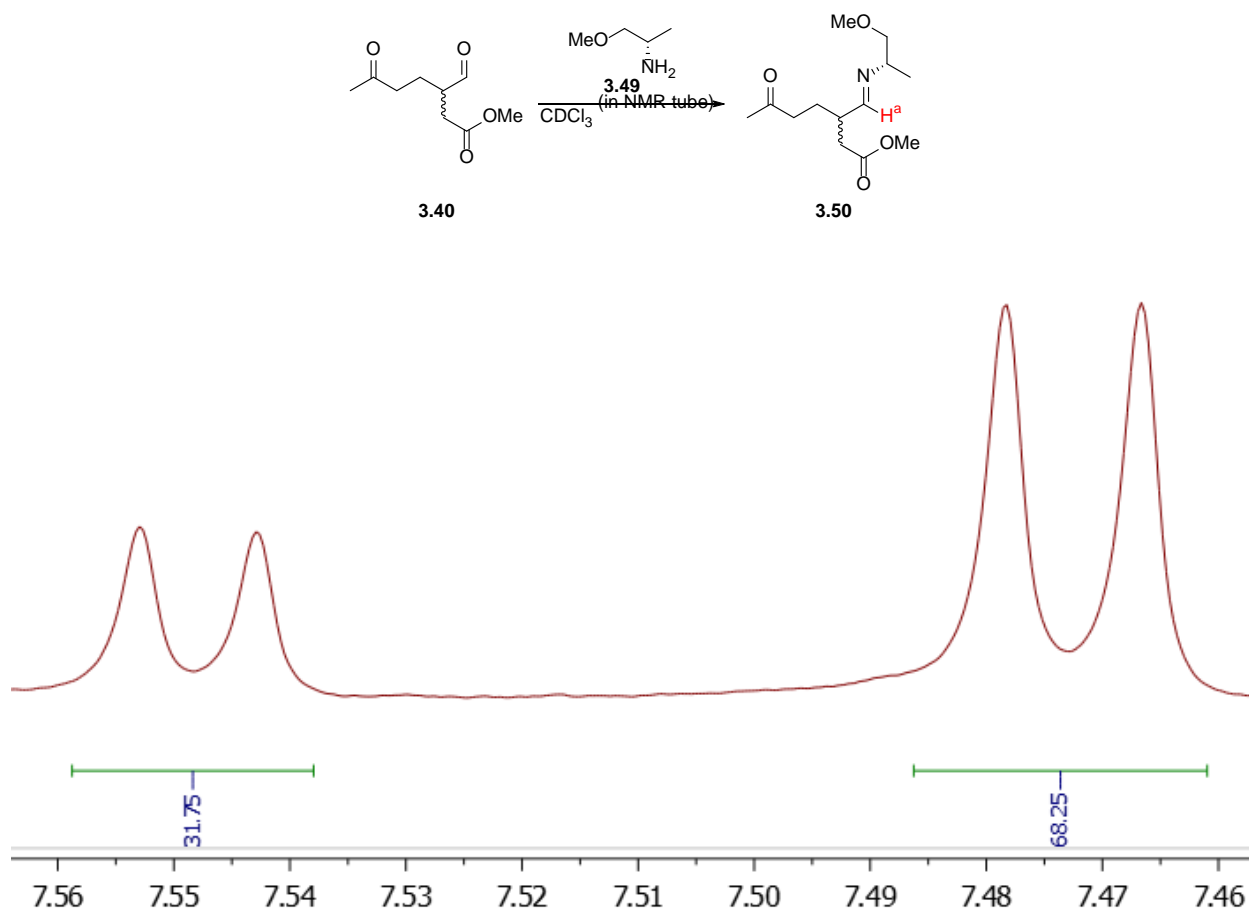
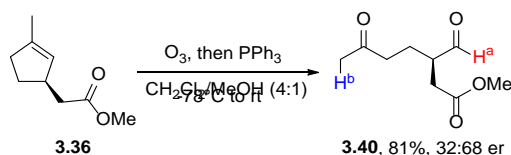


Figure 3.1. Determination of **3.40** enantiomeric ratio by reaction of chiral amine **3.49**, and ¹H NMR integration of imine **3.50** proton H^a.

concerning, as the enantiomeric ratio of commercially available (*R*)-linalool (**3.34**) was reported to be $\geq 95:5$, suggesting that epimerization had occurred at some point. As stated above, literature precedent indicates the RCM of tertiary alcohols similar to (*R*)-linalool (**3.34**) can be performed with complete retention of stereochemistry, and it is known that Claisen rearrangements result in complete retention of stereochemistry. Thus, we reasoned that epimerization had to be occurring either during or after the oxidative cleavage. To determine whether erosion of enantiopurity was occurring under the oxidative cleavage reaction conditions or simply upon standing, we subjected another sample of the 1:3 mixture of **3.40/3.48** that had been in the freezer for 3 days to the ^1H NMR procedure described above, and found the same 32:68 dr. Thus, we concluded that epimerization was occurring during ozonolysis. With this information in hand, we set out to find another reducing agent that would be more effective than dimethyl sulfide.

The terminal reductant most commonly employed, other than dimethyl sulfide, is triphenyl phosphine.¹¹⁸ We decided to repeat the ozonolysis experiment described above, but replace dimethyl sulfide with triphenyl phosphine (Scheme 3.17). Upon workup and purification, β -formyl ester **3.40** was isolated in 81% yield with a 32:68 dr. We saw no evidence of the formation of any



Scheme 3.17. Ozonolysis of γ,δ -unsaturated ester **3.36** in $\text{CH}_2\text{Cl}_2/\text{MeOH}$ with Me_2S as the terminal reductant.

ozonide, acetal, or hemiacetal products via TLC or ^1H NMR of the crude reaction mixture, suggesting that triphenyl phosphine was a suitable reducing agent for the complete conversion of γ,δ -unsaturated ester **3.36** to β -formyl ester **3.40** via ozonolysis. It was evident that epimerization

was occurring under the ozonolysis reaction conditions. We thus explored alternative methods for the oxidative cleavage of **3.36** that would not result in the epimerization of the α -stereocenter.

3.4.2 OsO₄-Catalyzed oxidative cleavage

Nicolaou and coworkers reported the use catalytic OsO₄ in the presence of *N*-morpholine-*N*-oxide (NMO) and 2,6-lutidine in 10:1 acetone/water as an effective protocol for the oxidation of alkenes, followed by oxidative cleavage with PhI(OAc)₂.¹²¹ We decided to apply these conditions to γ,δ -unsaturated ester **3.36** due to the high yields, mild reaction conditions, and broad substrate scope reported by Nicolaou. Thus, γ,δ -unsaturated ester **3.36** was dissolved in acetone/water (10:1) (Figure 3.2). To this solution was sequentially added 2,6-lutidine (2 equiv), NMO (1.5 equiv), and OsO₄ (0.03 equiv). The solution was stirred at room temperature for 16 h during which period the color changed from dark yellow/brown to light yellow. Once the starting material was fully consumed, as evidenced by TLC, PhI(OAc)₂ (1.5 equiv) was added and the solution stirred for 2 h. After complete conversion, as evidenced by TLC, saturated aq. Na₂S₂O₃ was added and the mixture transferred to a separatory funnel. The organic layer was extracted with saturated aq. CuSO₄ to remove the 2,6-lutidine. After concentration of the organic layer and purification of the resulting crude residue, β -formyl ester **3.40** was obtained in 89% yield. The enantiomeric ratio of β -formyl ester **3.40** was determined to be 91:9; significantly higher than when performing the oxidative cleavage via ozonolysis, and very close to the reported enantiomeric ratio (*R*)-linool (**3.34**) (95:5), though we did not verify the actual enantiomeric ratio of the commercially-supplied starting material via chiral HPLC or optical rotation.

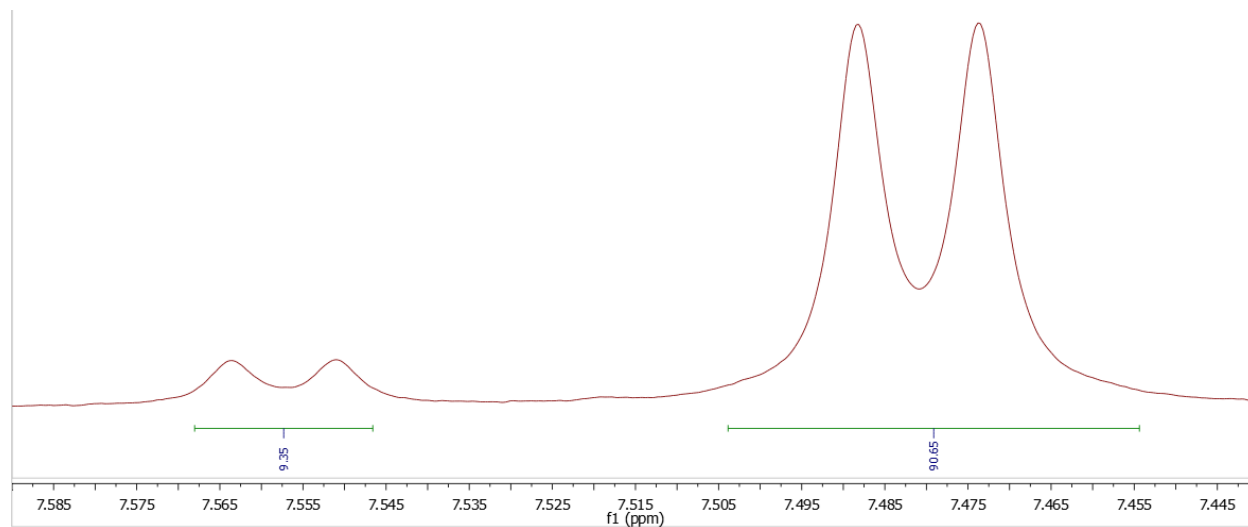
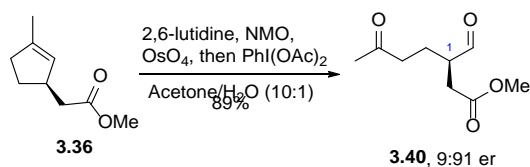
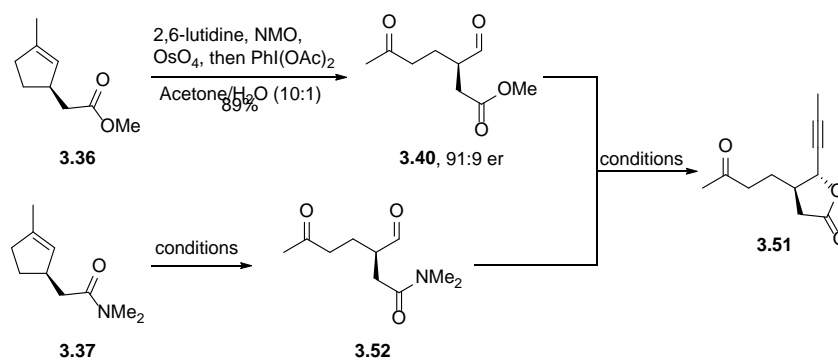


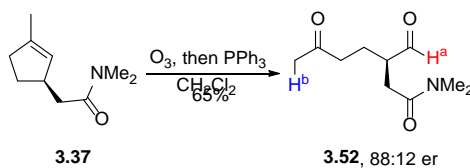
Figure 3.2. OsO₄ and PhI(OAc)₂-mediated oxidative cleavage of ester **3.36** with retention of C1 stereochemistry.

With the successful oxidative cleavage of γ,δ -unsaturated ester **3.36** affording β -formyl ester **3.40** in high yields and complete retention of stereochemistry, we wanted to effect an analogous oxidative cleavage on γ,δ -unsaturated amide **3.37** (Scheme 3.18). We reasoned that the resulting β -formyl amide **3.52** would be a valuable substrate going forward into the diastereoselective 1,2-addition/lactonization step to generate lactone **3.51**. In addition, it would provide a shorter route to lactone **3.51** in that we would not need to convert γ,δ -unsaturated amide **3.37** to γ,δ -unsaturated ester **3.36**. We wanted to first reexamine the ozonolysis conditions originally applied to γ,δ -unsaturated ester **3.36** due to the operational simplicity and clean reaction profile of this procedure. Because dimethyl sulfide had proven to be an ineffective reducing agent for the ozonolysis of γ,δ -unsaturated ester **3.36** to β -formyl ester **3.40**, we decided to adopt our



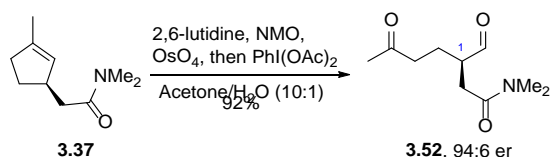
Scheme 3.18. Oxidative cleavage of γ,δ -unsaturated ester **3.36** and γ,δ -unsaturated amide **3.37**, and use of the resulting β -formyl ester **3.40** and β -formyl amide **3.52** to generate lactone **3.51**.

successful ozonolysis conditions, employing triphenyl phosphine as the terminal reductant. Thus, γ,δ -unsaturated amide **3.37** was dissolved in CH₂Cl₂ and the solution cooled to -78 °C (Scheme 3.19). A stream of O₃/O₂ was bubbled through the solution until a blue color was observed. This process took approximately 35 min, over twice as long as the analogous γ,δ -unsaturated ester **3.36**. A stream of O₂ was then bubbled through the solution until the color dissipated, then PPh₃ (3 equiv) added and the solution allowed to warm to room temperature while reacting for 24 h. Upon concentration and purification via SiO₂ flash column chromatography, β -formyl amide **3.52** was obtained in 65% yield. Key ¹H NMR resonances used for positive characterization were a signal at 9.75 ppm (s) corresponding to aldehyde proton H^a, singlets at 3.02 ppm and 2.93 ppm, corresponding to the protons on the amide methyl groups, and a singlet at 2.14 ppm, corresponding to the methyl protons H^b of the methyl ketone. Further structural confirmation was provided by



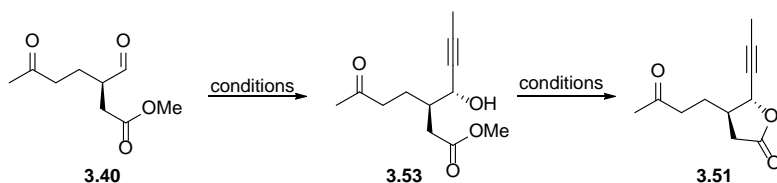
Scheme 3.19. Ozonolysis of γ,δ -unsaturated amide **3.37** in CH₂Cl₂ with PPh₃ as the terminal reductant.

By applying Nicolou's conditions to γ,δ -unsaturated amide **3.37**, β -formyl amide **3.52** was isolated in 92% yield, and the enantiomeric ratio determined to be 94:6 (Scheme 3.21). With efficient, optimized routes to both β -formyl ester **3.40** and β -formyl amide **3.52** in hand, we were able to show that the α -stereocenter was configurationally stable under the reported reaction conditions. Thus, we were poised to move forward to the key diastereoselective 1,2-addition/lactonization step of the synthesis.



Scheme 3.21. OsO_4 and $\text{PhI}(\text{OAc})_2$ -mediated oxidative cleavage of β -formyl amide **3.37** with retention of C1 stereochemistry.

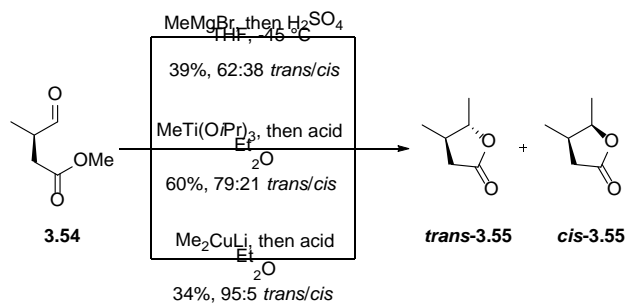
3.5 Diastereoselective 1,2-Addition/Lactonization to **3.40** and **3.52**



Scheme 3.22. Proposed diastereoselective 1,2-addition/lactonization of β -formyl ester **3.40**.

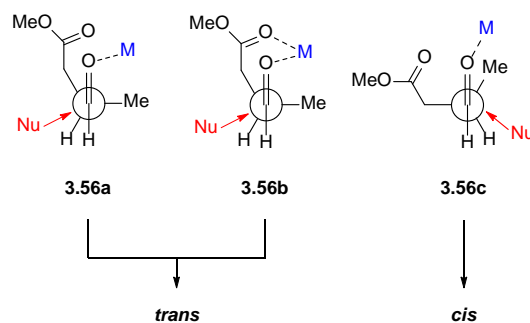
The next step in the total synthesis of (–)-dehydroleucodine (*ent*-**3.1**) was the diastereoselective addition of a propynyl nucleophile to β -formyl ester **3.40**, followed by acidic workup, leading to the lactonization of propargyl alcohol intermediate **3.53** (Scheme 3.22). A survey of the literature provides few reported methods for diastereoselective nucleophilic additions to acyclic aldehydes with a carboxylate at the β -position. Most work has been carried

out by Reissig on alkyl substituted β -formyl methyl esters (Scheme 3.23).⁹⁶ The diastereoselective addition of methylmagnesium bromide to β -formyl ester **3.54** afforded lactone **3.55** with a *trans/cis* diastereomeric ratio of 62:38. The authors saw both a yield enhancement as well as an enhancement of diastereoselectivity when triisopropoxy(methyl)titanium was used as the nucleophile, isolating lactone **3.55** in 60% yield with a diastereomeric ratio of 79:21. Excellent



Scheme 3.23. Precedent for the diastereoselective 1,2-addition/lactonization of β -formyl esters.

diastereoselectivity was achieved when a methyl cuprate was used as the nucleophile, affording lactone **3.55** with a diastereomeric ratio of 95:5, though only 34% of the lactone was isolated. Reissig proposes two possible mechanisms that give rise to the observed diastereomeric ratios. The authors propose that, in the case of the methylmagnesium bromide and triisopropoxy(methyl)titanium, competing Felkin-Ahn and Cram chelate transition states **3.56a** and **3.56b** (Scheme 3.24). The nucleophile approaches from the least hindered face of the aldehyde, resulting in the *trans*-lactone. The *cis*-lactone is generated via Felkin-Ahn transition state **3.56c**, where the methyl group and aldehyde carbonyl oxygen are more eclipsed. Thus, the nucleophile approaches from the opposite face. In the case of excellent diastereoselectivity achieved via addition of organocuprates, the authors propose Cram chelate **3.56b** is the predominate species in solution.

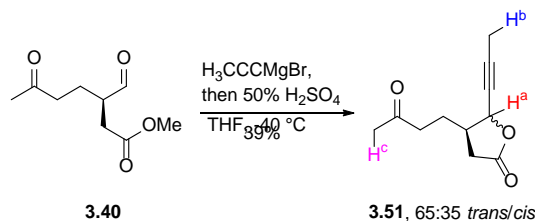


Scheme 3.24. Reissig's proposed transition states leading to the diastereoselective 1,2-addition of nucleophiles to β -formyl esters.

While the conditions reported by Reissig worked well on simple alkyl- and aryl substituted β -formyl esters, the concern with our system was that competitive 1,2-addition to the ketone could occur. While rates of nucleophilic additions to aldehydes are typically faster than rates of addition to ketones, we wanted to apply conditions that would ensure a chemoselective 1,2-addition to the aldehyde, leaving the ketone intact. Reetz and others have shown complete chemoselective 1,2-addition of organotitanium nucleophiles to aldehydes in the presence of ketones.⁹⁵ Because of Reissig's report of organotitanium reagents adding to β -formyl esters in a diastereoselective fashion, and Reetz's reports for the chemoselective 1,2-addition of organotitanium reagents, we reasoned that an alkynyltitanium nucleophile would be the best option to effect the chemo and diastereoselective 1,2-addition of an alkyne to β -formyl ester **3.40**. While the diastereoselectivity of organocuprates is significantly higher than the analogous organotitanium reagents, it is well known that copper acetylides are inert and do not add to carbonyls in a 1,2- fashion. This eliminated the use of organocuprates as a possible alkyne nucleophile source. With β -formyl ester **3.40** in hand and a proposed path to *trans*-lactone **3.51**, we set out to examine the feasibility of a diastereomeric 1,2-addition of an alkyne nucleophile to β -formyl ester **3.40**.

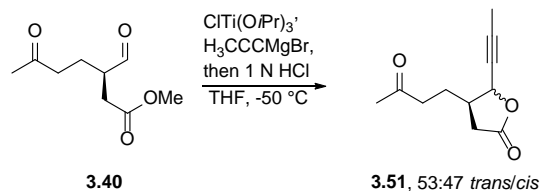
The first thing we wanted to do was benchmark our system against Reissig's simple alkyl-substituted systems. We wanted to probe the effect that the C4 ketone would have on both reaction

yield, as well as diastereoselectivity. To do this, we first employed commercially-available propynylmagnesium bromide as the nucleophile. Thus, β -formyl ester **3.40** was dissolved in THF and the solution cooled to $-40\text{ }^{\circ}\text{C}$ (Scheme 3.25). Propynylmagnesium bromide was added and allowed to react for 1 h while the solution was allowed to warm to room temperature. Upon complete consumption of starting material, as evidenced by TLC, a 50% aq. solution of H_2SO_4 was added. Upon concentration of the organic layer and purification of the crude residue via SiO_2 flash column chromatography, a mixture of *trans*-**3.51** and *cis*-**3.51** were isolated in 39% combined yield, with a diastereomeric ratio of 65:35 (*trans/cis*). Key ^1H NMR resonances at 5.13 ppm (dq, $J^1 = 7.0\text{ Hz}$, $J^2 = 2.0\text{ Hz}$, 0.34 H) and 4.65 ppm (dq, $J^1 = 7.0\text{ Hz}$, $J^2 = 2.0\text{ Hz}$, 0.65 H), corresponding to the lactone proton H_a of *cis*-**3.51** and *trans*-**3.51**, respectively. We used literature precedent for the assignment of these protons to a relative stereoisomer.¹²² With lactone **3.51** in hand, we were able to make a direct comparison between the diastereoselectivity achieved by Reissig on the simple methyl-substituted β -formyl ester **3.54**, and our system. We were encouraged that we observed a similar yield, and more importantly, a similar diastereomeric ratio to that reported by Reissig. With this information in hand, we reasoned that if we applied Reissig's organotitanium conditions, we would see both a yield increase, as well as an increase in the diastereomeric ratio. Thus, we set out to apply these conditions to β -formyl ester **3.40**.



Scheme 3.25. Addition of ethynylmagnesium bromide to β -formyl ester **3.40**.

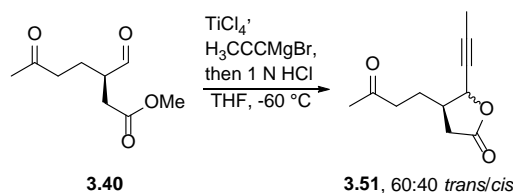
Chlorotitanium triisopropoxide (1.2 equiv) was dissolved in THF and cooled to -50 °C (Scheme 3.26). Propynylmagnesium bromide (0.5 M in THF, 1.2 equiv) was added and the solution reacted for 2 h. To this was added β -formyl ester **3.40**, and the solution reacted for 2 h at -50 °C. To the reaction vessel was added aq. 1 N HCl, and the mixture was warmed to room temperature and reacted for 24 h. A ^1H NMR spectrum was taken of the crude reaction mixture, which revealed that selective 1,2-addition to the aldehyde, followed by lactonization indeed occurred; however, the reaction proceeded with a diastereomeric ratio of 53:47 *trans/cis*; slightly worse than when using only propynylmagnesium bromide. We were unsure what had occurred to give us a lower diastereomeric ratio relative to the reaction being performed in the presence of only propynylmagnesium bromide, but we suspected the ketone carbonyl oxygen was interfering with chelate formation after propynylmagnesium bromide was transmetalated with the highly oxophilic titanium reagent. To test this hypothesis, we chose to transmetalate propynylmagnesium bromide with titanium tetrachloride instead of chlorotitanium triisopropoxide, as titanium tetrachloride is typically more Lewis acidic than its chlorotitanium alkoxide analogs.¹²³ We predicted we would see an even worse diastereomeric ratio with the more oxophilic titanium tetrachloride.



Scheme 3.26. Chlorotitaniumtriisopropoxide-mediated 1,2-addition of ethynylmagnesium bromide to β -formyl ester **3.40.**

The above conditions were repeated by using titanium tetrachloride instead of chlorotitanium triisopropoxide (Scheme 3.27). Upon completion of the reaction, as evidenced by

TLC, ^1H NMR was taken of the crude reaction mixture. We again observed selective 1,2-addition to the aldehyde, followed by lactonization; however, the reaction proceeded with diastereomeric



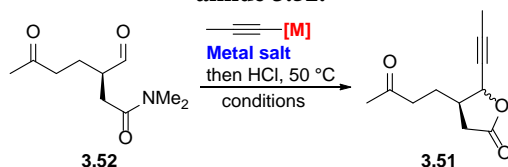
Scheme 3.27. Titanium tetrachloride-mediated 1,2-addition of propynylmagnesium bromide to β -formyl ester **3.40**.

ratio of 60:40 *trans/cis*. This result suggested that the oxophilicity of the organometallic reagent was not necessarily correlated to the diastereomeric outcome of the 1,2-addition.

With these results in hand, we wanted to explore the feasibility of performing a 1,2-addition/lactonization on β -formyl amide **3.52**. Doing so would allow us to access lactone **3.51** in fewer overall steps, as γ,δ -unsaturated amide **3.52** would not have to be converted to γ,δ -unsaturated ester **3.40**. In addition, diastereoselective additions to a β -formyl amide of this nature have never been reported. It was difficult to make a prediction as to whether we would see better or worse diastereoselectivities. The amide functionality would be expected form a stronger chelate with the organotitanium reagent, as the Lewis basicity of the amide carbonyl oxygen is greater than that of the ester carbonyl oxygen, leading to enhanced *trans/cis* diastereoselectivities. However, the increased steric demand of the *N,N*-dimethyl group would be expected to lower the *trans/cis* diastereoselectivity, based on the proposed transition state structures shown above (Scheme 3.25). We wanted to begin our studies by comparing the result of the addition of propynylmagnesium bromide to β -formyl amide **3.52** to the result of addition to β -formyl ester **3.40**. We reasoned that this would give us an idea of how this system behaves as opposed to the ester analog.

Thus, β -formyl amide **3.52** was dissolved in THF and cooled to $-78\text{ }^{\circ}\text{C}$ (Table 3.2, Entry 1). To this was added propynylmagnesium bromide (0.5 M in THF, 1.1 equiv). After reacting for 2 h, 1 N aq. HCl was added and the mixture heated to $50\text{ }^{\circ}\text{C}$ for 18 h. Upon workup and purification via SiO_2 flash column chromatography, lactone **3.51** was isolated in 55% yield, with a diastereomeric ratio of 66:34 *trans/cis*. We were encouraged by these results, as the diastereomeric ratio was nearly identical to when these conditions were applied to the β -formyl ester analog **3.40**; however, the reaction yield was slightly higher at 55%, versus 34% when performed on the **3.40**. With these results in hand, we reasoned that we could proceed with the 1,2-addition/lactonization of the β -formyl amide. We decided to screen a variety of different organometallic reagents in an effort to optimize both yield and diastereoselectivity. The second organometallic that we wanted to screen was propynyllithium, which can be generated *in situ* via deprotonation of 1-bromopropene, followed by elimination and subsequent deprotonation of the resulting propyne.¹²⁴

Table 3.2. Conditions for the diastereoselective 1,2-addition of propynylmagnesium bromide to β -formyl amide **3.52.**



Entry	[M] (equiv)	Metal salt (equiv)	Conditions	Yield	dr (trans/cis)
1	MgBr (1.1)	None	-78	55	66:34
2	Li (1.1)	None	-78	46	62:38
3	MgBr (1.1)	MnCl ₂ (1.1)	0	61	57:43
4	MgBr (1.1)	MnCl ₂ (1.1)/LiCl (2.2)	0	47	52:48
5	MgBr (1.1)	TiCl ₄ (1.1)	-60	45	50:50
6	MgBr (1.1)	ClTi(O <i>i</i> Pr) ₃ (1.1)	-60	86	38:62

Thus, 1-bromopropene was dissolved in THF and cooled to $-78\text{ }^{\circ}\text{C}$ (Table 3.2, Entry 2). To this was added *n*-butyllithium in a dropwise fashion. The mixture was reacted for 1 h before being

cannulated into a solution of β -formyl amide **3.52** in THF, also cooled to 78 °C. The mixture was reacted for 30 min then 1 N aq. HCl was added and the mixture heated to 50 °C for 18 h. Upon workup and purification via SiO₂ flash column chromatography, lactone **3.51** was isolated in 46% yield, with a diastereomeric ratio of 62:38 *trans/cis*. With similar yields and diastereomeric outcome to that of propynylmagnesium bromide, we drew the conclusion that the reactivity between the two were very similar. Due to the operational complexity of generating propynyllithium *in situ*, we decided to abandon this method for the generation of future organometallic nucleophiles, and opted to simply use the commercially available propynylmagnesium bromide in THF instead. The reaction profiles of both the organomagnesium and organolithium reactions were very complex by TLC, leading us to believe that, despite the depressed temperatures, 1,2-addition was taking place at both the aldehyde carbonyl carbon, as well as the ketone carbonyl carbon, leading to moderate to low reaction yields. Cahiez and coworkers have reported the chemoselective addition of organomanganese and manganate reagents to aldehydes in the presence of ketones.^{125–127} While no information is provided on the diastereoselective addition to β -formyl esters or amides such as **3.40** and **3.52**, we decided to examine these conditions as a potential solution towards chemoselective addition to the carbonyl carbon of the aldehyde.

Normant has described the preparation of various alkyl, alkenyl, and alkynyl manganese reagents, as well as more functionalized organomanganese reagents.^{125,128} Manganese(II) chloride (1.1 equiv) was first dehydrated by heating under vacuum with a Fisher burner, until no more condensation on the inside of the flask was observed (Table 3.2, entry 3). The flask was cooled under a constant flow of nitrogen, then suspended in THF. The suspension was cooled to 0 °C and propynylmagnesium bromide (1.1 equiv) added dropwise. After reacting for 1 h, amide **3.52** was

added as a solution in THF. The mixture was reacted for 3 h before 1 N HCl was added. The reaction was maintained at 50 °C overnight. Upon purification, the desired lactone **3.51** was isolated in 61% yield with a diastereomeric ratio of 57:43 (*trans/cis*). While the yield was improved with respect to the organolithium and organomagnesium reagents, the diastereomeric ratio was slightly depressed. Addition of LiCl has been shown to generate the corresponding organomanganate reagents, which we thought might provide enhanced yields or diastereoselectivities.¹²⁷ The preparation of these reagents is similar to that reported above; however, inclusion of LiCl (2 equiv with respect the MnCl₂) is necessary. Application of these conditions resulted in lactone **3.51** being isolated in 47% yield with a 52:48 diastereomeric ratio (Table 3.2, entry 4). The poor diastereomeric ratios and modest yields of **3.51** obtained when using the organomanganese reagents as the nucleophile led us to turn to the corresponding organotitanium reagents.

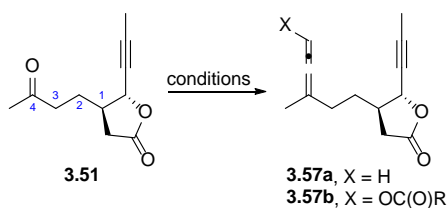
As stated above, organotitanium reagents chemoselectively add to aldehydes; however, we were concerned that we would observe low diastereoselectivity, as was seen in the case of β -formyl ester **3.40**. Nonetheless, we decided to apply both the titanium tetrachloride and chlorotitanium triisopropoxide conditions to β -formyl amide **3.52**. Both reactions were run in an analogous fashion as reported above on β -formyl ester **3.40**. In the presence of TiCl₄, lactone **3.51** was obtained in 45% yield, with a diastereomeric ratio of 50:50 (Table 3.2, entry 5), slightly worse than when performed on ester **3.40**. However, to our surprise, in the presence of chlorotitanium triisopropoxide, lactone **3.51** was generated in 86% yield (Table 3.2, entry 6). This was a very promising result, as the high yield suggested that the ketone remained intact throughout the reaction and did not affect the overall yield to any appreciable extent. To our surprise however, the diastereomeric ratio was 62:38, favoring the *cis* diastereomer. Despite the poor *trans*-

selectivity, the high yield of these conditions led us to move forward using propynyltitanium triisopropoxide as the preferred reagent for the transformation of amide **3.52** to lactone **3.51**.

3.6 Conversion of Ketone **3.51** to Allenes

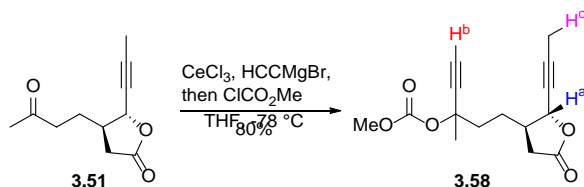
3.6.1 Formation of propargyl carbonate

With a rapid route to lactone **3.51** in hand, we set out to convert the C4 ketone to the desired allene, setting the stage for the Allenic Pauson–Khand reaction. We reasoned that lactone **3.51** could serve as a common intermediate towards the synthesis a variety of allenyl carboxyesters **3.57b**, as well as the terminal 3,3-disubstituted allene **3.57a** (Scheme 3.28). Having access to these different allene functional patterns would offer access to a wider variety of 6,12-guaianolides and analogs. We first examined the case of 3,3-disubstituted allene **3.57a**. We reasoned that we could use the Pd(0)-catalyzed propargyl carbonate hydrogenolysis conditions reported by Tsuji, and successfully applied by our group to other systems (*ad supra*).⁵² We thus set out to synthesize the propargyl carbonate precursor required for the hydrogenolysis reaction.



Scheme 3.28. Proposed conversion of ketone **3.51** to allenenes **3.57a** and **3.57b**.

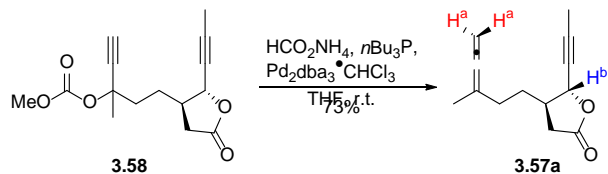
Application of the standard CeCl_3 -mediated addition of ethynylmagnesium bromide, followed by trapping with methyl chloroformate afforded propargyl carbonate **3.58** in 80% yield (Scheme 3.29). We were unable to separate any of the four diastereomers via chromatography, so the product was carried on as a mixture of these diastereomers; however, we observed no change in the lactone diastereomeric ratio during the course of this reaction. Analysis of the ^1H NMR spectrum revealed that the diastereomeric ratio of the *trans/cis* lactone remained constant throughout the reaction, as evidenced by a resonance at 5.15 ppm (dq, $J^1 = 7.2$ Hz, $J^2 = 2.1$ Hz, 0.63 H) corresponding to the H^a of *cis*-**3.58** and a resonance at 4.69 ppm (dq, $J^1 = 6.6$ Hz, $J^2 = 2.1$ Hz, 0.37 H) corresponding to H^a of *trans*-**3.58**. In addition, a methyl singlet at 3.78 ppm (3 H) confirmed the presence of a methyl carbonate. A singlet at 2.62 ppm (1 H) suggested the presence of alkynyl proton H^b , and a methyl singlet at 1.74 ppm (3 H) confirmed the presence of propargyl protons H^c . Due to the viscosity of propargyl carbonate **3.58**, it was exceedingly difficult to remove all of the EtOAc, even by azeotroping with a variety of solvents. With the desired propargyl carbonate **3.58** in hand, we were poised to apply Tsuji's conditions to access 3,3-disubstituted allene **3.57a**.



Scheme 3.29. Synthesis of propargyl carbonate **3.58**.

Application of the previously reported $\text{Pd}(0)$ -catalyzed hydrogenolysis conditions (see Chapter 2) afforded allene-yne **3.57a** in 73% yield (Scheme 3.30). A diagnostic ^1H NMR signal at 4.63 ppm (sept, $J = 3.2$ Hz, 2 H) provided evidence for the presence of allenyl protons H^a , and

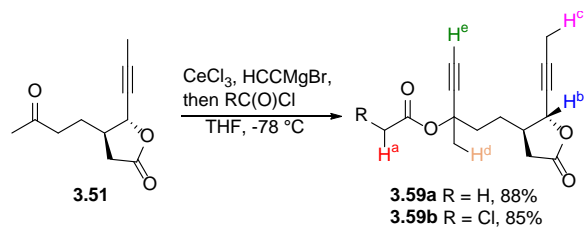
appear to be magnetically equivalent despite the fact that the two allenyl protons are diastereotopic due to the presence of the lactone. A resonance at 5.14 ppm (dq, $J^1 = 7.2$ Hz, $J^2 = 2.0$ Hz, 0.64 H) corresponding to H^b of *cis*-**3.57a** and 4.68 ppm (dq, $J^1 = 7.2$ Hz, $J^2 = 2.0$ Hz) corresponding to H^b of *trans*-**3.57a** confirmed that the lactone remained intact, though an accurate diastereomeric ratio could not be ascertained due to significant overlap of allenyl protons H^a with *trans*-**3.57a** proton H_b, though it was shown after the next synthetic step that the diastereomeric ratio had been maintained. With a successful route to 3,3-disubstituted allene **3.57a** in hand, we shifted our focus to the synthesis of the analogous allenyl carboxy esters **3.57b**, again by employing the same methodologies that we had previously shown to work on other systems.



Scheme 3.30. Synthesis of 3,3-disubstituted allene **3.57a**.

3.6.2 Synthesis of allenyl carboxyesters

We next wanted to synthesize both propargyl acetate **3.59a** as well as propargyl chloroacetate **3.59b** (Scheme 3.32), as we had previously shown greatly enhanced rates of hydrolysis under mild Sc(III) conditions in the case of the chloroacetate substrates (see Chapter 2). Thus, Lactone **3.51** was converted to propargyl acetate **3.59a** and propargyl chloroacetate **3.59b** in 88% and 85% yield, respectively via application of the previously reported conditions (see Chapter 2)(Scheme 3.31). Evidence for the formation of propargyl acetate **3.59a** was observed via

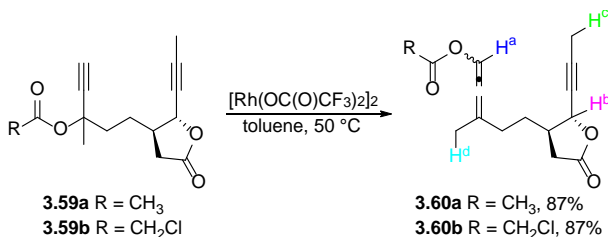


Scheme 3.31. Synthesis of propargyl esters 3.59a and 3.59b.

the presence of a methyl singlet at 2.04 ppm (3 H) corresponding to methyl protons H^a , a methyl singlet at 1.70 ppm (3 H) corresponding to methyl protons H^c , and a group of methyl singlets from 1.90-1.88 ppm integrating for a total of 3 H, corresponding to methyl protons H^d of each of the four possible diastereomers of **3.59a**. In addition, a signal at 2.58 ppm (s, 1 H) supported the presence of alkynyl proton H^a . The lactone diastereomeric ratio remained constant throughout the reaction, as evidenced by a signal at 5.15 ppm (m, 0.62 H) corresponding to H^b of *cis*-**3.59a**, and a signal at 4.70 ppm (m, 0.38 H) corresponding to H^b of *trans*-**3.59a**. Evidence for the formation of propargyl chloroacetate **3.59b** was observed via the presence of a ^1H NMR resonance at 4.02 ppm (s) corresponding to the chloroacetyl protons H^a . As was the case with propargyl carbonate **3.58**, we did not see individual signals for each diastereomer. The lactone remained intact and did not epimerize, as evidenced by a resonance at 5.16 ppm ($J^1 = 6.8$ Hz, $J^2 = 2.4$ Hz, 0.61 H) corresponding to H^b of *cis*-**3.59b** and a resonance at 4.70 ppm ($J^1 = 6.8$ Hz, $J^2 = 2.0$ Hz, 0.39 H) corresponding to H^b of *trans*-**3.59b**. A methyl singlet at 1.74 ppm (3 H) confirmed the presence of methyl protons H^c , and a group of singlets from 1.90-1.88 integrating for a total of 3 H corresponded to methyl protons H^d for the four expected diastereomers of **3.59b**. A singlet at 2.63 ppm confirmed the presence of alkynyl proton H^e . The ^{13}C NMR spectrum was very complex, as there were signals corresponding to each of the four possible diastereomers, many of which had a very similar chemical shift; however, based on the chemical shift regions, we reasoned that we had

the desired chloroacetate **3.59b**. For instance, four signals at 175.78 ppm, 175.76 ppm, 175.27 ppm, and 175.26 ppm provided evidence for the presence of four diastereomeric ester carbonyl carbons. Twelve signals from 76.7 ppm to 66.0 ppm provided evidence for the presence of four diastereomeric groups of four alkynyl carbons; however, the missing four signals are most likely buried in the CDCl₃ resonance, or do not resolve enough to be distinguished from the other signals.

With propargyl acetate **3.59a** and propargyl chloroacetate **3.59b** in hand, we were poised to apply the Rh(I)-catalyzed formal 3,3-sigmatropic rearrangement conditions which we have previously shown to be successful on other systems to access the corresponding allenyl carboxyesters. Thus, [Rh(OC(O)CF₃)₂]₂ (0.05 equiv) was dissolved in toluene and propargyl



Scheme 3.32. Rh(II)-catalyzed formal 3,3-sigmatropic rearrangement of allenyl carboxyesters **3.60a and **3.60b**.**

acetate **3.59a** or propargyl chloroacetate **3.59b** was added (Scheme 3.32). The solution was reacted at 50 °C until complete consumption of starting material was observed. In the case of propargyl acetate **3.59a**, the reaction time was 3 h; however, propargyl chloroacetate **3.59b** required 8 h to reach completion. The longer reaction time was expected, as we had also observed this to be the case with the propargyl chloroacetate previously reported (*ad supra*). Upon completion, the mixture was cooled to room temperature and SilaMetS® Thiourea was added to scavenge the Rh(I) catalyst. The mixture was allowed to stir for 16 h then filtered through a celite plug. After concentration and purification via SiO₂ flash column chromatography allenyl acetate **3.60a** or

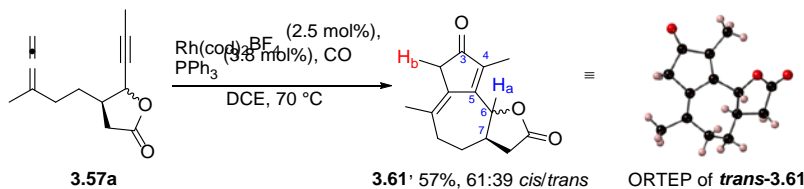
allenyl chloroacetate **3.60b** were isolated in 87% and 87% yield, respectively. Again, none of the diastereomers could be separated via chromatography, making the ^1H and ^{13}C NMR spectra very complex; however, by examining the chemical shift regions of the resonances, we were able to confirm structures. In the case of allenyl acetate **3.60a**, diagnostic allenyl proton H^{a} signals were observed from 7.36-7.30 ppm (1 H) and appeared to be two partially overlapping resonances, corresponding to two of the four diastereomers of **3.60a**. A signal at 5.14 ppm (m, 0.63 H) corresponding to H^{b} of *cis*-**3.60a** and 4.67 ppm (m, 0.37 H) corresponding to H^{b} of *trans*-**3.60a** confirmed that the lactone had remained intact and had not epimerized. Overlapping methyl resonances from 2.15-2.13 ppm integrating for a total of 3 H provided evidence for the presence of an acetyl group. Overlapping methyl resonances from 1.90-1.87 ppm (total 3 H), and 1.86-1.83 ppm (total 3 H) confirmed the presence of methyl protons H^{c} and H^{d} , respectively. With high-yield routes to both allene **3.57a** and **3.60a** and **3.60b** in hand, we were poised to explore the feasibility of allenic Pauson–Khand reaction on these substrates.

3.7 Allenic Pauson-Khand Reactions of **3.57a**, **3.60a**, and **3.60b**

3.7.1 APKR of 3,3-disubstituted allene **3.57a**

The successful application of cationic $\text{Rh}(\text{cod})_2\text{BF}_4$ to effect the APKR on our previously reported methyl-substituted allene-yne led us to reason that the conditions may also be applicable to methyl-substituted allene-ynes with a lactone installed in the tether (see Chapter 2). Thus, application of these conditions to lactone **3.57a** afforded the desired APKR adduct **3.61** in 57% yield and a 61:39 *trans/cis* ratio, confirming that no epimerization of the lactone had occurred

under the reaction conditions (Scheme 3.33). We were able to successfully separate *cis*-**3.61** and *trans*-**3.61** at this stage, *trans*-**3.61** eluting before *cis*-**3.61**. A ^1H NMR signal at 5.32 ppm (d, $J = 10.8$ Hz, 1H), corresponding to H^a , provided evidence for the formation of *trans*-**3.61**. Similarly, a signal at 5.59 ppm (d, $J = 5.6$ Hz, 1H) corresponded to H^a of *cis*-**3.61**. In addition, a resonance



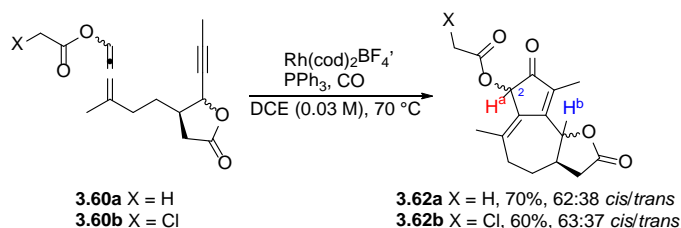
Scheme 3.33. APKR of 3,3-disubstituted allene-yne 3.57a.

at 2.97 ppm (s, 2H) corresponding to H^b of *trans*-**3.61** and 3.01 ppm (d, $J = 5.2$ Hz, 2H) corresponding to H^b of *cis*-**3.61** were observed. A resonance at 2.02 ppm (s, 3H) and 1.88 ppm (s, 3H) of *trans*-**3.61** confirmed the presence of two methyl groups. Likewise, resonances at 1.92 ppm (s, 3H) and 1.85 ppm (s, 3H) in the ^1H NMR spectrum of *cis*-**3.61** provided evidence for the presence of two methyl groups. The ^{13}C NMR spectra of *trans*-**3.61** and *cis*-**3.61** were very similar, with a signal at 204.4 ppm corresponding to the C3 carbonyl carbon of *trans*-**3.61** and 204.3 ppm corresponding to the carbonyl carbon of *cis*-**3.61**. Alkenyl resonances at 161.0, 139.2, and 132.9, and 129.8 ppm confirmed the presence of four alkenyl carbons in *trans*-**3.61**, with a lactone carbonyl carbon signal observed at 175.1 ppm. Similarly, resonances at 157.7, 143.4, 137.1, and 128.8 ppm provided evidence for the presence of four alkenyl carbons in *cis*-**3.61**, with a lactone carbonyl carbon signal at 176.2. To confirm the assignment of *cis*-**3.61** and *trans*-**3.61**, we were able to crystallize *trans*-**3.61** by dissolving a sample in EtOAc and allowing the solvent to slowly evaporate in the freezer (0 °C). X-ray crystallography confirmed both the C6-C7 relative stereochemistry, as well as the C7 absolute stereochemistry. We used this data to conclude that H^a

of *trans*-**3.61** is shifted upfield in the ^1H NMR spectrum, relative to H^a of *cis*-**3.61**. With the successful application of the APKR to lactone-containing 3,3-disubstituted allene-yne **3.57a**, we were poised to apply the conditions to the more functionalized allenyl carboxyesters **3.60a** and **3.60b**. If successful, we would have accessed the core carbon framework of (–)-dehydroleucodine (*ent*-**3.1**).

3.7.2 APKR of allenyl carboxyesters **3.60a** and **3.60b**

To this end, application of the previously reported cationic Rh(I) conditions to allenyl carboxy esters **3.60a** and **3.60b** afforded the desired APKR adducts **3.62a** and **3.62b** in 70% and 60% yields, respectively (Scheme 3.34). It was found that the substrate concentration had to be reduced to 0.03 M to achieve optimal yields for this reaction. As with the bicyclo[5.3.0]decadienone **3.61**, the *cis* and *trans* isomers of **3.62a** and **3.62b** were separable via flash column chromatography, and were characterized independently (Figure 3.3).



Scheme 3.34. APKR of allenyl carboxyesters **3.60a** and **3.60b**.

It was found that the APKR of both **3.60a** and **3.60b** proceeded with varying degrees of diastereocontrol at the C2 position. *Trans*-**3.62a** was generated in a 65:35 diastereomeric ratio at the C2 position, as evidenced by the presence of a ^1H NMR resonance at 5.40 ppm (d, $J = 10.8$

Hz, 0.65 H) corresponding to H^a of the major C2 diastereomer, and a resonance at 5.32 ppm (d, $J = 10.8$ Hz, 0.35 H) corresponding to H^a of the minor C2 diastereomer (Figure 3.3A). Further evidence was provided via resonances at 5.58 ppm (s, 0.59 H) and 5.56 ppm (s, 0.30 H) corresponding to H^b of the major and minor diastereomers, respectively. Interestingly, *cis*-**3.62a** was formed as a single C2 diastereomer, as evidenced by a ¹H NMR resonance at 5.63 ppm (d, $J = 6.0$ Hz, 1H) corresponding to H^a, and a resonance at 5.44 ppm (s, 1H) corresponding to H^b (Figure 3.3B).

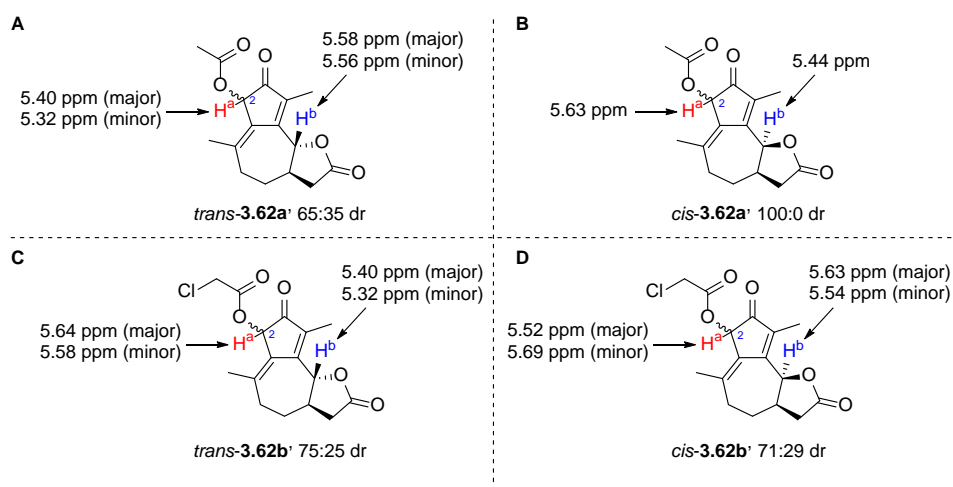


Figure 3.3. Chemical shift assignments for APKR C2 diastereomers.

Upon chromatographic separation of the lactone diastereomers of chloroacetate **3.62b**, it was found that *trans*-**3.62b** was formed in a 75:25 diastereomeric ratio at the C2 position; a slight enhancement over the 65:35 diastereomeric ratio observed for the acetate analog *trans*-**3.62a** (Figure 3.3C). Evidence of this was provided via ¹H NMR resonances at 5.64 ppm (s, 0.75H) and 5.58 ppm (s, 0.25H) corresponding to H^a of the major and minor C2 diastereomers, respectively. In addition, resonances at 5.40 ppm (d, $J = 10.8$ Hz, 0.75H) and 5.32 ppm (d, $J = 10.8$ Hz, 0.25H) were assigned as H^b of the major and minor diastereomers, respectively. Interestingly, it appeared

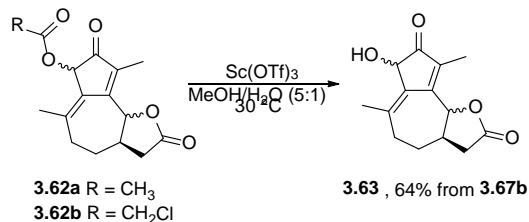
as though *cis*-**3.62b** had been generated in a 71:29 diastereomeric ratio at the C2 position, unlike the complete diastereoselectivity observed in the case of the acetate analog *cis*-**3.62a** (Figure 3.3D). Evidence for this was provided via ¹H NMR resonances at 5.69 ppm (s, 0.29H) and 5.52 ppm (s) corresponding to H^a of the minor and major C2 diastereomers, respectively, as well as resonances at 5.63 ppm (d, *J* = 6.0 Hz, 0.72H) and 5.54 ppm (d, *J* = 7.2 Hz) corresponding to H^b of the major and minor diastereomers, respectively. The origin of the differences in C2 diastereomeric outcome of *cis*-**3.62a** and *cis*-**3.62b** is still unclear.

With the success of the APKR on both allenyl carboxyesters **3.60a** and **3.60b**, the core carbon framework of (–)-dehydroleucodine was accessed in six linear steps, starting with a cheap, commercially available chiral pool material. We were now poised to deacetylate the C2 position and apply the isomerization conditions developed on the 2-hydroxy bicyclo[5.3.0]decadienone model system **2.59** to this system (see Chapter 2).

3.8 Hydrolysis of β-Keto Esters

With rapid access to lactone-containing α-acyloxy enones **3.62a** and **3.62b** in hand, we set out to apply the previously reported Sc(OTf)₃-catalyzed hydrolysis conditions to access the desired α-hydroxy enone **3.63** (Scheme 3.35).¹²⁹ Because of its slightly higher yielding APKR, the α-acetoxy enone **3.64a** was first subjected to the standard Sc(OTf)₃ conditions. Thus, **3.62a** was dissolved in MeOH/H₂O (5:1 v/v, 0.025 M). To this was added Sc(OTf)₃ (0.3 equiv) and the reaction maintained at 30 °C for 24 h. Analysis of the reaction mixture by TLC revealed that, while the desired hydrolysis product **3.63** appeared to be present in a small quantity, there was a substantial amount of starting material remaining, as well as multiple other reaction components.

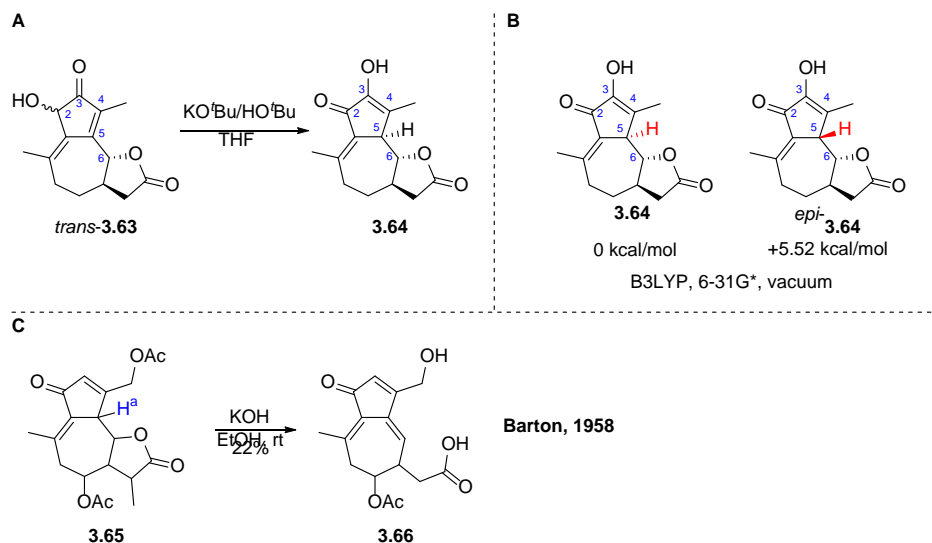
An additional portion of $\text{Sc}(\text{OTf})_3$ (1.7 equiv) was added and the reaction maintained for an additional 24 h. Despite the excess $\text{Sc}(\text{OTf})_3$, full conversion of **3.62a** was never achieved. In addition, the reaction profile was very complex, as visualized by the presence of multiple spots and streaks on TLC. We thus decided to shift our focus to the $\text{Sc}(\text{OTf})_3$ -mediated hydrolysis of



Scheme 3.35. Proposed hydrolysis of α -acyloxy enone **3.62a** or **3.62b** to access α -hydroxy enone **3.63**.

chloroacetate **3.62b**, which was shown to undergo hydrolysis at a significantly faster rate than the corresponding acetate (see Chapter 2). Thus, chloroacetate **3.62b** was dissolved in MeOH/H₂O (0.05 M, 5:1 v/v) and $\text{Sc}(\text{OTf})_3$ added. The reaction was maintained for 48 h, at which point it was deemed complete by TLC. It should be noted that the reaction time for the chloroacetoxy substrate **3.62b** is greatly increased with respect to our previous findings on chloroacetate **2.64b**. Upon workup and purification, 2-hydroxy enone **3.63** was isolated in 64% yield. The C2 diastereomers were not separated at this time. With the desired hydroxy enone **3.63** in hand, we were poised to apply the base-mediated isomerization conditions in an effort to transpose the C3-C5 enone to the C2-C4 position.

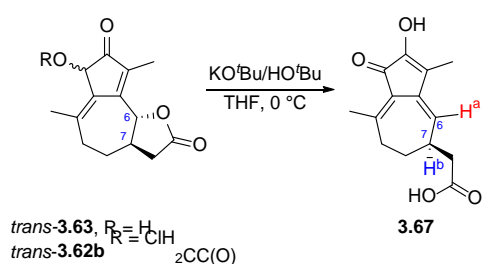
3.9 Base-Mediated Isomerization of α -Hydroxy Enone



Scheme 3.36. Proposed base-mediated isomerization of α -hydroxy enone **3.63** to α -keto enol **3.64**.

We wanted to examine the feasibility of applying the base-mediated isomerization conditions to each lactone diastereomer individually. With the assumption that the C5 diastereomeric outcome of the isomerization is under thermodynamic control (see Chapter 2), different C5 epimers could arise from the two lactone diastereomers. Barton showed that in the presence of potassium hydroxide, sesquiterpene lactone **3.65** underwent an elimination process to furnish acid **3.66**. This suggests that the pK_a of H^a is relatively low, lending support to the notion that the proposed isomerization process could proceed under thermodynamic control (Scheme 3.36C).¹³⁰ We thus proposed that base-mediated isomerization of *trans*-**3.63** would selectively afford the α -keto enol **3.64** with the desired stereochemistry at the C5 position (Scheme 3.36A). DFT calculations (B3LYP, 6-31G*, vacuum) supported this hypothesis, indicating that the desired C5 epimer of **3.64** was 5.52 kcal/mol more stable than its C5 epimer (Scheme 3.36B). With these predictions in hand, we set out to effect the base-mediated isomerization of *trans*-**3.63**.

Enone *trans*-**3.63** was dissolved in THF and cooled to 0 °C. Potassium *tert*-butoxide in *tert*-butanol (2 equiv of a 0.5 M solution) was added dropwise (Scheme 3.37). The mixture instantly turned dark yellow as a precipitate began to form. TLC revealed complete consumption of starting material to a baseline spot. The reaction was quenched with sat. aq. NH₄Cl, after which TLC indicated complete conversion of the baseline spot to another, slow-moving product. Upon workup and analysis of the crude residue via ¹H and ¹³C NMR, it was determined that the lactone at the C6



Scheme 3.37. Base-mediated isomerization/eliminative lactone opening of *trans*-3.63 and 3.62b.

position had opened via an elimination process, affording the acid **3.67** as the sole product. An alkenyl proton at 5.75 ppm (d, $J = 4.0$ Hz, 1H) was diagnostic of the C6 alkenyl proton H^a of **3.67**. In addition, the product consisted of only a single diastereomer as evidenced by the presence of only two methyl resonances (2.42 ppm and 2.00 ppm). A resonance at 3.04 ppm (m, 1H) provided evidence for C7 proton H^b. In addition to the ¹H NMR data, the ¹³C spectrum revealed a resonance at 189 ppm; confirming the presence of a ketone. Resonances at 177, 172, 155, 152, 134, 126, and 125 ppm suggested the presence of six olefinic carbons, as well as the carbonyl carbon of the carboxylic acid.

Application of these conditions to *trans*-**3.62b** also afforded acid **3.67**, thus confirming that a two-step, one-pot deprotection/isomerization process is possible as well. While the base-mediated isomerization conditions did not afford the desired product **3.64**, the

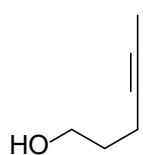
isomerization/eliminative lactone opening process to afford **3.67** did occur cleanly by TLC, and confirms that the C3-C5 enone of this more complex substrate can be transposed to the C2-C4 position.

3.10 Conclusions Towards the Total Synthesis of (-)-Dehydroleucodine (*ent*-**3.1**)

Starting with cheap chiral pool material (*R*)-linalool, we have shown that a C11 desmethyl 6,12-guaianolide framework can be accessed in an enantioselective fashion in six linear steps. The key APKR affords products with either a C2 methylenyl or acyloxy groups, enabling rapid access to fused cyclopentenones with two different oxidation states. Transposition of the C4-C5 double bond to the C3-C4 position was accomplished via hydrolysis of the 2-chloroacetoxy bicyclo[5.3.0]decadienone **3.62b**, followed by base-mediated isomerization affording **3.67**. However, ring-opening of the C6 lactone to generate the carboxylic acid occurred. Further optimization showed that both hydrolysis and isomerization reactions could be effected with potassium *tert*-butoxide in a single step. These conditions, while an effective method for the transposition of the C3-C5 enone motif of allenic Pauson-Khand adducts, afford the elimination product with ring-opening of the lactone, suggesting that this method is not applicable to substrates with leaving groups at the allylic C6 position.

Appendix A : Experimental Information for Chapter Two

General Methods. Unless otherwise indicated, all reactions were performed in flame-dried glassware under an atmosphere of dry nitrogen. All commercially available compounds used as received. Tetrahydrofuran (THF), dichloromethane (CH_2Cl_2), and diethyl ether (Et_2O) were purified by passing through alumina using the Sol-Tek ST-002 solvent purification system. Toluene was distilled over calcium hydride prior to use. Deuterated chloroform (CDCl_3) was dried over 3 Å molecular sieves prior to use. Gasses N_2 , H_2 , and CO were purchased from Matheson Tri Gas. Cerium chloride (anhydrous) was purchased and used as received. Flash column chromatography was performed using silica gel (40-63 μm particle size, 60 Å pore size). Thin-layer chromatography (TLC) was performed on silica gel F₂₅₄ glass-backed plates (250 μm thickness). ^1H and ^{13}C NMR were recorded on a Bruker Avance 400 MHz spectrometer. Spectra were referenced to residual chloroform (7.26 ppm, ^1H , 77.16 ppm, ^{13}C). Chemical shifts (δ) are reported in ppm and multiplicities are indicated by s (singlet), d (doublet), t (triplet), q (quartet), quint (quintet), and m (multiplet). Coupling constants, J , are reported in hertz (Hz). NMR spectra were obtained at room temperature. EI mass spectroscopy was performed on a Waters Micromass GCT high-resolution mass spectrometer, while ES mass spectroscopy was performed on a Waters Q-TOF Ultima API, Micromass UK Limited high-resolution mass spectrometer. IR spectra were obtained using a Nicolet Avatar E.S.P. 360 FT-IR.



Hex-4-yn-1-ol (2.10). To a 1-L, 3-necked round-bottom flask equipped with stir bar, nitrogen inlet adapter, thermometer adapter with thermometer, and septum was sequentially added hex-5-yn-1-ol (7.00 g, 71.3 mmol, 1.0 equiv) and DMSO (285

mL) via syringe. Potassium *tert*-butoxide (20.0 g, 178 mmol, 2.5 equiv) was added in a single portion by temporarily removing the septum. No temperature increase was observed upon addition of potassium *tert*-butoxide. The brown reaction mixture was maintained at rt for 4 h. Upon complete consumption of starting material, as evidenced by TLC, the flask was lowered into an ice/water bath (0 °C). The septum was replaced with an addition funnel containing 285 mL 1 N HCl which was added dropwise over the course of 20 min while maintaining an internal temperature between 20–30 °C. Upon complete addition, the mixture was transferred to a separatory funnel, the layers separated and the aqueous phase extracted with Et₂O (3 x 200 mL). The combined organic phases were dried over MgSO₄, filtered through a medium porosity fritted glass vacuum funnel, and concentrated via rotary evaporation. The crude residue was purified via SiO₂ flash column chromatography (40–70% Et₂O/hexanes) affording 5.75 g of the title compound as a clear yellow oil (82%). JEB03-122

Data for 2.10

¹H NMR: (400 MHz, CDCl₃)

3.75 (q, *J* = 5.6 Hz, 2H), 2.28–2.22 (m, 2H), 1.78 (t, *J* = 2.4 Hz, 3H), 1.73 (pent, *J* = 6.4 Hz, 2 H), 1.59–1.53 (m, 1 H) ppm;

¹³C NMR: (100 MHz, CDCl₃)

78.6, 76.4, 62.2, 31.7, 15.5, 3.6 ppm;

FTIR (neat)

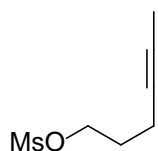
3328, 2921, 2874, 1436, 1350, 1329, 1175, 1054, 1034, 931, 909, 620, 551 cm⁻¹;

HRMS (HRMS ESI)

[M + H]⁺ calcd for C₆H₁₁O: 99.0804; found: 99.0835;

TLC $R_f = 0.18$ (40% Et₂O/hexanes)

Silica gel, visualized with p-anisaldehyde



Hex-4-yn-1-yl methanesulfonate (2.11). To a 250-mL, 2-necked round bottom flask equipped with stir bar, nitrogen inlet adapter, and septum was sequentially added hex-4-yn-1-ol **2.10** (5.60 g, 57.0 mmol, 1.0 equiv), CH₂Cl₂ (95 mL), and triethylamine (10.3 mL, 74.2 mmol, 1.3 equiv) via syringe. The flask was lowered into an ice/water bath (0 °C) and methanesulfonyl chloride (5.30 mL, 68.5 mmol, 1.2 equiv) was added dropwise over 5 min via syringe. Upon complete addition, the flask was removed from the ice/water bath and allowed to warm to rt at which it was maintained for 1.5 h. Upon complete consumption of starting material, as evidenced by TLC, the cloudy reaction mixture was transferred to a separatory funnel and washed with H₂O (2 x 100 mL). The layers were separated and the combined aqueous phases were extracted with CH₂Cl₂ (1 x 100 mL). The combined organic phases were dried over MgSO₄, filtered via medium porosity fritted glass vacuum filter, and concentrated via rotary evaporation. The crude residue was purified via SiO₂ flash column chromatography (60% Et₂O/hexanes), affording 9.80 g of the title compound as a pale-yellow oil (97%). JEB03-126

Data for 2.11

¹H NMR: (400 MHz, CDCl₃)

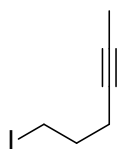
4.35 (t, $J = 6.4$ Hz, 2H), 3.02 (s, 3H), 2.33–2.26 (m, 2H), 1.90 (pent, $J = 6.4$ Hz, 2H), 1.78 (t, $J = 2.8$ Hz, 3H) ppm;

^{13}C NMR: (100 MHz, CDCl_3)
77.2, 76.9, 68.8, 37.4, 28.5, 15.1, 3.6 ppm;

FTIR (neat)
3028, 2923, 2855, 1439, 1348, 1332, 1169, 1089, 1007, 927, 924, 833, 792, 742, 526, 476 cm^{-1} ;

HRMS (HRMS ESI)
[$\text{M} + \text{H}$] $^+$ calcd for $\text{C}_7\text{H}_{13}\text{O}_3\text{S}$: 177.0579; found: 177.0577;

TLC $R_f = 0.49$ (60% Et_2O in hexanes)
Silica gel, visualized with p-anisaldehyde (mesylate stains purple)



6-iodo-hex-2-yne (2.8). To a 500-mL, 3-necked round bottom flask equipped with overhead stirrer, condenser with nitrogen inlet adapter, and septum was sequentially added sodium iodide (NaI) (20.6 g, 138 mmol, 2.5 equiv) and acetone (138 mL) via temporary removal of the septum. Upon complete dissolution of the NaI, hex-4-yn-yl methanesulfonate **2.11** (9.7 g, 55.0 mmol, 1.0 equiv) was added in a single portion via syringe. The flask was lowered into a preheated oil bath (65 °C) for 1.5 h, during which time a thick slurry formed. Upon complete consumption of the starting material, as evidenced by TLC, the flask was removed from the oil bath and allowed to cool to rt. Water was added (120 mL) via removal of the septum. The mixture transferred to a separatory funnel, the layers separated and the aqueous phase extracted with pentane (3 x 150 mL). The combined organic phases were dried over MgSO_4 , filtered via medium porosity fritted glass vacuum filter, and concentrated via rotary evaporation,

affording 11.0 g of the title compound as a pale-yellow oil (96%), which was taken on without further purification. JEB03-128

Data for 2.8

¹H NMR: (400 MHz, CDCl₃)

3.30 (t, *J* = 6.8 Hz, 2H), 2.29–2.23 (m, 2H), 1.95 (pent, *J* = 6.8 Hz, 2H), 1.78 (t, *J* = 2.4 Hz) ppm;

¹³C NMR: (100 MHz, CDCl₃)

76.9, 76.8, 32.5, 19.8, 5.7, 3.5 ppm;

FTIR (neat)

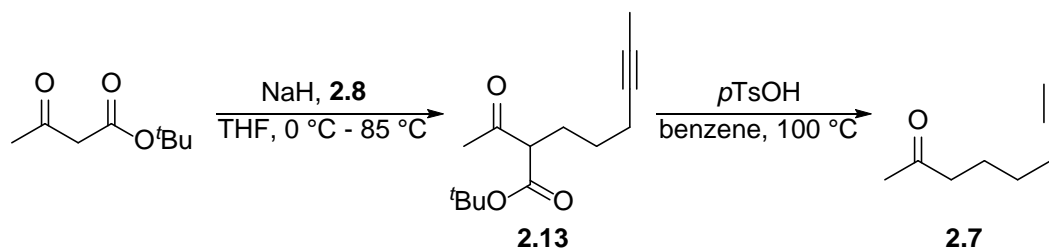
2917, 2841, 1430, 1347, 1245, 1221, 1167, 1155, 951, 847, 747, 607, 579, 532, 492 cm⁻¹;

HRMS (TOF MS ES+)

[M + H]⁺ calcd for C₆H₉I: 207.9749; found: 207.9735;

TLC R_f = 0.94 (30% Et₂O in hexanes)

Silica gel, visualized with KMnO₄



Non-7-yn-2-one (2.7). To a 250-mL, 2-necked round bottom flask equipped stir bar, condenser topped with nitrogen inlet adapter, and septum was added sodium hydride (NaH) (60% dispersion in mineral oil, 2.30 g, 58.0 mmol, 1.1 equiv) and THF (132 mL) via temporary removal of the septum. The flask was lowered into an ice/water bath (0 °C) and *tert*-butyl acetoacetate (10.5 mL 63.0 mmol, 1.2 equiv) was added dropwise over 20 min via syringe pump. Upon complete addition, the flask was removed from the ice/water bath and allowed to warm to rt, where it was maintained for 1 h. 6-Iodo-hex-2-yne **2.8** (11.0 g, 52.8 mmol, 1 equiv) was added in a single portion via syringe. The flask was lowered into a preheated oil bath (85 °C) and maintained for 18 h. Upon complete consumption of the starting material, as evidenced by TLC, the flask was removed from the oil bath and allowed to cool to rt. Sat. aq. NH₄Cl (100 mL) was added via removal of the septum, and the mixture was transferred to a separatory funnel. The layers were separated and the aqueous phase was extracted with Et₂O (2 x 50 mL). The combined organic phases were dried over MgSO₄, filtered via medium porosity fritted glass vacuum filter, and concentrated via rotary evaporation. The crude residue was transferred to a 250-mL 2-necked round bottom flask equipped with a condenser topped with nitrogen inlet adapter, and septum via syringe. Benzene (176 mL) and *p*-toluenesulfonic acid (2.00 g, 10.6 mmol, 0.2 equiv) were sequentially added via temporary removal of the septum. The flask was lowered into a preheated oil bath (100 °C) and maintained for 2 h at which point complete consumption of *t*-butyl acetoacetate **2.13** was observed via TLC. The flask was removed from the oil bath, allowed to cool to rt, transferred to a separatory funnel,

and washed with sat. aq. NaHCO₃ (1 x 100 mL), then brine (1 x 100 mL). The combined aqueous phases were extracted with Et₂O (2 x 100 mL), dried over MgSO₄, filtered via medium porosity fritted glass vacuum filter, and concentrated via rotary evaporation. The crude residue was purified via SiO₂ flash column chromatography (10%–20% Et₂O/hexanes) to afford 6.60 g of the title compound as a yellow oil (90%). JEB03-129

Data for 2.7

¹H NMR: (400 MHz, CDCl₃)

2.44 (t, *J* = 7.6 Hz, 2H), 2.16–2.10 (m, 2H), 2.14 (s, 3H), 1.77 (t, *J* = 2.4 Hz, 3H),
1.71–1.62 (m, 2H), 1.51–1.42 (m, 2H) ppm;

¹³C NMR: (100 MHz, CDCl₃)

209.0, 78.8, 76.0, 43.4, 30.0, 28.6, 23.2, 18.7, 3.6 ppm;

FTIR (neat)

2922, 2862, 1713, 1436, 1358, 1220, 1158, 952, 730, 592, 516 cm⁻¹;

HRMS (HRMS ESI)

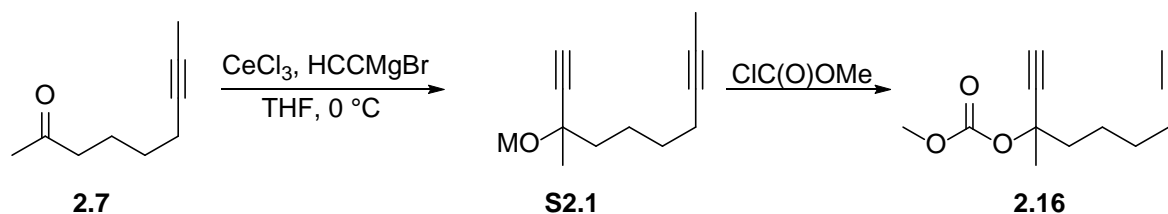
[M + H]⁺ calcd for C₉H₁₅O: 139.1117; found: 139.1113;

TLC R_f (**2.13**) = 0.41 (20% Et₂O/hexanes)

Silica gel, visualized with p-anisaldehyde

R_f (**2.7**) = 0.28 (20% Et₂O/hexanes)

Silica gel, visualized with p-anisaldehyde



Methyl (3-methyldeca-1,8-diyn-3-yl) carbonate (2.16). To a 250 mL, 3-necked round bottom flask equipped with stir bar, 125-mL addition funnel topped with septum, nitrogen inlet adapter, and septum was added anhydrous CeCl_3 (4.99 g, 20.3 mmol, 1.4 equiv) in a nitrogen-filled glovebox. The flask was removed from the glovebox and THF (145 mL) was added via syringe. The white suspension was allowed to stir under nitrogen at rt for 24 h at which point the flask was lowered into an ice/water bath (0°C). Ethynylmagnesium bromide (0.5 M solution in THF, 40.5 mL, 20.3 mmol, 1.4 equiv) was cannulated into the addition funnel, and then added dropwise to the flask over a period of 10 min. The resulting brown suspension was maintained at 0°C for 1.5 h, at which point non-7-yn-2-one **2.7** (2.00 g, 14.5 mmol, 1 equiv) was added in a single portion via syringe. The reaction was maintained at 0°C for 30 min until complete consumption of starting material was observed by TLC. Methyl chloroformate (2.24 mL, 28.9 mmol, 2 equiv) was added in a single portion via syringe and the flask was removed from the ice/water bath and warmed to rt, where it was maintained for 2 h. Upon complete consumption of intermediate **S2.1**, as evidenced by TLC, sat. aq. NH_4Cl was added (50 mL) via syringe, and the mixture transferred to a separatory funnel. Et_2O (150 mL) was added, the layers separated and the aqueous phase extracted with Et_2O (3 x 75 mL). The combined organic phases were dried over MgSO_4 , filtered via medium porosity fritted glass vacuum filter, and concentrated via rotary evaporation. The crude residue was purified via SiO_2 flash column chromatography (20% Et_2O /hexanes) to afford 3.18 g of the title compound as a yellow oil (98%). JEB03-163

Data for 2.16

¹H NMR: (400 MHz, CDCl₃)

3.77 (s, 3H), 2.58 (s, 1H), 2.18–2.11 (m, 2H), 2.00–1.92 (m, 1H), 1.88–1.79 (m, 1H), 1.77 (t, *J* = 2.4 Hz, 3H), 1.71 (s, 3H), 1.66–1.46 (m, 4H) ppm;

¹³C NMR: (100 MHz, CDCl₃)

153.7, 83.3, 78.9, 77.1, 75.9, 74.0, 54.5, 41.0, 29.0, 26.4, 23.5, 18.8, 3.6 ppm;

FTIR (neat)

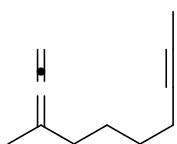
3283, 2952, 2863, 1751, 1439, 1376, 1256, 1163, 1088, 1028, 1013, 943, 869, 790, 663, 598, 582, 555 cm⁻¹;

HRMS (HRMS ESI)

[*M* + *H*]⁺ calcd for C₁₃H₁₉O₃: 223.1328; found: 223.1331;

TLC R_f = 0.68 (40% Et₂O/hexanes)

Silica gel, visualized with *p*-anisaldehyde



3-methyldeca-1,3-dien-8-yne (2.1). To a 250-mL, 2-necked round bottom flask

equipped with stir bar, septum, and nitrogen inlet adapter was sequentially added

ammonium formate (0.91 g, 14.4 mmol, 2 equiv), THF (58 mL) and

Pd₂dba₃•CHCl₃ (0.19 g, 0.18 mmol, 0.025 equiv) via temporary removal of the septum. To the red

reaction mixture was added tri-*n*-butylphosphine (0.23 mL, 0.90 mmol, 0.125 equiv) [CAUTION:

toxic, handle with care] via syringe, at which point the mixture turned yellow-green. The reaction

mixture was maintained at rt for 10 min before methyl (3-methyldeca-1,8-diyn-3-yl) carbonate

2.16 (1.6 g, 7.2 mmol, 1 equiv) was added in a single portion via syringe. The reaction was

maintained at rt for 18 h until complete consumption of the starting material was observed by TLC.

The mixture was filtered through a pad celite in a medium porosity fritted glass vacuum filter. The celite pad was rinsed with pentane (3 x 20 mL). The combined filtrates were evaporated via rotary evaporation and the crude residue purified via SiO₂ flash column chromatography (2% Et₂O/pentane) to afford 0.99 g of the title compound as a yellow oil (92%). The yellow color was removed by elution through a Silicycle FLH-R10030B-ISO40 SiliaSep™ 40g silica cartridge (100% pentane), affording 0.94 g of the title compound as a colorless oil; though this is not necessary for the success of the allenic Pauson-Khand reaction. JEB03-169

Data for 2.1

¹H NMR: (400 MHz, CDCl₃)

4.58 (sextet, *J* = 4.0 Hz, 2H), 2.16–2.10 (m, 2H), 1.94 (sept, *J* = 3.6 Hz, 2H), 1.78 (t, *J* = 3.6 Hz, 3H), 1.67 (t, *J* = 4.0 Hz, 3H), 1.54–1.48 (m, 4H) ppm;

¹³C NMR: (100 MHz, CDCl₃)

206.3, 98.3, 79.4, 75.6, 74.1, 33.1, 28.8, 26.7, 18.8, 18.7, 3.6 ppm;

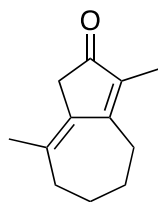
FTIR (neat)

2980, 2935, 2859, 1960, 1440, 1370, 1331, 1001, 845, 612, 590, 502;

TLC R_f = 0.74 (10% Et₂O/hexanes)

R_f = 0.40 (100% hexanes)

Silica gel, visualized with KMnO₄



3,8-dimethyl-4,5,6,7-tetrahydroazulen-2(1H)-one (2.2) (Table 2.2, Entry 6). A

15-mL 2-necked round bottom flask equipped with stir bar, condenser topped with a septum, and septum was sequentially charged with bis(1,5-

cyclooctadiene)rhodium(I) tetrafluoroborate (7 mg, 0.02 mmol, 0.025 equiv) and PPh₃ (7 mg, 0.02 mmol, 0.038 equiv) in a nitrogen-filled glovebox via temporary removal of the septum. The flask was removed from the glove box and a nitrogen inlet needle was inserted into the septum on the condenser. 1,2-Dichloroethane (6.8 mL) was added via syringe. The resulting dark yellow solution was maintained at rt for 10 min at which time the flask was evacuated and refilled five times with CO gas (100%), alternating between an inlet needle attached to a vacuum and an inlet needle attached to a balloon of CO. The light-yellow solution was maintained for 10 min before 3-methyldeca-1,3-dien-8-yne **2.1** (0.10 g, 0.67 mmol, 1 equiv) was added in a single portion via syringe. The flask was lowered into a preheated oil bath (70 °C) and maintained for 20 h until complete consumption of the starting material was observed by TLC. The flask was removed from the oil bath, allowed to cool to rt, and the contents transferred to a 200-mL recovery flask. The solvent was evaporated via rotary evaporation (40 °C bath temperature) and the crude residue was purified via SiO₂ flash column chromatography (20–40% Et₂O/hexanes) to afford 0.102 g of the title compound as a yellow oil which solidifies in the freezer (86%).

Data for 2.2

¹H NMR: (400 MHz, CDCl₃)
2.91 (s, 2H), 2.72–2.66 (m, 2H), 2.41–2.36 (m, 2H), 1.84 (s, 3H), 1.83–1.76 (m, 4H), 1.75 (t, 3H) ppm;

¹³C NMR: (100 MHz, CDCl₃)
205.0, 168.8, 137.7, 136.6, 131.6, 40.8, 35.7, 29.6, 26.9, 24.5, 24.2, 8.4 ppm;

FTIR (neat)

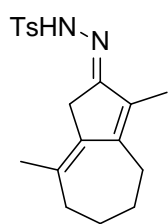
2924, 2860, 1682, 1597, 1579, 1449, 1422, 1389, 1331, 1276, 1218, 1159, 1119, 1090, 1071, 1050, 1002, 953, 916, 874, 845, 771, 680, 657, 637, 616, 560, 537, 509 cm^{-1} ;

HRMS (HRMS ESI)

$[\text{M} + \text{H}]^+$ calcd for $\text{C}_{12}\text{H}_{17}\text{O}$: 177.1273; found: 177.1269;

TLC $R_f = 0.28$ (40% Et_2O /hexanes)

Silica gel, visualized with KMnO_4



(E)-N'-(3,8-dimethyl-4,5,6,7-tetrahydroazulen-2(1H)-ylidene)-4-methylbenzenesulfonohydrazide (2.6). To a 10–20-mL microwave vial (Biotage 354833) equipped with a stir bar (Biotage 353930) was added tosyl hydrazide (0.38 g, 2.0 mmol, 1.2 equiv). The vial was sealed with a microwave vial cap with septum

(Biotage 352298), purged via nitrogen inlet needle, and ethanol (8.5 mL) was added via syringe. 3,8-Dimethyl-4,5,6,7-tetrahydroazulen-2(1H)-one **2.2** (0.57 g, 1.7 mmol, 1.0 equiv) was dissolved in EtOH (1 mL) and added to the vial via syringe. The nitrogen inlet needle was removed and the sealed vial was lowered into a preheated oil bath (85 °C) and maintained for 18 h, at which point complete consumption of starting material was observed by TLC. The vial was removed from the oil bath, allowed to cool to rt, and the contents transferred to a 25-mL recovery flask. The solvent was evaporated via rotary evaporation (40 °C bath temperature) and the crude residue purified via SiO_2 flash column chromatography (40%-75% Et_2O /hexanes), affording 0.45 g of the title compound as a yellow solid (77%).

Data for 2.6

¹H NMR: (400 MHz, CDCl₃)

7.88 (d, *J* = 8.4 Hz, 2H), 7.29 (d, *J* = 8.0 Hz, 2H), 7.13 (s, 1H), 2.89 (s, 3H), 2.56–2.50 (m, 2H), 2.41 (s, 3H), 2.32–2.27 (m, 2H), 1.77 (s, 3H), 1.75 (s, 3H), 1.74–1.62 (m, 4H) ppm;

¹³C NMR: (100 MHz, CDCl₃)

164.1, 154.8, 143.9, 136.0, 135.6, 133.1, 132.1, 129.5, 128.2, 35.8, 32.3, 28.7, 27.5, 25.0, 23.7, 21.7, 9.6 ppm;

FTIR (neat)

3208, 2923, 2859, 1597, 1399, 1332, 1164 cm⁻¹;

HRMS (HRMS ESI)

[M + H]⁺ calcd for C₁₉H₂₅O₂N₂S: 345.1631; found: 345.1623;

m.p. 168.0–173.1 °C

TLC R_f = 0.29 (40% Et₂O/hexanes)

Silica gel, visualized with KMnO₄

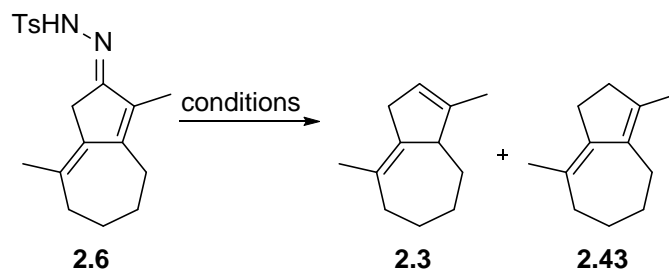


Table 2.5 Entry 1. To a 2–5 mL microwave vial (Biotage 351521) equipped with stir bar (Biotage 355543) was added N¹-(3,8-dimethyl-4,5,6,7-tetrahydroazulen-2(1H)-ylidene)-4-methylbenzenesulfonohydrazide **2.6** (0.090 g, 0.26 mmol, 1 equiv). The vial was sealed with a crimp-on microwave vial cap with septum (Biotage 352298) and purged with N₂ via nitrogen inlet needle. CDCl₃ (0.87 mL) was added via syringe. The vial was lowered into an ice/water bath (0 °C) and catecholborane (1 M in THF, 0.78 mL, 0.78 mmol, 3 equiv) was added dropwise over 1 min via syringe. The reaction was maintained for 1 h, at which point the cap was removed from the vial and NaOAc·3H₂O (0.106 g, 0.78 mmol, 3 equiv) was added in a single portion. A new cap was placed onto the vial and the reaction warmed to room temperature where it was maintained for 1 h. An additional volume of CDCl₃ (0.80 mL) was added as the mixture began to gel. The mixture was maintained for 1 h then lowered into a preheated oil bath (70 °C). After reacting for 1 h, the vial was removed from the oil bath and allowed to cool to room temperature, then filtered through a celite plug. The filtrate was concentration via rotary evaporation and purified via SiO₂ flash column chromatography (15% Et₂O/hexanes), affording 21 mg of a yellow oil (49%). ¹H NMR analysis of this oil revealed a **2.3** to **2.43** ratio of 43:57.

Table 2.5 Entry 2. To a 2–5 mL microwave vial (Biotage 351521) equipped with stir bar (Biotage 355543) was charged N'-(3,8-dimethyl-4,5,6,7-tetrahydroazulen-2(1H)-ylidene)-4-methylbenzenesulfonohydrazide **2.6** (0.050 g, 0.15 mmol, 1 equiv). The vial was sealed with a crimp-on microwave vial with septum (Biotage 352298) and purged with nitrogen via a nitrogen inlet needle. THF (1.5 mL) was added via syringe. The vial was lowered into an ice/water bath (0 °C) and catecholborane (1 M in THF, 0.73 mL, 0.73 mmol, 5 equiv) was added dropwise over 1 min via syringe. The yellow solution was maintained for 3 h, at which point the cap was removed from the vial and NaOAc·3H₂O (0.106 g, 0.78 mmol, 3 equiv) was added in a single portion. A new cap was placed onto the vial which was then lowered into a preheated oil (70 °C) where it was maintained for 1 h. The vial was removed from the oil bath and allowed to cool to room temperature, then filtered through a medium porosity fritted glass vacuum filter which was filled with celite. The filtrate was concentrated via rotary evaporation. The crude residue was purified via SiO₂ flash column chromatography (30% Et₂O/hexanes), affording 7 mg of a yellow oil (30%). ¹H NMR analysis of this oil revealed a **2.3** to **2.43** ratio of 79:21.

Data for **2.3** (79:21 ratio **2.3/2.43**)

¹H NMR: (400 MHz, CDCl₃)

5.35 (m, 1H), 3.03 (d, *J* = 11.2 Hz, 1H), 2.99–2.84 (m, 2H), 2.07–1.84 (m, 4H), 1.77–1.69 (m, 2H), 1.68 (s, 3H), 1.64 (s, 3H), 1.63–1.53 (m, 2H), 1.31–1.16 (m, 2H), 1.01–0.87 (m, 1H) ppm;

¹³C NMR: (100 MHz, CDCl₃)

73.2, 70.3, 60.0, 52.8, 16.4, 33.0, 33.7, 37.5, 36.8, 43.0, 47.8 54.7 ppm;

TLC $R_f = 0.96$ (40% Et₂O in hexanes)
Silica gel, visualized with KMnO₄

Table 2.5 Entry 3. To a 2–5 mL microwave vial (Biotage 351521) equipped with stir bar (Biotage 355543) was charged with benzoic acid (0.181 g, 1.5 mmol, 10.2 equiv). The vial was sealed with a crimp-on microwave vial cap with septum (Biotage 352298) and purged with nitrogen via a nitrogen inlet needle. CDCl₃ (0.48 mL) was added via syringe. The vial was lowered into an ice/water bath (0 °C) and BH₃ (1 M in THF, 0.73 mL, 0.73 mmol, 5 equiv) was added dropwise over 2 min via syringe, maintaining gentle bubbling. After reacting for 1 h, (E)-N'-(3,8-dimethyl-4,5,6,7-tetrahydroazulen-2(1H)-ylidene)-4-methylbenzenesulfonohydrazide **2.6** (0.050 g, 0.15 mmol, 1 equiv) was dissolved in CDCl₃ (0.30 mL) and added to the reaction mixture via syringe. The reaction was maintained for 3 h at 0 °C, at which point the cap was removed from the vial and NaOAc·3H₂O (0.138 g, 1.02 mmol, 7 equiv) was added in a single portion. A new cap was placed on the vial, which was then lowered into a preheated oil bath (70 °C). After reacting for 1 h, the vial was removed from the oil bath and allowed to cool to room temperature. The contents of the vial were transferred to a separatory funnel and washed with sat. aq. Na₂CO₃ (2 x 2 mL). The layers were separated and the organic phase dried over MgSO₄, concentrated via rotary evaporation, and purified via SiO₂ flash column chromatography (100% hexanes), affording 9 mg of a yellow oil (38%). ¹H NMR analysis of this oil revealed a **2.3** to **2.43** ratio of 4:96.

Data for 2.43 (4:96 ratio 2.3/2.43)

¹H NMR: (400 MHz, CDCl₃)

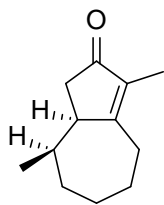
2.45–2.35 (m, 4H), 2.34–2.28 (m, 2H), 2.24 (t, *J* = 5.6 Hz, 2H), 1.78–1.71 (m, 2H)
1.71 (s, 3H), 1.69 (s, 3H), 1.65–1.58 (m, 2H) ppm; Impurities: 5.75–5.73 (m,
0.17H), 3.05–3.00 (m, 0.08H), 2.93–2.88 (m, 0.13H), 2.81–2.77 (m, 0.41H), 2.70–
2.62 (m, 0.29H), 1.96–1.88 (m, 1.07H), 1.30–1.22 (m, 1.52H), 1.22–1.78 (m,
0.94H), 1.04–0.99 (m, 0.33H), 0.97–0.92 (m, 0.29H), 0.91–0.80 (m, 1.00H) ppm;

¹³C NMR: (100 MHz, CDCl₃)

141.9, 139.7, 138.0, 123.5, 35.51, 35.50, 29.4, 28.5, 27.4, 26.0, 23.1, 15.1 ppm;
Impurities: 155.5, 142.0, 135.4, 119.7, 43.9, 3.5, 35.4, 29.9, 29.7, 27.5, 20.6, 13.6
ppm;

TLC R_f = 0.96 (15% Et₂O in hexanes)

Silica gel, PAA



3,8-dimethyl-4,5,6,7,8,8a-hexahydroazulen-2(1H)-one (2.35). A 25-mL two-necked round bottom flask equipped with stir bar, nitrogen inlet adapter, and septum, was charged with palladium on carbon (10% Pd, 0.18 g, 0.17 mmol, 0.1 equiv) via temporary removal of the septum. Ethyl acetate (3.4 mL) was added via syringe. 3,8-dimethyl-4,5,6,7-tetrahydroazulen-2(1H)-one **2.2** (0.300 g, 1.7 mmol, 1 equiv) was dissolved in methanol (13.6 mL) and added to the flask via syringe. A balloon filled with hydrogen gas (100%) was attached to a needle, and the needle inserted through the septum and into the reaction mixture. Hydrogen was bubbled through the mixture while being allowed to vent through the nitrogen inlet adapter at rt for 20 min. A small aliquot of the reaction mixture (0.1 mL) was removed via syringe,

filtered through a small plug of celite in a cotton-filled pipette, and concentrated via rotary evaporation. The residue was dissolved in CDCl_3 and subjected to ^1H NMR, which revealed complete consumption of starting material. After reacting for a total of 30 min, the reaction mixture was filtered through a celite-filled (6 x 4 cm) medium porosity fritted glass vacuum filter, and the filtrate concentrated via rotary evaporation. The crude residue was purified via SiO_2 flash column chromatography (20–40% Et_2O /hexanes), affording 0.272 g of the title compound as a colorless oil (90%).

Data for 2.35

^1H NMR: (400 MHz, CDCl_3)

3.09–3.03 (m, 1H), 2.76–2.67 (m, 1H), 2.53 (dd, $J^1 = 18.8$ Hz, $J^2 = 6.4$ Hz, 1H),
2.47–2.37 (m, 1H), 2.14–2.07 (m, 1H). 2.02 (dd, $J^1 = 18.4$ Hz, $J^2 = 1.2$ Hz, 1H),
1.80–1.72 (m, 2H), 1.70–1.63 (m, 5H), 1.61–1.43 (m, 3H), 0.69 (d, $J = 7.2$ Hz, 3H)
ppm;

^{13}C NMR: (100 MHz, CDCl_3)

208.8, 177.6, 137.2, 46.4, 40.8, 36.3, 35.6, 31.8, 26.6, 26.5, 13.9, 8.0 ppm;

FTIR (neat)

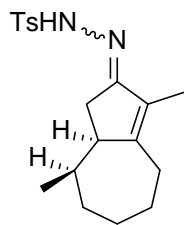
2918, 2867, 1691, 1630, 1453, 1380, 1358, 1312 cm^{-1} ;

HRMS (HRMS ESI)

$[\text{M} + \text{H}]^+$ calcd for $\text{C}_{12}\text{H}_{19}\text{O}$: 179.1430; found: 179.1428;

TLC $R_f = 0.28$ (40% Et_2O /hexanes)

Silica gel, visualized with KMnO_4



N'-(3,8-dimethyl-4,5,6,7,8,8a-hexahydroazulen-2(1H)-ylidene)-4-methylbenzenesulfonylhydrazide (2.36). A 2–5 mL microwave vial (Biotage

351521) equipped with a stir bar (Biotage 353930) was charged with *p*-toluenesulfonyl hydrazide (104 mg, 0.56 mmol, 2 equiv). The vial was sealed with

a crimp-on microwave vial cap with septum (Biotage 352298) and purged with nitrogen via nitrogen inlet needle. EtOH was added via syringe, followed by 3,8-dimethyl-4,5,6,7,8,8a-hexahydroazulen-2(1H)-one **2.35** (50 mg, 0.28 mmol, 1 equiv) which had been dissolved in EtOH (0.4 mL) via syringe. The nitrogen inlet needle was removed and the sealed vial lowered into a preheated oil bath (85 °C) where it was maintained for 18 h. Upon complete consumption of starting material, as evidenced by TLC, the vial was removed from the oil bath and allowed to cool to rt. The contents were transferred to a 10-mL recovery flask and concentrated via rotary evaporation. The crude residue was purified via SiO₂ flash column chromatography (20%–40% Et₂O/hexanes), affording 90 mg of the title compound as a white solid (93%). The isomeric ratio of the hydrazone was determined to be 29:71 based on the integrations of the methyl doublets at 0.97 ppm and 0.62 ppm, respectively; though we did not separate the major and minor isomers.

Data for 2.36

¹H NMR: (400 MHz, CDCl₃, *major isomer, **minor isomer)

7.90–7.85 (m, 2H), 7.30 (d, *J* = 8.0 Hz, 2H), 6.90–6.84 (m, 1H), 3.02–2.97 (m, 0.71H), 2.59–2.44 (m, 2.17H), 2.42 (s, 3.13H), 2.40–2.34 (m, 0.65H), 2.04–1.88 (m, 1.90H), 1.86–1.79 (m, 0.41H), 1.70–1.61 (m, 5.03H), 1.60–1.52 (m, 1.76H), 1.53–1.40 (m, 2.50H), 1.32–1.22 (0.97H), 0.97** (d, *J* = 6.4 Hz, 0.87H), 0.62* (d, *J* = 7.2 Hz, 2.13H) ppm;

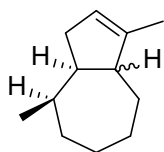
^{13}C NMR: (100 MHz, CDCl_3 , *major isomer, **minor isomer)
168.1*, 167.6**, 160.7**, 160.4*, 143.89**, 143.87*, 135.6, 133.1, 132.3**,
129.5, 128.31**, 128.29*, 52.6**, 49.2*, 40.8**, 36.6**, 36.2*, 36.0, 32.8**,
31.4*, 30.3*, 28.8**, 27.4**, 27.0*, 26.8*, 25.0**, 22.6**, 21.7*, 13.9*, 9.1* ppm;

FTIR (neat)
3213, 2912, 1619, 1443, 1402, 1387, 1334, 1308, 1289, 1186, 1163, 1089, 1019,
927, 811, 769, 733, 704, 669, 623, 596, 575, 546, 500, 458 cm^{-1} ;

HRMS (HRMS ESI)
[M + H]⁺ calcd for $\text{C}_{19}\text{H}_{27}\text{O}_2\text{N}_2\text{S}$: 347.1788; found: 347.1778;

m.p. 133.2-135.4 °C

TLC $R_f = 0.23$ (30% Et_2O /hexanes)
Silica gel, visualized with KMnO_4



3,8-dimethyl-1,3a,4,5,6,7,8,8a-octahydroazulene (2.38) (Table 2.4, Entry 8). A 0.5–2 mL microwave vial (Biotage 352016) equipped with stir bar (Biotage 355544) was charged with N¹-(3,8-dimethyl-4,5,6,7,8,8a-hexahydroazulen-2(1H)-ylidene)-4-methylbenzenesulfonohydrazide **2.36** (50 mg, 0.14 mmol, 1 equiv). The vial was sealed with a crimp-on microwave vial cap (Biotage 352298) and flushed with N_2 via an inlet needle. CDCl_3 (0.72 mL) was added via syringe and the vial lowered into an ice/water (0 °C) bath. Catecholborane (0.72 mL of a 1 M solution in THF, 0.72 mmol, 5 equiv) was added dropwise over 1 min, and the reaction maintained for 3 h. $\text{NaOAc}\cdot 3\text{H}_2\text{O}$ (87 mg, 1.01 mmol, 7 equiv) was added via removal of the microwave vial cap. A new cap was placed onto the vial, which was removed from the ice/water bath and lowered into a preheated oil bath (70 °C). The white mixture was

maintained for 1 h before the vial was removed from the oil bath and cooled to rt. The contents were transferred to a separatory funnel, diluted with Et₂O (2 mL), and washed with sat. NaHCO₃ (2 x 2 mL). The phases were separated and the combined aqueous phases extracted with Et₂O (2 x 2 mL). The combined organic phases were dried over MgSO₄, filtered through a cotton plug, and concentrated via rotary evaporation. The crude residue was purified via SiO₂ flash column chromatograph (10% Et₂O/hexanes) affording 12 mg of the title compound as a colorless oil (48%) as a 63:37 diastereomeric ratio.

Data for 2.38

¹H NMR: (400 MHz, CDCl₃)

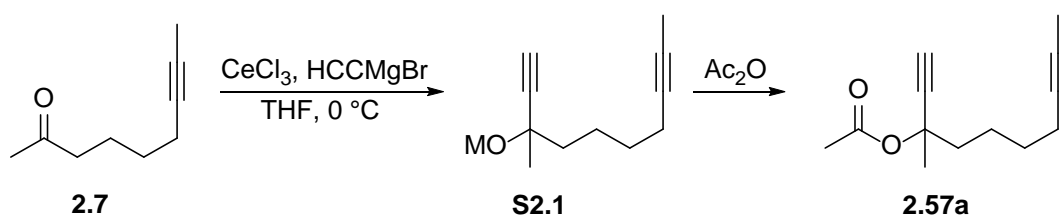
5.30–5.27 (m, 0.37H), 5.27–5.24 (m, 0.63H), 2.43–2.23 (m, 2.39H), 2.19–2.13 (m, 1.44H), 2.07–1.97 (m, 1.29H), 1.97–1.84 (m, 1.96H), 1.83–1.71 (m, 1.68H), 1.70–1.64 (0.91H), 1.63–1.60 (m, 3.08H), 1.59–1.47 (m, 2.53H), 1.47–1.39 (m, 1.53H), 1.38–1.15 (m, 2.46H), 1.09–0.93 (m, 1.48H), 0.91 (d, *J* = 6.4 Hz, 1.12H), 0.82 (d, *J* = 6.4 Hz, 2.08H) ppm;

¹³C NMR: (100 MHz, CDCl₃)

143.7, 143.3, 123.5, 123.3, 53.2, 51.2, 48.6, 46.3, 38.9, 38.4, 38.24, 38.22, 34.8, 33.3, 32.4, 32.6, 30.0, 29.1, 23.6, 23.4, 21.9, 16.8, 15.2, 15.1 ppm;

TLC R_f = 0.94 (40% Et₂O/hexanes)

Silica gel, visualized with KMnO₄



(R)-3-methyldeca-1,8-diyne-3-yl acetate (2.57a). To a 50-mL 2-necked round bottom flask equipped with stir bar and two septa was added anhydrous CeCl_3 (1.25 g, 5.1 mmol, 1.4 equiv) in a nitrogen-filled glove box, via temporary removal of a septum. The flask was removed from the glovebox and one of the septa was replaced with a nitrogen inlet adapter. THF (14 mL) was added via syringe and the resulting suspension was stirred under N_2 at rt for 18 h. The flask was lowered into an ice/water bath (0°C) and ethynylmagnesium bromide (10.1 mL of a 0.5 M solution in THF, 5.1 mmol, 1.4 equiv) was added dropwise over 10 min via syringe. The resulting brown suspension was maintained at 0°C for 1 h, at which point non-7-yn-2-one **2.7** (0.50 g, 3.6 mmol, 1 equiv) was added dropwise over 2 min via syringe. After reacting for 10 min at 0°C , complete consumption of starting material was observed by TLC. Acetic anhydride (1.03 mL, 10.9 mmol, 3 equiv) was added in a single portion via syringe, and the mixture maintained at 0°C for 20 min, over which time the reaction mixture partially gelled. Upon complete consumption of intermediate **S2.1**, as evidenced by TLC, sat. aq. NH_4Cl was added via syringe and the mixture transferred to a separatory funnel. The layers were separated and the aqueous phase extracted with Et_2O (3 x 50 mL). The combined organic phases were dried over MgSO_4 , filtered through a medium porosity fritted glass vacuum funnel, and concentrated via rotary evaporation. The crude residue was purified via SiO_2 flash column chromatography (5% Et_2O /hexanes) affording 0.71 g of the title compound as a yellow oil (94%).

Data for 2.57a

¹H NMR: (400 MHz, CDCl₃)

2.55 (s, 1H), 2.19–2.12 (m, 2H), 2.03 (s, 3H), 1.98–1.90 (m, 1H), 1.85–1.79 (m, 1H), 1.78 (t, *J* = 2.4 Hz, 3H), 1.67 (s, 3H), 1.62–1.48 (m 4H) ppm;

¹³C NMR: (100 MHz, CDCl₃)

169.5, 84.0, 79.0, 75.8, 74.9, 73.4, 41.0, 29.0, 26.5, 23.5, 22.1, 18.8, 3.6 ppm;

FTIR (neat)

3279, 2940, 2864, 1742, 1438, 1368, 1237, 1166, 1097, 1015, 943, 851, 660, 611, 536 cm⁻¹;

HRMS (HRMS ESI)

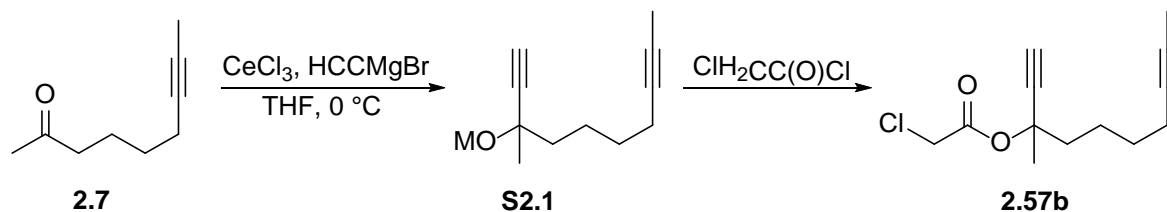
[*M* + *H*]⁺ calcd for C₁₃H₁₉O₂: 207.13796; found: 207.13838;

TLC R_f (**S2.1**) = 0.07 (10% Et₂O/hexanes)

Silica gel, visualized with p-anisaldehyde

R_f (**2.57a**) = 0.34 (10% Et₂O/hexanes)

Silica gel, visualized with p-anisaldehyde)



3-methyldeca-1,8-diyne-3-yl 2-chloroacetate (2.57b). A 250-mL 3-necked round bottom flask equipped with stir bar, 100-mL addition funnel topped with septum, and two septa was charged

with anhydrous CeCl_3 (4.64 g, 18.8 mmol, 1.3 equiv) in a nitrogen-filled glovebox. The flask was removed from the glovebox and one of the septa replaced with a nitrogen inlet adapter. THF (110 mL) was added via temporary removal of the septum, and the resulting white suspension stirred under N_2 at rt for 18 h. The flask was lowered into an ice/water bath (0 °C). Ethynylmagnesium bromide (34.7 mL of a 0.5 M solution in THF, 17.4 mmol, 1.2 equiv) was cannulated into the addition funnel, then added dropwise to the flask over 20 min. Upon complete addition, the resulting brown suspension was maintained for 1.5 h at 0 °C, at which point Non-7-yn-2-one **2.7** (2.00 g, 14.5 mmol, 1 equiv) was added dropwise over 2 min via syringe. Complete consumption of starting material was evidenced by TLC after 15 min. Chloroacetyl chloride (1.73 mL, 21.7 mmol, 1.5 equiv) was added dropwise over 2 min via syringe. The flask was removed from the ice/water bath and allowed to warm to rt, where it was maintained for 2 h. Upon complete consumption of intermediate **S2.1**, as evidenced by TLC, sat. aq. NH_4Cl was added (~100 mL) via removal of the septum, and the mixture transferred to a 500-mL separatory funnel. The layers were separated and the aqueous phase extracted with Et_2O (~100 mL x 2). The combined organic phases were dried over MgSO_4 , filtered through a medium porosity fritted glass vacuum funnel, and concentrated via rotary evaporation. The crude residue was purified via SiO_2 flash column chromatography (10–20% Et_2O /hexanes) affording 3.17 g of the title compound as a yellow oil (91%).

Data for **2.57b**

^1H NMR: (400 MHz, CDCl_3)

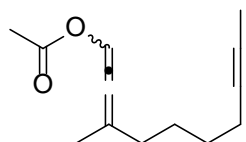
4.02 (s, 2H), 2.60 (s, 1H), 2.19–2.12 (m, 2H), 2.03–1.93 (m, 1H), 1.89–1.80 (m, 1H), 1.78 (t, $J = 2.4$ Hz, 3H), 1.72 (s, 3H), 1.63–1.48 (m, 4H) ppm;

¹³C NMR: (100 MHz, CDCl₃)
165.5, 82.9, 78.9, 77.3, 76.0, 74.4, 41.5, 40.8, 28.9, 26.4, 23.4, 18.7, 3.6 ppm;

FTIR (neat)
3288, 2942, 2864, 1763, 1742, 1437, 1411, 1376, 1289, 1262, 1151, 1093, 1016,
948, 859, 793, 637, 545 cm⁻¹;

HRMS (HRMS ESI)
[M + H]⁺ calcd for C₁₃H₁₈O₂Cl: 241.0995; found: 241.0984;

TLC R_f (**S2.1**) = 0.19 (20% Et₂O/hexanes)
Silica gel, visualized with p-anisaldehyde
R_f (**2.57b**) = 0.45 (20% Et₂O/hexanes)
Silica gel, visualized with p-anisaldehyde



3-methyldeca-1,2-dien-8-yn-1-yl acetate (2.56a). A 10–20-mL microwave vial (Biotage 354833) equipped with stir bar (Biotage 353930) was charged with rhodium(II) trifluoroacetate dimer (116 mg, 0.18 mmol, 0.05 equiv) in

a nitrogen-filled glovebox. The vial was sealed with a crimp-on microwave vial cap with septum (Biotage 352298) and removed from the glove box. The septum was pierced with a nitrogen inlet needle and toluene (17.7 mL) was added via syringe. 3-Methyldeca-1,8-dien-3-yl acetate **2.57a** (0.73 g, 3.5 mmol, 1 equiv) was dissolved in toluene (1 mL) and added in a single portion via syringe. The nitrogen inlet needle was removed and the sealed vial was lowered into a preheated oil bath (50 °C), where it was maintained for 1.5 h. Upon complete consumption of the starting material, as evidenced by TLC, the vial was removed from the oil bath and allowed to cool to rt. The contents were transferred to a 50-mL recover flask and concentrated via rotary evaporation

(40 °C bath temperature). The crude residue was purified via SiO₂ flash column chromatography (1–3% Et₂O/hexanes), affording 0.65 g of the title compound as a pale-yellow oil (88%).

Data for 2.56a

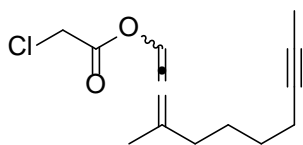
¹H NMR: (400 MHz, CDCl₃)
7.32–7.28 (m, 1H), 2.13 (s, 3H), 2.12–2.01 (m, 4H) 1.83 (s, 3H), 1.79–1.76 (m, 3H), 1.58–1.46 (m, 4H) ppm;

¹³C NMR: (100 MHz, CDCl₃)
189.5, 169.0, 116.0, 109.8, 79.1, 75.7, 34.8, 28.6, 26.5, 21.1, 20.6, 18.7, 3.6 ppm;

FTIR (neat)
2937, 2860, 1974, 1746, 1440, 1367, 1209, 1147, 1035, 990, 920, 787, 626, 598, 550 cm⁻¹;

HRMS (HRMS ESI)
[M+H⁺] calcd for C₁₃H₁₉O₂: 207.13796; found: 207.13767;

TLC R_f = 0.41 (10% Et₂O/hexanes)
Silica gel, visualized with p-anisaldehyde



3-methyldeca-1,2-dien-8-yn-1-yl 2-chloroacetate (2.56b). A 50-mL 2-necked round bottom flask equipped with stir bar, reflux condenser topped with septum, and septum was charged with rhodium(II) trifluoroacetate dimer (100 mg, 0.15 mmol, 0.037 equiv) in a nitrogen-filled glovebox. The flask was removed from the glovebox and the septum on top of the condenser replaced with a nitrogen

inlet adapter. Toluene was added (24 mL) via syringe, followed by 3-methyldeca-1,8-diyn-3-yl 2-chloroacetate **2.57b** (1.00 g, 4.15 mmol, 1 equiv) dissolved in toluene, in a single portion via syringe. The flask was lowered into a preheated oil bath (50 °C) where it was maintained for 8 h. Upon complete consumption of starting material, as evidenced by TLC, the flask was removed from the oil bath and allowed to cool to rt. SilametS Thiourea (350 mg, 1.07 mmol/g, 2.5 equiv with respect to rhodium(II) trifluoroacetate dimer) was added via temporary removal of the septum. The mixture was maintained at rt for 16 h then filtered through a medium porosity fritted glass vacuum filter filled with celite (6 x 4 cm). The filtrate was concentrated via rotary evaporation and the crude residue purified via SiO₂ flash column chromatography (5% Et₂O/hexanes), affording 0.89 g of the title compound as a yellow oil (89%).

Data for 2.56b

¹H NMR: (400 MHz, CDCl₃)

7.32 (sextet, *J* = 2.0 Hz, 1H), 4.16 (s, 2H), 2.19–2.08 (m, 4H), 1.86 (d, *J* = 2.0 Hz, 3H), 1.80 (t, *J* = 2.4 Hz, 3H), 1.60–1.49 (m, 4H) ppm;

¹³C NMR: (100 MHz, CDCl₃)

189.5, 165.4, 117.3, 110.3, 79.1, 75.8, 40.9, 34.7, 28.6, 26.4, 20.6, 18.7, 3.6 ppm;

FTIR (neat)

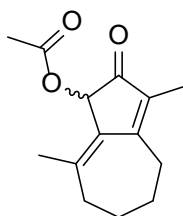
1769, 1746, 1308, 1285, 1236, 1149, 1057, 1004, 942, 787 cm⁻¹;

HRMS (HRMS ESI)

[*M* + *H*]⁺ calcd for C₁₃H₁₈O₂Cl: 241.09898; found: 241.09919;

TLC R_f = 0.69 (20% Et₂O/hexanes)

Silica gel, visualized with p-anisaldehyde



3,8-dimethyl-2-oxo-1,2,4,5,6,7-hexahydroazulen-1-yl acetate (2.58a). A 100-mL 2-necked round bottom flask equipped with stir bar, reflux condenser topped with septum, and a septum, was sequentially charged with bis(1,5-cyclooctadiene)rhodium(I) tetrafluoroborate (31 mg, 0.08 mmol, 0.025 equiv) and PPh₃ (30 mg, 0.11 mmol, 0.038 equiv) in a nitrogen-filled glovebox. The flask was removed from the glovebox and a nitrogen inlet needle was inserted into the septum on top of the reflux condenser. 1,2-Dichloroethane (30 mL) was added via syringe. The resulting dark yellow solution was maintained at rt for 10 min at which time the flask was evacuated and refilled five times with CO gas (100%), alternating between an inlet needle attached to a vacuum and an inlet needle attached to a balloon of CO. The light-yellow solution was maintained for 10 min before 3-methyldeca-1,2-dien-8-yn-1-yl acetate **2.56a** (0.62 g, 3.0 mmol, 1 equiv) was added in a single portion via syringe. The flask was lowered into a preheated oil bath (70 °C) and maintained for 20 h. Upon complete consumption of starting material, as evidenced by TLC, the flask was removed from the oil bath, allowed to cool to rt, and the contents transferred to a 100-mL recovery flask. The solvent was evaporated via rotary evaporation (40 °C bath temperature) and the crude residue purified via SiO₂ flash column chromatography (20–40% Et₂O/hexanes) affording 0.60 g of the title compound as a pale-yellow solid (85%).

Data for 2.58a

¹H NMR: (400 MHz, CDCl₃)

5.66 (s, 1H), 2.72 (t, *J* = 5.6 Hz, 2H), 2.48–2.34 (m, 2H), 2.13 (s, 3H), 1.89–1.69 (m, 4H), 1.82 (s, 3H), 1.78 (s, 3H);

^{13}C NMR: (100 MHz, CDCl_3)

200.3, 170.0, 169.2, 140.5, 134.8, 131.9, 72.2, 35.6, 29.0, 26.5, 24.2, 23.5, 20.8, 8.3
ppm;

FTIR (neat)

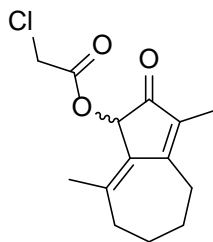
2923, 1739, 1694, 1574, 1433, 1371, 1338, 1277, 1224, 1024, 968, 929, 747, 586,
518 cm^{-1} ;

HRMS (HRMS ESI)

$[\text{M} + \text{H}]^+$ calcd for $\text{C}_{14}\text{H}_{19}\text{O}_3$: 235.1334; found: 235.1348;

TLC $R_f = 0.36$ (40% Et_2O /hexanes)

Silica gel, visualized with KMnO_4



3,8-dimethyl-2-oxo-1,2,4,5,6,7-hexahydroazulen-1-yl 2-chloroacetate

(2.58b). A 50-mL 2-necked round bottom flask equipped with stir bar, reflux condenser topped with septum, and a septum was sequentially charged with bis(1,5-cyclooctadiene)rhodium(I) tetrafluoroborate (51 mg, 0.13 mmol, 0.05

equiv) and PPh_3 (49 mg, 0.19 mmol, 0.075 equiv) in a nitrogen-filled glovebox. The flask was removed from the glovebox and a nitrogen inlet needle was inserted into the septum on top of the reflux condenser. 1,2-dichloroethane (25 mL) was added via syringe. The resulting dark yellow solution was maintained at rt for 10 min at which time the flask was evacuated and refilled five times with CO gas (100%), alternating between an inlet needle attached to a vacuum and an inlet needle attached to a balloon of CO. The light-yellow solution was maintained for 10 min before 3-methyldeca-1,2-dien-8-yn-1-yl 2-chloroacetate **2.56b** (0.60 g, 2.5 mmol, 1 equiv) was added in a single portion via syringe. The flask was lowered into a preheated oil bath (70 °C) and maintained

for 20 h. Upon complete consumption of starting material, as evidenced by TLC, the flask was removed from the oil bath, allowed to cool to rt, and the contents transferred to a 100-mL recovery flask. The solvent was evaporated via rotary evaporation (40 °C bath temperature) and the crude residue purified via SiO₂ flash column chromatography (30% Et₂O/hexanes) affording 0.58 g of the title compound as a pale-yellow solid (86%).

Data for 2.58b

¹H NMR: (400 MHz, CDCl₃)

5.69 (s, 1H), 4.12 (d, *J* = 0.4 Hz, 2H), 2.73 (t, *J* = 5.6 Hz, 2H), 2.46–2.37 (m, 2H), 1.92–1.71 (m, 4H), 1.85 (s, 3H), 1.79 (s, 3H) ppm;

¹³C NMR: (100 MHz, CDCl₃)

199.2, 169.7, 166.5, 141.4, 134.9, 131.1, 73.6, 40.8, 35.6, 29.0, 26.4, 24.1, 23.7, 8.3 ppm;

FTIR (neat)

2936, 1735, 1689, 1568, 1454, 1415, 1392, 1323, 1257, 1162, 1026, 977, 855, 799, 782, 746, 690, 557, 542, 508, 455, 429 cm⁻¹;

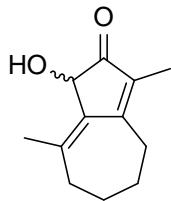
HRMS (HRMS ESI)

[*M* + *H*]⁺ calcd for C₁₄H₁₈O₃Cl: 269.0945; found: 269.0931;

m.p. 83.4–84.4 °C

TLC R_f = 0.37 (40% Et₂O/hexanes)

Silica gel, visualized with KMnO₄



1-hydroxy-3,8-dimethyl-4,5,6,7-tetrahydroazulen-2(1H)-one (2.53). A 100-mL 2-necked round bottom flask equipped with stir bar, reflux condenser topped with nitrogen inlet adapter, and septum, was charged with 3,8-dimethyl-2-oxo-1,2,4,5,6,7-hexahydroazulen-1-yl 2-chloroacetate **2.58b** (0.52 g, 1.94 mmol, 1 equiv) via temporary removal of the septum, and MeOH (32 mL) via syringe. Scandium(III) triflate (48 mg, 0.097 mmol, 0.05 equiv) was added to a scintillation vial and dissolved in 6.5 mL H₂O. This solution was added to the flask via syringe. The flask was lowered into a preheated oil bath (30 °C) and maintained for 3.5 h, at which point complete consumption of starting material was evidenced by TLC. The flask was removed from the oil bath, allowed to cool to rt, and the contents transferred to a 125-mL separatory funnel. Brine (20 mL) was added, the layers separated, and the aqueous phase extracted with EtOAc (2 x 20 mL). The combined organic phases were dried over MgSO₄, filtered through a medium porosity fritted glass vacuum filter, and concentrated via rotary evaporation. The crude residue was purified via SiO₂ flash column chromatography (40–60% Et₂O/hexanes) affording 0.33 g of the title compound as a white solid (88%).

Data for 2.53

¹H NMR: (400 MHz, CDCl₃)
4.44 (d, *J* = 2 Hz, 1H), 2.74–2.68 (m, 3H), 2.50–2.34 (m, 2H), 2.05 (s, 3H), 1.90–1.69 (m, 4H), 1.77 (s, 3H) ppm;

¹³C NMR: (100 MHz, CDCl₃)
205.7, 170.2, 141.5, 134.2, 133.6, 72.0, 35.8, 29.3, 26.5, 24.2, 23.8, 8.2 ppm;

FTIR (neat)
3286, 2918, 1667, 1563, 1394, 1335, 1256, 1129, 1041, 801, 762, 580

cm⁻¹;

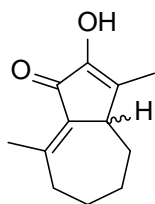
HRMS (HRMS ESI)

[M + H]⁺ calcd for C₁₂H₁₇O₂: 193.12231; found: 193.12232;

m.p. 81.6-83.7 °C

TLC R_f = 0.12 (40% Et₂O/hexanes)

Silica gel, visualized with KMnO₄



2-hydroxy-3,8-dimethyl-4,5,6,7-tetrahydroazulen-1(3aH)-one (2.54). A 25-mL

2-necked round bottom flask equipped with stir bar, nitrogen inlet adapter, and septum was sequentially charged with 1-hydroxy-3,8-dimethyl-4,5,6,7-tetrahydroazulen-2(1H)-one **2.53** (105 mg, 0.55 mmol, 1 equiv) via temporary removal of the septum, and THF (10.9 mL) via syringe. To this solution was added potassium *tert*-butoxide (1.3 mL of a 0.5 M solution in *t*BuOH, 0.66 mmol, 1.2 equiv) via syringe, and the reaction maintained at rt for 5 min, during which period a yellow precipitate formed. After complete consumption of starting material, as evidenced by TLC, the mixture was diluted with EtOAc (10 mL), transferred to a 60-mL separatory funnel and sat. NH₄Cl (20 mL) added. The layers were separated and the organic phase was dried over MgSO₄ and concentrated via rotary evaporation, affording 104 mg of the title compound as an off-white solid (99%).

Data for 2.54

¹H NMR: (400 MHz, CDCl₃)

5.75 (s, 1H), 2.93 (d, *J* = 11.6 Hz, 1H), 2.43 (t, *J* = 13.2 Hz, 1H), 2.39 (s, 3H),
2.23–2.03 (m, 3H), 1.95 (s, 3H), 1.90–1.81 (m, 1H), 1.64–1.51 (m, 1H), 1.30–1.17
(m, 1H), 0.94–0.81 (m, 1H) ppm;

¹³C NMR: (100 MHz, CDCl₃)

189.9, 153.4, 150.5, 136.8, 134.0, 45.2, 38.8, 31.5, 31.2, 25.5, 21.2, 11.4 ppm;

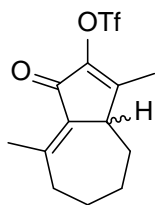
FTIR (neat)

3304, 2930, 2850, 1666, 1614, 1436, 1401, 1353, 1331, 1292, 1215, 1184, 1158,
1091, 1048, 989, 965, 948, 835, 818, 785, 672, 653, 599, 556, 535, 508, 483 cm⁻¹;

HRMS (HRMS ESI)

[*M* + *H*]⁺ calcd for C₁₂H₁₇O₂: 193.12231; found: 193.12213;

TLC R_f = 0.65 (40% Et₂O/hexanes, visualized with KMnO₄)



3,8-dimethyl-1-oxo-1,3a,4,5,6,7-hexahydroazulen-2-yl trifluoromethanesulfonate (2.59). A 0.5–2 mL microwave vial (Biotage 352016) equipped with stir bar (Biotage 355544) was charged with 2-hydroxy-3,8-dimethyl-

4,5,6,7-tetrahydroazulen-1(3aH)-one **2.54** (18 mg, 0.09 mmol, 1 equiv). The vial was sealed with a crimp-on microwave vial cap (Biotage 352298) and flushed with N₂ via an inlet needle. CH₂Cl₂ (0.94 mL) was added via syringe and the vial lowered into an ice/water (0 °C) bath. Triethylamine (26 μL, 0.19 mmol, 2.0 equiv) and triflic anhydride (19 μL, 0.11 mmol, 1.2 equiv) were sequentially added dropwise via syringe. The reaction was maintained for 1 h at which point complete consumption of starting material was observed by TLC. The vial was removed from the

ice/water bath and the contents transferred to a recovery flask. Upon concentration and purification of the crude residue via SiO₂ flash column chromatography (20% Et₂O/hexanes), 24 mg of the title compound were isolated as a pale-yellow oil (79%). The product was contaminated with a small amount of an identified product which was not observable by TLC.

Data for 2.59

¹H NMR: (400 MHz, CDCl₃)

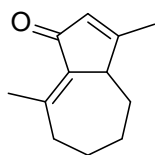
3.12 (d, *J* = 11.6 Hz, 1H), 2.48–2.41 (m, 1H), 2.40 (s, 3H), 2.28–2.21 (m, 1H), 2.17–2.12 (m, 2H) 2.09 (s, 3H), 1.92–1.86 (m, 1H), 1.69–1.58 (m, 1H) 1.33–1.24 (m, 1H), 1.09–1.00 (m, 1H) ppm;

¹³C NMR: (100 MHz, CDCl₃)

185.0, 156.9, 156.8, 146.3, 132.2, 118.7 (q, *J* = 318.3 Hz), 46.1, 38.9, 31.2, 30.7, 25.0, 21.4, 12.6 ppm;

TLC R_f = 0.53 (40% Et₂O/hexanes)

Silica gel, visualized with KMnO₄



3,8-dimethyl-4,5,6,7-tetrahydroazulen-1(3aH)-one (2.55). A 2–5 mL microwave vial (Biotage 521521) equipped with stir bar (Biotage 355543) was charged with Tetrakis(triphenylphosphine)-palladium(0) (34 mg, 0.03 mmol, 0.5 equiv) and lithium chloride (22 mg, 0.51 mmol, 8.75 equiv). The vial was sealed with a crimp-on microwave vial cap (Biotage 352298), and flushed with nitrogen via an inlet needle. 3,8-Dimethyl-1-oxo-1,3a,4,5,6,7-hexahydroazulen-2-yl trifluoromethanesulfonate **2.59** (19 mg, 0.06 mmol, 1 equiv) was dissolved in DMF (5.9 mL) and added to the vial via syringe. The solution was degassed for

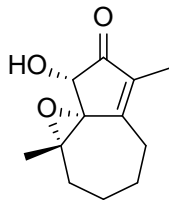
10 min by bubbling nitrogen through the solution via an inlet needle. Triethylsilane (0.19 mL, 1.2 mmol, 20.4 equiv) was added via syringe. The inlet needle was removed and the sealed vial lowered into a preheated oil bath (90 °C), where it was maintained for 15 min. Upon complete consumption of starting material, as evidenced by TLC, the vial was removed from the oil bath and allowed to cool to rt. The contents were transferred to a separator funnel, diluted with Et₂O (5 mL), and washed with H₂O (2 x 3 mL). The organic phase was dried over MgSO₄ and concentrated via rotary evaporation. The crude residue was purified via SiO₂ flash column chromatography (20% Et₂O/hexanes) affording 5.6 mg of the title compound as a colorless oil (54%). The product was contaminated with triethylsilane.

Data for 2.55

¹H NMR: (400 MHz, CDCl₃)
6.02 (pent, *J* = 1.2 Hz, 1H), 3.08 (d, *J* = 11.6 Hz, 1H), 2.43–2.37 (m, 1H), 2.35 (s, 3H), 2.19–2.13 (m, 1H), 2.12–2.06 (m, 2H), 2.05 (m, 3H), 1.88–1.80 (m, 1H), 1.67–1.54 (m, 2H), 1.32–1.26 (m, 1H) ppm; Impurities: 0.97 (t, *J* = 8.0 Hz, 2.13H), 0.59 (q, *J* = 8.0 Hz, 1.46H) ppm (triethyl silane);

¹³C NMR: (100 MHz, CDCl₃)
197.4, 172.1, 151.5, 136.8, 133.5, 50.4, 39.1, 31.5, 31.0, 25.5, 20.8, 16.8 ppm;
Impurities: 6.7, 5.9 ppm (triethyl silane);

TLC R_f = 0.51 (30% Et₂O/hexanes)
Silica gel, visualized with KMnO₄



8-hydroxy-1a,6-dimethyl-1a,2,4,5-tetrahydro-3H-azuleno[3a,4-b]oxirene-

7(8H)-one (2.61). A 100-mL 2-necked round bottom flask equipped with stir bar, nitrogen inlet adapter, and septum was charged with vanadyl acetylacetonate (4

mg, 0.016 mmol, 0.01 equiv) via temporary removal of the septum. Benzene (31 mL) was added via syringe, followed by 1-hydroxy-3,8-dimethyl-4,5,6,7-tetrahydroazulen-2(1H)-one **2.53** (300 mg, 1.56 mmol, 1 equiv), which had been dissolved in benzene (3 mL), via syringe. *Tert*-butyl hydroperoxide (~5 M in decanes, 0.37 mL, 1.87 mmol, 1.2 equiv) was added dropwise over 1 min via syringe, during which period the reaction mixture turned deep red. The reaction was maintained at rt for 1 h, during which period the color changed to light yellow. Upon complete consumption of starting material, as evidenced by TLC, the mixture was concentrated via rotary evaporation. The crude residue was purified via SiO₂ flash column chromatography (40% Et₂O/hexanes), affording 307 mg of the title compound as a white solid and single diastereomer (94%).

Data for 2.61

¹H NMR: (400 MHz, CDCl₃)

3.89 (d, *J* = 3.2 Hz, 1H), 2.91 (m, 1H), 2.39 (d, *J* = 4 Hz, 1H), 2.32–2.25 (m, 1H)
2.21–2.11 (m, 1H), 2.02–1.87 (m, 2H) 1.82 (d, *J* = 1.6 Hz, 3H), 1.76–1.66 (m, 1H),
1.66–1.57 (m, 1H), 1.48 (s, 3H), 1.20–1.07 (m, 1H) ppm;

¹³C NMR: (100 MHz, CDCl₃)

203.9, 167.8, 140.9, 71.5, 68.3, 67.9, 35.5, 29.1, 25.9, 24.4, 23.5, 8.7 ppm;

FTIR (neat)

1769, 1746, 1308, 1285, 1236, 1149, 1057, 1004, 942, 787 cm⁻¹;

HRMS (HRMS ESI)

3432, 2927, 1684, 1615, 1441, 1389, 1339, 1326, 1281, 1225, 1175, 1158, 1127,
1108, 1045, 1028, 982, 886, 854, 824, 768, 724, 653, 610, 545, 475 cm^{-1} ;

$[\text{M} + \text{H}]^+$ calcd for $\text{C}_{12}\text{H}_{17}\text{O}_3$: 209.11722; found: 209.11741;

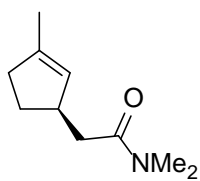
TLC

$R_f = 0.20$ (60% Et_2O /hexanes)

Silica gel, visualized with KMnO_4

Appendix B : Experimental Information for Chapter Three

General Methods. Unless otherwise indicated, all reactions were performed in flame-dried glassware under an atmosphere of dry nitrogen. All commercially available compounds used as received. Tetrahydrofuran (THF), dichloromethane (CH₂Cl₂), and diethyl ether (Et₂O) were purified by passing through alumina using the Sol-Tek ST-002 solvent purification system. Toluene was distilled over calcium hydride prior to use. Deuterated chloroform (CDCl₃) was dried over 3 Å molecular sieves prior to use. Gasses N₂, H₂, and CO were purchased from Matheson Tri Gas. Flash column chromatography was performed using silica gel (40-63 μm particle size, 60 Å pore size). Thin-layer chromatography (TLC) was performed on silica gel F₂₅₄ glass-backed plates (250 μm thickness). ¹H and ¹³C NMR were recorded on a Bruker Avance 400 MHz spectrometer. Spectra were referenced to residual chloroform (7.26 ppm, ¹H, 77.16 ppm, ¹³C). Chemical shifts (δ) are reported in ppm and multiplicities are indicated by s (singlet), d (doublet), t (triplet), q (quartet), quint (quintet), and m (multiplet). Coupling constants, *J*, are reported in hertz (Hz). NMR spectra were obtained at room temperature. EI mass spectroscopy was performed on a Waters Micromass GCT high-resolution mass spectrometer, while ES mass spectroscopy was performed on a Waters Q-TOF Ultima API, Micromass UK Limited high-resolution mass spectrometer. IR spectra were obtained using a Nicolet Avatar E.S.P. 360 FT-IR.



(*R*)-*N,N*-dimethyl-2-(3-methylcyclopent-2-en-1-yl)acetamide (3.37). Two-step, two-pot procedure. A 2–5-mL microwave vial (Biotage 351521) equipped with stir bar (Biotage 355543) was charged with Hoveyda-Grubbs 2nd

generation catalyst (2.0 mg, 0.003 mmol, 0.1 mol%). The vial was sealed with a crimp-on

microwave vial cap with septum (Biotage 352298) and purged with N₂ via an inlet needle. (*R*)-linalool (0.50 g, 0.57 mL, 3.2 mmol, 1 equiv) was added and a second needle attached to an oil bubbler was inserted into the septum. The mixture was reacted at rt while being allowed to vent through the oil bubbler for 1 h, at which point complete consumption of starting material was observed by TLC. The nitrogen inlet needle was removed and a needle attached to an air line was inserted through the septum and into the reaction mixture. Air was bubbled through the green solution for 20 min during which time the solution turned black. A syringe was used to transfer the solution to a 50-mL 2-necked round bottom flask which was equipped with a stir bar, septum, and reflux condenser topped with nitrogen inlet adapter. Freshly distilled toluene (13 mL) was added via syringe, followed by *N,N*-dimethylacetamide dimethyl acetal (1.4 mL, 9.7 mmol, 3 equiv) via syringe. The flask was lowered into a preheated oil bath set to 115 °C and reacted for 24 h at which point TLC revealed the reaction to be complete. The flask was removed from the oil bath, allowed to cool to rt, transferred to a 100-mL recovery flask, and concentrated via rotary evaporation (40 °C bath temperature). Purification via SiO₂ flash column chromatography (40–60% Et₂O/hexanes), afforded 0.40 g of the title compound as an orange oil (75%).

Two-step, one-pot procedure. This reaction was performed as described above with the following modifications: Hoveyda-Grubbs 2nd generation catalyst (< 1 mg, spatula tip) was dissolved in toluene (2.6 mL). (*R*)-Linalool (0.100 g, 0.12 mL, 0.65 mmol, 1 equiv) was added in a single portion via syringe. Reacted at rt for 1.5 h. Air was bubbled through the reaction mixture for 40 min before *N,N*-dimethylacetamide dimethyl acetal (0.24 mL, 1.62 mmol, 2.5 equiv) was added in a single portion via syringe. Reacted at 115 °C for 24 h. Contents transferred to a recovery flask and concentrated via rotary evaporation. 0.083 g of the title compound as an orange oil (77%).

NOTE: This one-pot procedure was scaled up to 5 g and 68% of the title compound was isolated; however, catalyst loading had to be increased to 0.3 mol% for the metathesis to reach completion.

Data for 3.37

¹H NMR: (400 MHz, CDCl₃)

5.31–5.27 (m, 1H), 3.16–3.06 (m, 1H), 2.99 (s, 3H), 2.94 (s, 3H), 2.39–2.27 (m, 2H), 2.27–2.14 (m, 3H), 1.71 (s, 3H) 1.53–1.42 (m, 1H) ppm;

¹³C NMR: (100 MHz, CDCl₃)

172.7, 141.1, 128.4, 42.5, 39.9, 37.5, 36.3, 35.4, 31.1, 16.8 ppm;

FTIR (neat)

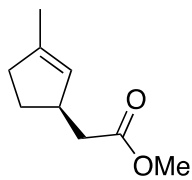
2920, 1738, 1641, 1493, 1445, 1393, 1327, 1266, 1129, 1084, 1056, 1005, 986, 815, 824, 614, 455 cm⁻¹;

HRMS (HRMS ESI)

calcd for C₁₀H₁₈NO (M+H⁺): 168.1382; found: 168.1375;

TLC R_f = 0.13 (50% Et₂O in hexanes)

Silica gel, visualized with KMnO₄



Methyl (*R*)-2-(3-methylcyclopent-2-en-1-yl)acetate (3.36). A 250-mL 2-necked round-bottom flask equipped with stir bar, nitrogen inlet adapter, and septum was charged with (*R*)-*N,N*-dimethyl-2-(3-methylcyclopent-2-en-1-yl)acetamide **3.37** (1.75 g, 10.5 mmol, 1 equiv) via syringe. Dichloromethane (105 mL) was added via temporary removal of the septum, followed by pyridine (2.5 mL, 31.4 mmol, 3 equiv) via syringe. The flask was lowered into an ethanol bath cooled to -40 °C via immersion chiller. Triflic

anhydride (2.3 mL, 13.6 mmol, 1.3 equiv) was added dropwise over 20 min via syringe pump. Upon complete addition, the ethanol bath was warmed to 0 °C over 2 h by gradually increasing the temperature of the immersion chiller. Upon reaching 0 °C the reaction was maintained for 2 h, at which point the starting material had been consumed as evidenced by TLC. Methanol (12.7 mL, 314 mmol, 30 equiv) was added dropwise over 3 min via syringe, and the flask removed from the ethanol bath and allowed to warm to rt, where it was maintained for 16 h. 1 N HCl was added (50 mL) via temporary removal of the septum, and the biphasic mixture was stirred at rt for 3 h. The reaction mixture was transferred to a separatory funnel and the layers separated. The aqueous phase was extracted with CH₂Cl₂ (1 x). The combined organic phases were dried over MgSO₄, filtered through a medium-porosity fritted glass vacuum filter, and concentrated via rotary evaporation. The crude residue was purified via SiO₂ flash column chromatography (40% Et₂O/pentane), affording 1.36 g of the title compound as a pale-yellow oil (85%).

Data for 3.36

¹H NMR: (400 MHz, CDCl₃)
5.27–5.23 (m, 1H), 3.67 (s, 3H), 3.10–2.99 (m, 1H), 2.38–2.10 (m, 5H), 1.71 (s, 3H), 1.53–1.44 (m, 1H) ppm;

¹³C NMR: (100 MHz, CDCl₃)
173.7, 141.6, 127.6, 51.5, 42.4, 40.7, 36.3, 30.7, 16.7 ppm;

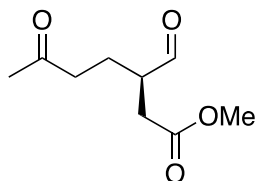
FTIR (neat)
2951, 2844, 1736, 1657, 1436, 1360, 1315, 1253, 1190, 1156, 1074, 1014, 996, 883, 821, 655, 593

HRMS (HRMS ESI)

calcd for C₉H₁₅O₂ (M+H⁺): 155.1066; found: 155.1060;

TLC R_f = 0.74 (40% Et₂O/hexanes)

Silica gel, visualized via KMnO₄



Methyl (*R*)-3-formyl-6-oxoheptanoate (3.40). A 25-mL 2-necked round

bottomed flask equipped with stir bar, nitrogen inlet adapter, and septum

was charged with methyl (*R*)-2-(3-methylcyclopent-2-en-1-yl)acetate **3.36**

(150 mg, 0.97 mmol, 1 equiv). Acetone (8.8 mL), deionized water (0.9 mL), and 2,6-lutidine (0.23

mL, 1.95 mmol, 2 equiv) were sequentially added via syringe. *N*-Methylmorpholine *N*-oxide (170

mg, 1.46 mmol, 1.5 equiv) was added, followed by osmium tetroxide (7 mg, 0.03 mmol, 0.03

equiv) via temporary removal of the septum. The brown-yellow reaction mixture was maintained

at rt for 16 h, at which point complete consumption of starting material was observed by TLC.

Iodobenzene diacetate (470 mg, 1.46 mmol, 1.5 equiv) was added via temporary removal of the

septum and the mixture maintained at rt for 2 h. Upon completion, as evidenced by TLC, saturated

aqueous Na₂S₂O₃ (10 mL) was added and the mixture stirred for 10 min. The mixture was

transferred to a separatory funnel and EtOAc (10 mL) was added. The layers were separated and

the aqueous phase extracted with EtOAc (2 x 10 mL). The combined organic phases were washed

with saturated aqueous CuSO₄ (3 x 10 mL). The organic phase was dried over MgSO₄, filtered

through a medium porosity fritted glass vacuum filter, and concentrated via rotary evaporation.

The crude residue was purified via SiO₂ flash column chromatography (40–80% EtOAc/hexanes),

affording 161 mg of the title compound as a colorless oil (89%).

Data for 3.40

¹H NMR: (400 MHz, CDCl₃)

9.68 (d, 0.8 Hz, 1H), 3.68 (s, 3H), 2.85–2.77 (m, 1H), 2.72 (dd, $J^1 = 16.4$ Hz, $J^2 = 8$ Hz, 1H), 2.57–2.48 (m, 2H), 2.42 (dd, $J^1 = 16.4$ Hz, $J^2 = 5.6$ Hz, 1H), 2.14 (s, 3H), 2.06–1.95 (m, 1H), 1.83–1.71 (m, 1H) ppm;

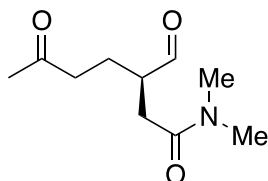
¹³C NMR: (100 MHz, CDCl₃)

207.3, 202.3, 172.1, 52.1, 46.9, 40.3, 33.2, 30.1, 22.3 ppm;

TLC $R_f = 0.24$ (40% EtOAc in hexanes)

$R_f = 0.05$ (40% Et₂O in hexanes)

Silica gel, visualized with p-anisaldehyde



(R)-3-formyl-*N,N*-dimethyl-6-oxoheptanamide (3.52). To a 250 mL 2-

necked round-bottom flask equipped with stir bar, nitrogen inlet adapter,

and septum were sequentially added (*R*)-*N,N*-dimethyl-2-(3-

methylcyclopent-2-en-1-yl)acetamide **3.37** (2.18 g, 13.0 mmol, 1 equiv), acetone (118 mL),

deionized water (12 mL), 2,6-lutidine (3.00 mL, 26.0 mmol, 2 equiv), *N*-methylmorpholine *N*-

oxide (2.29 g, 19.6 mmol, 1.5 equiv), and osmium tetroxide (99 mg, 0.39 mmol, 0.03 equiv), via

temporary removal of the septum. The brown-yellow mixture was reacted at rt for 20 h, at which

point the starting material had been fully consumed, as evidenced by TLC. Iodobenzene diacetate

(6.30 g, 19.6 mmol, 1.5 equiv) was added in a single portion via temporary removal of the septum,

and the mixture reacted at rt for 1.5 h. Upon completion, as evidenced by TLC, sat. aq. Na₂S₂O₃

(50 mL) was added. The biphasic mixture was allowed to stir for 5 min before being transferred

to a separatory funnel and diluted with EtOAc (30 mL). The layers were separated and the aqueous

layer extracted with EtOAc (3 x 50 mL). The combined organic layers were dried over MgSO₄, filtered through a fritted glass vacuum filter, and concentrated via rotary evaporation. The crude residue was purified via SiO₂ flash column chromatography (5% MeOH/45% EtOAc/50% hexanes), affording 2.40 g of the title compound as a yellow oil (92%). The enantiomeric ratio was determined to be 94:6, following a procedure developed by Gellman and coworkers.¹²⁰ A pipette tip of the title compound was dissolved in CDCl₃ (~0.6 mL) in an NMR tube. To this was added a drop of (*S*)-1-methoxypropan-2-amine via pipette. The mixture was shaken vigorously and subjected to ¹H NMR within 10 min of addition of (*S*)-1-methoxypropan-2-amine.

Data for 3.52

¹H NMR: (400 MHz, CDCl₃)

9.74 (d, *J* = 1.2 Hz, 1H), 3.02 (s, 3H), 2.93 (s, 3H), 2.88 (pent, *J* = 6.8 Hz, 1H), 2.76 (dd, *J*¹ = 16.4 Hz, *J*² = 8 Hz, 1H), 2.63-2.46 (m, 2H), 2.42 (dd, *J*¹ = 16.4 Hz, *J*² = 5.2 Hz, 1H), 2.14 (s, 3H), 2.04-1.92 (m, 1H), 1.80-1.69 (m, 1 H) ppm;

¹³C NMR: (100 MHz, CDCl₃)

207.9, 203.4, 170.5, 46.9, 40.9, 37.4, 35.7, 33.5, 30.1, 22.9 ppm;

FTIR (neat)

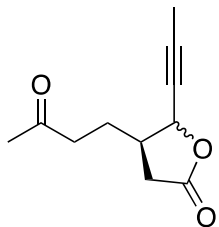
2928, 1711, 1635, 1498, 1401, 1364, 1263, 1146, 1060, 964, 901, 801, 742, 621, 589 cm⁻¹;

HRMS (HRMS ESI)

calcd for C₁₀H₁₈O₃N (M+H⁺): 200.1281; found: 200.1271;

TLC R_f = 0.24 (5% MeOH/60% EtOAc/35% hexanes)

Silica gel, visualized with *p*-anisaldehyde (product stained pink)



4R)-4-(3-oxobutyl)-5-(prop-1-yn-1-yl)dihydrofuran-2(3H)-one (3.51). To a 10-mL 2-necked round bottom flask equipped with stir bar, nitrogen inlet adapter, and septum, were sequentially added chlorotriisopropoxytitanium(IV) (0.50 mL of a 1 M solution in hexane, 0.50 mmol, 2 equiv) and THF (1.0 mL)

via syringe. The flask was lowered into an ethanol-filled immersion chilled bath set to $-60\text{ }^{\circ}\text{C}$. 1-Propynylmagnesium bromide (1.0 mL of a 0.5 M solution in THF, 0.50 mmol, 2 equiv) was added dropwise over a period of 5 min via syringe. The solution was reacted for 1 h, during which period a precipitate was formed. To this mixture was added (*R*)-3-formyl-*N,N*-dimethyl-6-oxoheptanamide **3.52** (50 mg, 0.25 mmol, 1 equiv) in a single portion at $-60\text{ }^{\circ}\text{C}$. The mixture was maintained for 2 h at which point TLC indicated complete consumption of starting material. 1 N HCl was added (1 mL) via syringe, and the flask was removed from the ethanol bath and immediately transferred to a preheated oil bath set to $50\text{ }^{\circ}\text{C}$. The mixture was reacted for 16 h at which point the flask was removed from the oil bath, allowed to cool to rt, and the contents transferred to a separatory funnel. The layers were separated and the aqueous phase extracted with EtOAc (3 x 5 mL). The combined organic layers were dried over MgSO_4 , filtered through a cotton plug and concentrated via rotary evaporation. The crude residue was purified via SiO_2 flash column chromatography (40% EtOAc in hexanes) affording 42 mg of the title compound as a pale-yellow oil (86%) in a 62:38 cis/trans ratio.

Data for 3.51

¹H NMR: (400 MHz, CDCl₃)

5.18-5.13 (m, 0.62H, *cis*-), 4.70-4.66 (m, 0.38H, *trans*-), 2.75 (dd, $J^1 = 17.2$ Hz, $J^2 = 8.0$ Hz, 0.47H), 2.65-2.49 (m, 3.75H), 2.35 (dd, $J^1 = 16.8$ Hz, $J^2 = 10.8$ Hz, 0.77H), 2.26-2.20 (m, 0.45H), 2.19 (s, 3H), 1.97-1.85 (m, 5H), 1.18-1.71 (m, 0.64H) ppm;

¹³C NMR: (100 MHz, CDCl₃)

207.4, 207.0, 175.6, 175.0, 87.3, 85.2, 75.2, 74.5, 73.1, 72.4, 43.1, 41.0, 40.9, 39.1, 34.7, 33.6, 30.1, 26.1, 24.4, 3.8 ppm;

FTIR (neat)

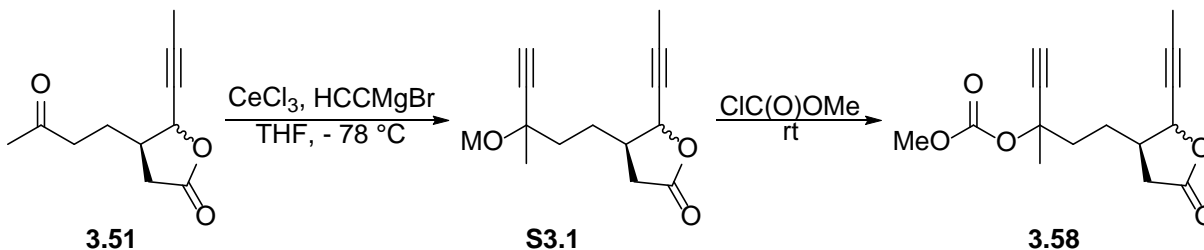
2924, 2245, 1775, 1711, 1417, 1359, 1290, 1264, 1218, 1159, 1086, 971, 900, 859, 838, 800, 744, 693, 591, 524 cm⁻¹;

HRMS (HRMS ESI)

calcd for C₁₁H₁₅O₃ (M+H⁺): 195.1015; found: 195.1012;

TLC R_f = 0.68 (100% EtOAc)

Silica gel, visualized with p-anisaldehyde



Methyl ((3R)-3-methyl-5-((3R)-5-oxo-2-(prop-1-yn-1-yl)tetrahydrofuran-3-yl)pent-1-yn-3-yl) carbonate (3.58). A 25-mL 2-necked round bottom flask equipped with stir bar and two septa

was charged with anhydrous CeCl_3 (0.36 g, 1.4 mmol, 1.4 equiv) in a nitrogen-filled glovebox. The flask was removed from the glovebox and one of the septa replaced with a nitrogen inlet adapter. THF (7.4 mL) was added via syringe and the resulting suspension stirred at rt for 16 h. The flask was lowered into an ice/water bath (0 °C) and ethynylmagnesium bromide (2.9 mL of a 0.5 M solution in THF, 1.4 mmol, 1.4 equiv) was added dropwise over a period of 5 min via syringe. The resulting brown suspension maintained at 0 °C for 1 h before the flask was removed from the ice/water bath and lowered into a dry ice/acetone bath (-78 °C). (4*R*)-4-(3-Oxobutyl)-5-(prop-1-yn-1-yl)dihydrofuran-2(3*H*)-one **3.51** (0.20 g, 1.0 mmol, 1 equiv) was added in a single portion via syringe and the reaction maintained for 10 min at which point complete consumption of starting material was observed by TLC. Methyl chloroformate (0.16 mL, 2.1 mmol, 2 equiv) was added in a single portion via syringe, and the flask was removed from the dry ice/acetone bath and allowed to warm to rt, where it was maintained for 1 h. Upon complete consumption of intermediate **S3.1**, as evidenced by TLC, sat. aq. NH_4Cl (5 mL) was added via syringe and the mixture transferred to a separatory funnel. EtOAc (5 mL) was added, the layers separated, and the aqueous phase extracted with EtOAc (3 x 5 mL). The combined organic phases were dried over MgSO_4 , gravity filtered through a cotton plug, and concentrated via rotary evaporation. The crude residue was purified via SiO_2 flash column chromatography (20% EtOAc/hexanes) affording 0.23 g of the title compound as a viscous yellow oil (80%).

Data for **3.58**

^1H NMR: (400 MHz, CDCl_3)

5.17-5.13 (m, 0.50H), 4.71-4.67 (m, 0.50H), 3.80-3.75 (m, 3.34H), 2.81-2.75 (dd, $J^1 = 14.0$ Hz, $J^2 = 6.8$ Hz, 0.55 H), 2.62 (s, 1H), 2.60-2.55 (m, 0.61H), 2.55-2.45

(m, 1H), 2.40-2.31 (m, 0.63H), 2.27-2.18 (m, 0.58H), 2.05-1.94 (m, 1.27H), 1.92-1.84 (m, 5.49H), 1.74 (s, 3H), 1.72-1.61 (m, 1.54H) ppm;

^{13}C NMR: (100 MHz, CDCl_3)

175.7, 175.1, 153.6, 87.2, 87.1, 85.2, 82.8, 82.6, 76.44, 76.39, 76.36, 74.7, 74.6, 74.5, 74.4, 54.7, 54.6, 43.44, 43.40, 39.64, 39.6, 39.4, 39.2, 39.1, 34.64, 34.56, 33.8, 33.7, 27.4, 27.3, 26.5, 26.4, 3.81, 3.77 ppm;

FTIR (neat)

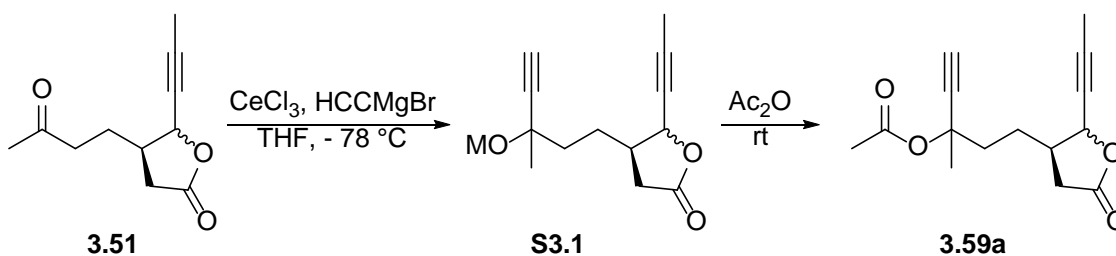
2249, 1779, 1749, 1440, 1375, 1262, 1149 cm^{-1} ;

HRMS (HRMS ESI)

calcd for $\text{C}_{15}\text{H}_{18}\text{O}_5\text{Na}$ ($\text{M}+\text{Na}^+$): 301.1046; found: 301.1055;

TLC $R_f = 0.55$ (30% EtOAc in hexanes)

Silica gel, visualized with p-anisaldehyde



(3R)-3-methyl-5-((3R)-5-oxo-2-(prop-1-yn-1-yl)tetrahydrofuran-3-yl)pent-1-yn-3-yl acetate

(3.59a). A 100-mL two-necked round bottom flask equipped with a stir bar and two septa was charged with anhydrous CeCl_3 (1.35 g, 5.5 mmol, 1.4 equiv) in a nitrogen-filled glovebox by temporary removal of a septum. The flask was removed from the glovebox and one septum was replaced with a nitrogen inlet adapter. THF (16 mL) was added via syringe and the white suspension stirred at rt under N_2 for 16 h. The flask was placed in an ice/water bath ($0\text{ }^\circ\text{C}$) and

ethynylmagnesium bromide (10.2 mL of a 0.5 M solution in THF, 5.1 mmol, 1.3 equiv) was added dropwise over 10 min via syringe. The flask was removed from the ice/water bath and lowered into a dry ice/acetone bath (-78 °C), where it was maintained for 1.5 h. (4*R*)-4-(3-oxobutyl)-5-(prop-1-yn-1-yl)dihydrofuran-2(3*H*)-one **3.51** (0.76 g, 3.9 mmol, 1 equiv) was dissolved in THF (2 mL) and added dropwise to the reaction mixture via syringe over 2 min. Upon completion of addition, the mixture was maintained for 2 h then the flask was removed from the dry ice/acetone bath and allowed to warm to rt. After 30 min at this temperature, complete consumption of the starting material was evidenced by TLC, and acetic anhydride (0.74 mL, 7.8 mmol, 2 equiv) was added in a single portion via syringe at rt. The mixture was allowed to react for 16 h, after which time complete consumption of the intermediate **S3.1** was evidenced by TLC. The mixture was transferred to a separatory funnel, diluted with EtOAc (15 mL) and washed with sat. aq. NH₄Cl (2 x 20 mL). The layers were separated and the combined aqueous phases were extracted with EtOAc (2 x 20 mL). The combined organic phases were dried over MgSO₄, concentrated via rotary evaporation, and the crude residue purified via SiO₂ flash column chromatography (20–40% EtOAc/hexanes), affording 0.90 g of the title compound as a viscous orange oil (88%).

Data for 3.59a

¹H NMR: (400 MHz, CDCl₃)

5.18–5.13 (m, 0.62H), 4.73–4.68 (m, 0.38H), 2.78 (ddd, $J^1 = 17.2$ Hz, $J^2 = 8.0$ Hz, $J^3 = 1.2$ Hz, 0.51H), 2.58 (s, 1.19H), 2.65–2.60 (m, 0.43H), 2.56–2.46 (m, 1.02H), 2.41–2.33 (m, 0.66H), 2.26–2.18 (m, 0.58H), 2.04 (s, 3.27H), 1.92–1.87 (m, 3.66H), 1.87–1.73 (m, 3.17H), 1.71–1.68 (m, 2.92H) ppm;

¹³C NMR: (100 MHz, CDCl₃)

175.7, 175.3, 169.3, 87.1, 85.1, 83.5, 83.3, 83.2, 74.43, 74.40, 74.0, 73.9, 73.3, 73.2, 58, 43.4, 39.7, 39.3, 39.10, 39.07, 34.62, 34.59, 33.78, 33.72, 28.2, 27.4, 26.6, 26.5, 25.4, 25.3, 22.0, 15.4, 3.82, 3.80 ppm;

FTIR (neat)

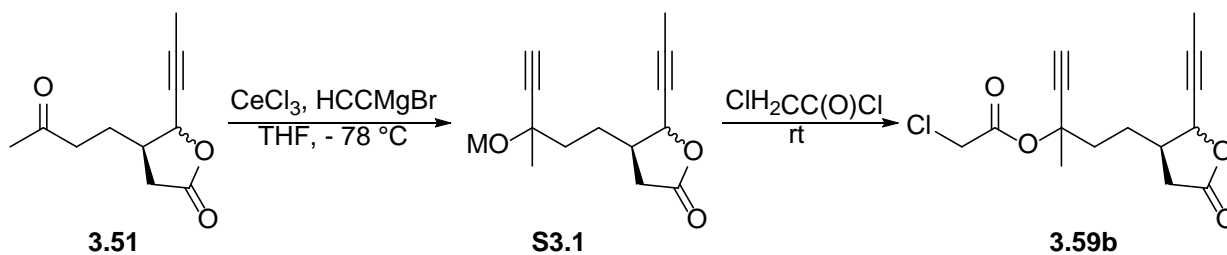
13276, 2925, 2245, 1779, 1739, 1441, 1368, 1239, 1153, 1097, 1013, 975, 856, 672, 611, 535 cm^{-1} ;

HRMS (HRMS ESI)

calcd for $\text{C}_{15}\text{H}_{19}\text{O}_4$ ($\text{M}+\text{H}^+$): 263.1278; found: 263.1305;

TLC $R_f = 0.71$ (50% EtOAc)

Silica gel, p-anisaldehyde



(3R)-3-methyl-5-((3R)-5-oxo-2-(prop-1-yn-1-yl)tetrahydrofuran-3-yl)pent-1-yn-3-yl 2-chloroacetate (3.59b). A 25-mL two-necked round bottom flask equipped with a stir bar and two septa was charged with anhydrous CeCl_3 (0.533 g, 2.16 mmol, 1.4 equiv) in a nitrogen-filled glovebox by temporary removal of a septum. The flask was removed from the glovebox and one septum was replaced with a nitrogen inlet adapter. THF (6.3 mL) was added via syringe and the white suspension stirred at rt under N_2 for 16 h. The flask was placed in an ice/water bath ($0\text{ }^\circ\text{C}$) and ethynylmagnesium bromide (4.0 mL of a 0.5 M solution in THF, 2.00 mmol, 1.3 equiv) was added dropwise over 10 min via syringe. The flask was removed from the ice/water bath and

allowed to warm to rt. After 2 h, the flask was lowered into a dry ice/acetone bath (-78 °C) and (4*R*)-4-(3-oxobutyl)-5-(prop-1-yn-1-yl)dihydrofuran-2(3*H*)-one **3.51** (0.300 g, 1.55 mmol, 1 equiv) was dissolved in THF (2 mL) and added dropwise to the reaction mixture via syringe over 2 min. Upon completion of addition, the mixture was maintained for 15 min then the flask was removed from the dry ice/acetone bath and allowed to warm to rt. After 30 min at this temperature, an additional portion of ethynylmagnesium bromide (4.0 mL of a 0.5 M solution in THF, 2.00 mmol, 1.3 equiv) was added dropwise over 10 min. After 30 min complete consumption of the starting material was evidenced by TLC, and chloroacetyl chloride (0.37 mL, 4.64 mmol, 3 equiv) was added in a single portion via syringe at rt. The mixture was allowed to react for 1 h, at which point the reaction had reached completion based upon consumption of the intermediate **S3.1**, as evidenced by TLC. The mixture was transferred to a separatory funnel, diluted with EtOAc (10 mL) and washed with sat. aq. NH₄Cl (2 x 15 mL). The layers were separated and the combined aqueous phases were extracted with EtOAc (2 x 15 mL). The combined organic phases were dried over MgSO₄, concentrated via rotary evaporation, and the crude residue purified via SiO₂ flash column chromatography (20% to 40% EtOAc/hexanes), affording 0.390 g of the title compound as a viscous yellow oil (85%).

Data for 3.59b

¹H NMR: (400 MHz, CDCl₃)

5.18-5.13 (m, 0.6H), 5.42-4.68 (m, 0.4H), 4.02 (s, 2H), 2.79 (ddd, $J^1 = 17.2$ Hz, $J^2 = 8.0$ Hz, $J^3 = 1.2$ Hz, 0.4H), 2.63 (s, 1H), 2.61-2.48 (m, 1.5H), 2.41-2.30 (m, 0.6H), 2.22 (ddd, $J^1 = 17.2$ Hz, $J^2 = 8.0$ Hz, $J^3 = 3.2$ Hz, 0.4H), 2.10-1.95 (m, 1.1H), 1.91-1.87 (m, 3.6H), 1.87-1.80 (m, 1.7H), 1.76-1.71 (m, 3.2H) ppm;

^{13}C NMR: (100 MHz, CDCl_3)

175.78, 175.76, 175.27, 175.26, 165.43, 165.38, 87.3, 87.2, 85.3, 82.4, 82.2, 82.13, 82.11, 76.7, 76.6, 75.2, 75.15, 75.13, 75.09, 74.9, 74.58, 74.51, 73.23, 73.18, 72.3, 43.35, 43.32, 41.4, 40.6, 39.57, 39.55, 39.16, 39.14, 38.99, 38.97, 34.62, 34.57, 33.73, 33.69, 27.28, 27.26, 26.52, 26.49, 26.4, 25.3, 25.2 ppm;

FTIR (neat)

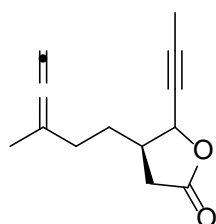
1762, 1310, 1233, 1148, 1035, 972, 864, 792, 672, 529 cm^{-1} ;

HRMS (HRMS ESI)

calcd for $\text{C}_{15}\text{H}_{18}\text{O}_4\text{Cl}$ ($\text{M}+\text{H}^+$): 297.0888; found: 297.0891;

TLC $R_f = 0.71$ (50% EtOAc)

Silica gel, p-anisaldehyde



(4R)-4-(3-methylpenta-3,4-dien-1-yl)-5-(prop-1-yn-1-yl)dihydrofuran-

2(3H)-one (3.57a). A 25-mL 2-necked round bottom flask equipped with stir

bar, nitrogen inlet adapter, and septum, was sequentially charged with

ammonium formate (102 mg, 1.6 mmol, 2 equiv), THF (6.5 mL), and

$\text{Pd}_2\text{dba}_3 \cdot \text{CHCl}_3$ (21 mg, 0.02 mmol, 0.025 equiv) via temporary removal of the septum. To the red

reaction mixture was added tri-*n*-butylphosphine (30 μL , 0.12 mmol, 0.13 equiv) via syringe, at

which point the mixture turned yellow-green. The reaction mixture was maintained at rt for 10 min

before methyl ((3*R*)-3-methyl-5-((3*R*)-5-oxo-2-(prop-1-yn-1-yl)tetrahydrofuran-3-yl)pent-1-yn-

3-yl) carbonate **3.58** (225 mg, 0.81 mmol, 1 equiv) was dissolved in 0.5 mL THF and added in a

single portion via syringe. The reaction was maintained at rt for 18 h, at which point complete

consumption of starting material was observed by TLC. The mixture was filtered through a pad of

celite in a medium porosity fritted glass vacuum filter. The celite pad was rinsed with Et₂O (2 x 20 mL). The combined filtrates were concentrated via rotary evaporation, and the crude residue purified via SiO₂ flash column chromatography (10% to 20% Et₂O in hexanes gradient), affording 120 mg of the title compound as a pale-yellow oil (73%).

Data for 3.57a

¹H NMR: (400 MHz, CDCl₃)

5.16-5.11 (m, 0.38H), 4.70-4.59 (m, 2.62H), 2.75 (dd, $J^1 = 17.2$ Hz, $J^2 = 8.4$ Hz, 0.69H), 2.66-2.58 (m, 0.43H), 2.56-2.47 (m, 1.07H), 2.34 (dd, $J^1 = 16.8$ Hz, $J^2 = 11.2$ Hz, 0.45H), 2.20 (dd, $J^1 = 17.2$ Hz, $J^2 = 8.4$ Hz, 0.57H), 2.03-1.93 (m, 2.22H), 1.90-1.87 (m, 3.18H), 1.86-1.72 (m, 1.54H), 1.72-1.67 (m, 3.26H), 1.57-1.48 (m, 1.17H) ppm;

¹³C NMR: (100 MHz, CDCl₃)

206.2, 206.1, 176.1, 175.5, 97.5, 97.4, 86.9, 84.9, 75.4, 75.2, 74.8, 74.7, 73.4, 72.8, 43.3, 39.3, 34.7, 33.6, 31.3, 31.1, 30.2, 28.1, 18.9, 18.7, 3.8, 3.7 ppm;

FTIR (neat)

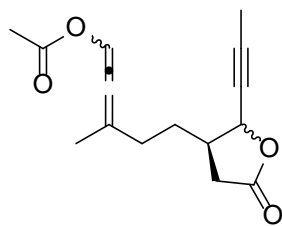
2246, 1959, 1778, 1442, 1149, 977, 847 cm⁻¹;

HRMS (HRMS ESI)

calcd for C₁₃H₁₇O₂ (M+H⁺): 205.1223; found: 205.1219;

TLC R_f = 0.46 (20% EtOAc in hexanes)

Silica gel, KMnO₄



3-methyl-5-((3R)-5-oxo-2-(prop-1-yn-1-yl)tetrahydrofuran-3-yl)penta-1,2-dien-1-yl acetate (3.60a). A 50-mL 2-necked round bottom flask equipped with stir bar, reflux condenser topped with septum, and septum was added rhodium(II) trifluoroacetate dimer (0.107 g, 0.16 mmol, 0.05 equiv) in a nitrogen-filled glovebox via temporary removal of the septum. The flask was removed from the glovebox and the septum on top of the condenser replaced with a nitrogen inlet adapter. Freshly distilled toluene (13 mL) was added via syringe, followed by (3R)-3-methyl-5-((3R)-5-oxo-2-(prop-1-yn-1-yl)tetrahydrofuran-3-yl)pent-1-yn-3-yl acetate **3.59a** (0.850 g, 3.2 mmol, 1 equiv), which was dissolved in toluene (3.2 mL), in a single portion via syringe. The flask was lowered into a preheated oil bath (50 °C), and the mixture maintained for 3 h. Upon complete consumption of starting material, as evidenced by TLC, the flask was removed from the oil bath and allowed to cool to rt. SilametS Thiourea (1.08 g, 1.07 mmol/g, 7.2 equiv with respect to rhodium(II) trifluoroacetate dimer) was added via temporary removal of the septum, and the mixture maintained for 16 h. The mixture was filtered through a pad of celite in a medium porosity fritted glass vacuum filter. The celite pad was rinsed with EtOAc (2 x 10 mL). The combined filtrates were concentrated via rotary evaporation, and the crude residue purified via SiO₂ flash column chromatography (10–30% EtOAc/Hexanes), affording 0.742 g of the title compound as a yellow oil (87%).

Data for 3.60a

¹H NMR: (400 MHz, CDCl₃)

7.36–7.30 (m, 1H), 5.17–5.10 (m, 0.63H), 4.70–4.65 (m, 0.37H), 2.79–2.70 (m, 0.46H), 2.65–2.57 (m, 0.90H), 2.56–2.46 (m, 1H), 2.39–2.29 (m, 0.83H), 2.16–2.08 (m, 3.42H), 1.90–1.87 (m, 2.75H), 1.86–1.83 (m, 3H) ppm;

¹³C NMR: (100 MHz, CDCl₃)

189.8, 189.7, 175.9, 175.3, 174.1, 168.8, 123.8, 114.8, 113.9, 110.6, 110.4, 110.3, 107.7, 100.1, 87.0, 75.2, 74.6, 73.3, 72.6, 66.0, 64.9, 43.1, 39.3, 39.2, 34.6, 33.6, 33.6, 32.9, 32.7, 32.6, 30.0, 29.9, 28.0, 21.1, 21.0, 20.6, 15.4, 3.8 ppm;

FTIR (neat)

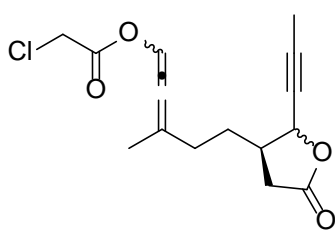
1777, 1744, 1369, 1212, 1154, 1040, 970, 794, 599, 548 cm⁻¹;

HRMS (HRMS ESI)

calcd for C₁₅H₁₉O₄ (M+H⁺): 263.1278; found: 263.1279;

TLC R_f = 0.42 (30% EtOAc in hexanes)

Silica gel, visualized with p-anisaldehyde



3-methyl-5-((3R)-5-oxo-2-(prop-1-yn-1-yl)tetrahydrofuran-3-yl)penta-1,2-dien-1-yl 2-chloroacetate (3.60b).

A 15-mL 2-necked round bottom flask equipped with stir bar, reflux condenser topped with nitrogen septum, and septum was added rhodium(II) trifluoroacetate dimer (0.039 g, 0.06 mmol, 0.05 equiv) in a nitrogen-filled glovebox via temporary removal of the septum. The flask was removed from the glovebox and the septum on top of the

condenser replaced with a nitrogen inlet adapter. Freshly distilled toluene (5.9 mL) was added via syringe, followed by (3R)-3-methyl-5-((3R)-5-oxo-2-(prop-1-yn-1-yl)tetrahydrofuran-3-yl)pent-1-yn-3-yl 2-chloroacetate **3.59b** (0.350 g, 1.18 mmol, 1 equiv), which was dissolved in toluene (2 mL), in a single portion via syringe. The flask was lowered into a preheated oil bath (50 °C), and the mixture maintained for 8 h. Upon complete consumption of starting material, as evidenced by TLC, the flask was removed from the oil bath and allowed to cool to rt. SilametS Thiourea (0.393 g, 1.07 mmol/g, 7 equiv with respect to rhodium(II) trifluoroacetate dimer) was added via temporary removal of the septum, and the mixture maintained for 11 h. The mixture was filtered through a pad of celite in a medium porosity fritted glass vacuum filter. The celite pad was rinsed with EtOAc (2 x 10 mL). The combined filtrates were concentrated via rotary evaporation, and the crude residue purified via SiO₂ flash column chromatography (15%-20% EtOAc/Hexanes), affording 0.303 g of the title compound as a pale yellow oil (87%).

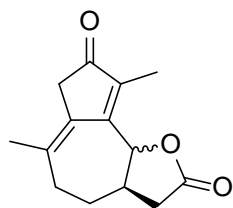
Data for 3.60b

¹H NMR: (400 MHz, CDCl₃)

7.35-7.29 (m, 1H), 5.16-5.10 (m, 0.65H), 4.69-4.65 (m, 0.36H), 4.15-4.12 (m, 2.06H), 2.79-2.70 (m, 0.35H), 2.64-2.47 (m, 1.63H), 2.39-2.29 (m, 0.72H), 2.24-2.10 (m, 2.41H), 1.90-1.85 (m, 6.42H), 1.84-1.71 (m, 2.11H) ppm;

TLC R_f = 0.43 (30% EtOAc in hexanes)

Silica gel, visualized with p-anisaldehyde



(3aR)-6,9-dimethyl-3a,5,7,9b-tetrahydroazuleno[4,5-b]furan-2,8(3H,4H)-

dione (3.61). A 15-mL 2-necked round bottom flask equipped with stir bar,

reflux condenser topped with septum, and septum was sequentially added

bis(1,5-cyclooctadiene)rhodium(I) tetrafluoroborate (5.0 mg, 0.013 mmol,

0.025 equiv) and PPh₃ (5.0 mg, 0.019 mmol, 0.038 equiv) in a nitrogen-filled glovebox via

temporary removal of the septum. The flask was removed from the glove box and a nitrogen inlet

needle was inserted into the septum on the condenser. 1,2-Dichloroethane (5 mL) was added via

syringe. The resulting dark yellow solution was maintained at rt for 10 min at which time the flask

was evacuated and refilled five times with CO gas (100%), alternating between an inlet needle

attached to a vacuum and an inlet needle attached to a balloon of CO. The light-yellow solution

was maintained for 10 min before (4R)-4-(3-methylpenta-3,4-dien-1-yl)-5-(prop-1-yn-1-

yl)dihydrofuran-2(3H)-one **3.57a** (0.10 g, 0.51 mmol, 1 equiv) was added in a single portion via

syringe, using 0.5 mL 1,2-dichloroethane to rinse the syringe. The flask was lowered into a

preheated oil bath (70 °C), and the reaction maintained for 18 h. Very little starting material had

been consumed at this point, as evidenced by TLC. Bis-(1,5-cyclooctadiene)rhodium(I)

tetrafluoroborate (12 mg, 0.06 equiv) and PPh₃ (12 mg, 0.09 equiv) were added to a flame-dried

scintillation vial in a nitrogen-filled glove box. The vial was sealed with a septum, removed from

the glovebox and 1,2-dichloroethane (0.1 mL) added via syringe. The resulting solution was

transferred to the reaction flask via syringe. The reaction was maintained at 70 °C for an additional

24 h at which point complete consumption of starting material was observed by TLC. The flask

was removed from the oil bath and allowed to cool to rt. The contents were transferred to a 50-mL

recovery flask, using CH₂Cl₂ to rinse the flask forward. Concentration via rotary evaporation (40

°C bath temperature), followed by purification of the crude residue via SiO₂ flash column

chromatography (40% EtOAc/hexanes) afforded 67 mg of the title compound as an off-white solid (57%). *Cis*-**3.61** and *trans*-**3.61** isomers were separable at this stage. 8 mg of *cis*-**3.61** and 8 mg of *trans*-**3.61** were isolated, along with 51 mg of combined *cis*-**3.61** and *trans*-**3.61**.

Data for *trans*-**3.61**

¹H NMR: (400 MHz, CDCl₃)

5.32 (d, $J = 10.8$ Hz, 1H), 2.97 (s, 2H), 2.77 (dd, $J^1 = 16.8$ Hz, $J^2 = 8$ Hz, 1H), 2.66-2.54 (m, 2H), 2.39 (dd, $J^1 = 16.8$ Hz, $J^2 = 12.4$ Hz, 1H), 2.29-2.19 (m, 2H), 2.03 (s, 3H), 1.88 (s, 3H), 1.78-1.71 (m, 1H) ppm;

¹³C NMR: (100 MHz, CDCl₃)

204.4, 175.1, 161.0, 139.2, 132.9, 129.8, 82.3, 40.4, 40.3, 36.5, 32.6, 28.0, 24.6, 9.9 ppm;

FTIR (neat)

2249, 1779, 1749, 1440, 1375, 1262, 1149 cm⁻¹;

HRMS (HRMS ESI)

calcd for C₁₄H₁₇O₃ (M+H⁺): 233.1172; found: 233.1174;

TLC R_f = 0.30 (40%EtOAc in hexanes)

Silica gel, visualized with KMnO₄

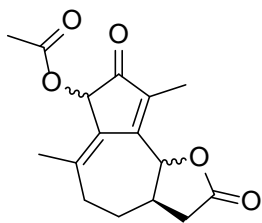
Data for *cis*-**3.61**

¹H NMR: (400 MHz, CDCl₃)

5.59 (d, $J = 5.6$ Hz, 1H), 3.07-2.98 (m, 2H), 2.98-2.88 (m, 2H), 2.50-2.24 (m, 4H), 1.92 (s, 3H), 1.90-1.87 (m, 1H), 1.85 (s, 3H) ppm;

^{13}C NMR: (100 MHz, CDCl_3)

204.4, 176.2, 157.7, 143.4, 137.1, 128.8, 79.7, 41.2, 38.4, 36.3, 32.8, 31.2, 24.1, 9.0
ppm;



(3aR)-6,9-dimethyl-2,8-dioxo-2,3,3a,4,5,7,8,9b-octahydroazuleno[4,5-b]furan-7-yl acetate (3.62a). To a 500-mL 2-necked round bottom flask

equipped with stir bar, reflux condenser topped with septum, and septum was sequentially added bis-(1,5-cyclooctadiene)rhodium(I) tetrafluoroborate (20 mg, 0.049 mmol, 0.025 equiv) and PPh_3 (20 mg, 0.076 mmol, 0.038 equiv) in a nitrogen-filled glovebox via temporary removal of the septum. The flask was removed from the glovebox, a nitrogen inlet needle was inserted into the septum on the condenser, and 1,2-dichloroethane (200 mL) added via syringe. The resulting dark yellow solution was maintained at rt for 10 min at which time the flask was evacuated and refilled five times with CO gas (100%), alternating between an inlet needle attached to a vacuum and an inlet needle attached to a balloon of CO. The light-yellow solution was maintained for 10 min before 3-methyl-5-((3R)-5-oxo-2-(prop-1-yn-1-yl)tetrahydrofuran-3-yl)penta-1,2-dien-1-yl acetate **3.60a** (0.525 g, 2.00 mmol, 1 equiv) dissolved in 1,2-dichloroethane (5 mL), was added in a single portion via syringe. The flask was lowered into a preheated oil bath set to 70 °C, and the mixture reacted for 19 h, at which point an addition portion of bis-(1,5-cyclooctadiene)rhodium(I) tetrafluoroborate (20 mg, 0.049 mmol, 0.025 equiv) and PPh_3 (20 mg, 0.076 mmol, 0.038 equiv) were added via temporary removal of the septum. The reaction was maintained for 24 h at which point the starting material had been consumed, as evidenced by TLC. The flask was removed from the oil bath and allowed to cool to rt. The contents were transferred to a recovery flask and concentrated via rotary evaporation (40

°C bath temperature). The crude residue was purified via SiO₂ flash column chromatography (40–60% EtOAc/hexanes), affording 0.405 g of the title compound as a stick, off-white solid (70%). A small amount of the *cis* and *trans* lactone isomers were semi-separable at this stage, affording 0.010 g *trans*-**3.62a**, 0.010 g *cis*-**3.62a**.

Data for **3.62a**

¹H NMR: (400 MHz, CDCl₃)

5.65–5.61 (m, 1H), 5.58 (s, 0.59H), 5.56–5.54 (m, 0.39H), 5.44 (s, 0.71H), 5.39 (d, *J* = 10.8 Hz, 0.67H), 5.32 (d, *J* = 10.8 Hz, 0.33H), 3.04–2.92 (m, 2.11H), 2.83–2.73 (m, 1.24H), 2.72–2.54 (m, 2.38H), 2.49–2.35 (m, 3.52H), 2.34–2.15 (m, 4.11H), 2.51–2.10 (m, 5.93H), 2.06–2.03 (m, 3.03H), 2.03–1.95 (m, 1.83H), 1.95–1.92 (m, 2.71H), 1.89–1.87 (m, 2.86H), 1.85–1.82 (m, 3.30H), 1.81–1.71 (m, 2.35H) ppm;

¹³C NMR: (100 MHz, CDCl₃)

200.4, 200.1, 176.4, 174.8, 169.7, 169.5, 161.5, 161.1, 156.9, 140.0, 139.3, 137.6, 136.6, 135.9, 135.6, 130.7, 129.5, 128.8, 82.0, 81.5, 81.0, 18.5, 73.7, 72.0, 71.2, 39.9, 39.8, 37.0, 36.4, 36.2, 35.7, 34.3, 33.0, 32.5, 31.7, 31.6, 29.8, 28.3, 27.9, 24.2, 23.6, 23.3, 23.1, 20.8, 20.6, 20.5, 15.4, 10.1, 9.8, 9.5, 8.8 ppm;

FTIR (neat)

2927, 1781, 1743, 1703, 1217, 1160, 1039, 732 cm⁻¹;

HRMS (HRMS ESI)

calcd for C₁₆H₁₉O₅ (M+H⁺): 291.1227; found: 291.1246;

TLC R_f = 0.29 (50% EtOAc/hexanes)

Silica gel, visualized with KMnO₄

¹H NMR *trans*-3.62a

¹H NMR: (400 MHz, CDCl₃)

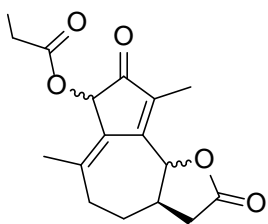
5.58 (s, 0.59H), 5.56 (s, 0.30H), 5.40 (d, *J* = 12.0 Hz 0.65H), 5.32 (d, *J* = 8.0 Hz),
2.84–2.74 (m, 1.14H), 2.72–2.53 (m, 2.58H), 2.45–2.32 (m, 1.52H), 2.32–2.15 (m,
3.37H), 2.15–2.11 (m, 2.77H), 2.07–2.03 (m, 2.64H), 1.90–1.87 (m, 2.93H), 1.80–
1.69 (m, 1.58H) ppm;

¹H NMR for *cis*-3.62a

¹H NMR: (400 MHz, CDCl₃)

5.63 (d, *J* = 6.0 Hz, 1H), 5.44 (s, 0.90H), 3.04–2.94 (m, 2.68H), 2.46–2.36 (m,
2.82H), 2.29–2.17 (m, 2.68H), 2.16–2.10 (m, 3.73H), 2.07–1.95 (m, 3.22H), 1.95–
1.90 (m, 3.92H), 1.90–1.82 (m, 4.44H), 1.81–1.73 (m, 2.22H) ppm;

Cl



3 a R) - 6 , 9 - d i m e t h y l - 2 , 8 - d i o x o - 2 , 3 , 3 a , 4 , 5 , 7 , 8 , 9 b -
octahydroazuleno[4,5-b]furan-7-yl 2-chloroacetate (3.62b). To a 50-
mL 2-necked round bottom flask equipped with stir bar, reflux condenser
topped with septum, and septum was sequentially added bis-(1,5-

cyclooctadiene)rhodium(I) tetrafluoroborate (5.0 mg, 0.013 mmol, 0.025 equiv) and PPh₃ (5.0 mg,
0.019 mmol, 0.038 equiv) in a nitrogen-filled glovebox via temporary removal of the septum. The
flask was removed from the glovebox, a nitrogen inlet needle was inserted into the septum on the
condenser, and 1,2-dichloroethane (21 mL) added via syringe. The resulting dark yellow solution
was maintained at rt for 10 min at which time the flask was evacuated and refilled five times with
CO gas (100%), alternating between an inlet needle attached to a vacuum and an inlet needle

attached to a balloon of CO. The light-yellow solution was maintained for 10 min before 3-methyl-5-((3R)-5-oxo-2-(prop-1-yn-1-yl)tetrahydrofuran-3-yl)penta-1,2-dien-1-yl 2-chloroacetate **3.60b** (0.185 g, 0.62 mmol, 1 equiv) dissolved in 1 mL 1,2-dichloroethane, was added in a single portion via syringe. The flask was lowered into a preheated oil bath set to 70 °C, and the mixture reacted for 28 h, at which point the starting material had been consumed, as evidenced by TLC. The flask was removed from the oil bath and allowed to cool to rt. The contents were transferred to a recovery flask and concentrated via rotary evaporation (40 °C bath temperature). The crude residue was purified via SiO₂ flash column chromatography (20% to 50% EtOAc/hexanes), affording 0.121 g of the title compound as a yellow solid (60%). The *cis* and *trans* lactone isomers were semi-separable at this stage, affording 0.026 g *trans*-**3.62b**, 0.036 g *cis*-**3.62b**, and 0.059 g **3.62b** as a mixture.

Data for *trans*-**3.62b**

¹H NMR: (400 MHz, CDCl₃)

5.64 (s, 0.75H), 5.58 (s, 0.25H), 5.40 (d, *J* = 10.8 Hz, 0.75H), 5.32 (d, *J* = 10.8 Hz, 0.25H), 4.15-4.08 (m, 2H), 2.83-2.75 (m, 1H) 2.71-2.53 (m, 2.28H), 2.43-2.35 (m, 1.26H), 2.32-2.16 (m, 3.04H), 2.07-2.03 (m, 2.90H), 1.94-1.85 (m, 4.18H), 1.82-1.72 (m, 1.35H) ppm;

¹³C NMR: (100 MHz, CDCl₃)

199.6, 199.1, 174.7, 174.6, 166.33, 161.8, 161.5, 138.6, 136.9, 136.6, 135.7, 129.9, 128.7, 127.7, 81.9, 81.4, 73.3, 73.0, 72.7, 40.6, 40.5, 39.8, 39.4, 38.2, 36.4, 36.2, 33.6, 33.0, 32.5, 28.3, 27.8, 24.5, 23.7, 17.7, 10.1, 9.8, 3.8 ppm;

FTIR (neat)

2924, 1768, 1704, 1157, 1008, 954, 784, 478 cm⁻¹;

HRMS (HRMS ESI)

calcd for C₁₆H₁₈O₅Cl (M+H⁺): 325.0837; found: 325.0837;

TLC R_f = 0.29 (50% EtOAc/hexanes)

Silica gel, visualized with KMnO₄

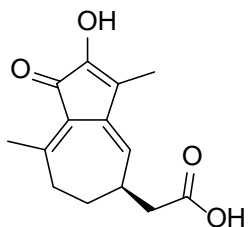
Data for *cis*-3.62b

¹H NMR: (400 MHz, CDCl₃)

5.69 (s, 0.29H), 5.63 (d, *J* = , 0.72H), 5.54 (d, *J* = ,), 5.56-5.50 (m, 1H), 4.15-4.10 (m, 2H), 3.04-2.95 (m, 1.77H), 2.82-2.74 (0.67H) 2.47-2.37 (m, 2.22H), 2.31-2.21 (m, 1.54H), 2.08-1.99 (m, 1.38H), 1.98 (s, 1H), 1.95 (s, 2H), 1.88-1.84 (m, 3H), 1.82-1.75 (m, 1.30H) ppm;

¹³C NMR: (100 MHz, CDCl₃)

199.4, 199.0, 176.3, 175.6, 166.3, 166.0, 158.6, 157.4, 141.2, 141.0, 139.4, 138.8, 128.6, 128.0, 80.9, 78.4, 74.9, 74.1, 40.7, 40.6, 40.5, 40.4, 37.0, 35.7, 35.6, 34.3, 31.7, 31.5, 29.8, 23.6, 23.4, 9.5, 8.8 ppm;



(R)-2-(2-hydroxy-3,8-dimethyl-1-oxo-1,5,6,7-tetrahydroazulen-5-yl)acetic acid (3.67). A 0.5–2-mL microwave vial (Biotage 3532016) equipped with stir bar (Biotage 355544) was charged with (3aR)-6,9-dimethyl-2,8-dioxo-2,3,3a,4,5,7,8,9b-octahydroazuleno[4,5-b]furan-7-yl 2-

chloroacetate **3.62b** (10 mg, 0.031 mmol, 1 equiv). The vial was sealed with a crimp-on microwave

vial cap with septum (Biotage 352298) and flushed with nitrogen via an inlet needle. THF (1 mL) was added via syringe, and the vial was lowered into an ice/water (0 °C) bath. Potassium *tert*-butoxide (0.18 mL of a 0.5 M solution in *tert*-butanol, 0.09 mmol, 3 equiv) was added dropwise over 1 min, during which period the solution turned dark orange as a precipitate formed. The mixture was maintained for 10 min, at which point complete consumption of the starting material was evidenced by TLC. Sat. NH₄Cl (1 mL) was added, and the mixture transferred to a separatory funnel. The layers were separated and the organic layer dried over MgSO₄ and concentrated via rotary evaporation, affording 7 mg of a red residue. ¹H NMR and ¹³C NMR of this residue was used for characterization. The NMR was contaminated with *tert*-butanol and a product of the chloroacetate deprotection.

Data for 3.67 (crude)

¹H NMR: (400 MHz, CDCl₃)

5.75 (d, 4.0 Hz, 1H), 3.08–2.99 (m, 1H), 2.61–2.56 (m, 2H), 2.54 (d, *J* = 6.8 Hz, 1H), 2.48 (d, *J* = 8.0 Hz, 1H), 2.42 (s, 3H), 2.00 (s, 3H), 1.98–1.94 (m, 1H), 1.92–1.87 (m, 1H), 1.87–1.78 (m, 2H) ppm;

¹³C NMR: (100 MHz, CDCl₃)

189.4, 177.4, 171.6, 155.4, 151.6, 134.3, 125.7, 125.0, 40.3, 37.9, 37.0, 30.6, 22.0, 8.5 ppm;

FTIR (neat)

2922, 1701, 1644, 1600, 1414, 1153, 1054, 907, 787, 590, 471 cm⁻¹;

HRMS (HRMS ESI)

calcd for C₁₄H₁₇O₄ (M+H⁺): 249.1121; found: 249.1123;

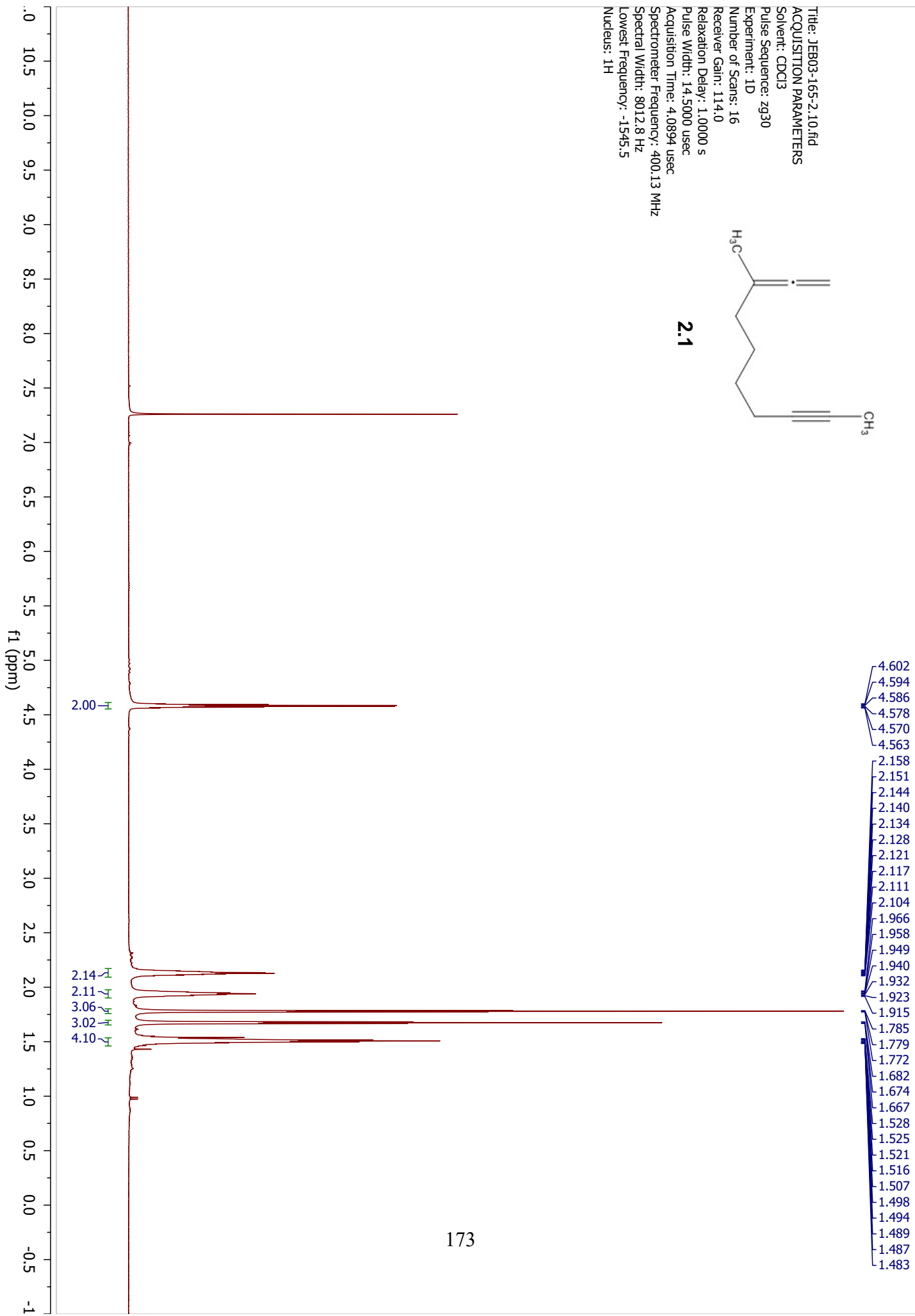
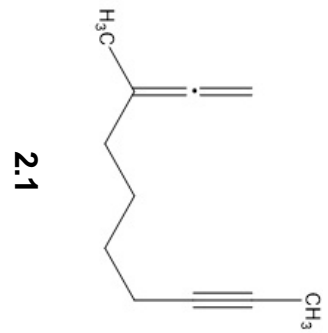
TLC

$R_f = 0.23$ (60% EtOAc in hexanes)

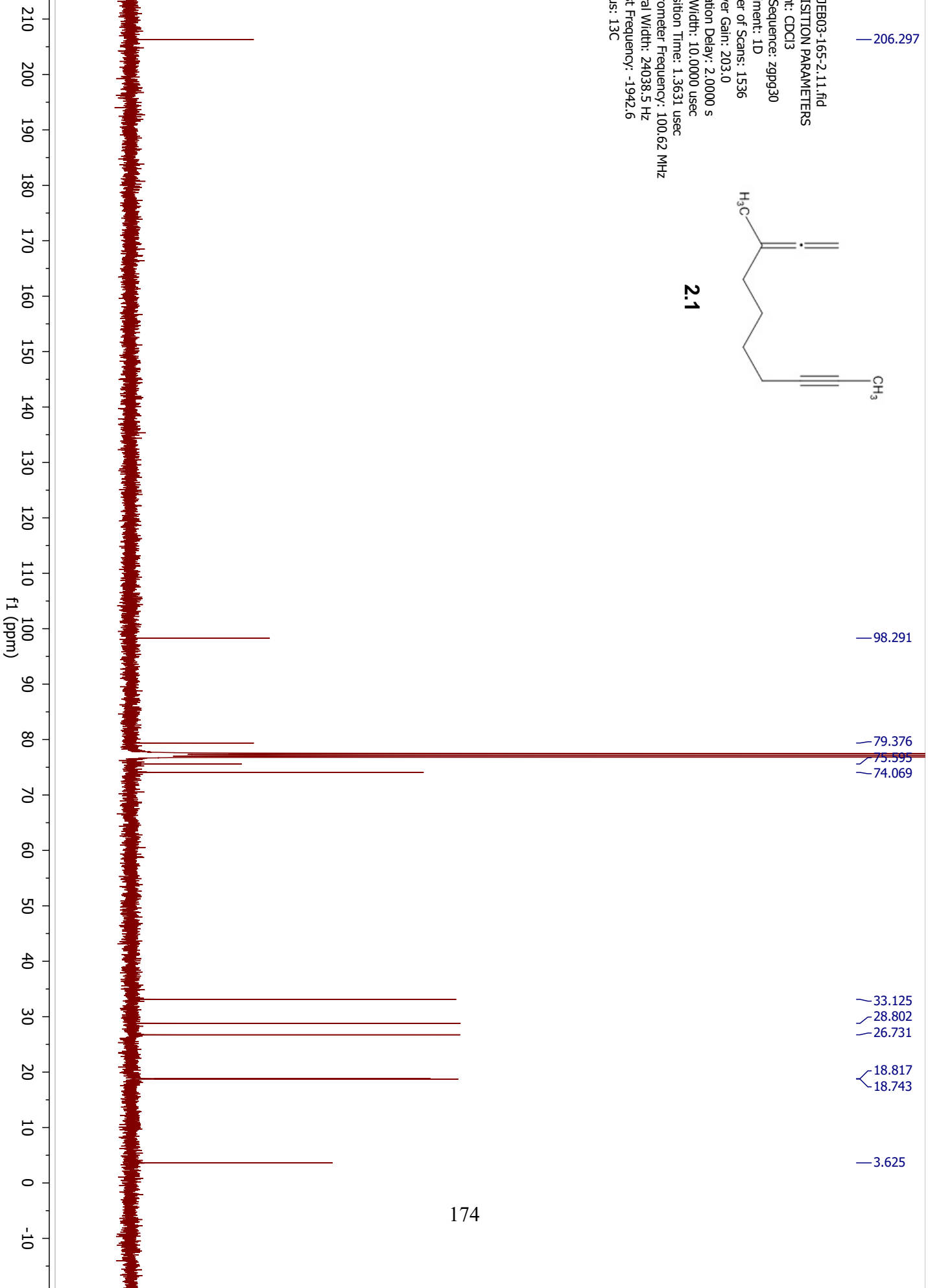
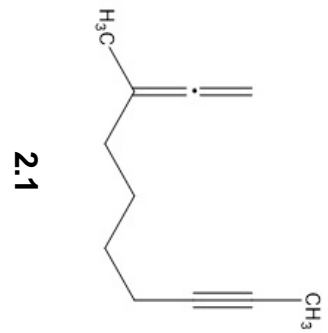
Silica gel, visualized with UV

Appendix C : NMR Spectra

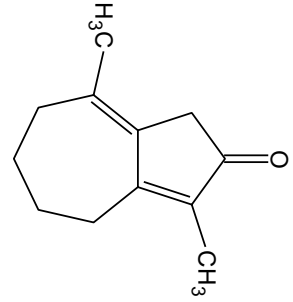
Title: JEB03-165-2.10.fid
ACQUISITION PARAMETERS
Solvent: CDCl3
Pulse Sequence: zg30
Experiment: 1D
Number of Scans: 16
Receiver Gain: 114.0
Relaxation Delay: 1.0000 s
Pulse Width: 14.5000 usec
Acquisition Time: 4.0894 usec
Spectrometer Frequency: 400.13 MHz
Spectral Width: 8012.8 Hz
Lowest Frequency: -1545.5
Nucleus: 1H



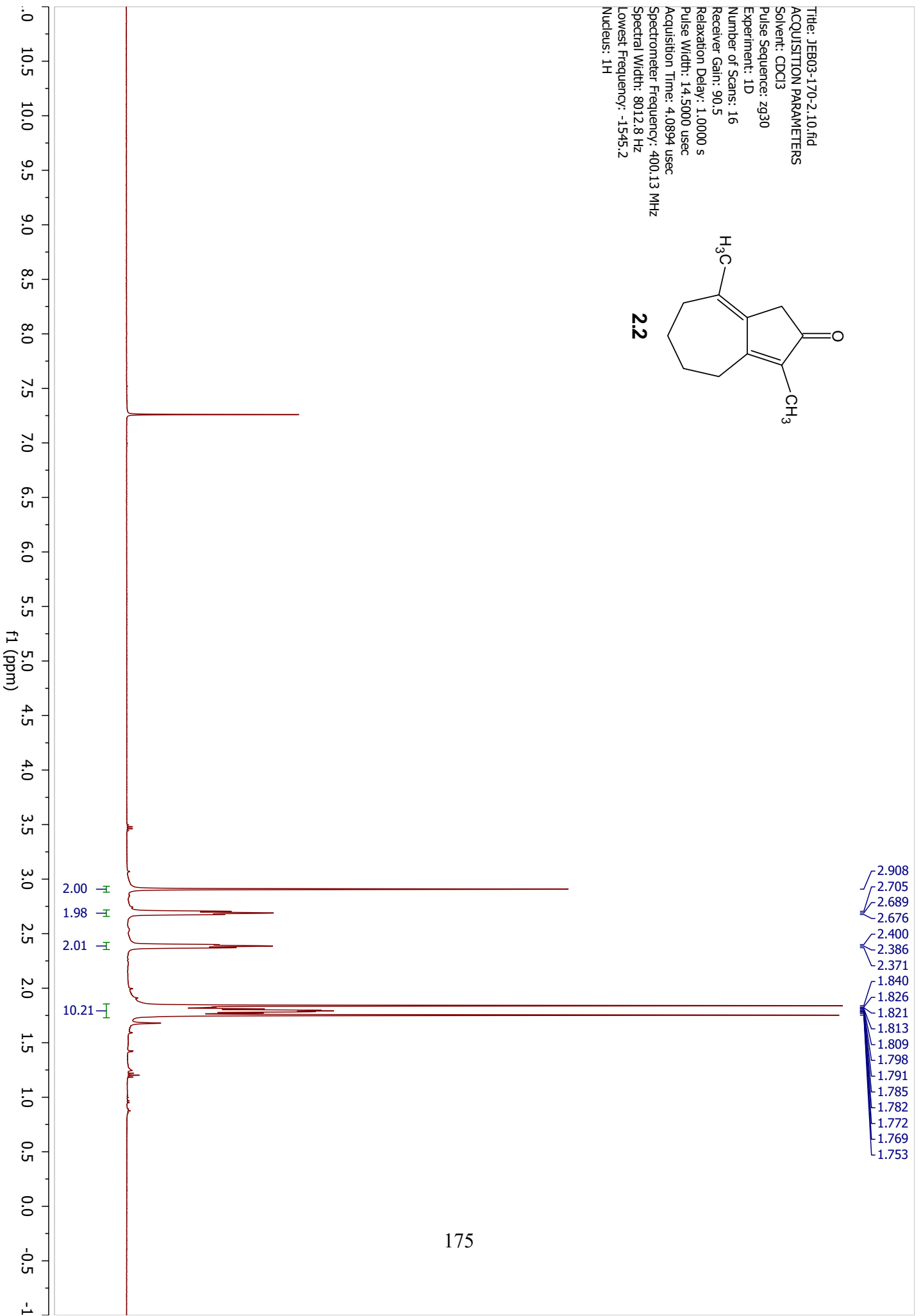
Title: JEB03-165-2.11.fid
ACQUISITION PARAMETERS
Solvent: CDCl3
Pulse Sequence: zppg30
Experiment: 1D
Number of Scans: 1536
Receiver Gain: 203.0
Relaxation Delay: 2.0000 s
Pulse Width: 10.0000 usec
Acquisition Time: 1.3631 usec
Spectrometer Frequency: 100.62 MHz
Spectral Width: 24038.5 Hz
Lowest Frequency: -1942.6
Nucleus: 13C



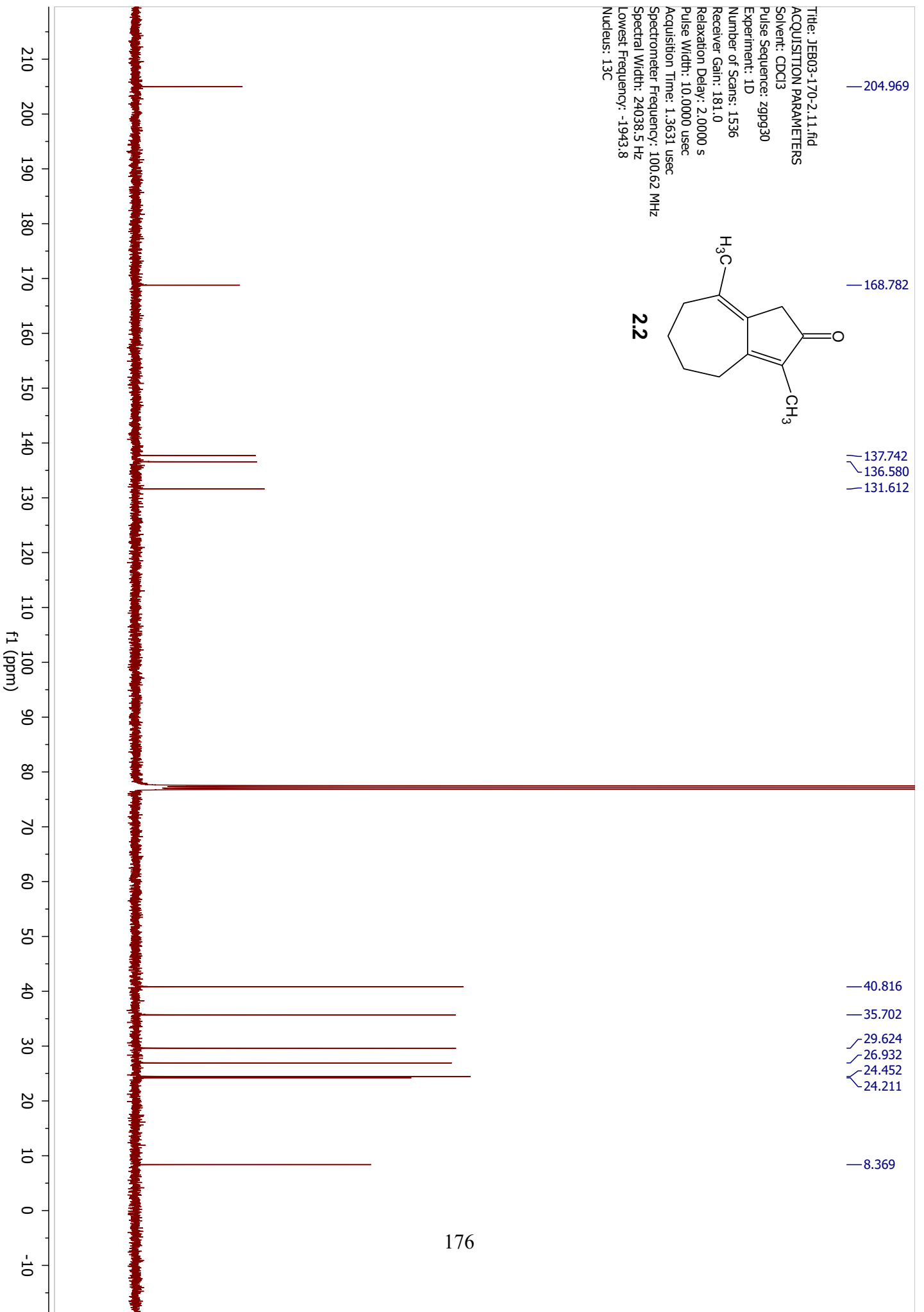
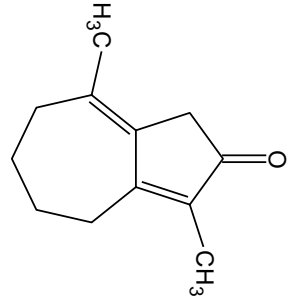
Title: JEB03-170-2.10.fid
ACQUISITION PARAMETERS
Solvent: CDCl3
Pulse Sequence: zg30
Experiment: 1D
Number of Scans: 16
Receiver Gain: 90.5
Relaxation Delay: 1.0000 s
Pulse Width: 14.5000 usec
Acquisition Time: 4.0894 usec
Spectrometer Frequency: 400.13 MHz
Spectral Width: 8012.8 Hz
Lowest Frequency: -1545.2
Nucleus: 1H



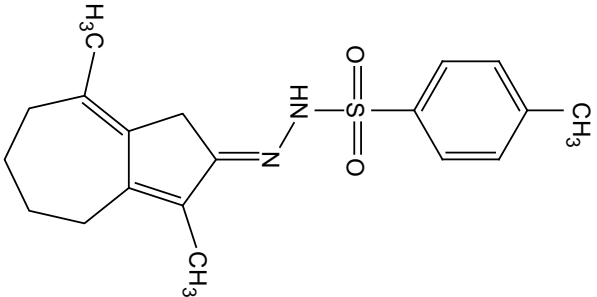
2.2



Title: JEB03-170-2.11.fid
ACQUISITION PARAMETERS
Solvent: CDCl3
Pulse Sequence: zppg30
Experiment: 1D
Number of Scans: 1536
Receiver Gain: 181.0
Relaxation Delay: 2.0000 s
Pulse Width: 10.0000 usec
Acquisition Time: 1.3631 usec
Spectrometer Frequency: 100.62 MHz
Spectral Width: 24038.5 Hz
Lowest Frequency: -1943.8
Nucleus: 13C

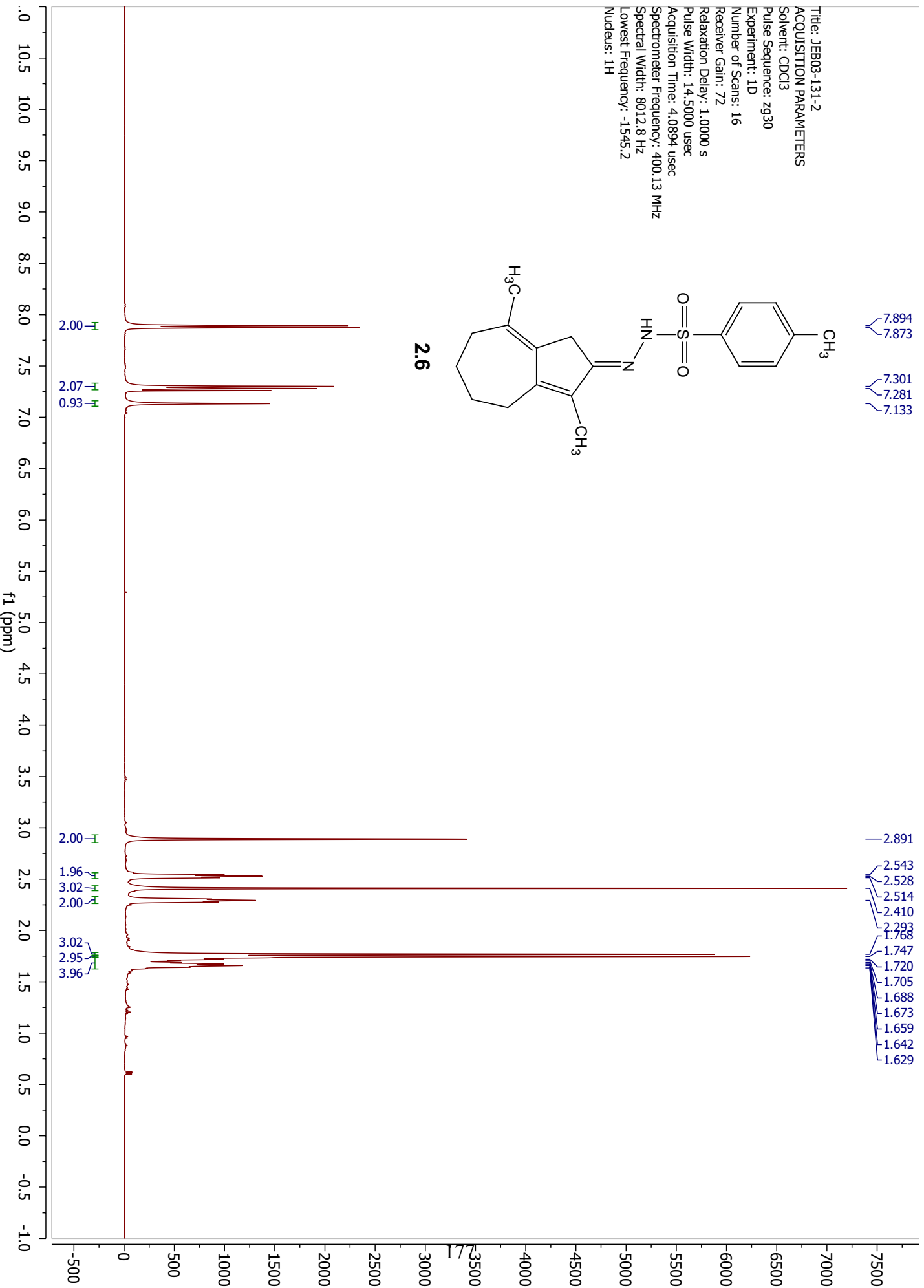


Title: JEB03-131-2
ACQUISITION PARAMETERS
Solvent: CDCl3
Pulse Sequence: zg30
Experiment: 1D
Number of Scans: 16
Receiver Gain: 72
Relaxation Delay: 1.0000 s
Pulse Width: 14.5000 usec
Acquisition Time: 4.0894 usec
Spectrometer Frequency: 400.13 MHz
Spectral Width: 8012.8 Hz
Lowest Frequency: -1545.2
Nucleus: 1H

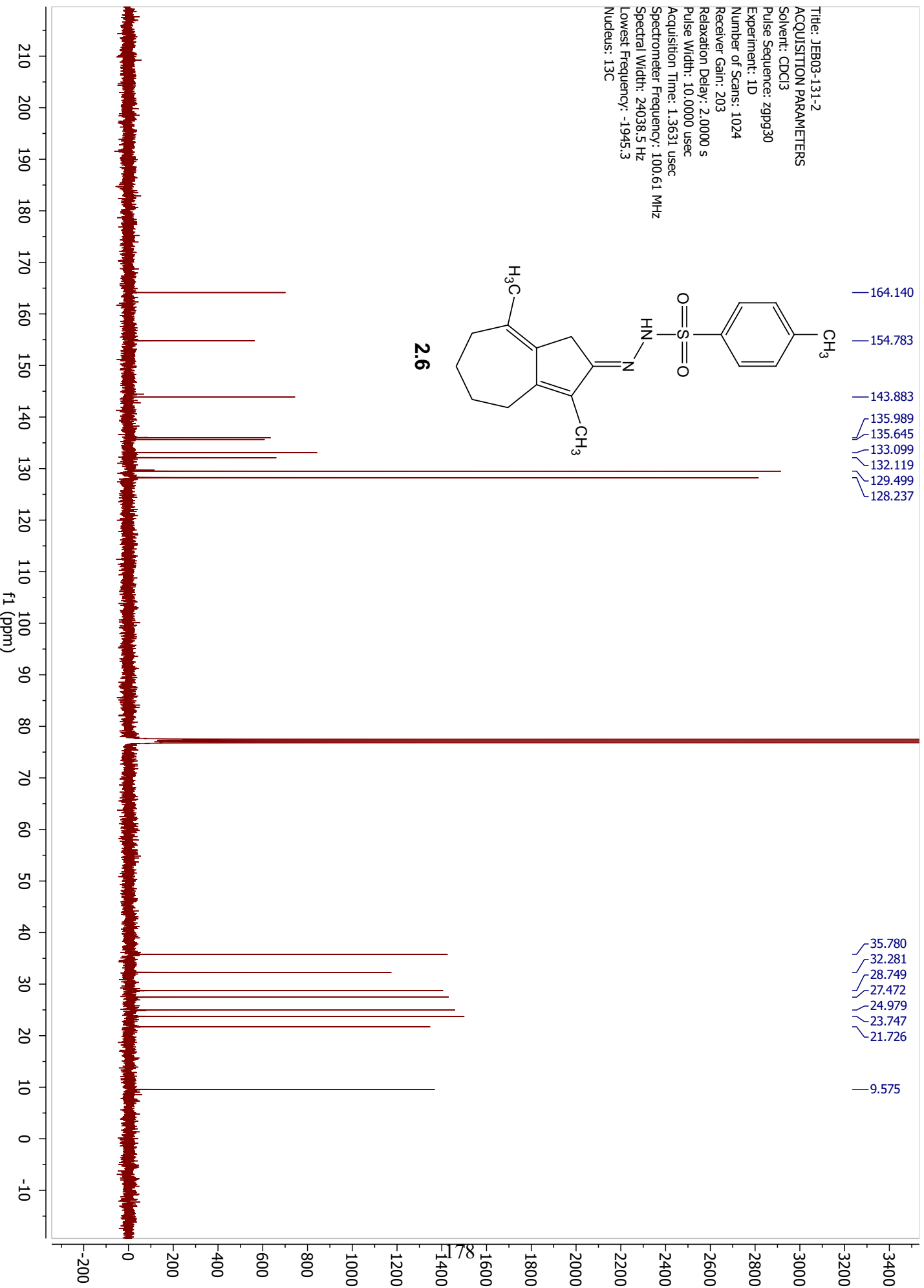
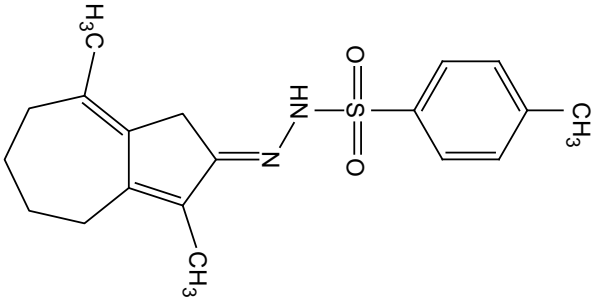


7.894
7.873
7.301
7.281
7.133

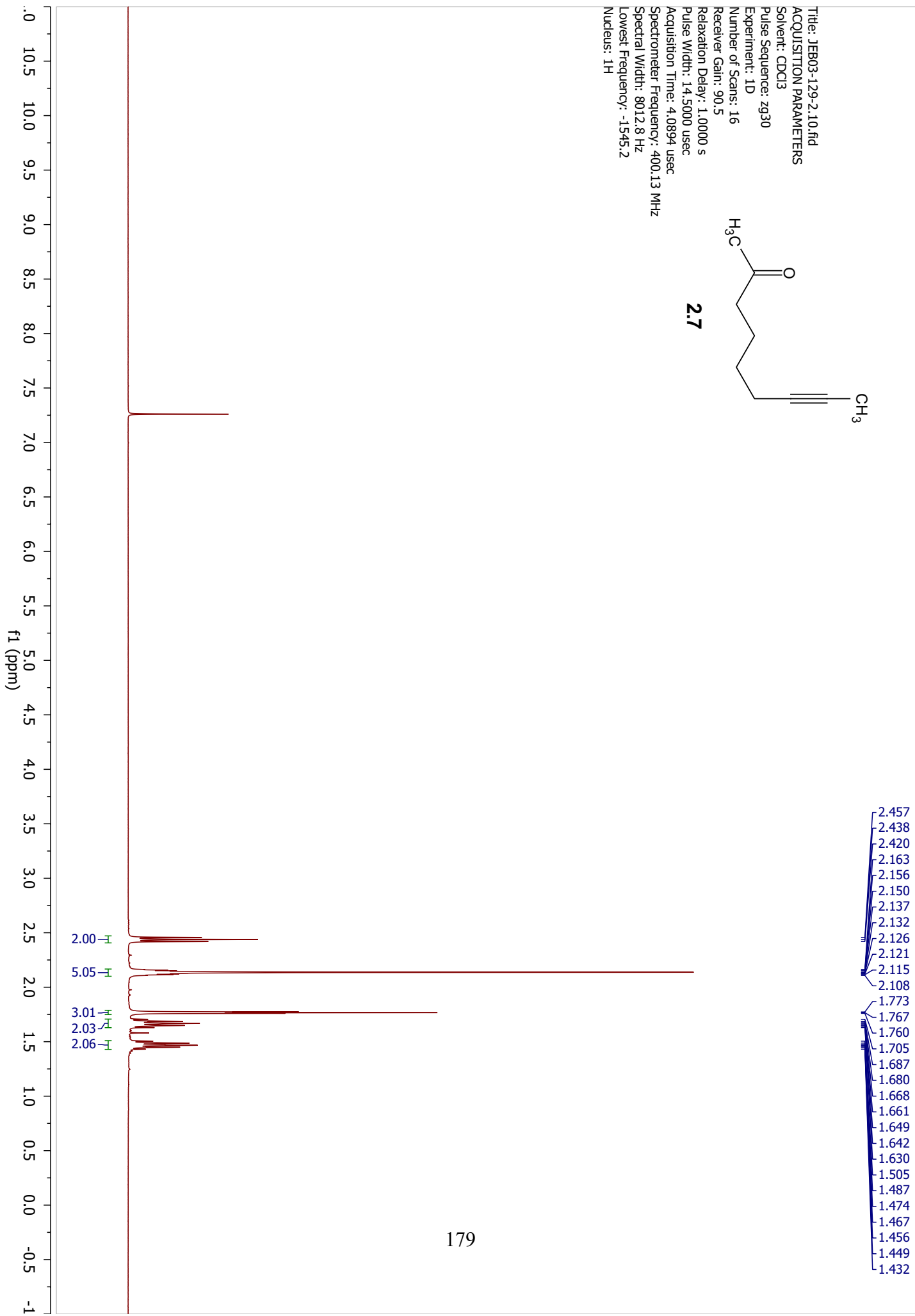
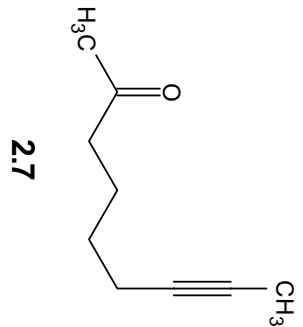
2.6



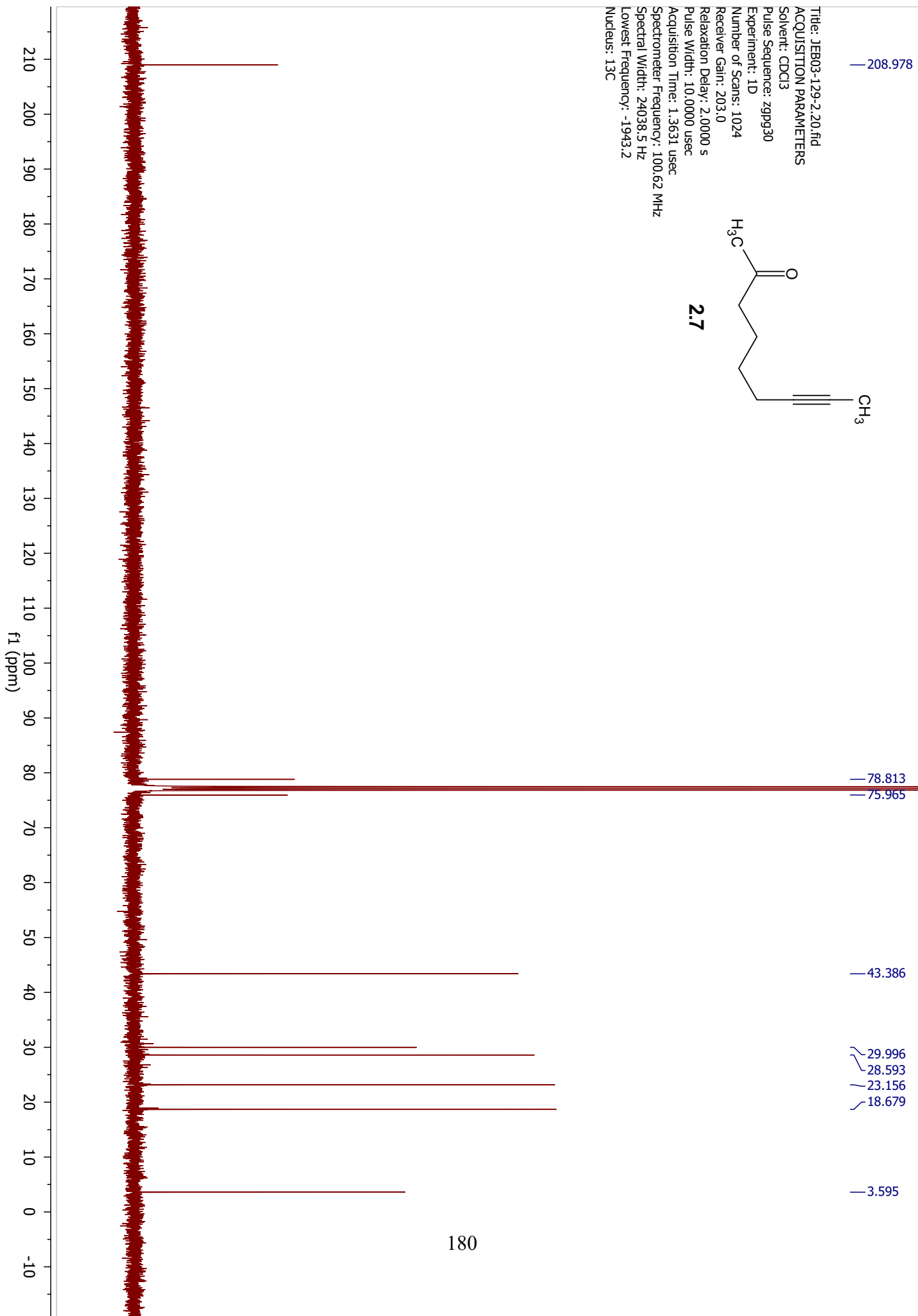
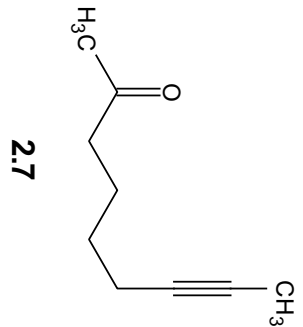
Title: JEB03-131-2
 ACQUISITION PARAMETERS
 Solvent: CDCl3
 Pulse Sequence: zpgp30
 Experiment: 1D
 Number of Scans: 1024
 Receiver Gain: 203
 Relaxation Delay: 2.0000 s
 Pulse Width: 10.0000 usec
 Acquisition Time: 1.3631 usec
 Spectrometer Frequency: 100.61 MHz
 Spectral Width: 24038.5 Hz
 Lowest Frequency: -1945.3
 Nucleus: 13C



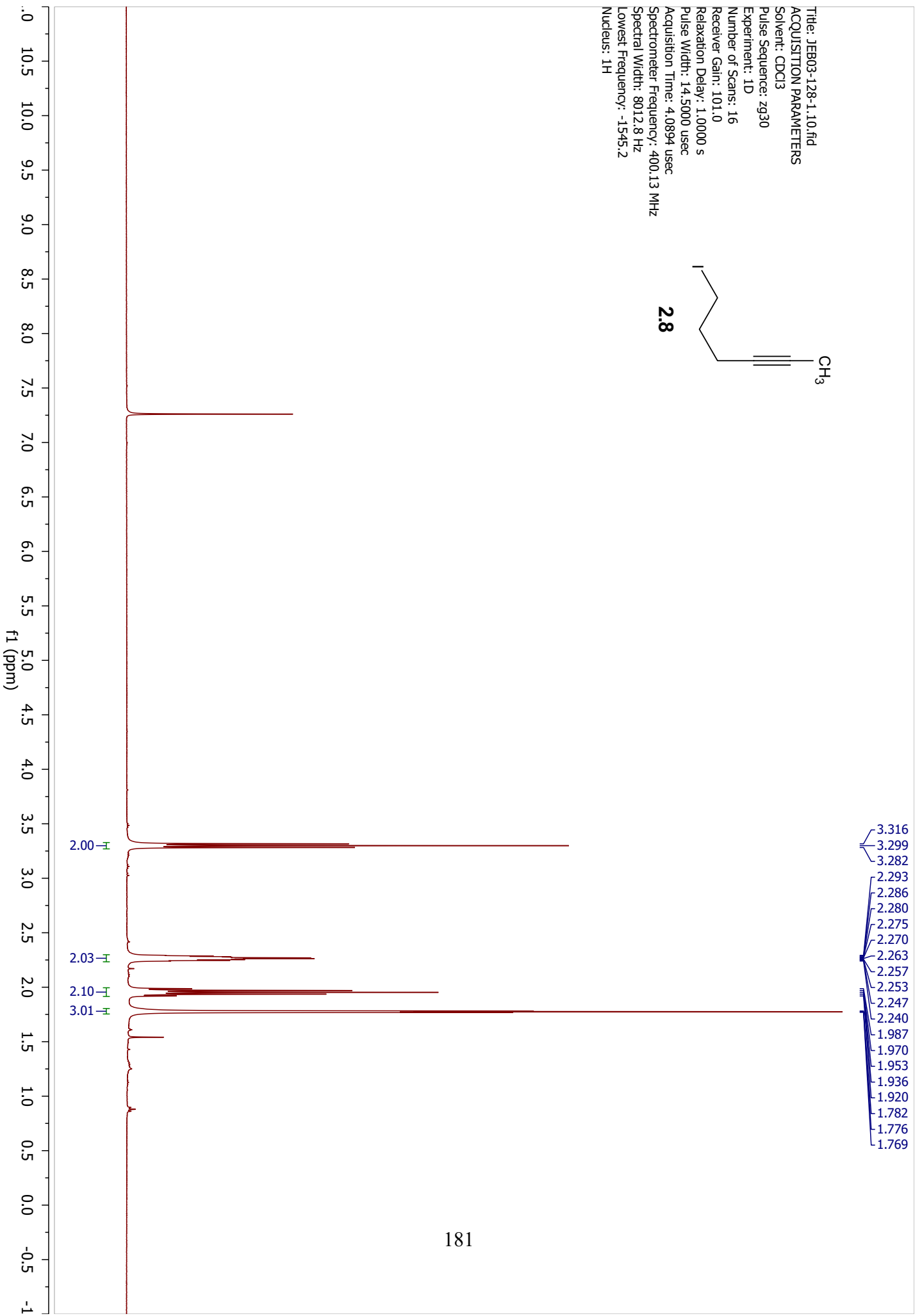
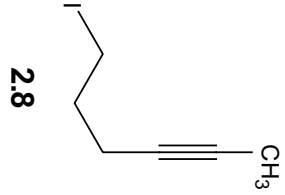
Title: JEB03-129-2.10.fid
ACQUISITION PARAMETERS
Solvent: CDCl3
Pulse Sequence: zg30
Experiment: 1D
Number of Scans: 16
Receiver Gain: 90.5
Relaxation Delay: 1.0000 s
Pulse Width: 14.5000 usec
Acquisition Time: 4.0894 usec
Spectrometer Frequency: 400.13 MHz
Spectral Width: 8012.8 Hz
Lowest Frequency: -1545.2
Nucleus: 1H



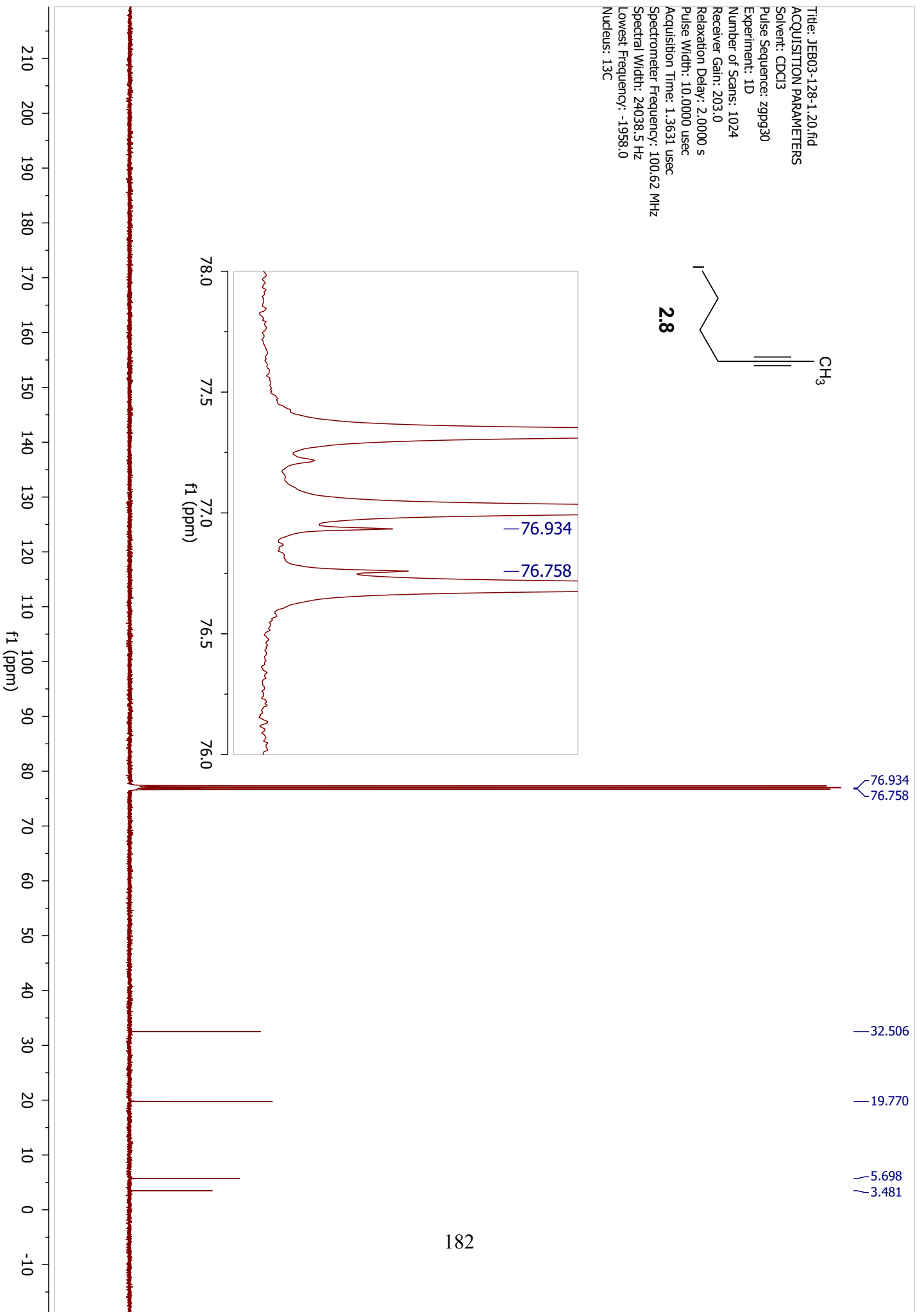
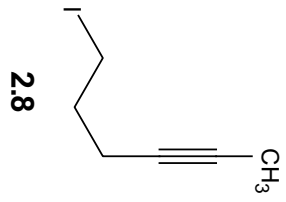
Title: JEB03-129-2.20.fid
ACQUISITION PARAMETERS
Solvent: CDCl3
Pulse Sequence: zpgp30
Experiment: 1D
Number of Scans: 1024
Receiver Gain: 203.0
Relaxation Delay: 2.0000 s
Pulse Width: 10.0000 usec
Acquisition Time: 1.3631 usec
Spectrometer Frequency: 100.62 MHz
Spectral Width: 24038.5 Hz
Lowest Frequency: -1943.2
Nucleus: 13C



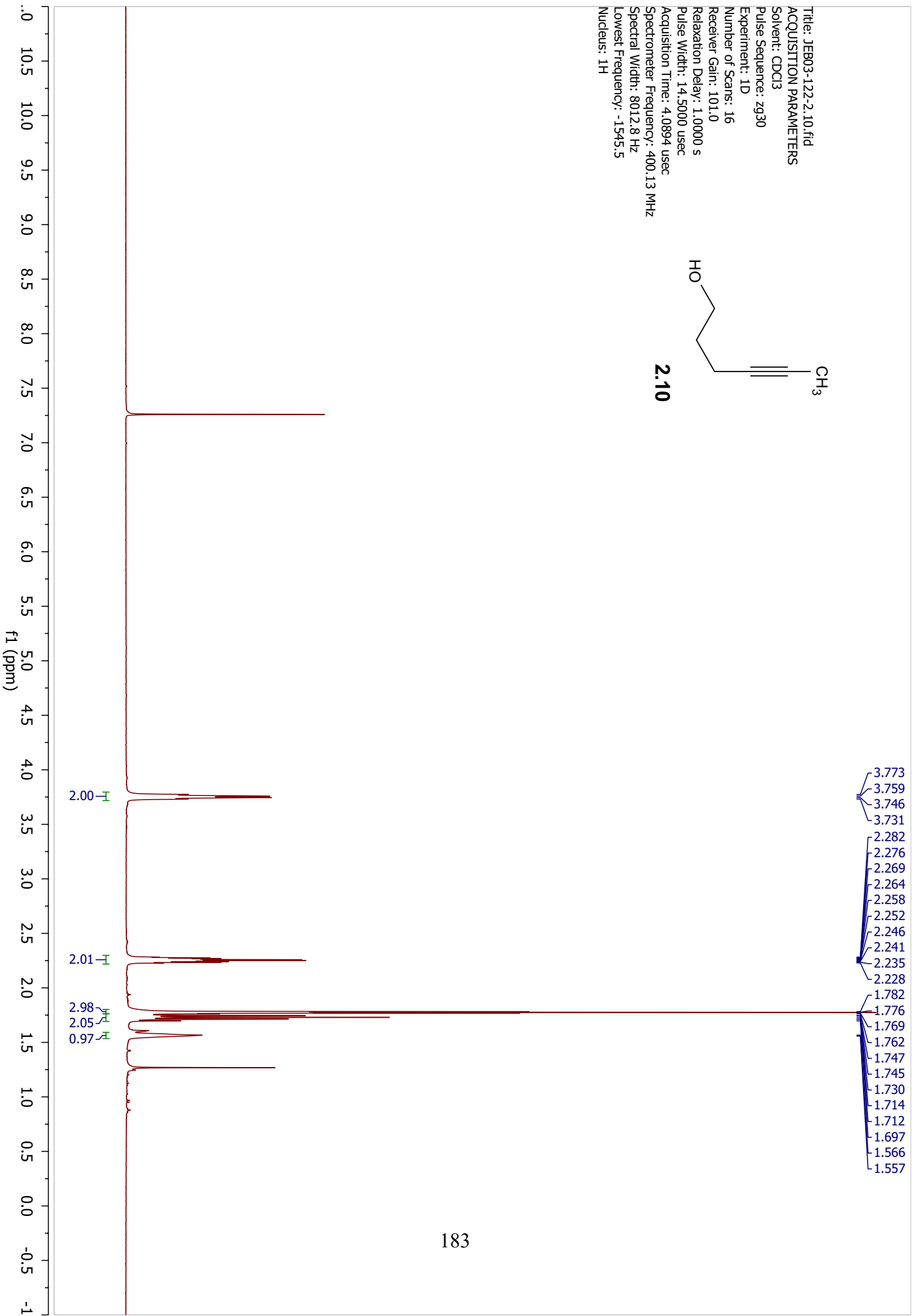
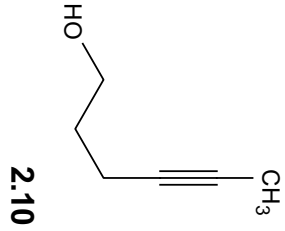
Title: JEB03-128-1.10.fid
ACQUISITION PARAMETERS
Solvent: CDCl3
Pulse Sequence: zg30
Experiment: 1D
Number of Scans: 16
Receiver Gain: 101.0
Relaxation Delay: 1.0000 s
Pulse Width: 14.5000 usec
Acquisition Time: 4.0894 usec
Spectrometer Frequency: 400.13 MHz
Spectral Width: 8012.8 Hz
Lowest Frequency: -1545.2
Nucleus: 1H



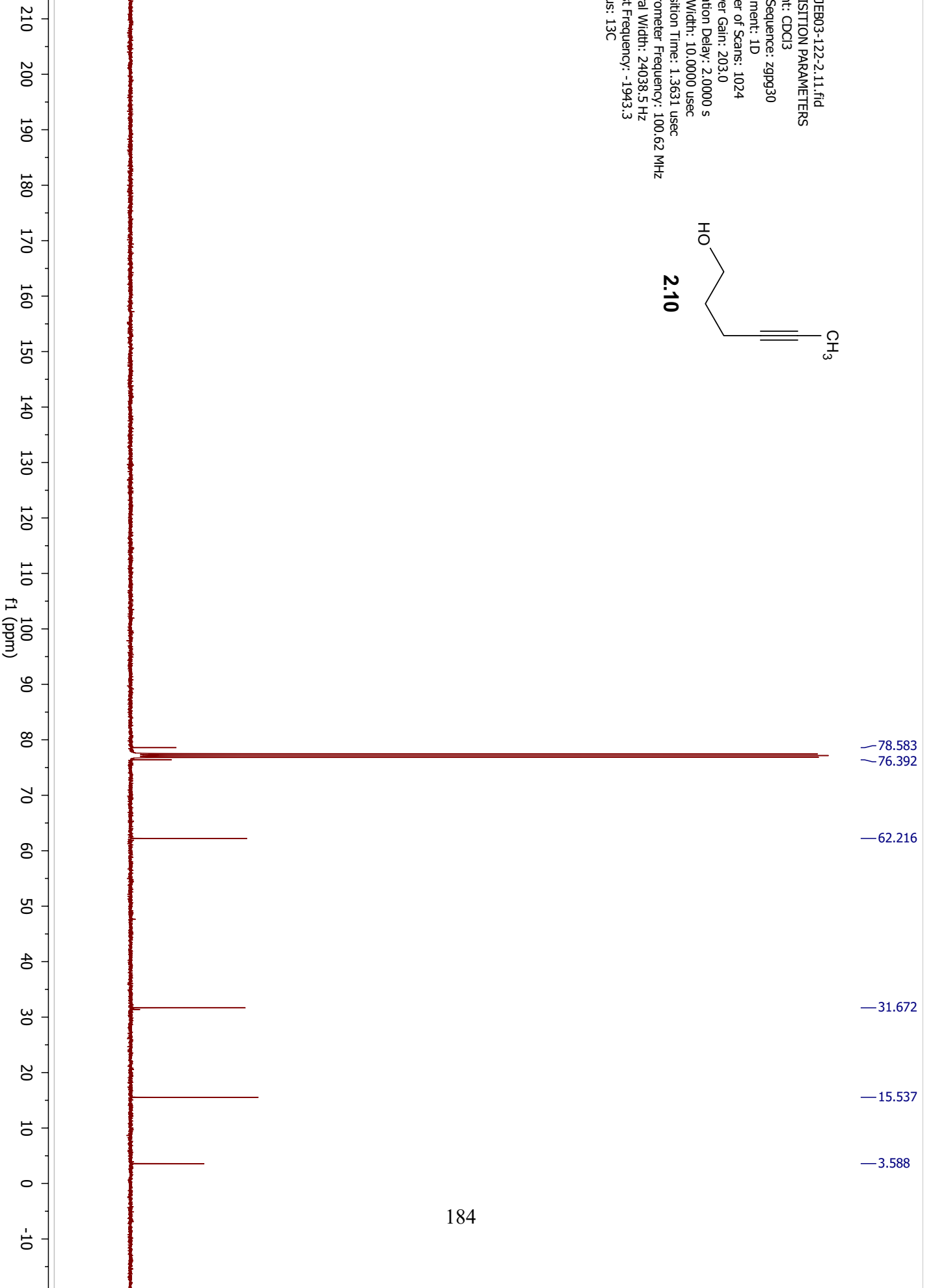
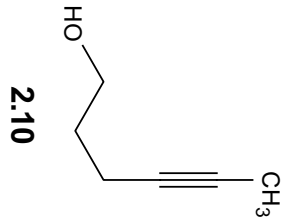
Title: JEB03-128-1.20.fid
ACQUISITION PARAMETERS
Solvent: CDCl3
Pulse Sequence: zppg30
Experiment: 1D
Number of Scans: 1024
Receiver Gain: 203.0
Relaxation Delay: 2.0000 s
Pulse Width: 10.0000 usec
Acquisition Time: 1.3631 usec
Spectrometer Frequency: 100.62 MHz
Spectral Width: 24038.5 Hz
Lowest Frequency: -1958.0
Nucleus: 13C



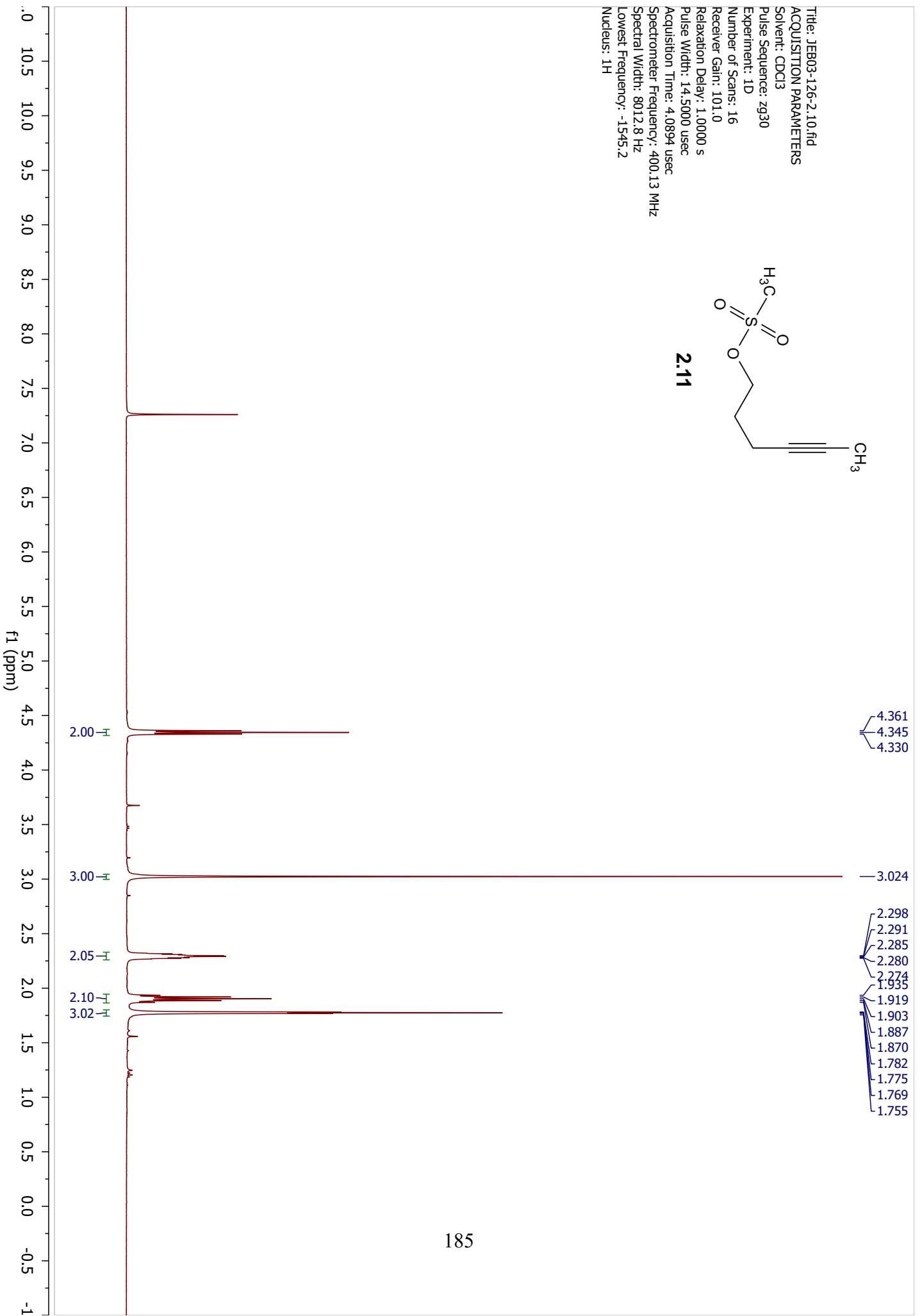
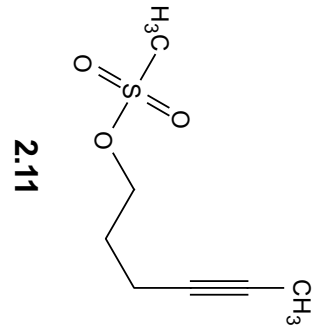
Title: JEB03-122-2.10.fid
ACQUISITION PARAMETERS
Solvent: CDCl3
Pulse Sequence: zg30
Experiment: 1D
Number of Scans: 16
Receiver Gain: 101.0
Relaxation Delay: 1.0000 s
Pulse Width: 14.5000 usec
Acquisition Time: 4.0894 usec
Spectrometer Frequency: 400.13 MHz
Spectral Width: 8012.8 Hz
Lowest Frequency: -1545.5
Nucleus: 1H



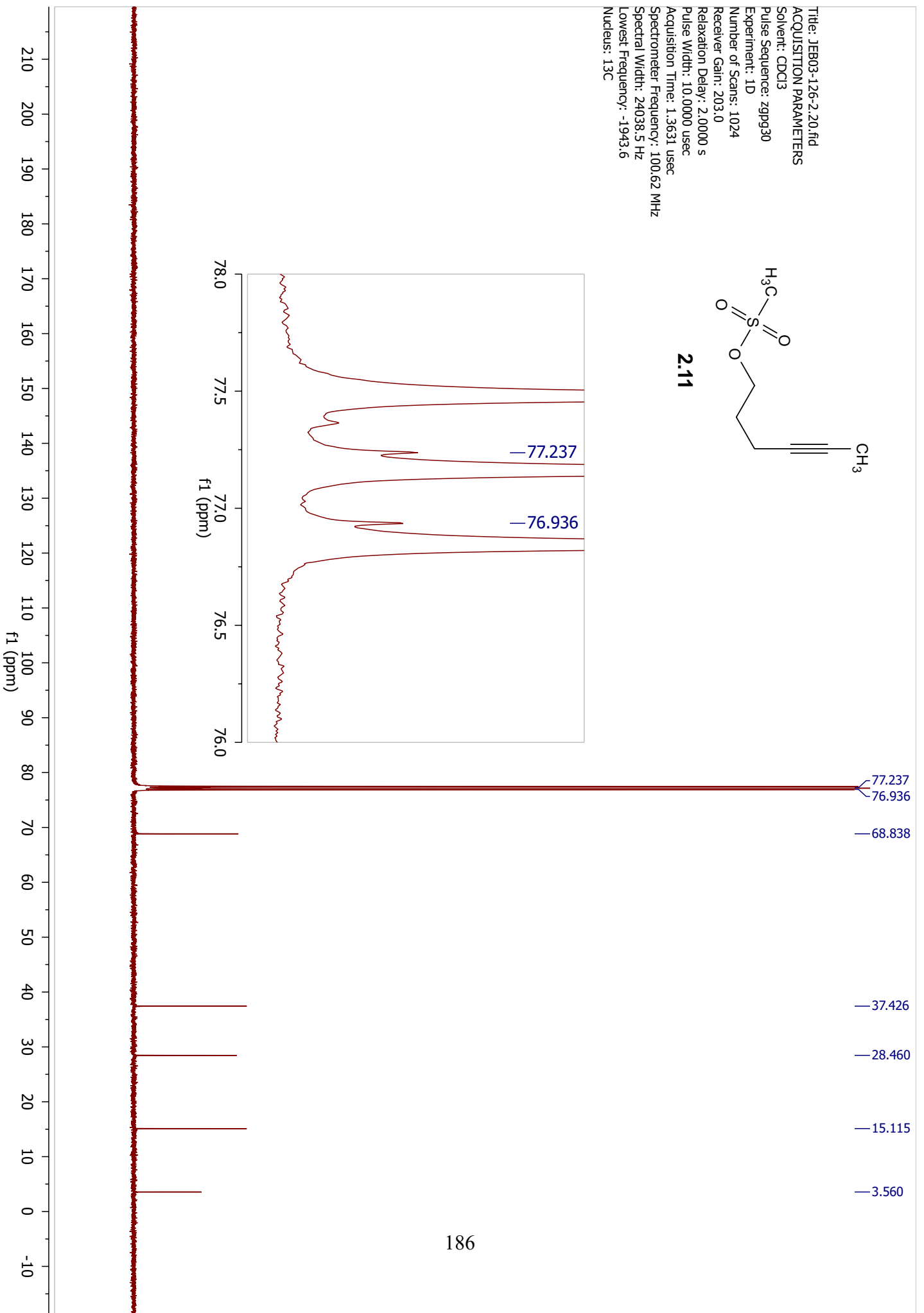
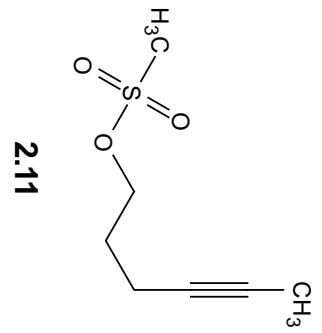
Title: JEB03-122-2.11.fid
ACQUISITION PARAMETERS
Solvent: CDCl3
Pulse Sequence: zgpg30
Experiment: 1D
Number of Scans: 1024
Receiver Gain: 203.0
Relaxation Delay: 2.0000 s
Pulse Width: 10.0000 usec
Acquisition Time: 1.3631 usec
Spectrometer Frequency: 100.62 MHz
Spectral Width: 24038.5 Hz
Lowest Frequency: -1943.3
Nucleus: 13C



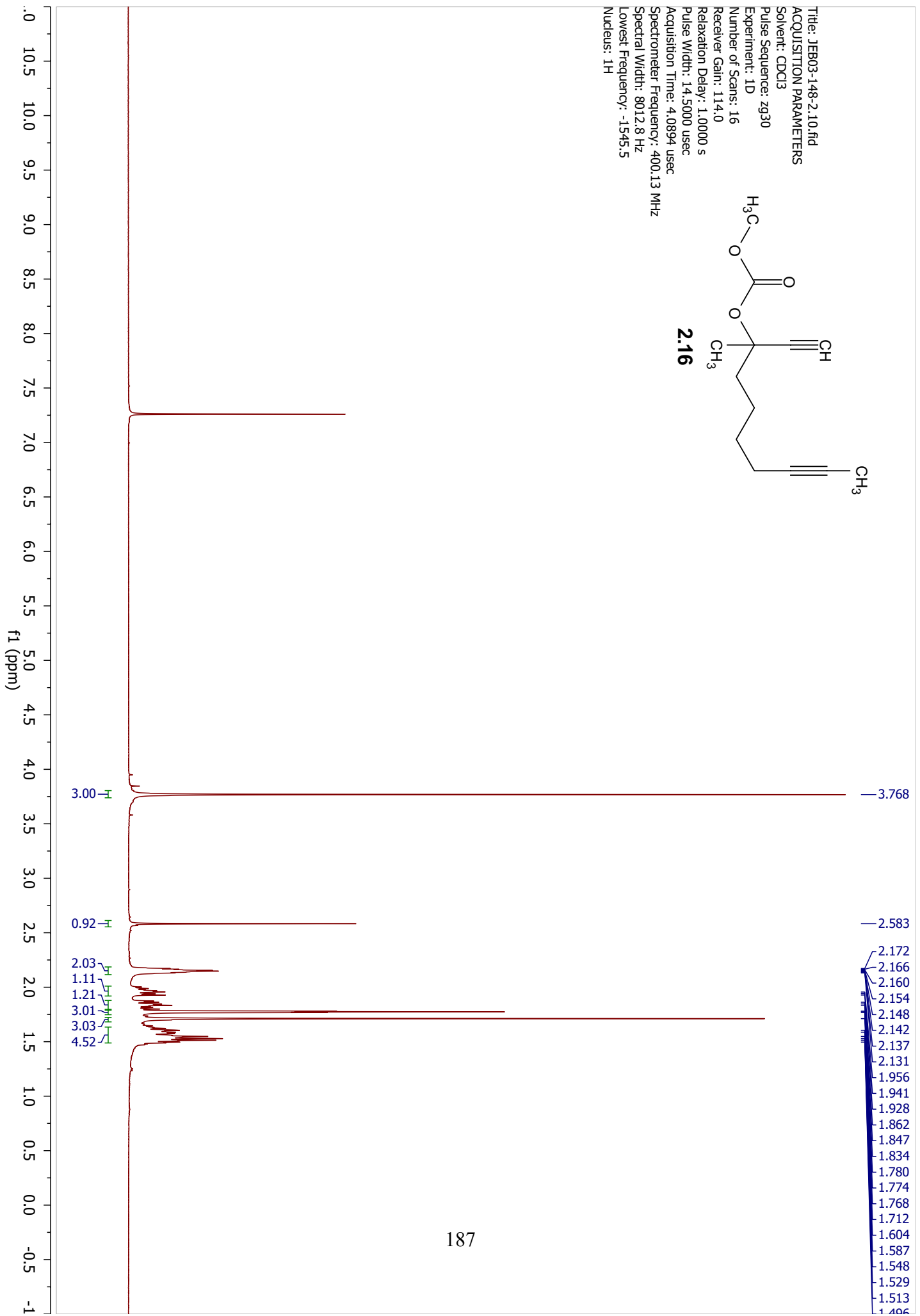
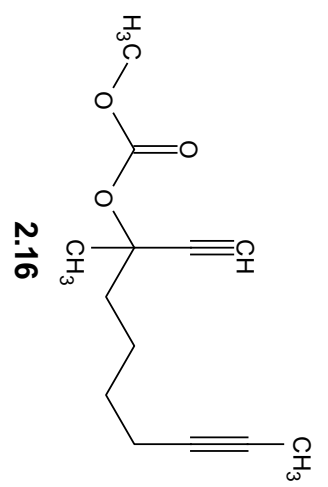
Title: JEB03-126-2.10.fid
ACQUISITION PARAMETERS
Solvent: CDCl3
Pulse Sequence: zg30
Experiment: 1D
Number of Scans: 16
Receiver Gain: 101.0
Relaxation Delay: 1.0000 s
Pulse Width: 14.5000 usec
Acquisition Time: 4.0894 usec
Spectrometer Frequency: 400.13 MHz
Spectral Width: 8012.8 Hz
Lowest Frequency: -1545.2
Nucleus: 1H



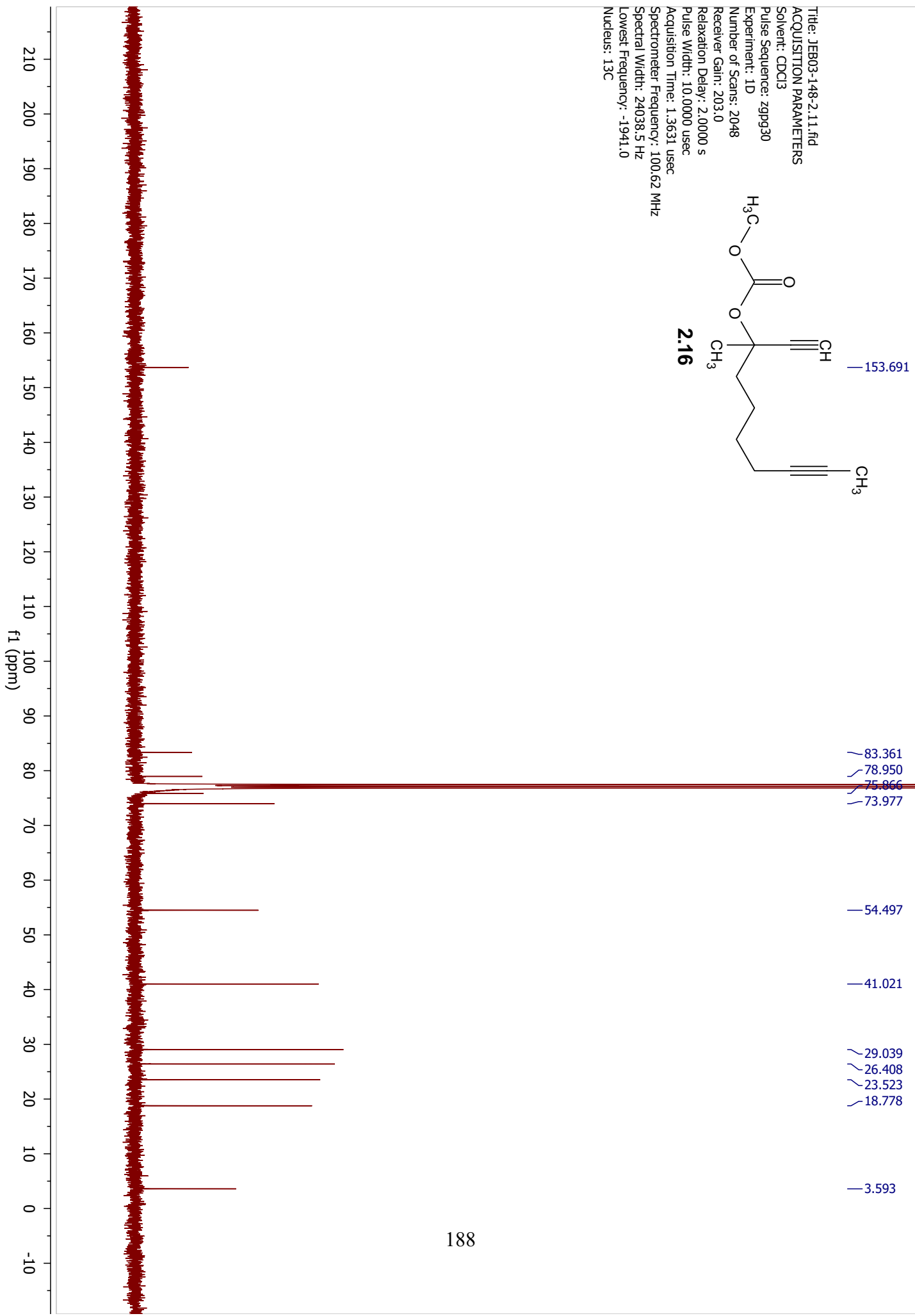
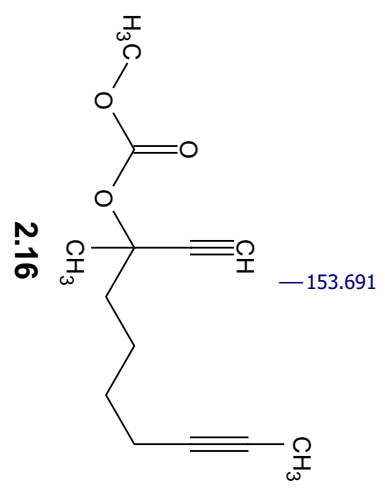
Title: JEB03-126-2.20.fid
ACQUISITION PARAMETERS
Solvent: CDCl3
Pulse Sequence: zpgp30
Experiment: 1D
Number of Scans: 1024
Receiver Gain: 203.0
Relaxation Delay: 2.0000 s
Pulse Width: 10.0000 usec
Acquisition Time: 1.3631 usec
Spectrometer Frequency: 100.62 MHz
Spectral Width: 24038.5 Hz
Lowest Frequency: -1943.6
Nucleus: 13C



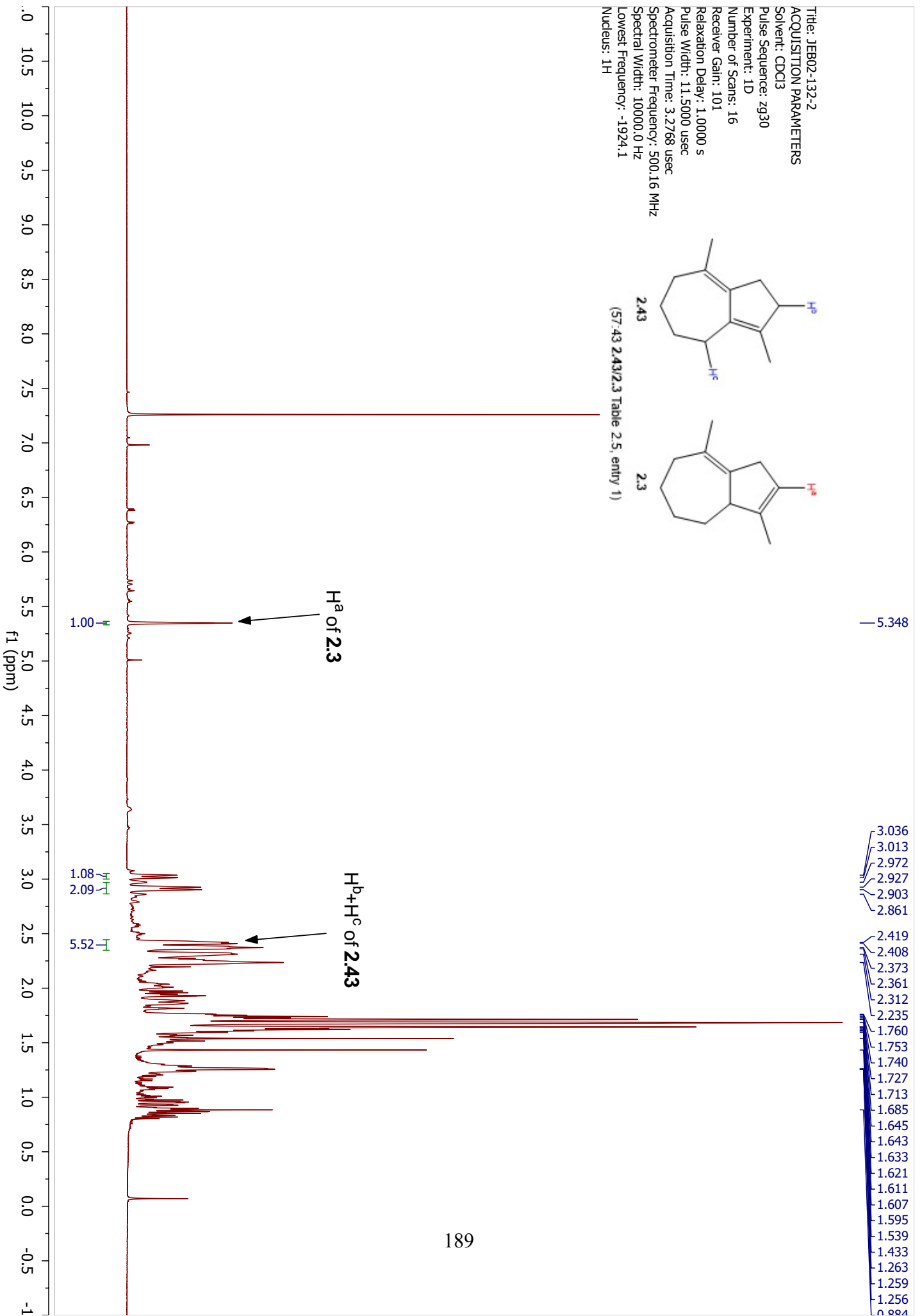
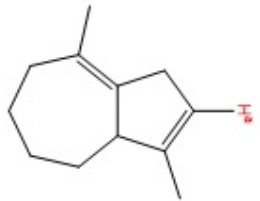
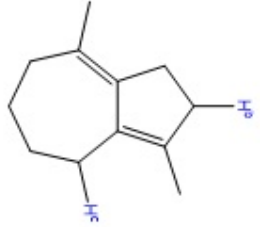
Title: JEB03-148-2.10.fid
ACQUISITION PARAMETERS
Solvent: CDCl3
Pulse Sequence: zg30
Experiment: 1D
Number of Scans: 16
Receiver Gain: 114.0
Relaxation Delay: 1.0000 s
Pulse Width: 14.5000 usec
Acquisition Time: 4.0894 usec
Spectrometer Frequency: 400.13 MHz
Spectral Width: 8012.8 Hz
Lowest Frequency: -1545.5
Nucleus: 1H



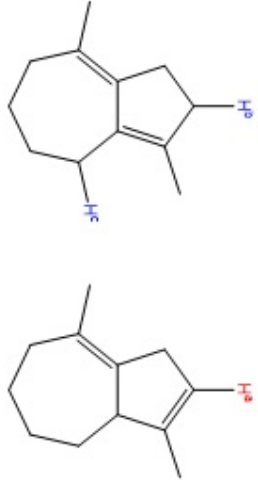
Title: JEB03-148-2.11.fid
ACQUISITION PARAMETERS
Solvent: CDCl3
Pulse Sequence: zppg30
Experiment: 1D
Number of Scans: 2048
Receiver Gain: 203.0
Relaxation Delay: 2.0000 s
Pulse Width: 10.0000 usec
Acquisition Time: 1.3631 usec
Spectrometer Frequency: 100.62 MHz
Spectral Width: 24038.5 Hz
Lowest Frequency: -1941.0
Nucleus: 13C



Title: JEB02-132-2
 ACQUISITION PARAMETERS
 Solvent: CDCl3
 Pulse Sequence: zg30
 Experiment: 1D
 Number of Scans: 16
 Receiver Gain: 101
 Relaxation Delay: 1.0000 s
 Pulse Width: 11.5000 usec
 Acquisition Time: 3.2768 usec
 Spectrometer Frequency: 500.16 MHz
 Spectral Width: 10000.0 Hz
 Lowest Frequency: -1924.1
 Nucleus: 1H

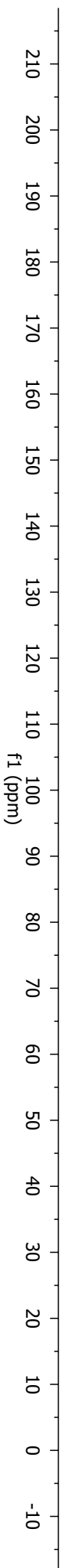


Title: JEB02-132-2
ACQUISITION PARAMETERS
Solvent: CDCl3
Pulse Sequence: zppg30
Experiment: 1D
Number of Scans: 1024
Receiver Gain: 203
Relaxation Delay: 2.0000 s
Pulse Width: 10.5000 usec
Acquisition Time: 1.1010 usec
Spectrometer Frequency: 125.77 MHz
Spectral Width: 29761.9 Hz
Lowest Frequency: -2284.7
Nucleus: 13C

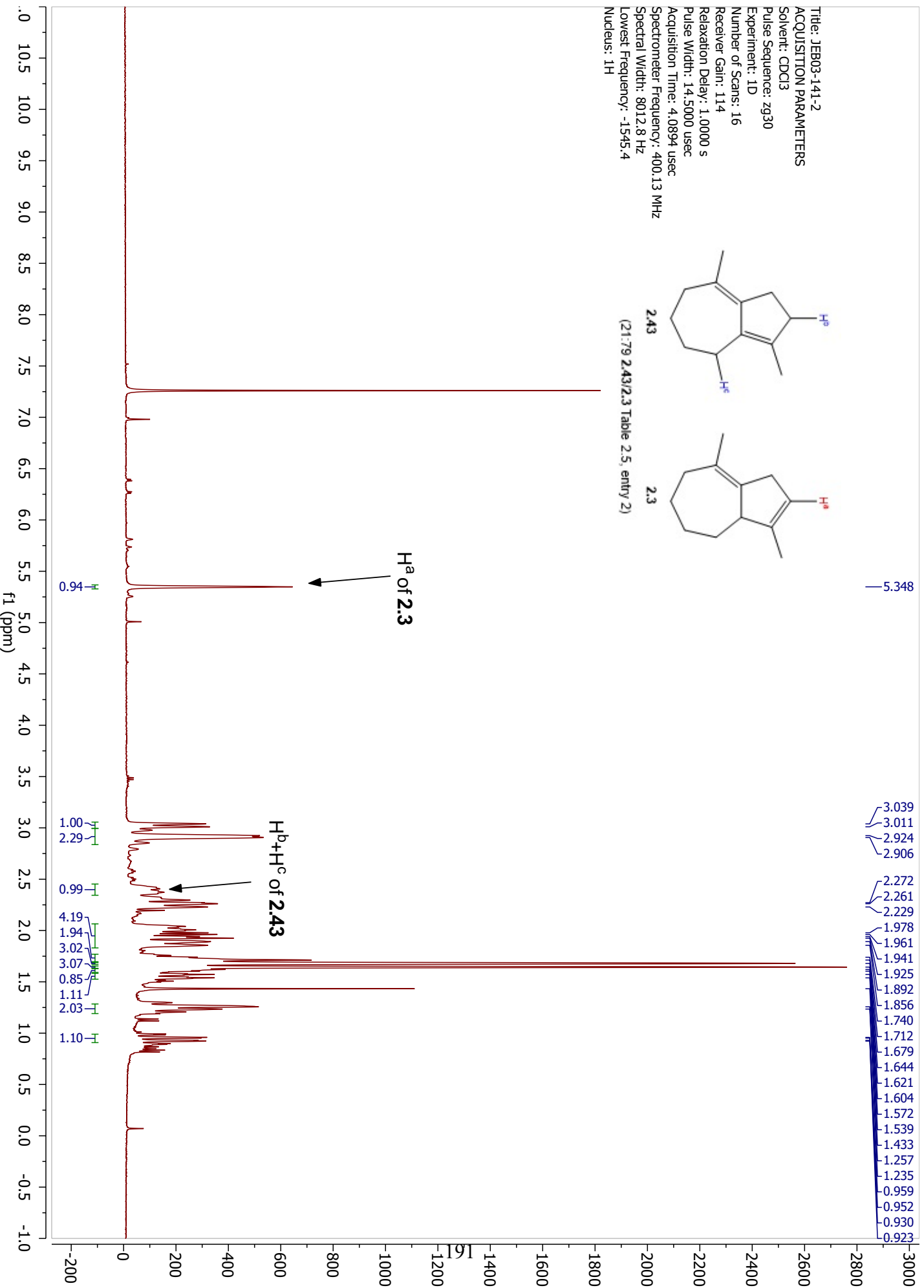
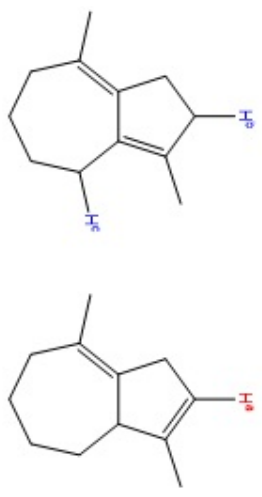


143.135
141.876
140.227
139.686
138.057
129.878
123.460
122.697

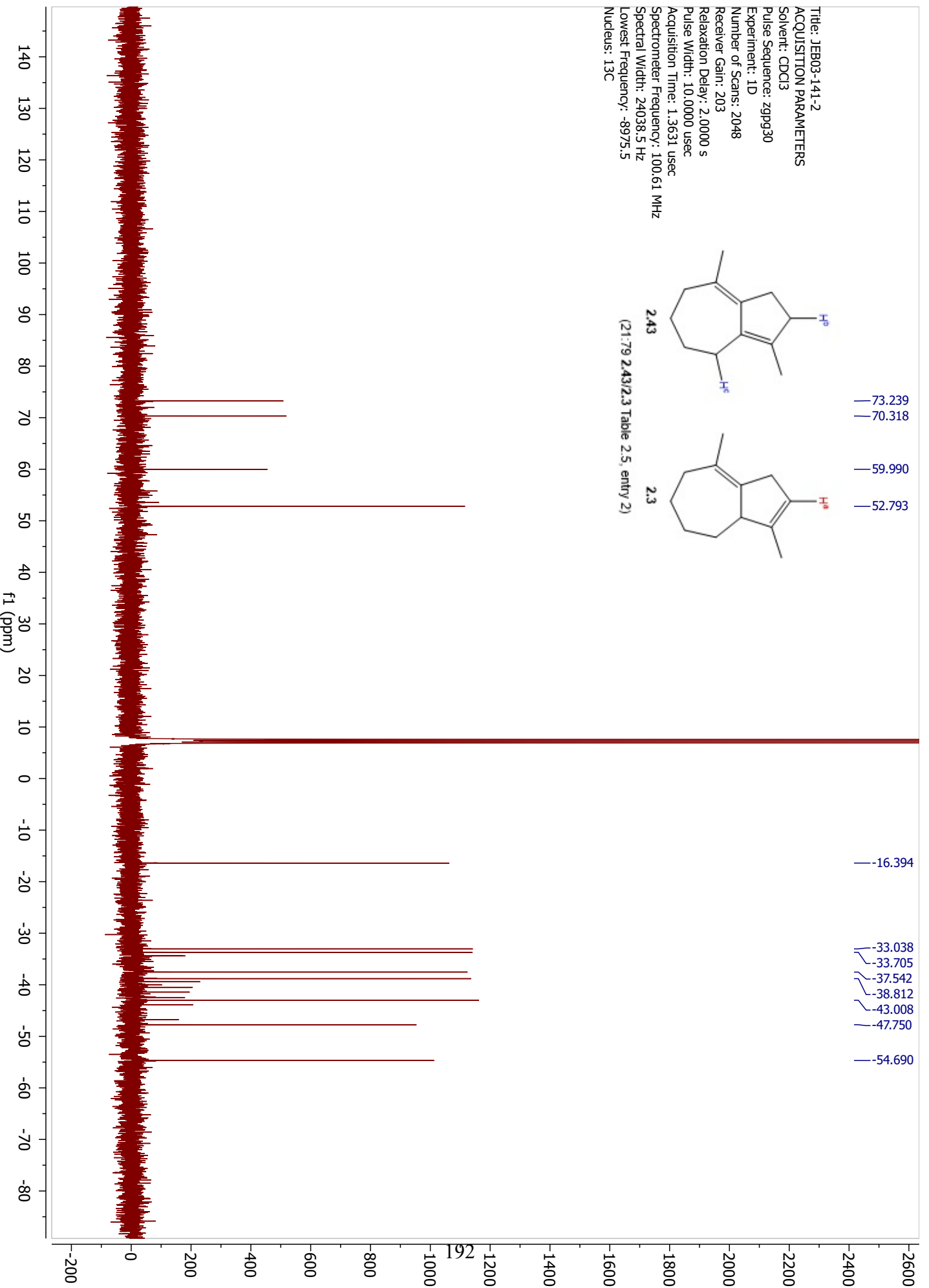
53.510
36.867
36.208
35.529
35.499
32.352
31.096
29.368
28.472
27.431
26.896
26.001
15.195
15.119
14.254



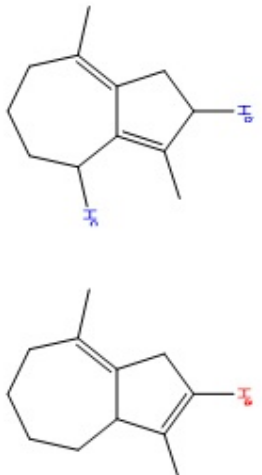
Title: JEB03-141-2
ACQUISITION PARAMETERS
Solvent: CDCl3
Pulse Sequence: zg30
Experiment: 1D
Number of Scans: 16
Receiver Gain: 114
Relaxation Delay: 1.0000 s
Pulse Width: 14.5000 usec
Acquisition Time: 4.0894 usec
Spectrometer Frequency: 400.13 MHz
Spectral Width: 8012.8 Hz
Lowest Frequency: -1545.4
Nucleus: 1H



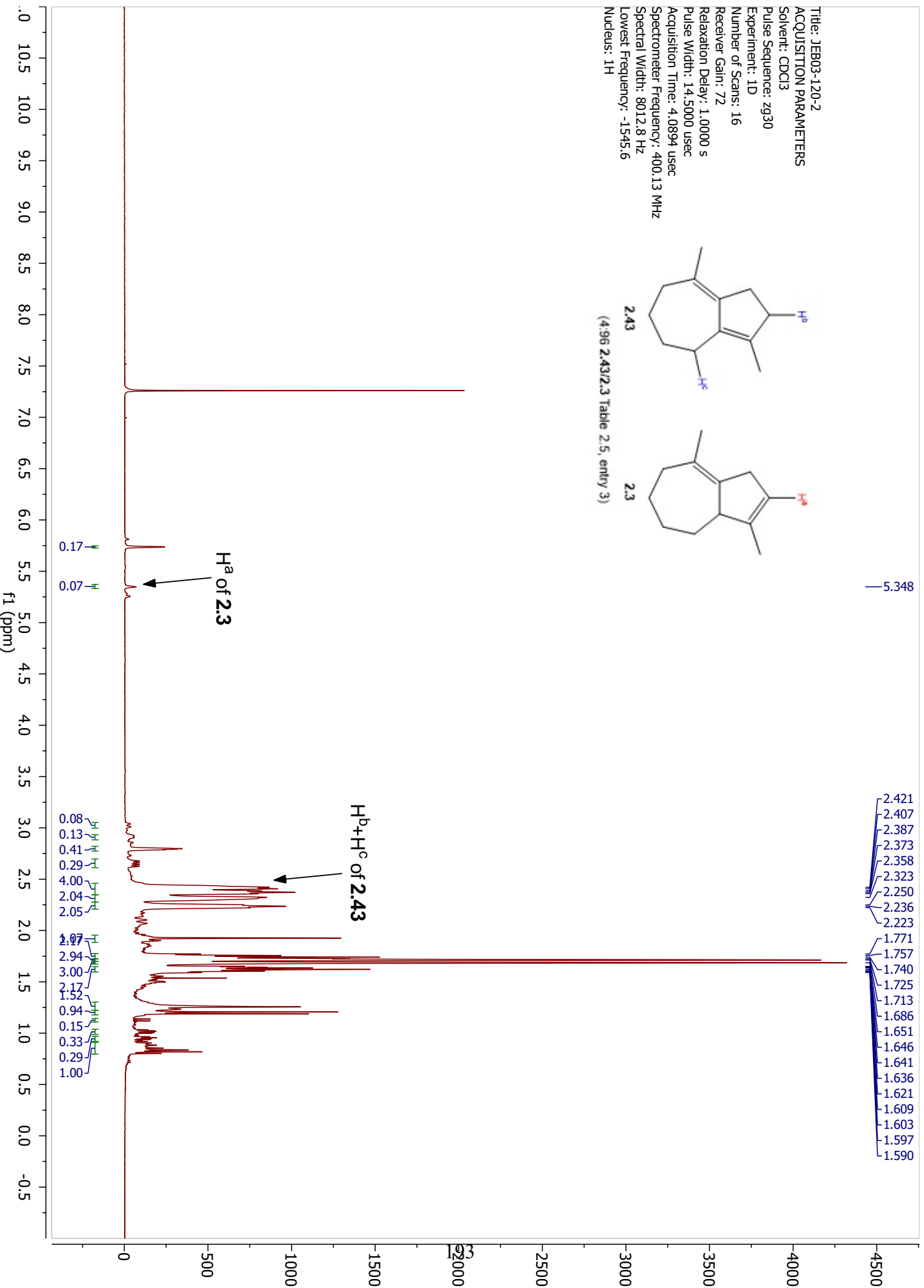
Title: JEB03-141-2
ACQUISITION PARAMETERS
Solvent: CDCl3
Pulse Sequence: zppg30
Experiment: 1D
Number of Scans: 2048
Receiver Gain: 203
Relaxation Delay: 2.0000 s
Pulse Width: 10.0000 usec
Acquisition Time: 1.3631 usec
Spectrometer Frequency: 100.61 MHz
Spectral Width: 24038.5 Hz
Lowest Frequency: -8975.5
Nucleus: 13C



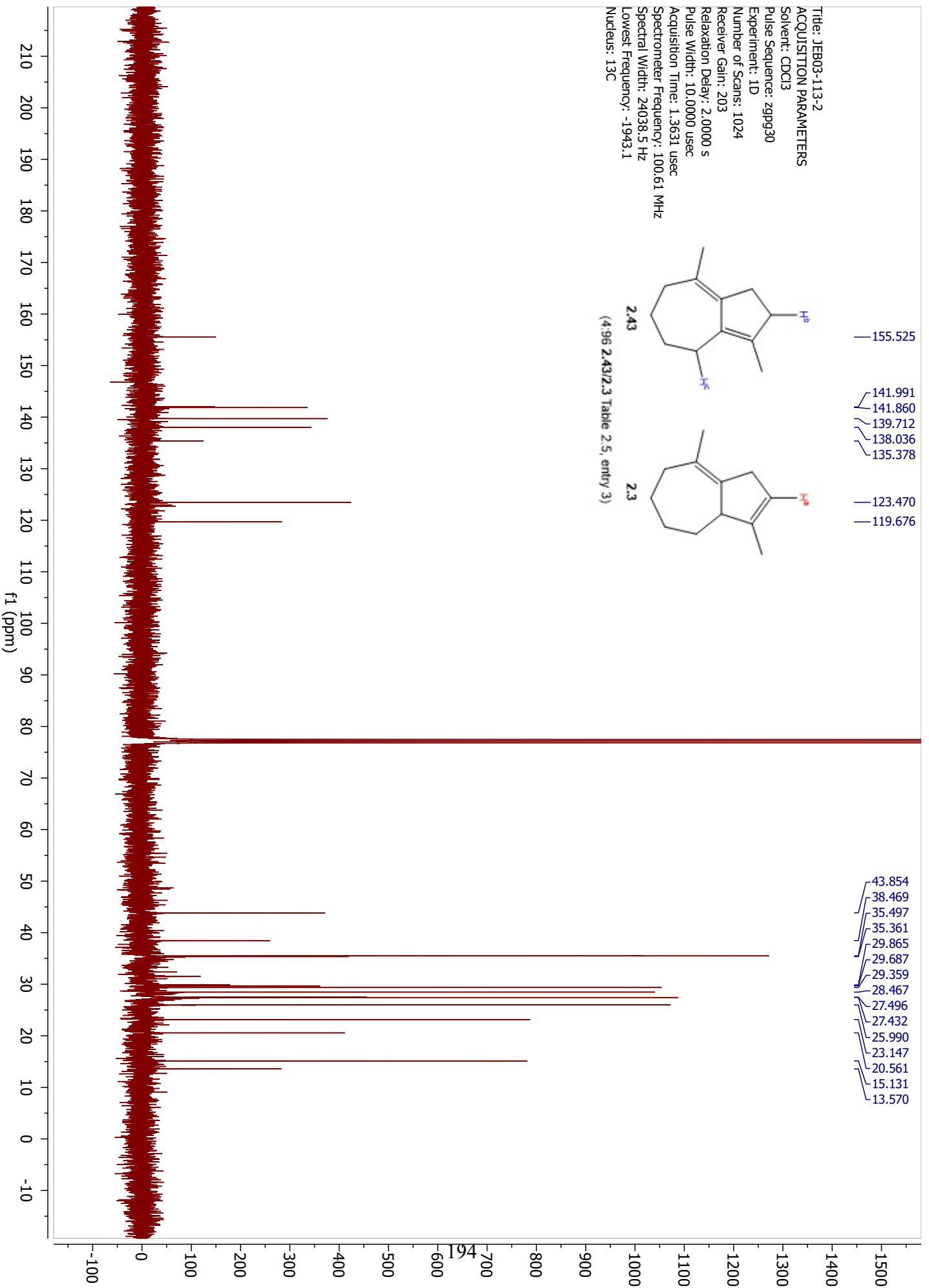
Title: JEB03-120-2
 ACQUISITION PARAMETERS
 Solvent: CDCl3
 Pulse Sequence: zg30
 Experiment: 1D
 Number of Scans: 16
 Receiver Gain: 72
 Relaxation Delay: 1.0000 s
 Pulse Width: 14.5000 usec
 Acquisition Time: 4.0894 usec
 Spectrometer Frequency: 400.13 MHz
 Spectral Width: 8012.8 Hz
 Lowest Frequency: -1545.6
 Nucleus: 1H

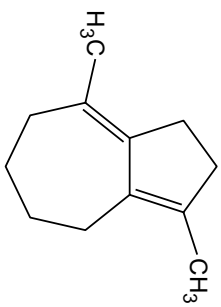


2.43
 (4.96 2.43/2.3 Table 2.5, entry 3)
 2.3

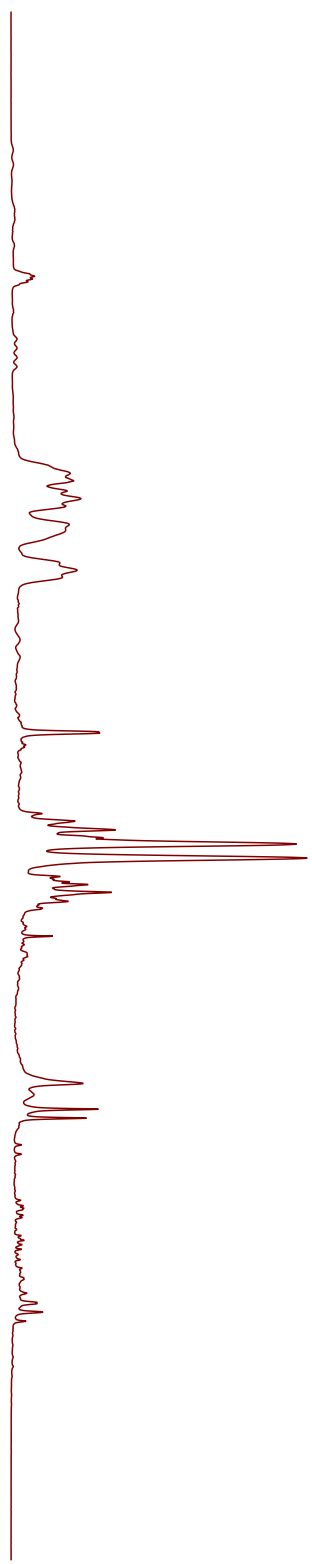


Title: JEB03-113-2
ACQUISITION PARAMETERS
Solvent: CDCl3
Pulse Sequence: zppg30
Experiment: 1D
Number of Scans: 1024
Relaxation Delay: 2.0000 s
Pulse Width: 10.0000 usec
Acquisition Time: 1.3631 usec
Spectrometer Frequency: 100.61 MHz
Spectral Width: 24038.5 Hz
Lowest Frequency: -1943.1
Nucleus: 13C

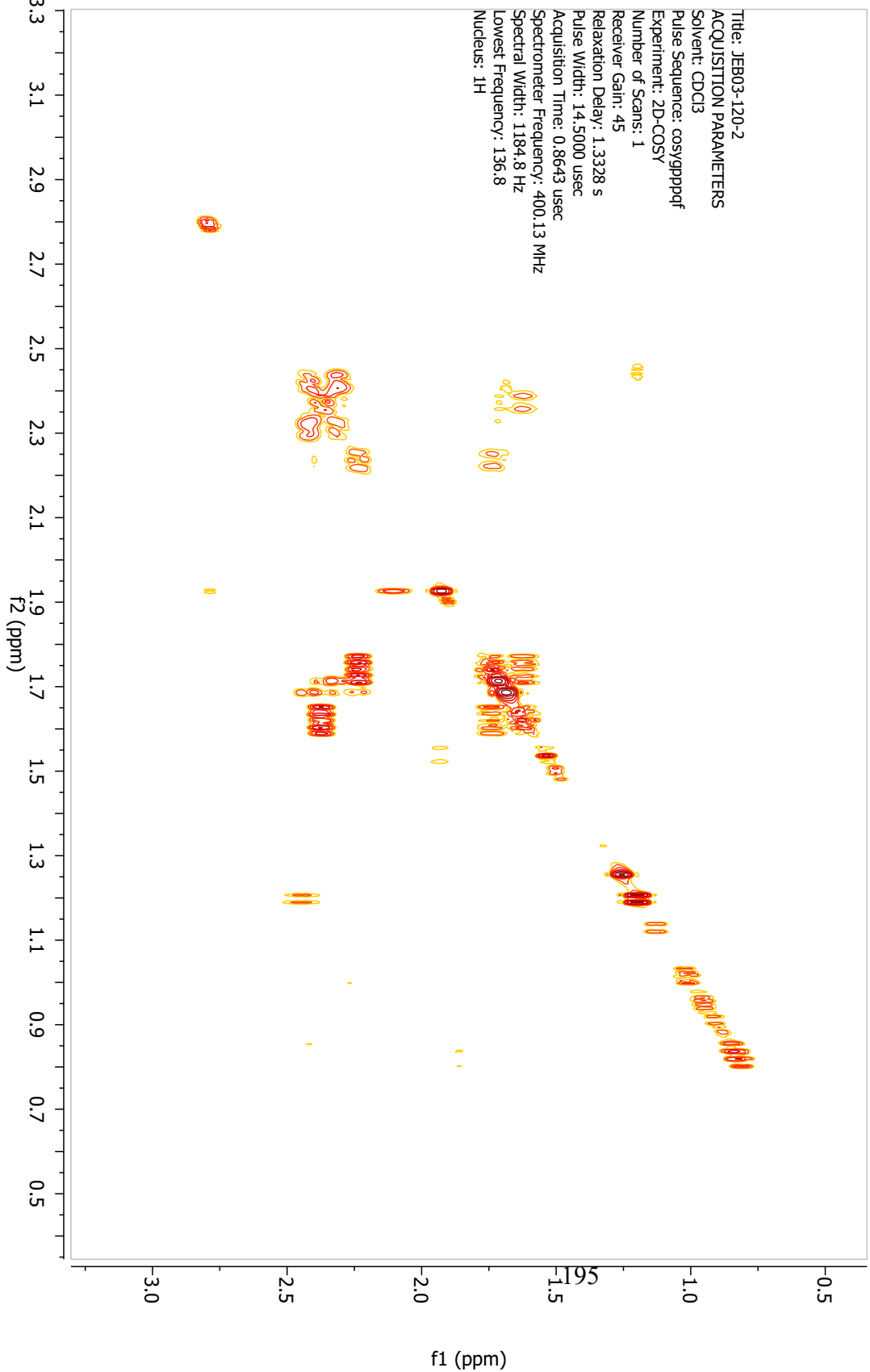


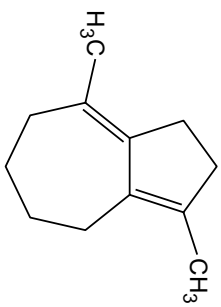


2.43

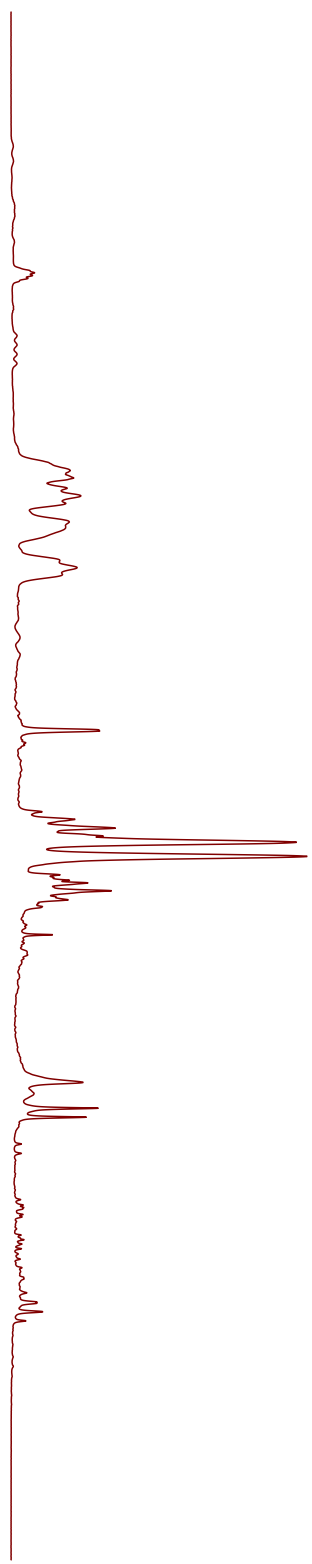


Title: JEB03-120-2
ACQUISITION PARAMETERS
Solvent: CDCl3
Pulse Sequence: cosypppppf
Experiment: 2D-COSY
Number of Scans: 1
Receiver Gain: 45
Relaxation Delay: 1.3328 s
Pulse Width: 14.5000 usec
Acquisition Time: 0.8643 usec
Spectrometer Frequency: 400.13 MHz
Spectral Width: 1184.8 Hz
Lowest Frequency: 136.8
Nucleus: 1H

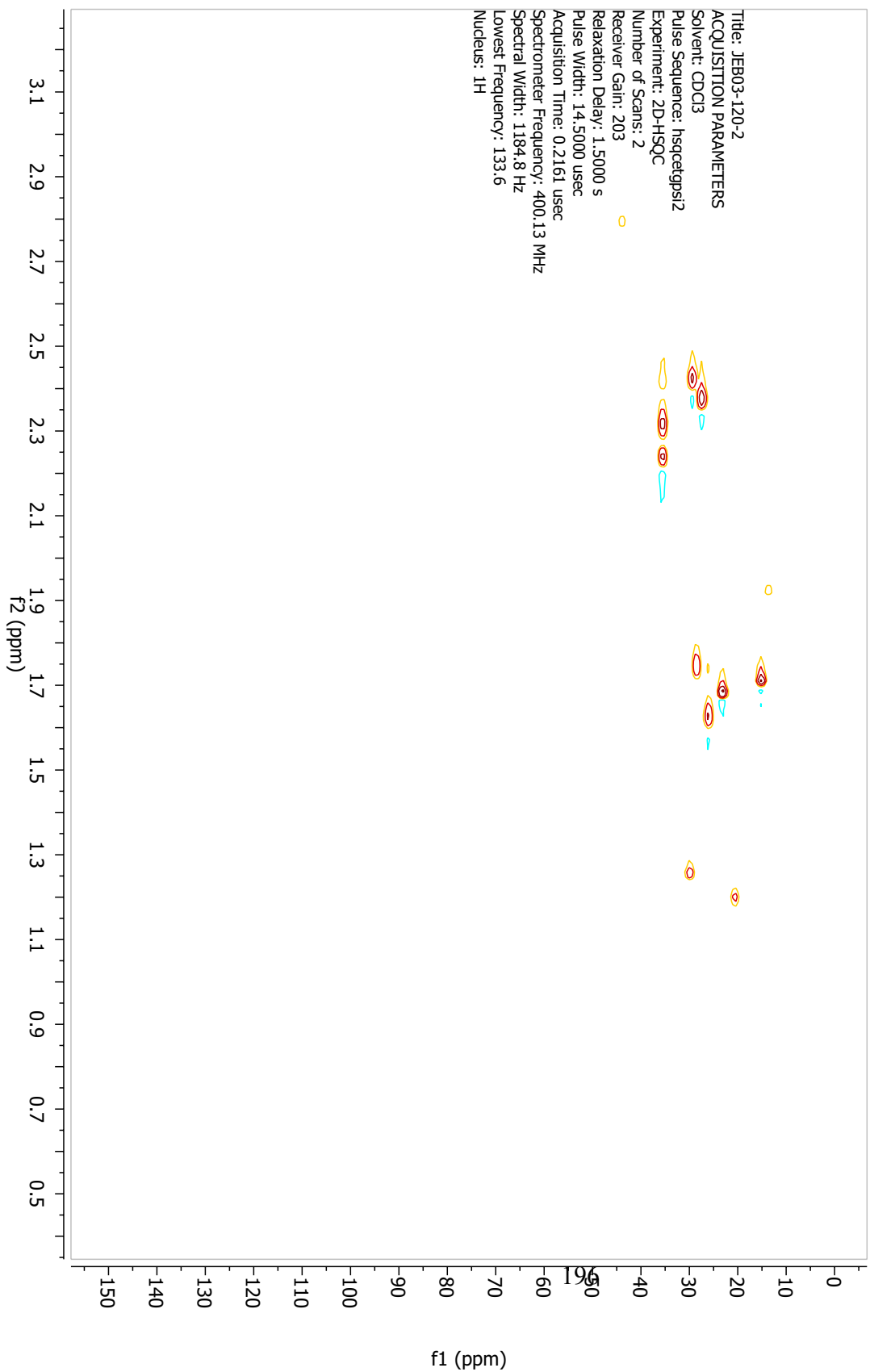


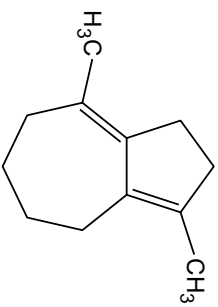


2.43

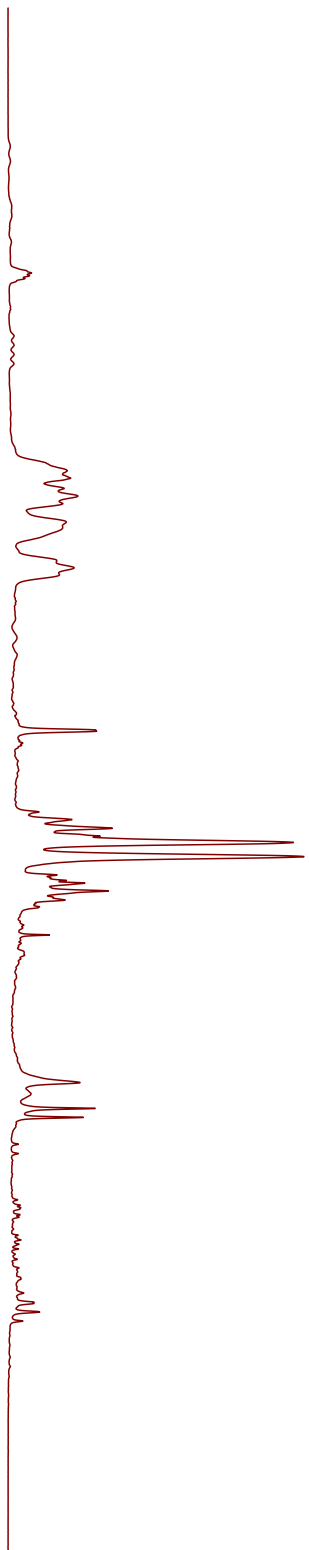


Title: JEB03-120-2
ACQUISITION PARAMETERS
Solvent: CDCl3
Pulse Sequence: hsqcetgps12
Experiment: 2D-HSQC
Number of Scans: 2
Receiver Gain: 203
Relaxation Delay: 1.5000 s
Pulse Width: 14.5000 usec
Acquisition Time: 0.2161 usec
Spectrometer Frequency: 400.13 MHz
Spectral Width: 1184.8 Hz
Lowest Frequency: 133.6
Nucleus: 1H

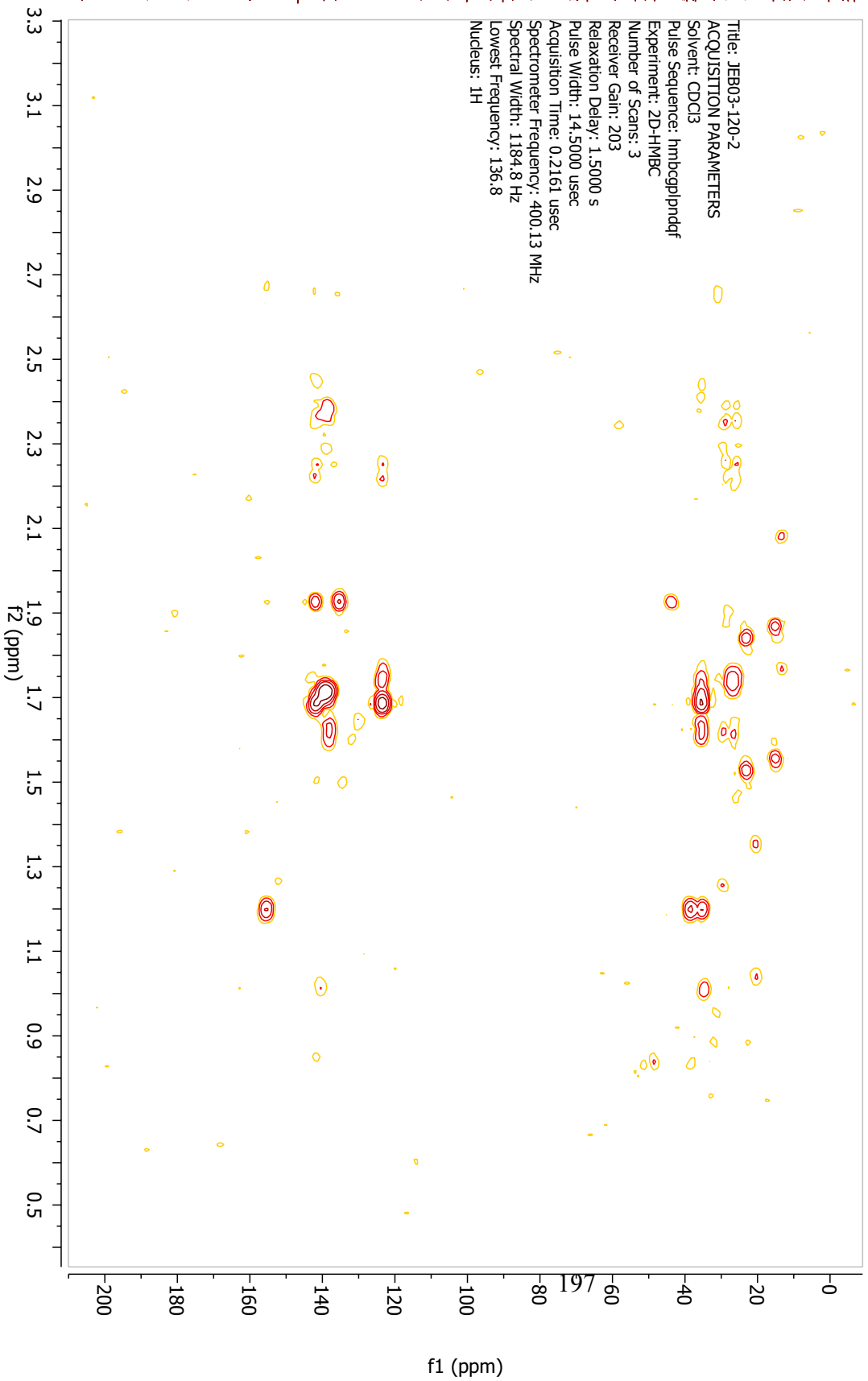




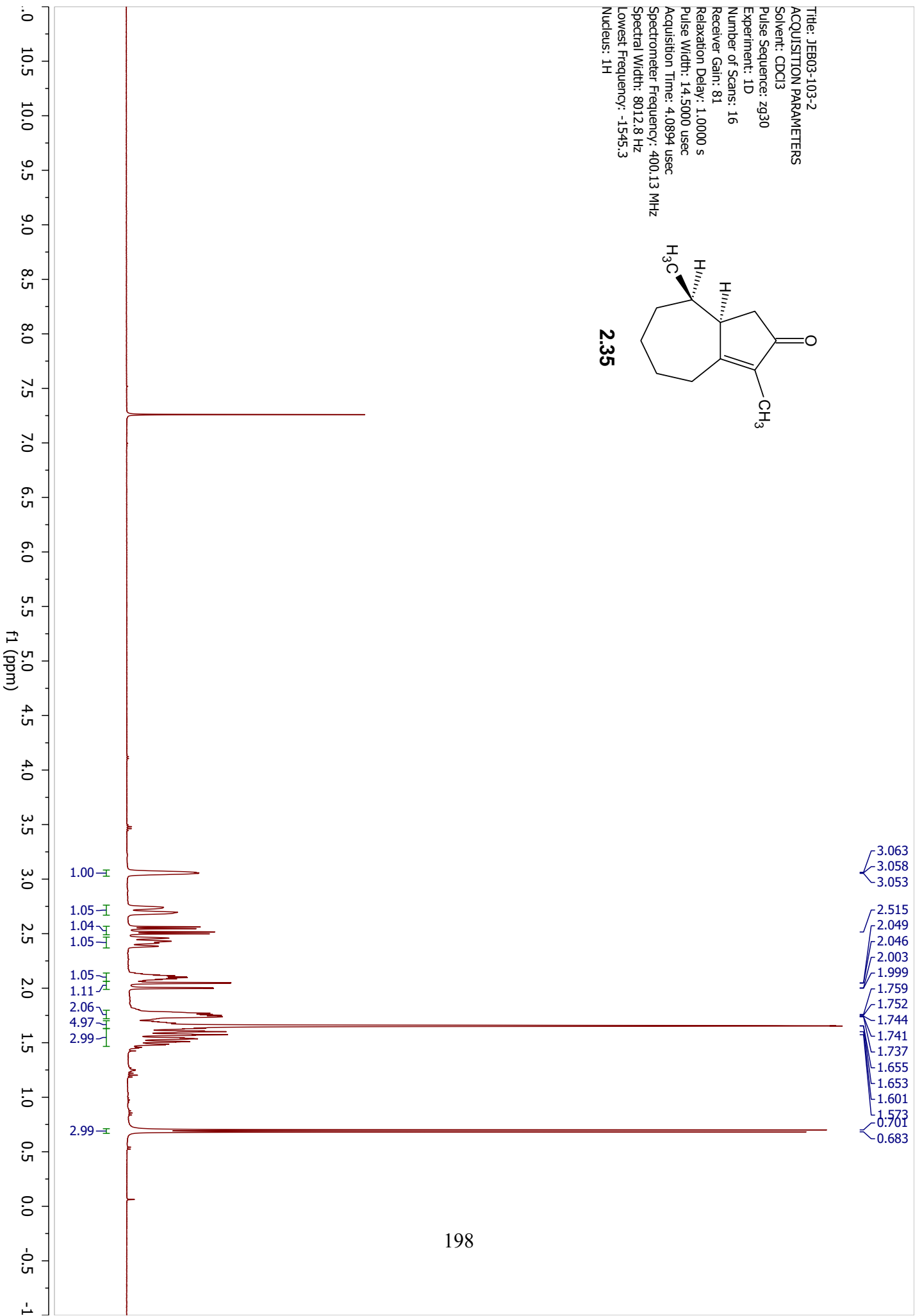
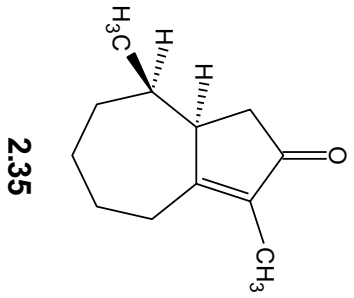
2.43



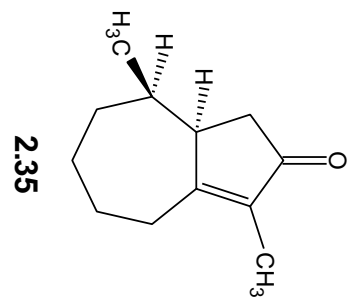
Title: JEB03-120-2
ACQUISITION PARAMETERS
Solvent: CDCl3
Pulse Sequence: hmbcgp1pndqf
Experiment: 2D-HMBC
Number of Scans: 3
Receiver Gain: 203
Relaxation Delay: 1.5000 s
Pulse Width: 14.5000 usec
Acquisition Time: 0.2161 usec
Spectrometer Frequency: 400.13 MHz
Spectral Width: 1184.8 Hz
Lowest Frequency: 136.8
Nucleus: 1H



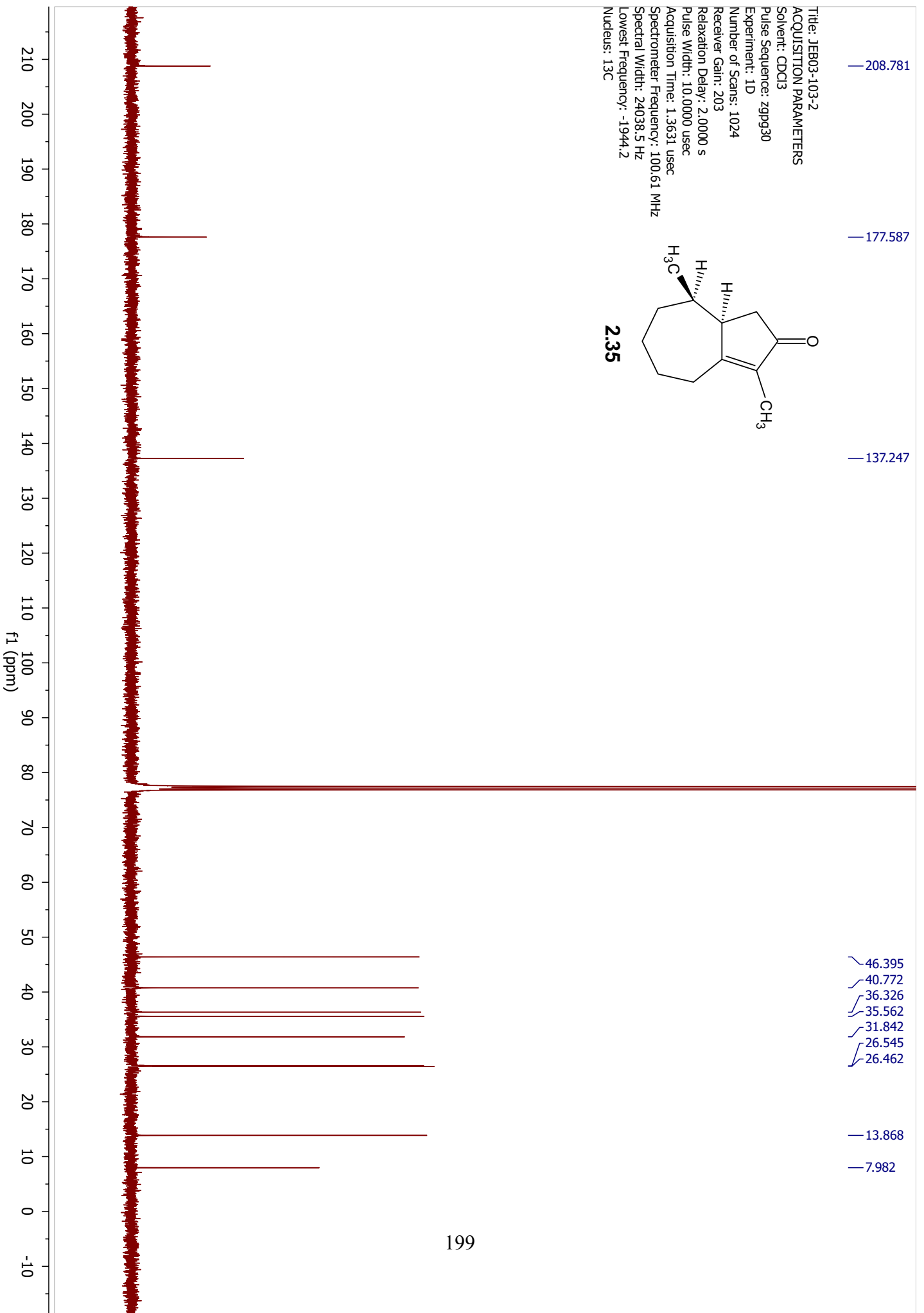
Title: JEB03-103-2
ACQUISITION PARAMETERS
Solvent: CDCl3
Pulse Sequence: zg30
Experiment: 1D
Number of Scans: 16
Receiver Gain: 81
Relaxation Delay: 1.0000 s
Pulse Width: 14.5000 usec
Acquisition Time: 4.0894 usec
Spectrometer Frequency: 400.13 MHz
Spectral Width: 8012.8 Hz
Lowest Frequency: -1545.3
Nucleus: 1H



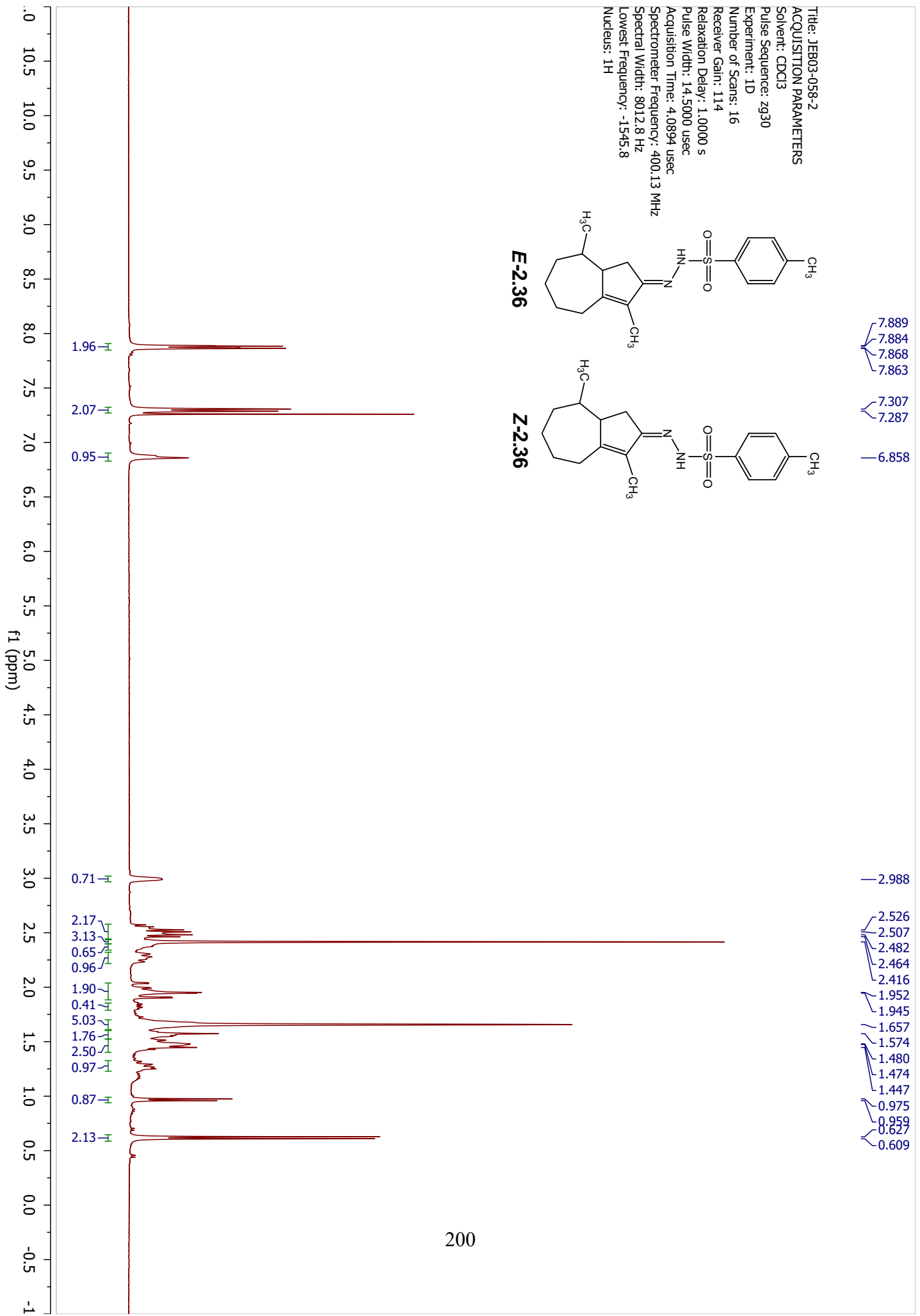
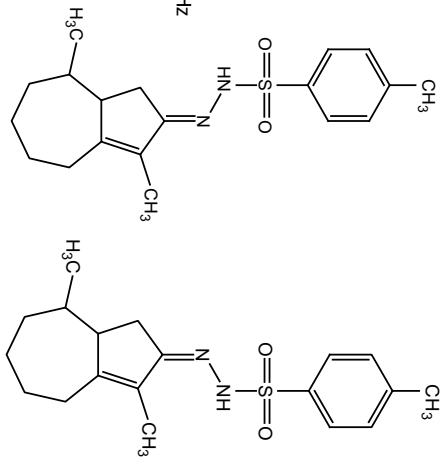
Title: JEB03-103-2
ACQUISITION PARAMETERS
Solvent: CDCl3
Pulse Sequence: zppg30
Experiment: 1D
Number of Scans: 1024
Receiver Gain: 203
Relaxation Delay: 2.0000 s
Pulse Width: 10.0000 usec
Acquisition Time: 1.3631 usec
Spectrometer Frequency: 100.61 MHz
Spectral Width: 24038.5 Hz
Lowest Frequency: -1944.2
Nucleus: 13C



2.35



Title: JEB03-058-2
 ACQUISITION PARAMETERS
 Solvent: CDCl3
 Pulse Sequence: zg30
 Experiment: 1D
 Number of Scans: 16
 Receiver Gain: 114
 Relaxation Delay: 1.0000 s
 Pulse Width: 14.5000 usec
 Acquisition Time: 4.0894 usec
 Spectrometer Frequency: 400.13 MHz
 Spectral Width: 8012.8 Hz
 Lowest Frequency: -1545.8
 Nucleus: 1H



Title: JEB03-058-2
ACQUISITION PARAMETERS
Solvent: CDCl3
Pulse Sequence: zppg30
Experiment: 1D
Number of Scans: 1024
Receiver Gain: 203
Relaxation Delay: 2.0000 s
Pulse Width: 10.0000 usec
Acquisition Time: 1.3631 usec
Spectrometer Frequency: 100.61 MHz
Spectral Width: 24038.5 Hz
Lowest Frequency: -1945.8
Nucleus: 13C

168.062
167.595

160.418

143.870

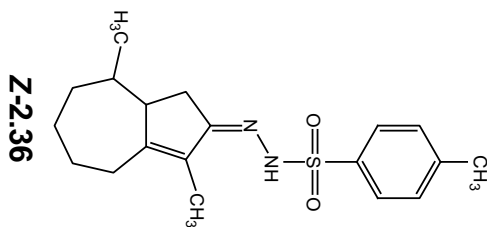
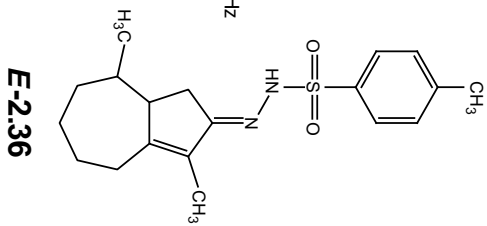
135.604

133.060

132.259

129.477

128.297



52.588

49.238

36.623

36.192

36.001

31.425

30.332

28.755

27.426

26.950

26.816

25.024

23.742

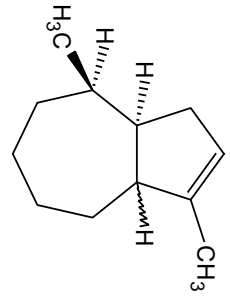
21.742

9.128

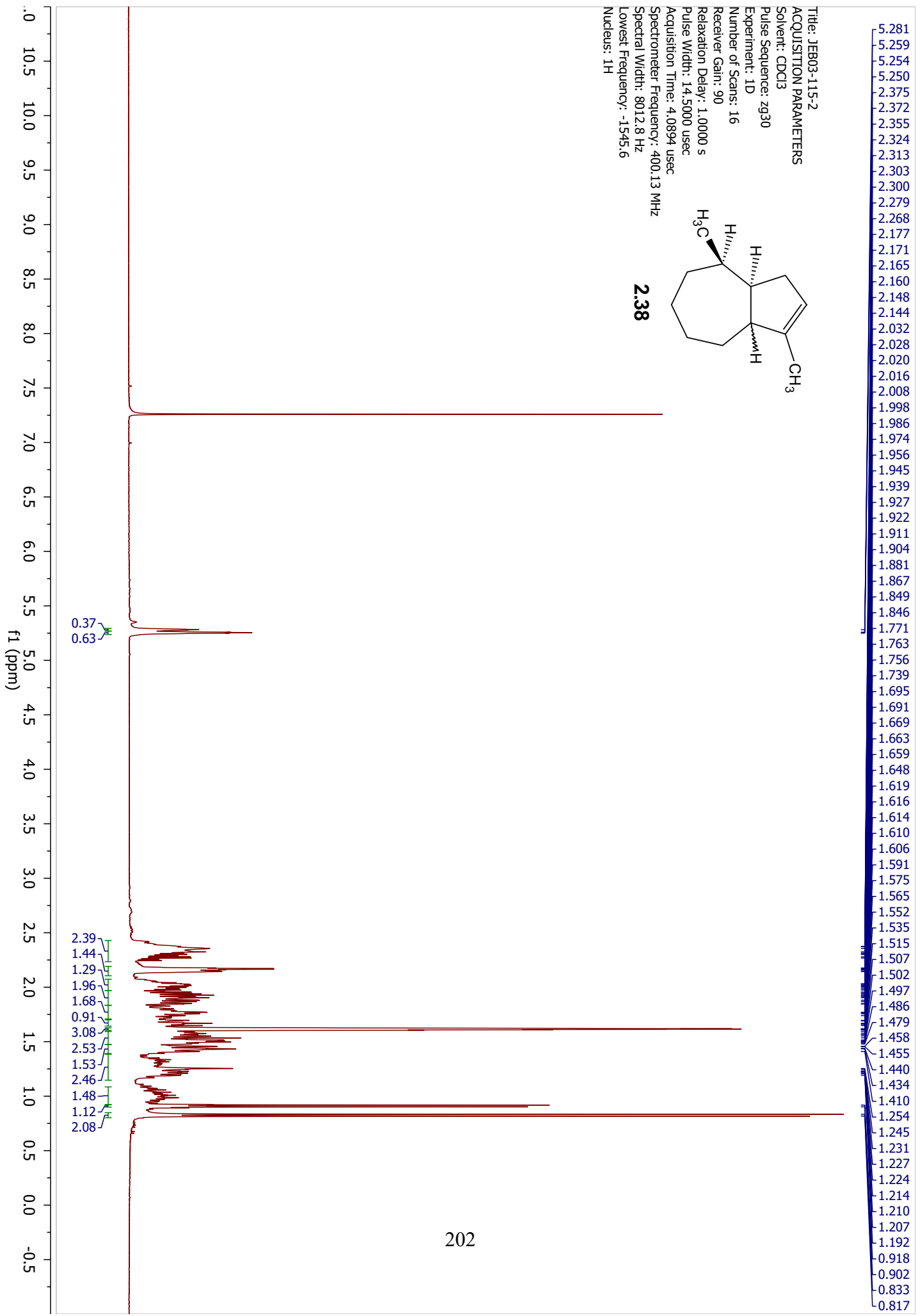
210
200
190
180
170
160
150
140
130
120
110
100
90
80
70
60
50
40
30
20
10
0
-10

f1 (ppm)

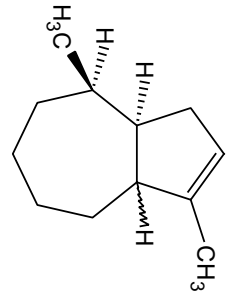
Title: JEB03-115-2
ACQUISITION PARAMETERS
Solvent: CDCl3
Pulse Sequence: zg30
Experiment: 1D
Number of Scans: 16
Receiver Gain: 90
Relaxation Delay: 1.0000 s
Pulse Width: 14.5000 usec
Acquisition Time: 4.0894 usec
Spectrometer Frequency: 400.13 MHz
Spectral Width: 8012.8 Hz
Lowest Frequency: -1545.6
Nucleus: 1H



2.38



Title: JEB03-115-2
ACQUISITION PARAMETERS
Solvent: CDCl3
Pulse Sequence: zppg30
Experiment: 1D
Number of Scans: 1024
Receiver Gain: 203
Relaxation Delay: 2.0000 s
Pulse Width: 10.0000 usec
Acquisition Time: 1.3631 usec
Spectrometer Frequency: 100.61 MHz
Spectral Width: 24038.5 Hz
Lowest Frequency: -1943.3
Nucleus: 13C

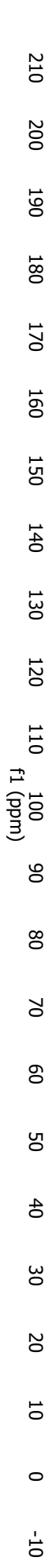


2.38

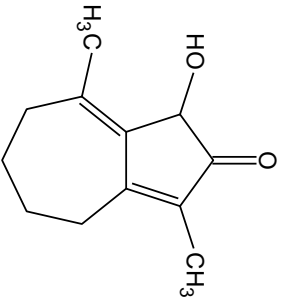
143.680
143.264

123.454
123.310

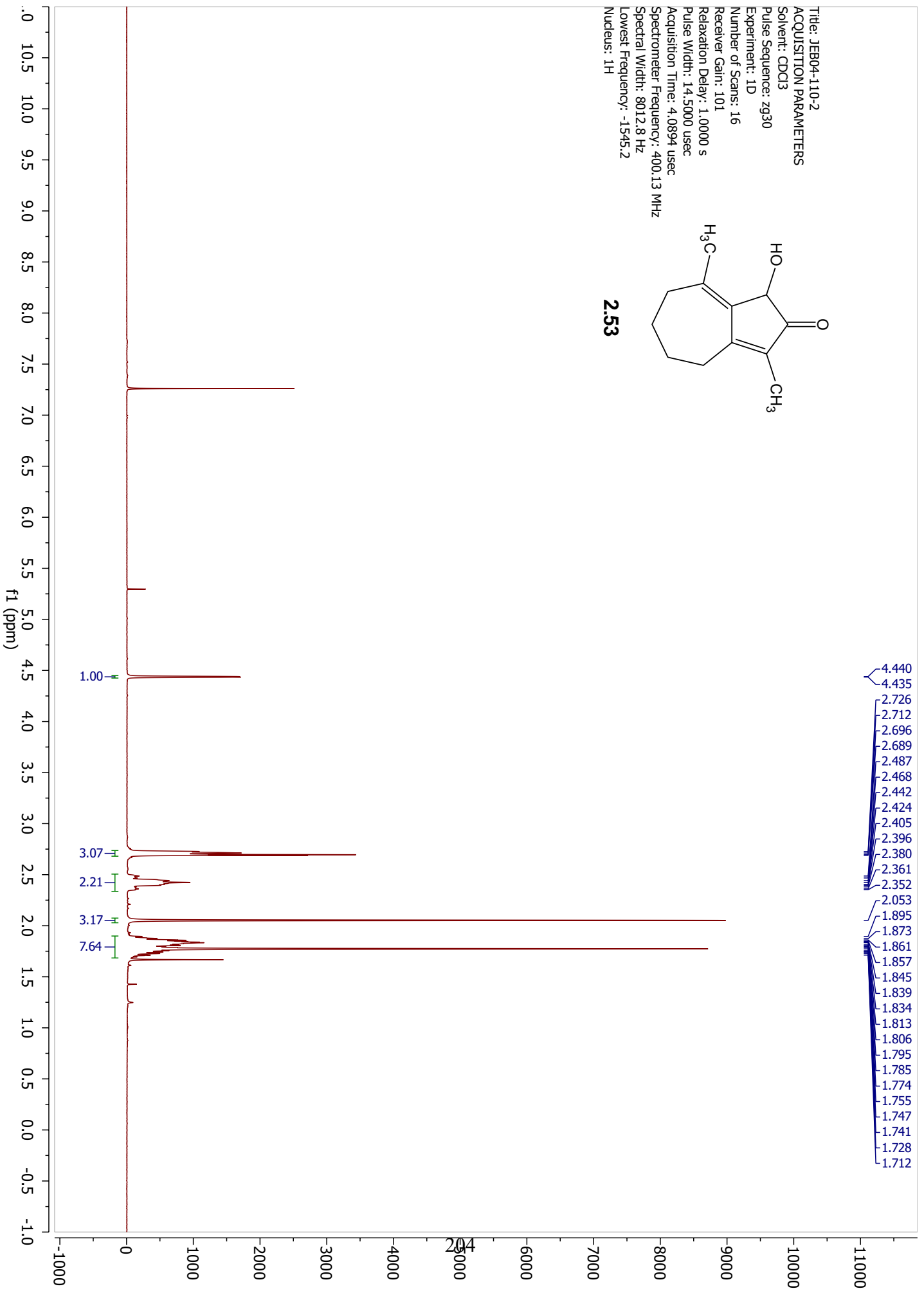
53.217
51.152
48.568
46.273
38.875
38.387
38.244
38.218
34.764
33.266
32.362
31.647
30.044
29.133
23.558
23.367
21.934
16.771
15.246
15.143



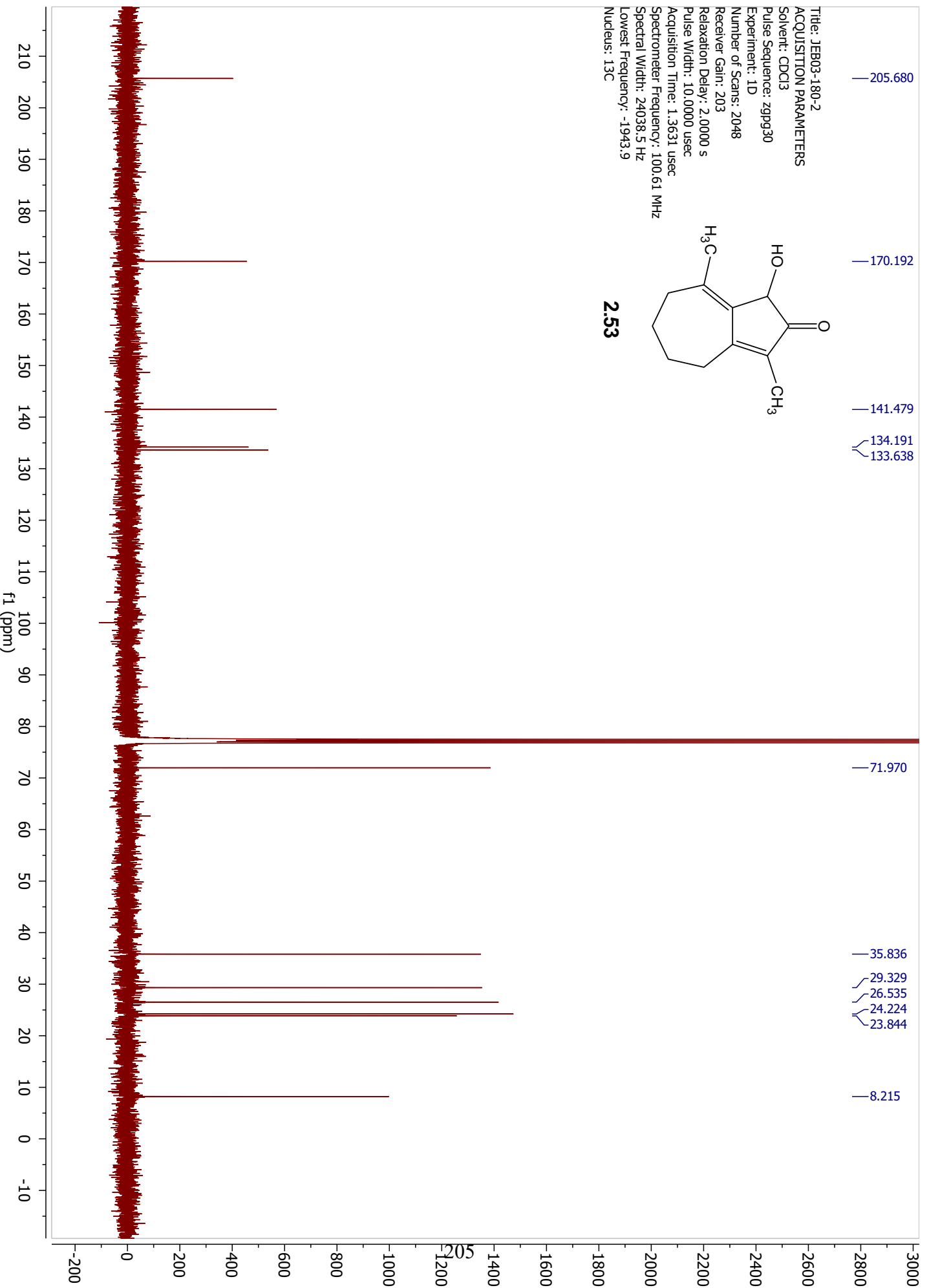
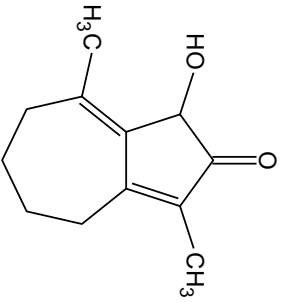
Title: JEB04-110-2
ACQUISITION PARAMETERS
Solvent: CDCl3
Pulse Sequence: zg30
Experiment: 1D
Number of Scans: 16
Receiver Gain: 101
Relaxation Delay: 1.0000 s
Pulse Width: 14.5000 usec
Acquisition Time: 4.0894 usec
Spectrometer Frequency: 400.13 MHz
Spectral Width: 8012.8 Hz
Lowest Frequency: -1545.2
Nucleus: 1H



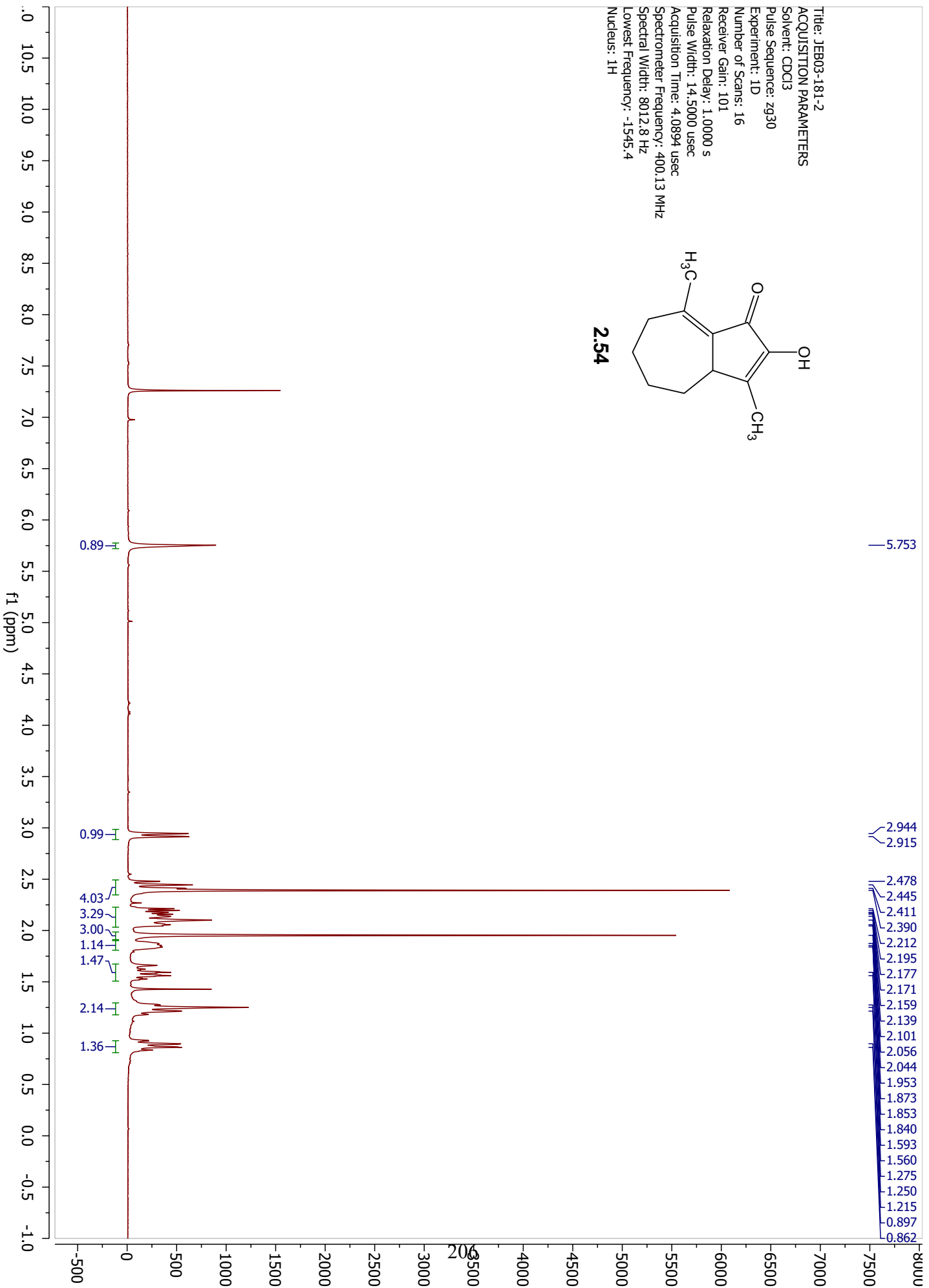
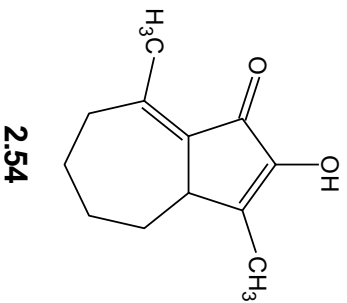
2.53



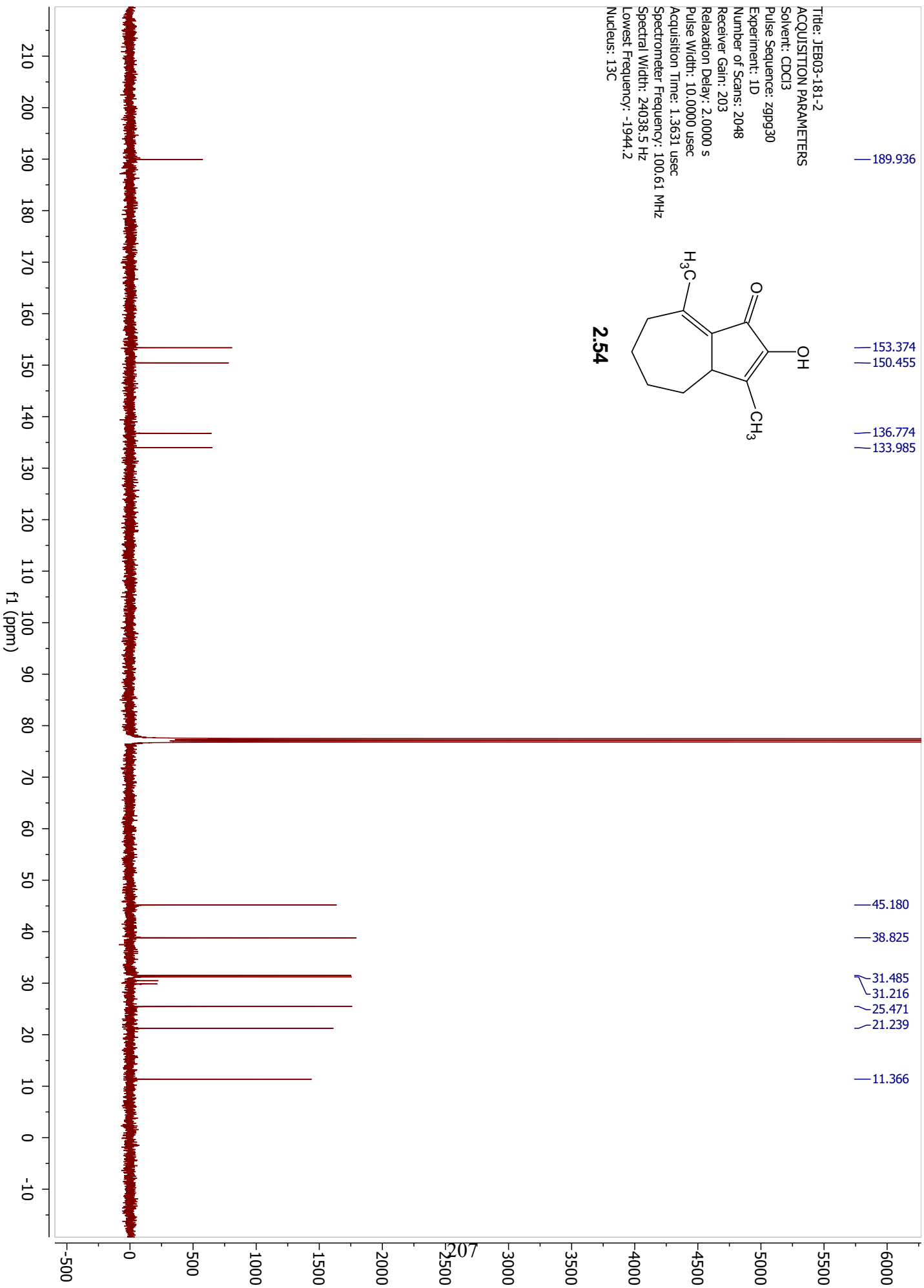
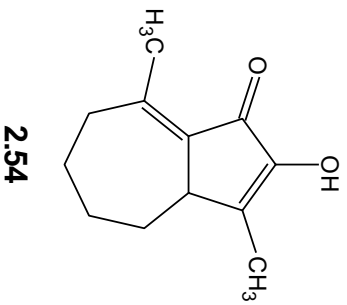
Title: JEB03-180-2
ACQUISITION PARAMETERS
Solvent: CDCl3
Pulse Sequence: zgpg30
Experiment: 1D
Number of Scans: 2048
Receiver Gain: 203
Relaxation Delay: 2.0000 s
Pulse Width: 10.0000 usec
Acquisition Time: 1.3631 usec
Spectrometer Frequency: 100.61 MHz
Spectral Width: 24038.5 Hz
Lowest Frequency: -1943.9
Nucleus: 13C



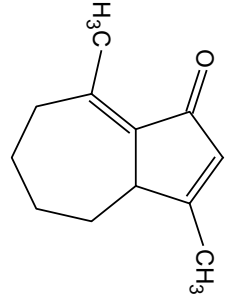
Title: JEB03-181-2
ACQUISITION PARAMETERS
Solvent: CDCl3
Pulse Sequence: zg30
Experiment: 1D
Number of Scans: 16
Receiver Gain: 101
Relaxation Delay: 1.0000 s
Pulse Width: 14.5000 usec
Acquisition Time: 4.0894 usec
Spectrometer Frequency: 400.13 MHz
Spectral Width: 8012.8 Hz
Lowest Frequency: -1545.4
Nucleus: 1H



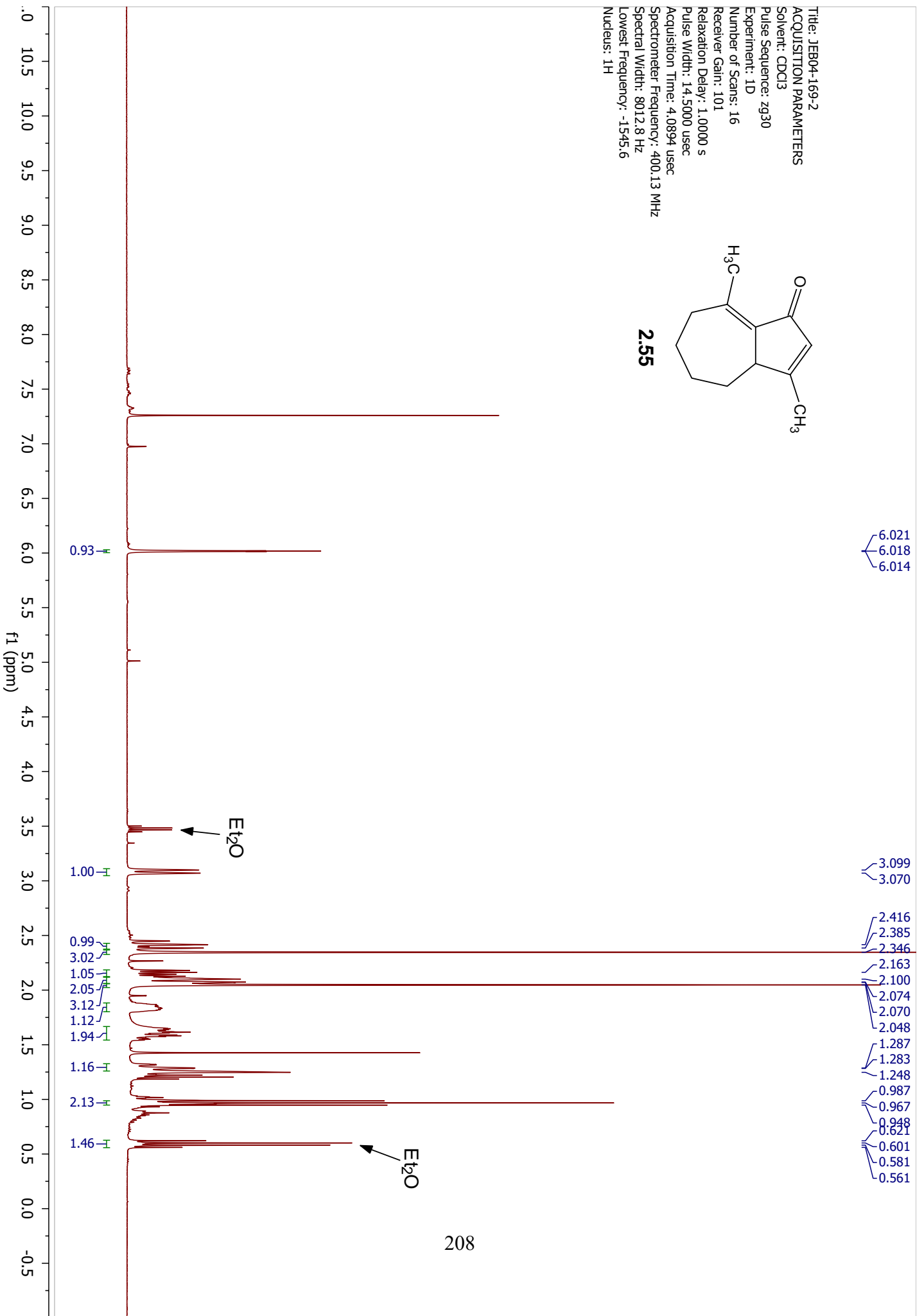
Title: JEB03-181-2
ACQUISITION PARAMETERS
Solvent: CDCl3
Pulse Sequence: zpgp30
Experiment: 1D
Number of Scans: 2048
Receiver Gain: 203
Relaxation Delay: 2.0000 s
Pulse Width: 10.0000 usec
Acquisition Time: 1.3631 usec
Spectrometer Frequency: 100.61 MHz
Spectral Width: 24038.5 Hz
Lowest Frequency: -1944.2
Nucleus: 13C



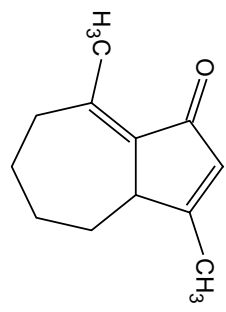
Title: JEB04-169-2
ACQUISITION PARAMETERS
Solvent: CDCl3
Pulse Sequence: zg30
Experiment: 1D
Number of Scans: 16
Receiver Gain: 101
Relaxation Delay: 1.0000 s
Pulse Width: 14.5000 usec
Acquisition Time: 4.0894 usec
Spectrometer Frequency: 400.13 MHz
Spectral Width: 8012.8 Hz
Lowest Frequency: -1545.6
Nucleus: 1H



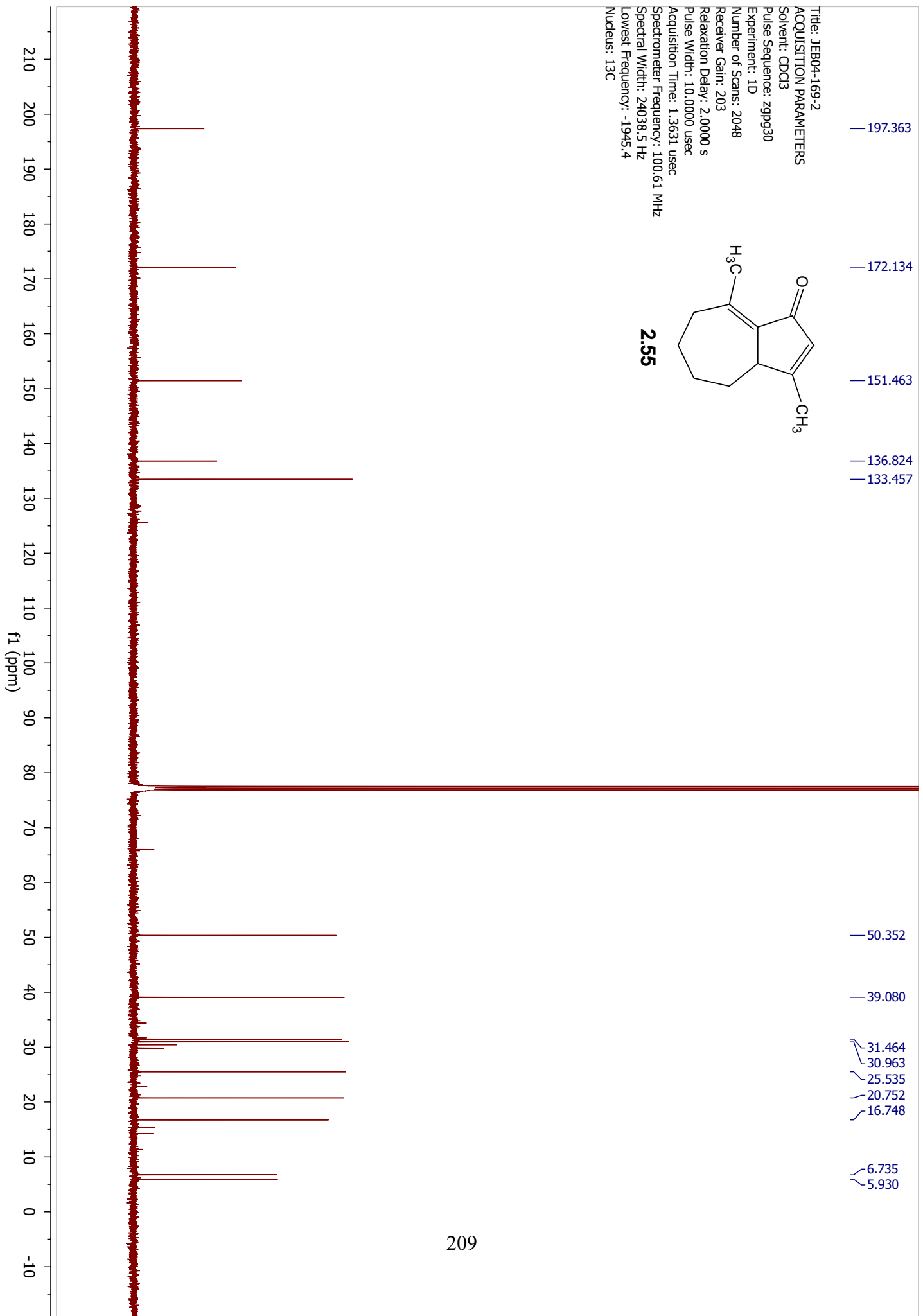
2.55



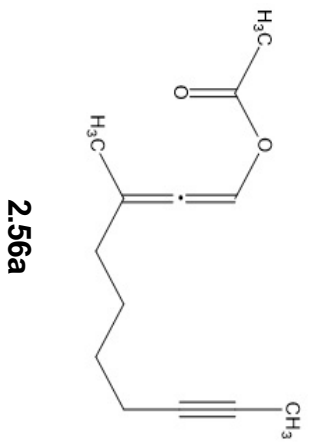
Title: JEB04-169-2
ACQUISITION PARAMETERS
Solvent: CDCl3
Pulse Sequence: zpgp30
Experiment: 1D
Number of Scans: 2048
Receiver Gain: 203
Relaxation Delay: 2.0000 s
Pulse Width: 10.0000 usec
Acquisition Time: 1.3631 usec
Spectrometer Frequency: 100.61 MHz
Spectral Width: 24038.5 Hz
Lowest Frequency: -1945.4
Nucleus: 13C



2.55



Title: JEB03-178-2
ACQUISITION PARAMETERS
Solvent: CDCl3
Pulse Sequence: zg30
Experiment: 1D
Number of Scans: 16
Receiver Gain: 128
Relaxation Delay: 1.0000 s
Pulse Width: 14.5000 usec
Acquisition Time: 4.0894 usec
Spectrometer Frequency: 400.13 MHz
Spectral Width: 8012.8 Hz
Lowest Frequency: -1545.2
Nucleus: 1H



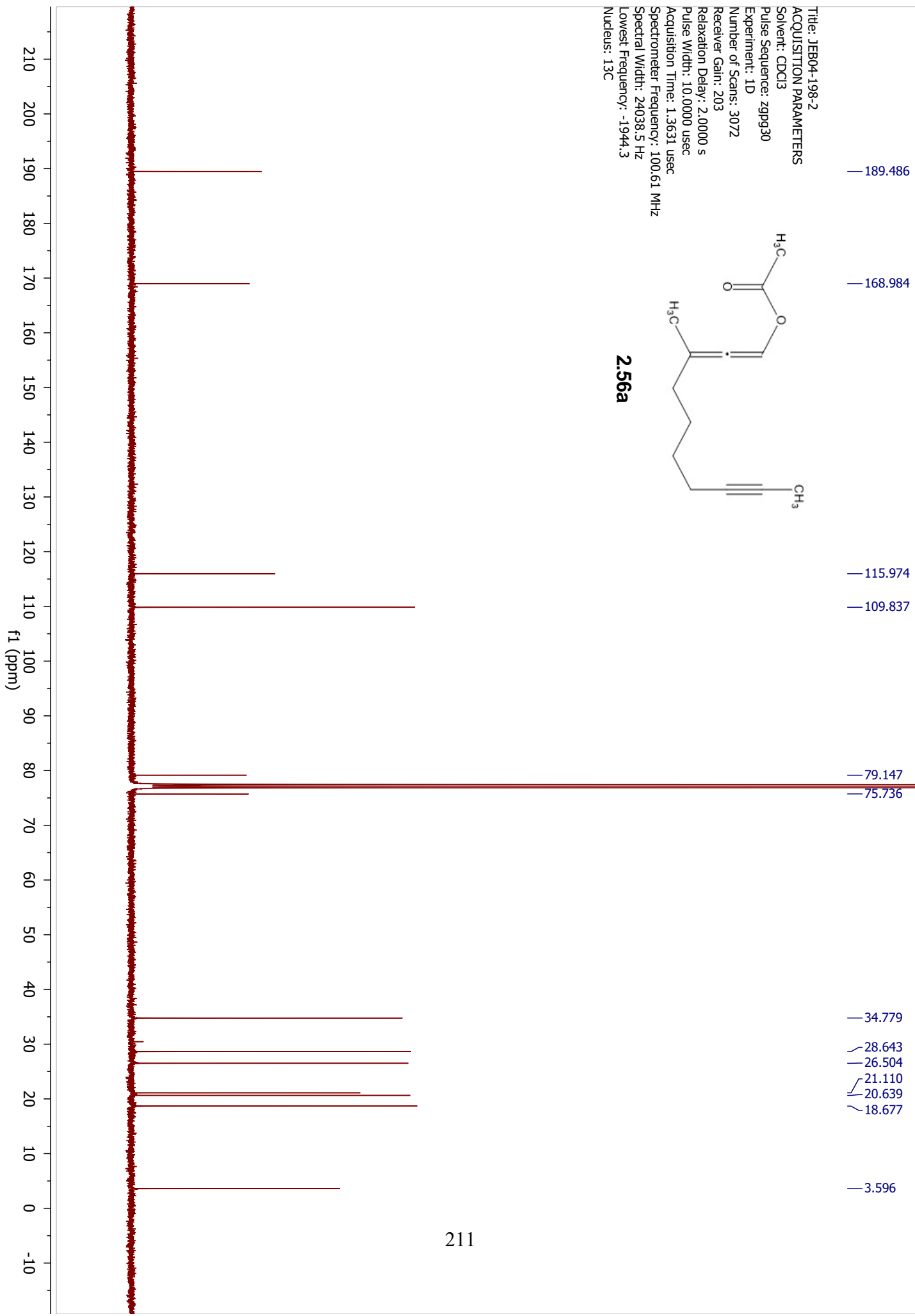
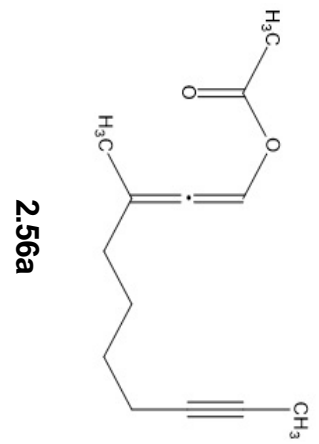
7.301
7.297

2.133
2.091
2.071
2.052
1.827
1.780
1.775

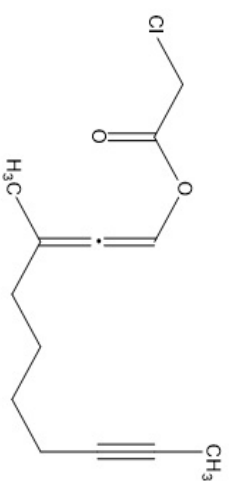
2.56a



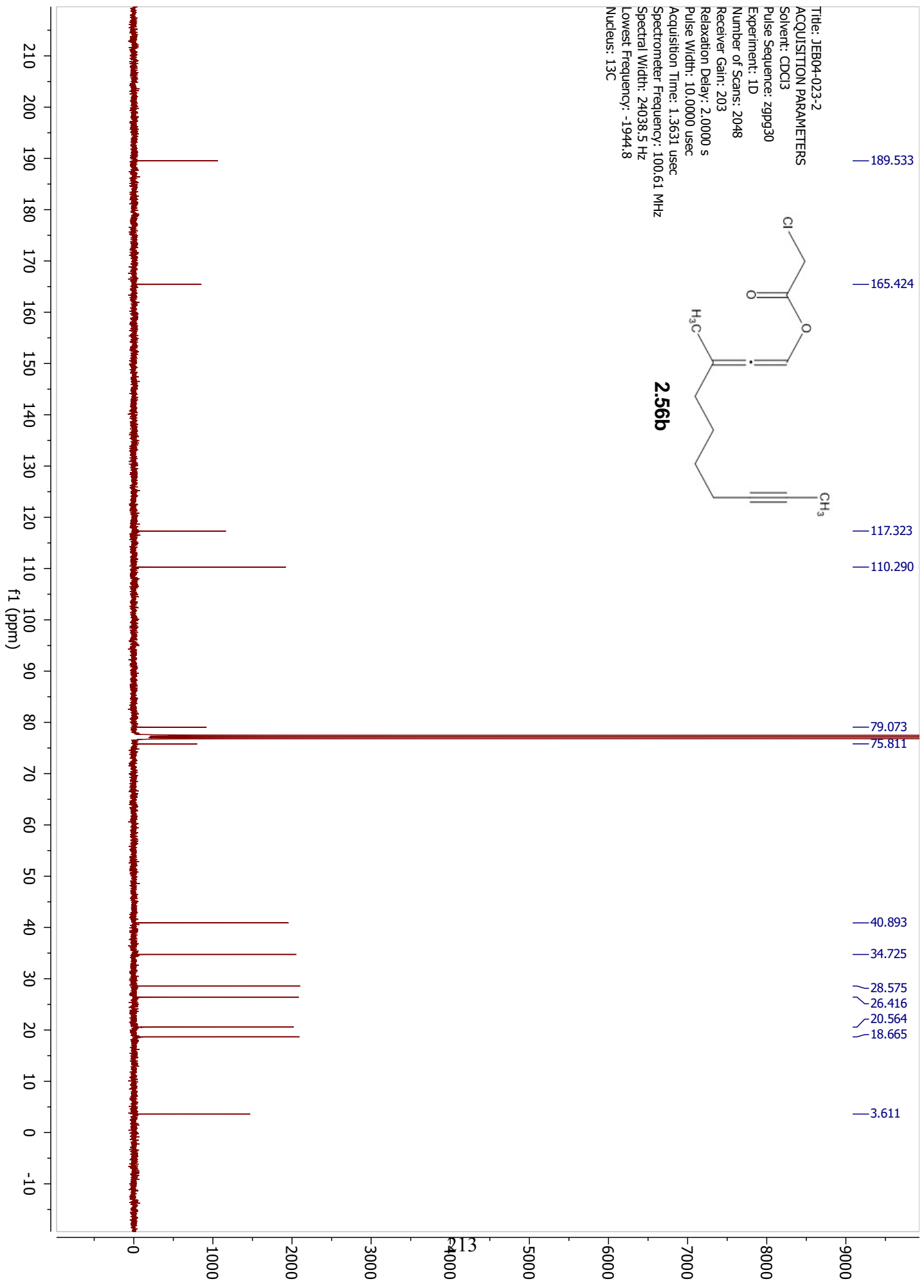
Title: JEB04-198-2
ACQUISITION PARAMETERS
Solvent: CDCl3
Pulse Sequence: zppg30
Experiment: 1D
Number of Scans: 3072
Receiver Gain: 203
Relaxation Delay: 2.0000 s
Pulse Width: 10.0000 usec
Acquisition Time: 1.3631 usec
Spectrometer Frequency: 100.61 MHz
Spectral Width: 24038.5 Hz
Lowest Frequency: -1944.3
Nucleus: 13C



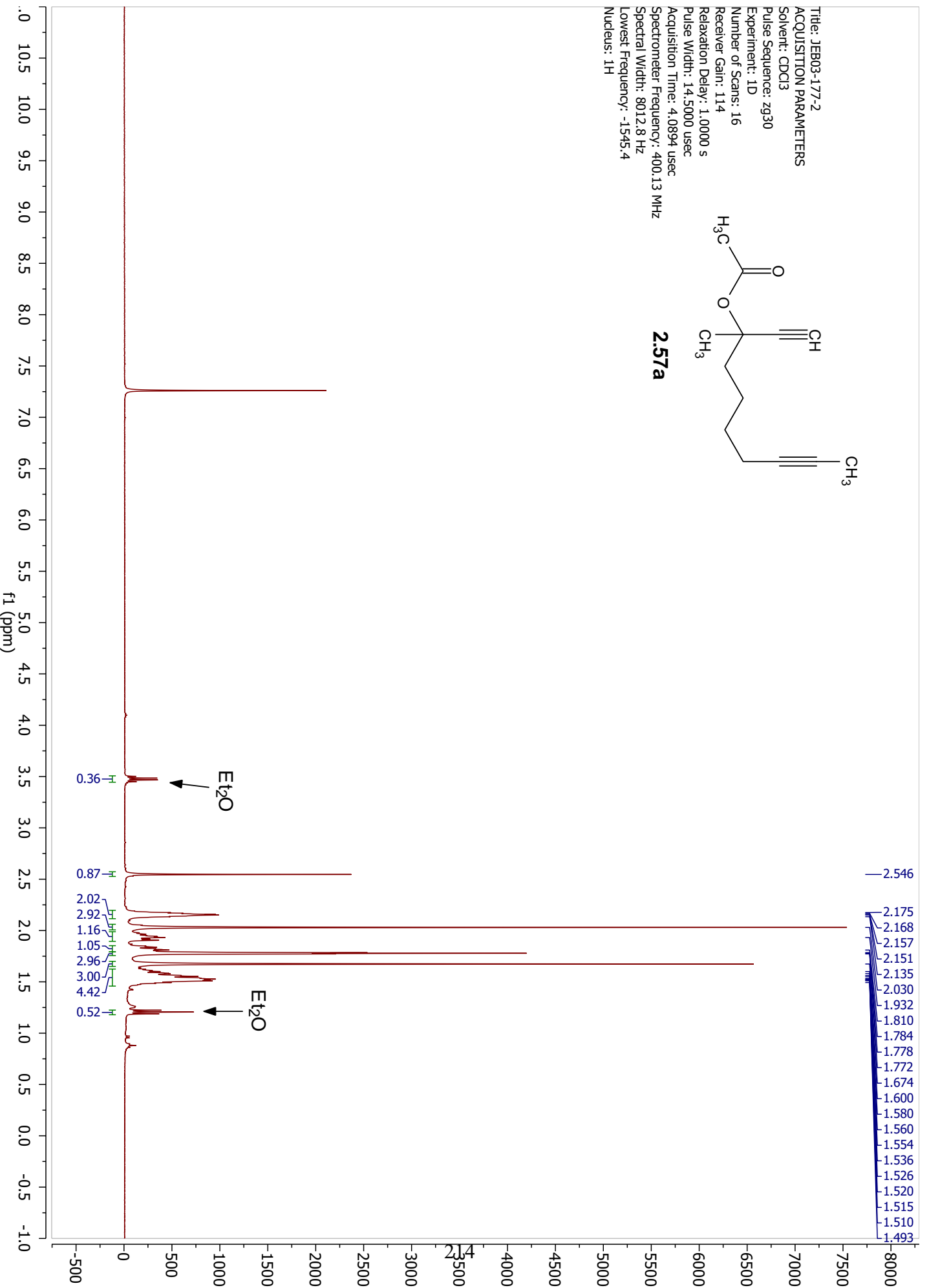
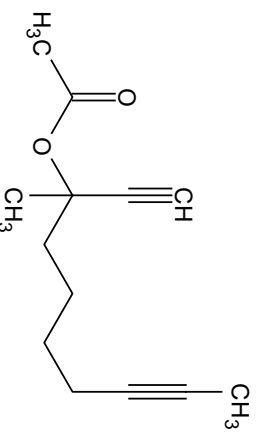
Title: JEB04-023-2
ACQUISITION PARAMETERS
Solvent: CDCl3
Pulse Sequence: zppg30
Experiment: 1D
Number of Scans: 2048
Receiver Gain: 203
Relaxation Delay: 2.0000 s
Pulse Width: 10.0000 usec
Acquisition Time: 1.3631 usec
Spectrometer Frequency: 100.61 MHz
Spectral Width: 24038.5 Hz
Lowest Frequency: -1944.8
Nucleus: 13C



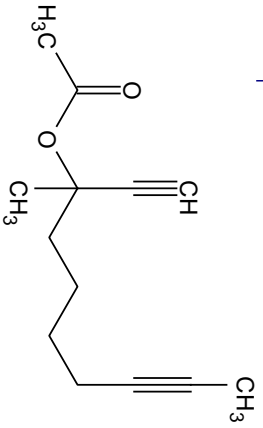
2.56b



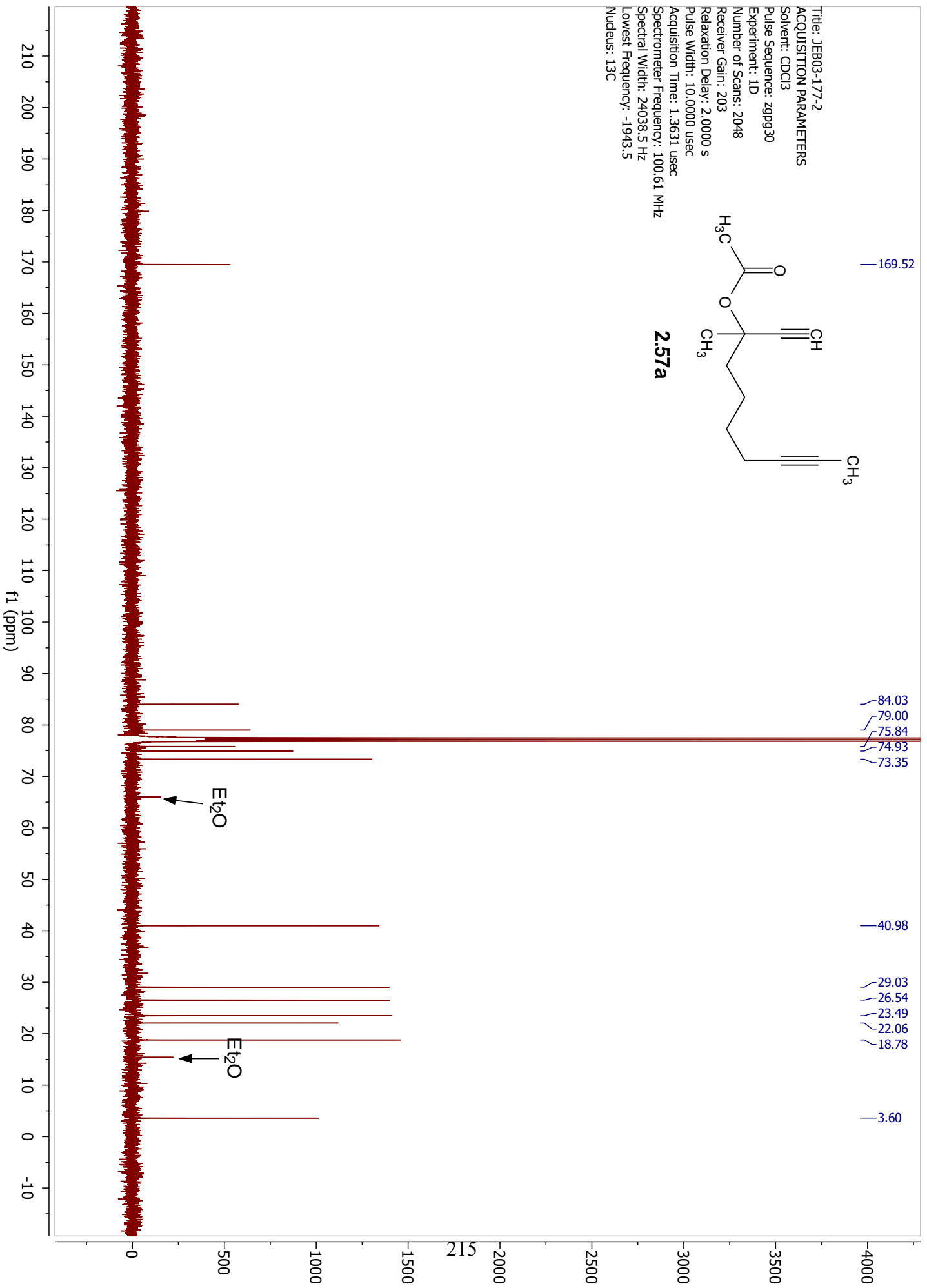
Title: JEB03-177-2
ACQUISITION PARAMETERS
Solvent: CDCl3
Pulse Sequence: zg30
Experiment: 1D
Number of Scans: 16
Receiver Gain: 114
Relaxation Delay: 1.0000 s
Pulse Width: 14.5000 usec
Acquisition Time: 4.0894 usec
Spectrometer Frequency: 400.13 MHz
Spectral Width: 8012.8 Hz
Lowest Frequency: -1545.4
Nucleus: 1H



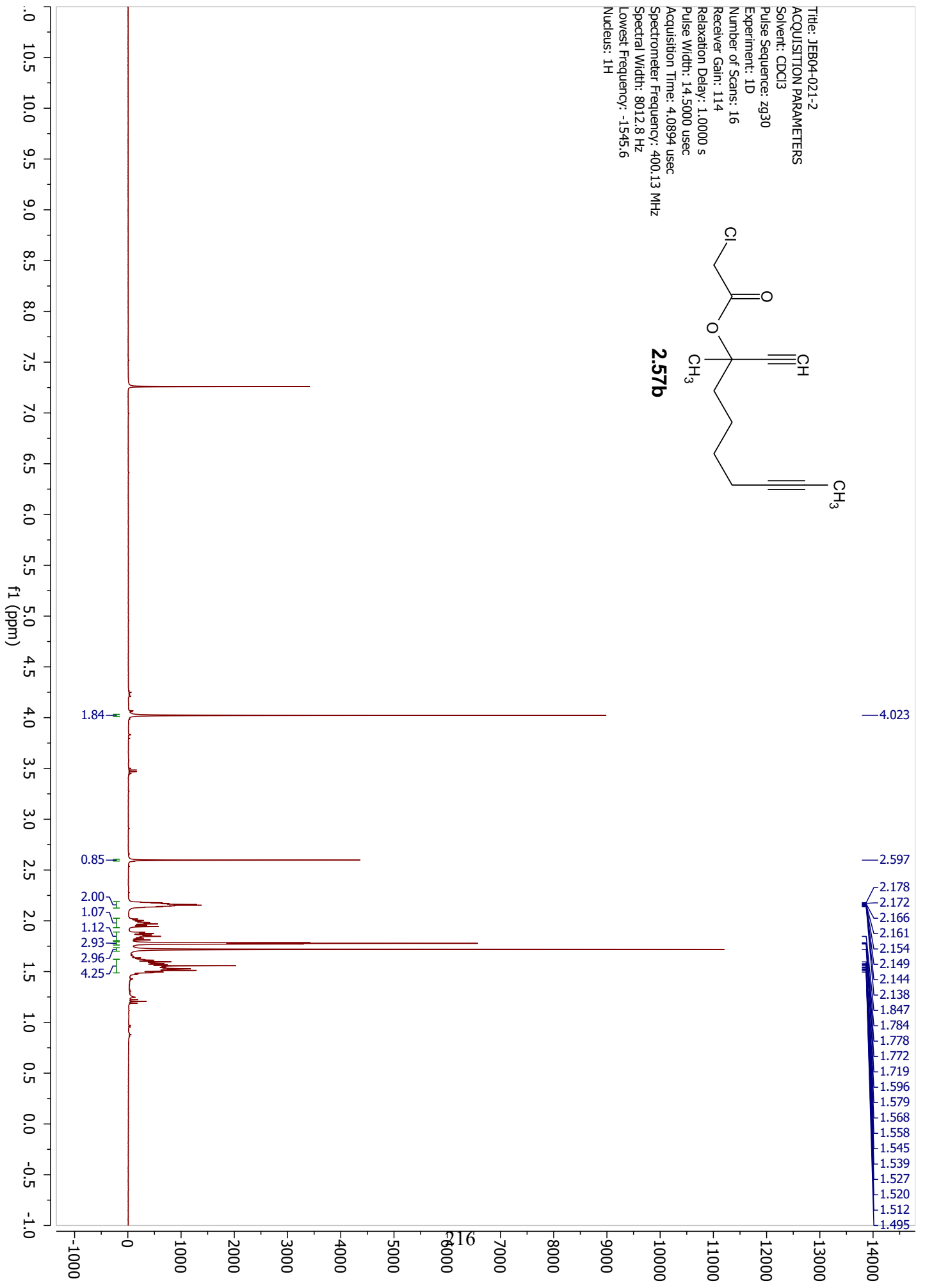
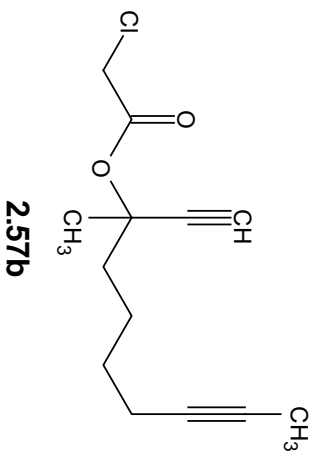
Title: JEB03-177-2
ACQUISITION PARAMETERS
Solvent: CDCl3
Pulse Sequence: zgpg30
Experiment: 1D
Number of Scans: 2048
Receiver Gain: 203
Relaxation Delay: 2.0000 s
Pulse Width: 10.0000 usec
Acquisition Time: 1.3631 usec
Spectrometer Frequency: 100.61 MHz
Spectral Width: 24038.5 Hz
Lowest Frequency: -1943.5
Nucleus: 13C



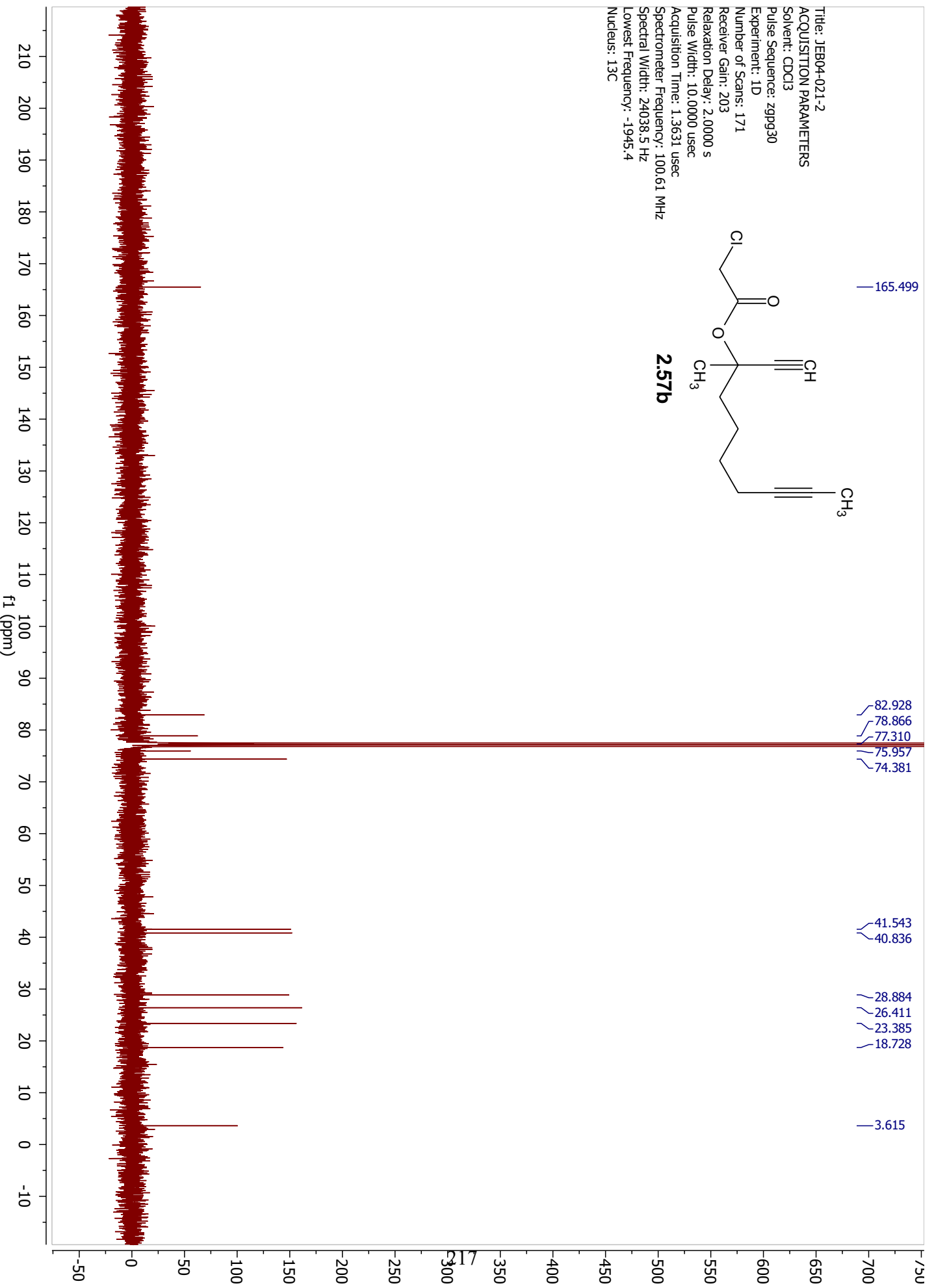
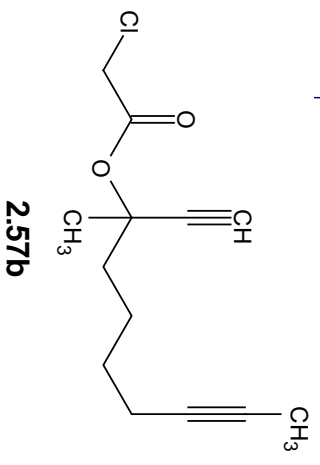
2.57a



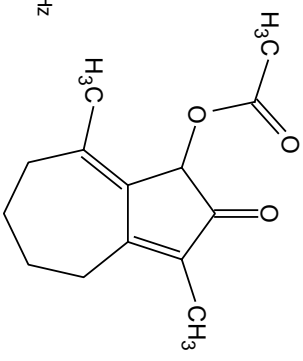
Title: JEB04-021-2
ACQUISITION PARAMETERS
Solvent: CDCl3
Pulse Sequence: zg30
Experiment: 1D
Number of Scans: 16
Receiver Gain: 114
Relaxation Delay: 1.0000 s
Pulse Width: 14.5000 usec
Acquisition Time: 4.0894 usec
Spectrometer Frequency: 400.13 MHz
Spectral Width: 8012.8 Hz
Lowest Frequency: -1545.6
Nucleus: 1H



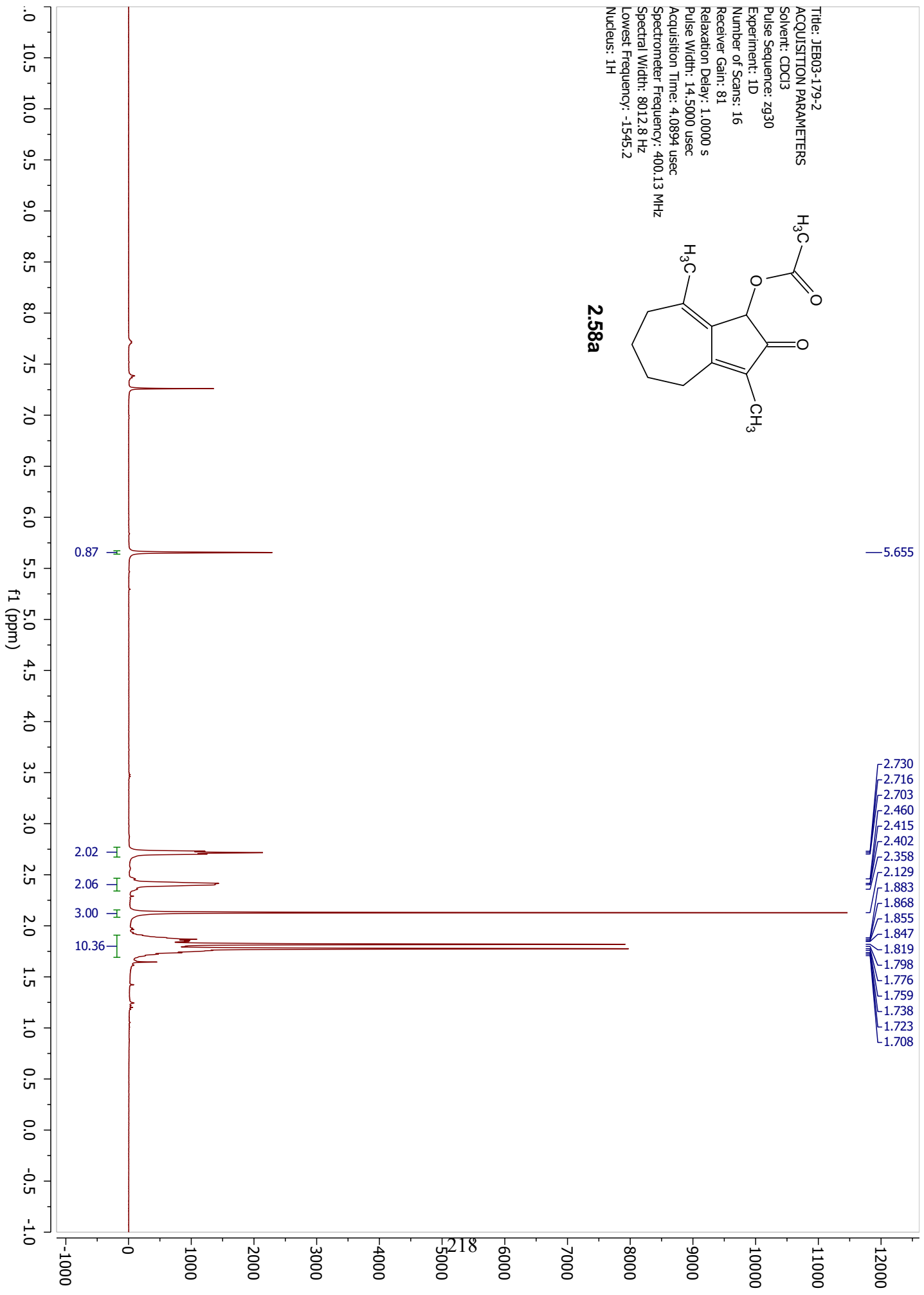
Title: JEB04-021-2
ACQUISITION PARAMETERS
Solvent: CDCl3
Pulse Sequence: zpgp30
Experiment: 1D
Number of Scans: 171
Receiver Gain: 203
Relaxation Delay: 2.0000 s
Pulse Width: 10.0000 usec
Acquisition Time: 1.3631 usec
Spectrometer Frequency: 100.61 MHz
Spectral Width: 24038.5 Hz
Lowest Frequency: -1945.4
Nucleus: 13C



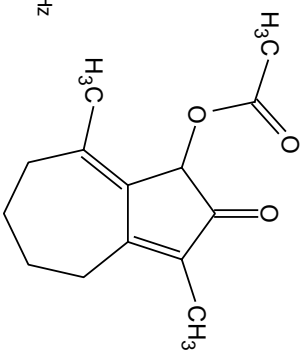
Title: JEB03-179-2
ACQUISITION PARAMETERS
Solvent: CDCl3
Pulse Sequence: zg30
Experiment: 1D
Number of Scans: 16
Receiver Gain: 81
Relaxation Delay: 1.0000 s
Pulse Width: 14.5000 usec
Acquisition Time: 4.0894 usec
Spectrometer Frequency: 400.13 MHz
Spectral Width: 8012.8 Hz
Lowest Frequency: -1545.2
Nucleus: 1H



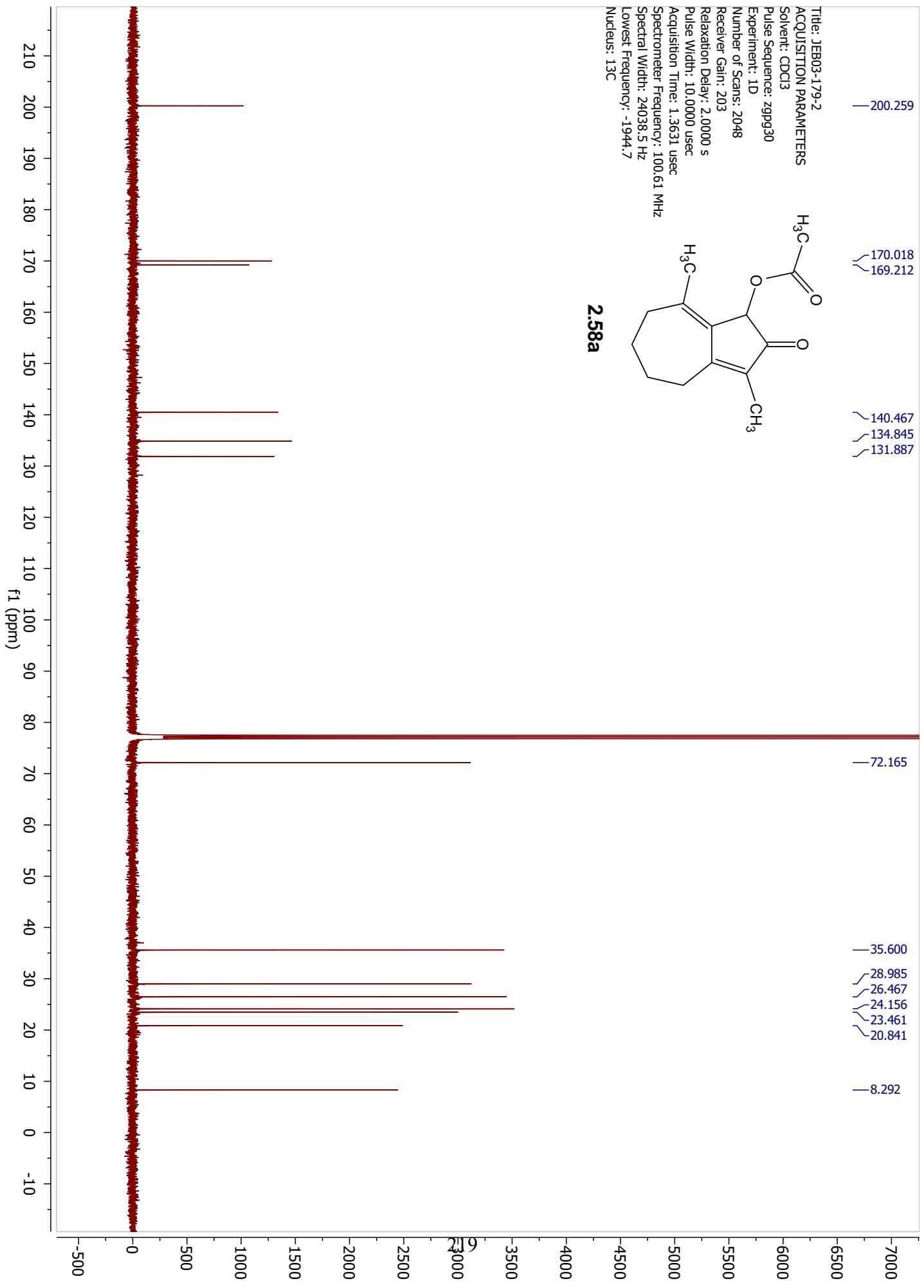
2.58a



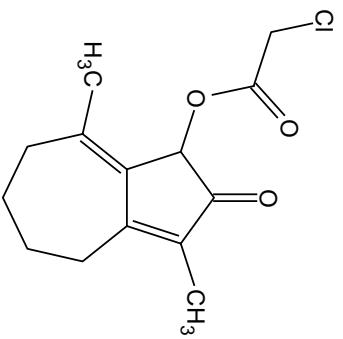
Title: JEB03-179-2
ACQUISITION PARAMETERS
Solvent: CDCl3
Pulse Sequence: zppg30
Experiment: 1D
Number of Scans: 2048
Receiver Gain: 203
Relaxation Delay: 2.0000 s
Pulse Width: 10.0000 usec
Acquisition Time: 1.3631 usec
Spectrometer Frequency: 100.61 MHz
Spectral Width: 24038.5 Hz
Lowest Frequency: -1944.7
Nucleus: 13C



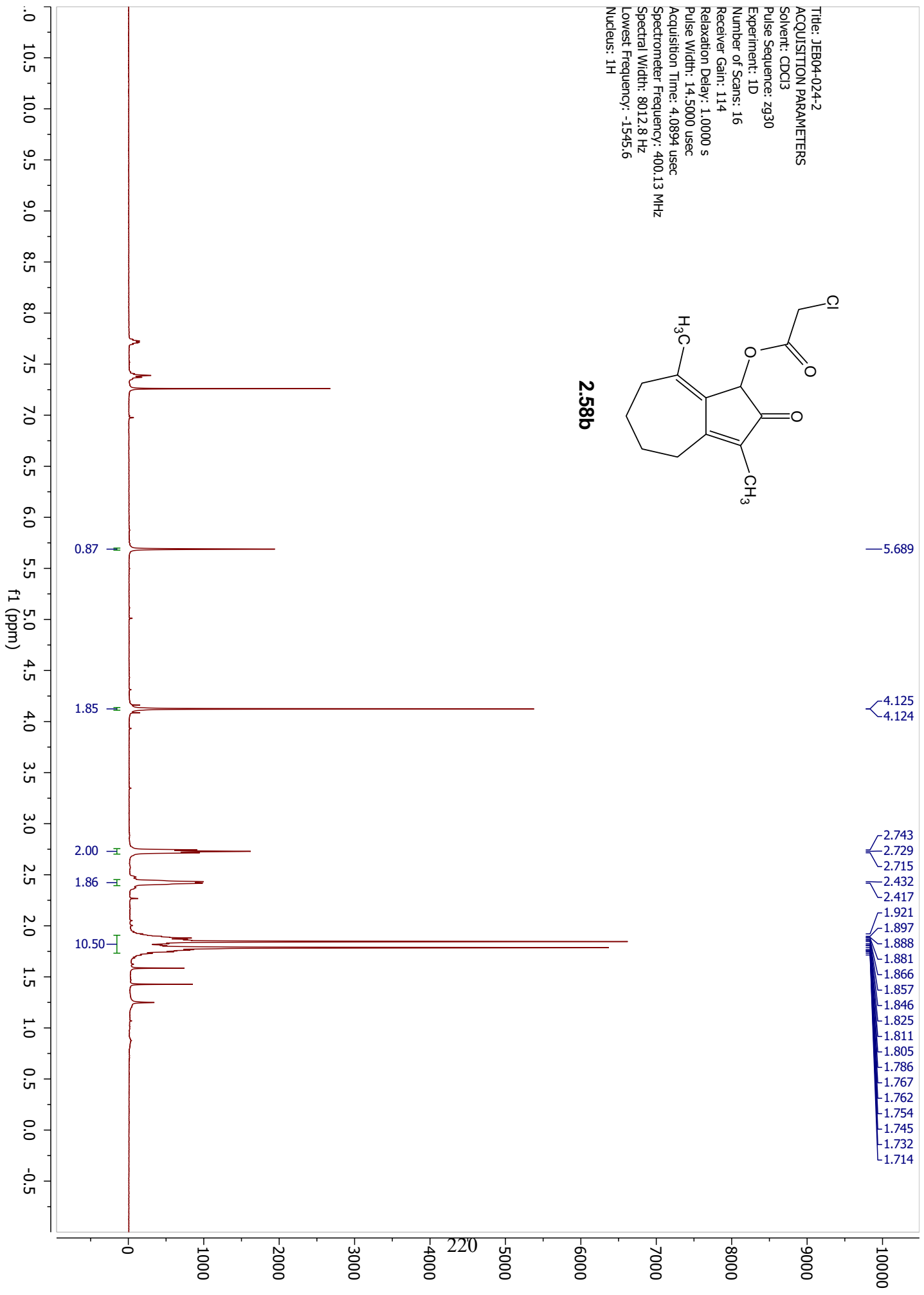
2.58a



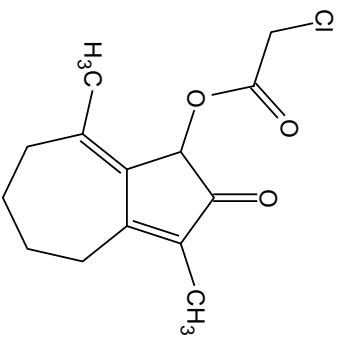
Title: JEB04-024-2
ACQUISITION PARAMETERS
Solvent: CDCl3
Pulse Sequence: zg30
Experiment: 1D
Number of Scans: 16
Receiver Gain: 114
Relaxation Delay: 1.0000 s
Pulse Width: 14.5000 usec
Acquisition Time: 4.0894 usec
Spectrometer Frequency: 400.13 MHz
Spectral Width: 8012.8 Hz
Lowest Frequency: -1545.6
Nucleus: 1H



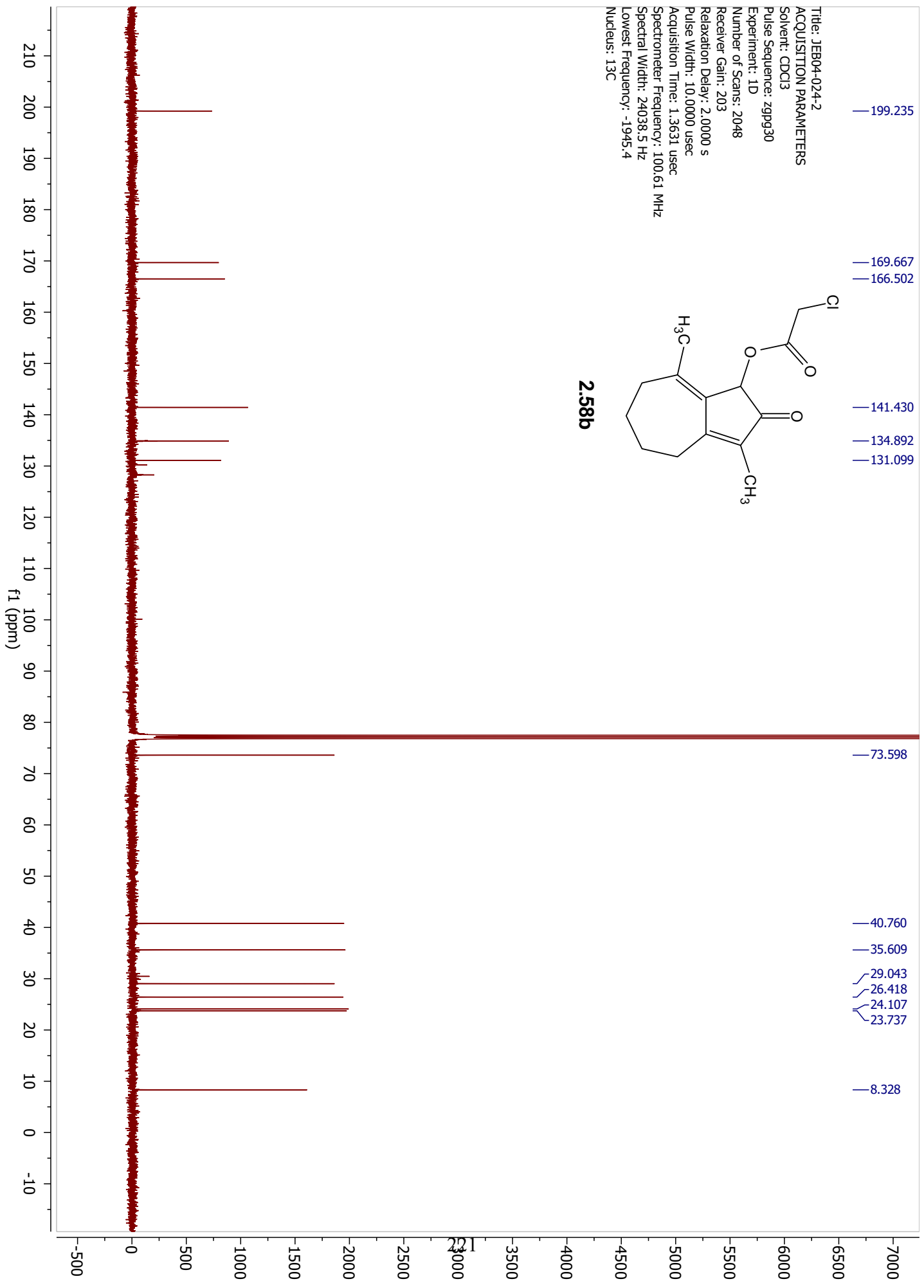
2.58b



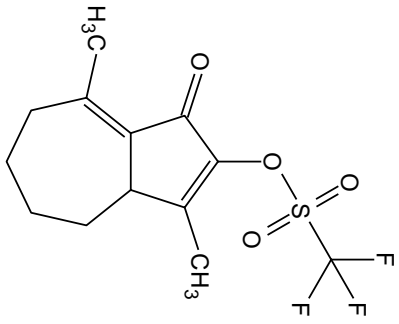
Title: JEB04-024-2
ACQUISITION PARAMETERS
Solvent: CDCl3
Pulse Sequence: zppg30
Experiment: 1D
Number of Scans: 2048
Receiver Gain: 203
Relaxation Delay: 2.0000 s
Pulse Width: 10.0000 usec
Acquisition Time: 1.3631 usec
Spectrometer Frequency: 100.61 MHz
Spectral Width: 24038.5 Hz
Lowest Frequency: -1945.4
Nucleus: 13C



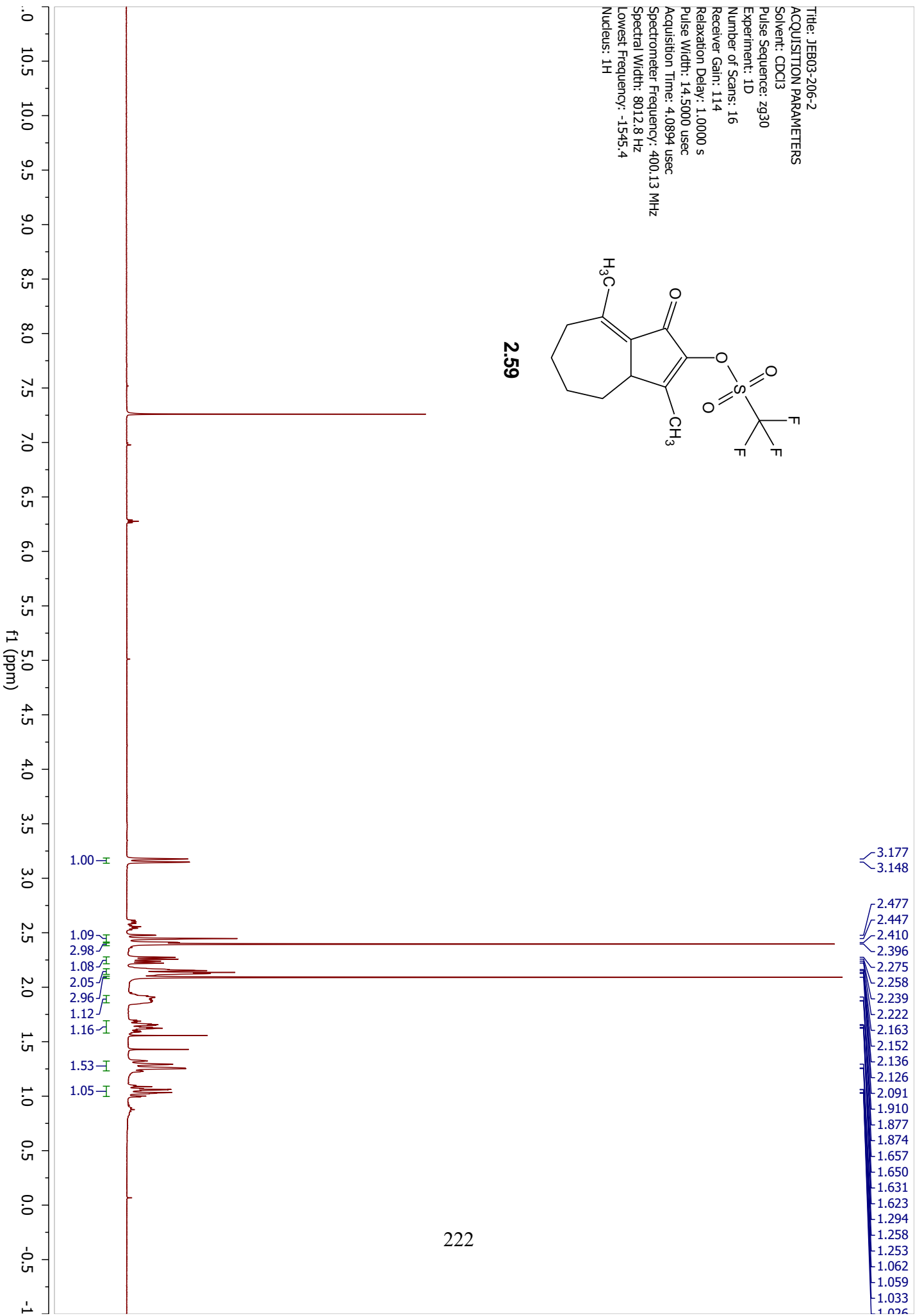
2.58b



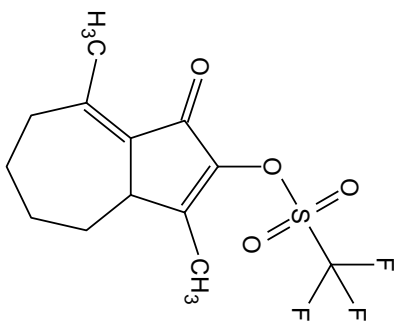
Title: JEB03-206-2
ACQUISITION PARAMETERS
Solvent: CDCl3
Pulse Sequence: zg30
Experiment: 1D
Number of Scans: 16
Receiver Gain: 114
Relaxation Delay: 1.0000 s
Pulse Width: 14.5000 usec
Acquisition Time: 4.0894 usec
Spectrometer Frequency: 400.13 MHz
Spectral Width: 8012.8 Hz
Lowest Frequency: -1545.4
Nucleus: 1H



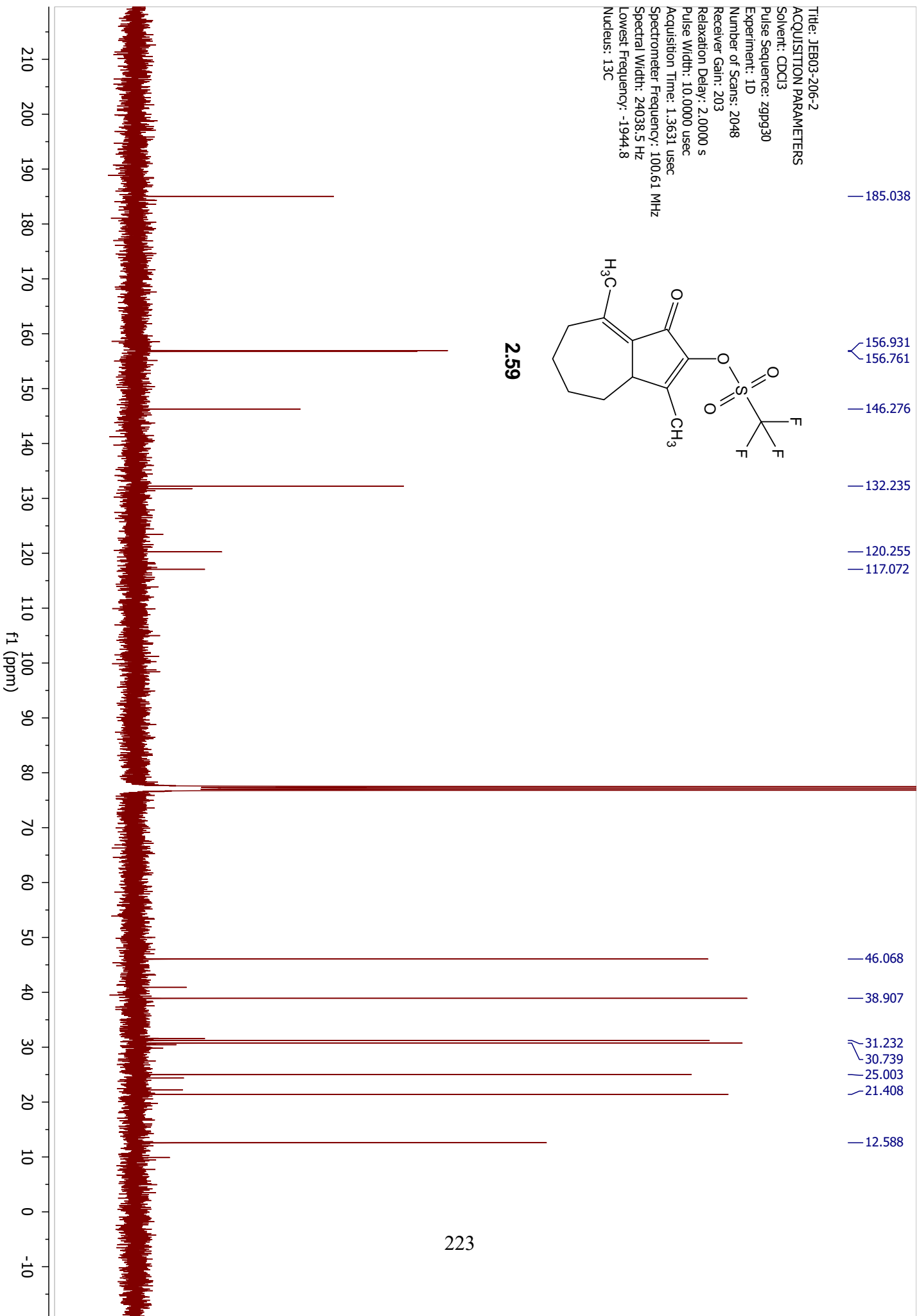
2.59



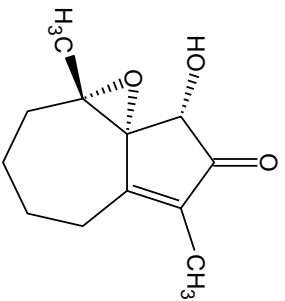
Title: JEB03-206-2
ACQUISITION PARAMETERS
Solvent: CDCl3
Pulse Sequence: zppg30
Experiment: 1D
Number of Scans: 2048
Receiver Gain: 203
Relaxation Delay: 2.0000 s
Pulse Width: 10.0000 usec
Acquisition Time: 1.3631 usec
Spectrometer Frequency: 100.61 MHz
Spectral Width: 24038.5 Hz
Lowest Frequency: -1944.8
Nucleus: 13C



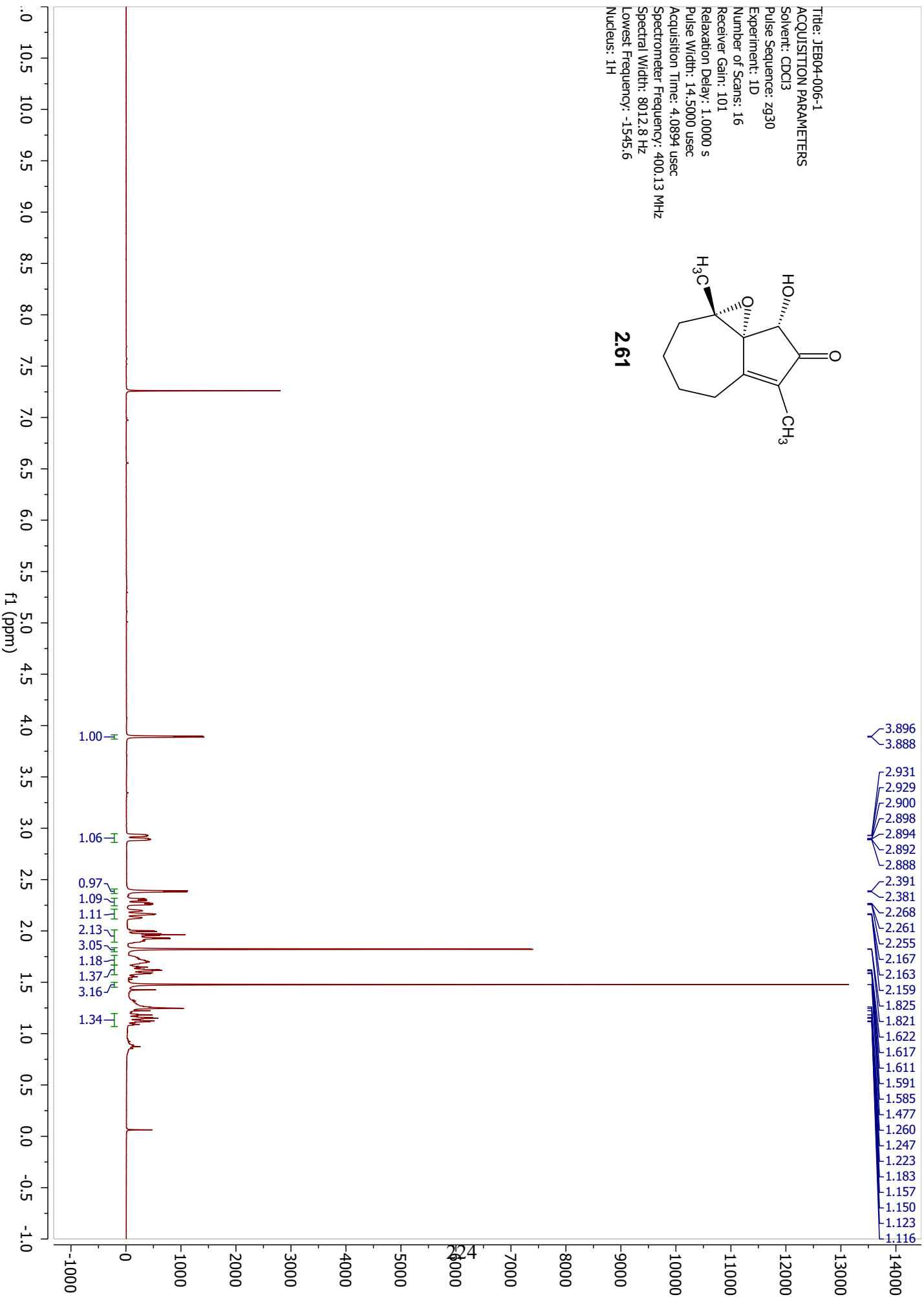
2.59



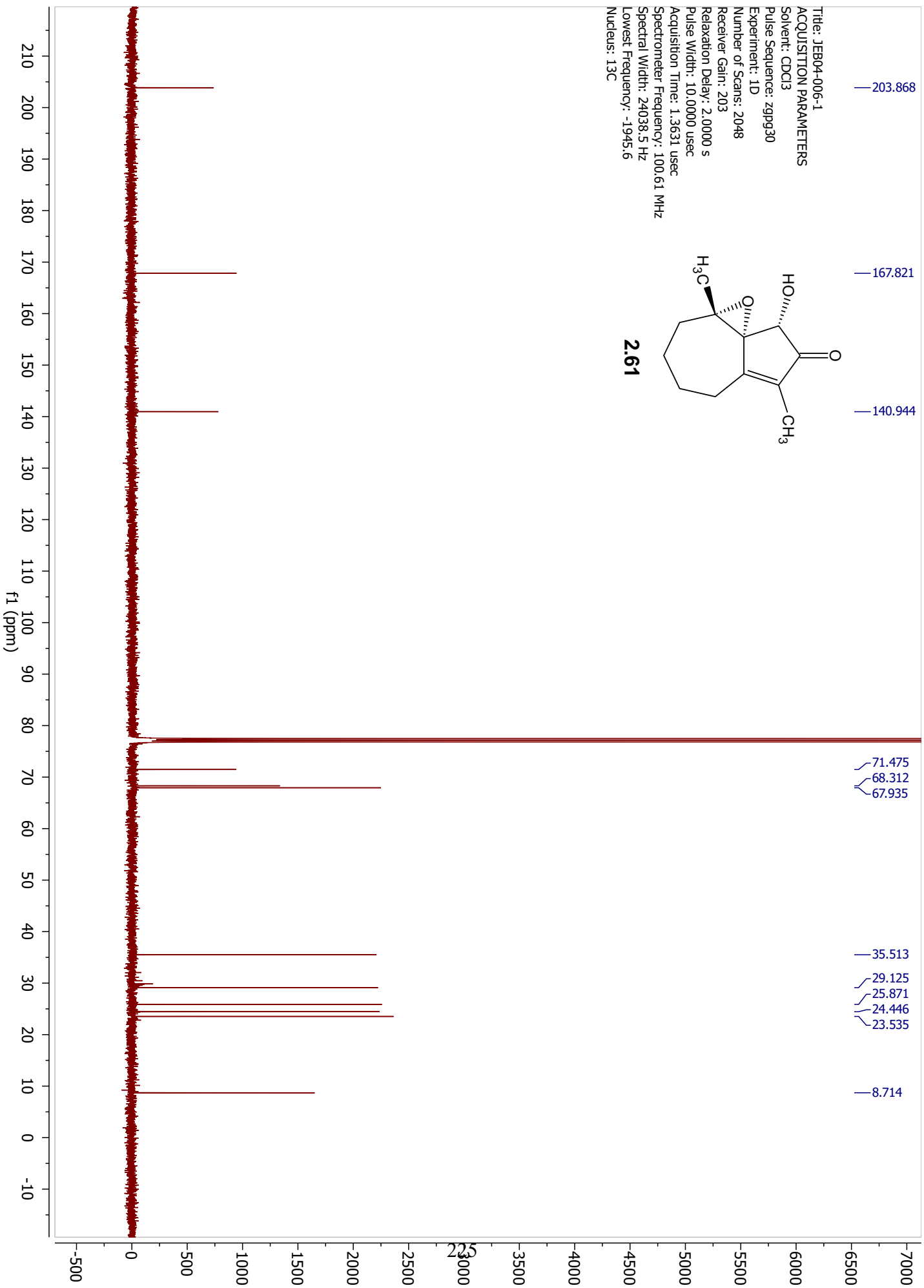
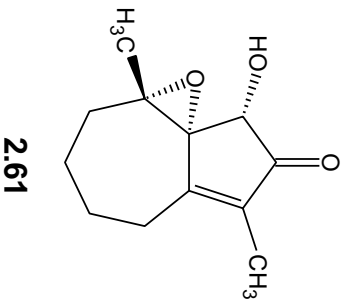
Title: JEB04-006-1
ACQUISITION PARAMETERS
Solvent: CDCl3
Pulse Sequence: zg30
Experiment: 1D
Number of Scans: 16
Receiver Gain: 101
Relaxation Delay: 1.0000 s
Pulse Width: 14.5000 usec
Acquisition Time: 4.0894 usec
Spectrometer Frequency: 400.13 MHz
Spectral Width: 8012.8 Hz
Lowest Frequency: -1545.6
Nucleus: 1H



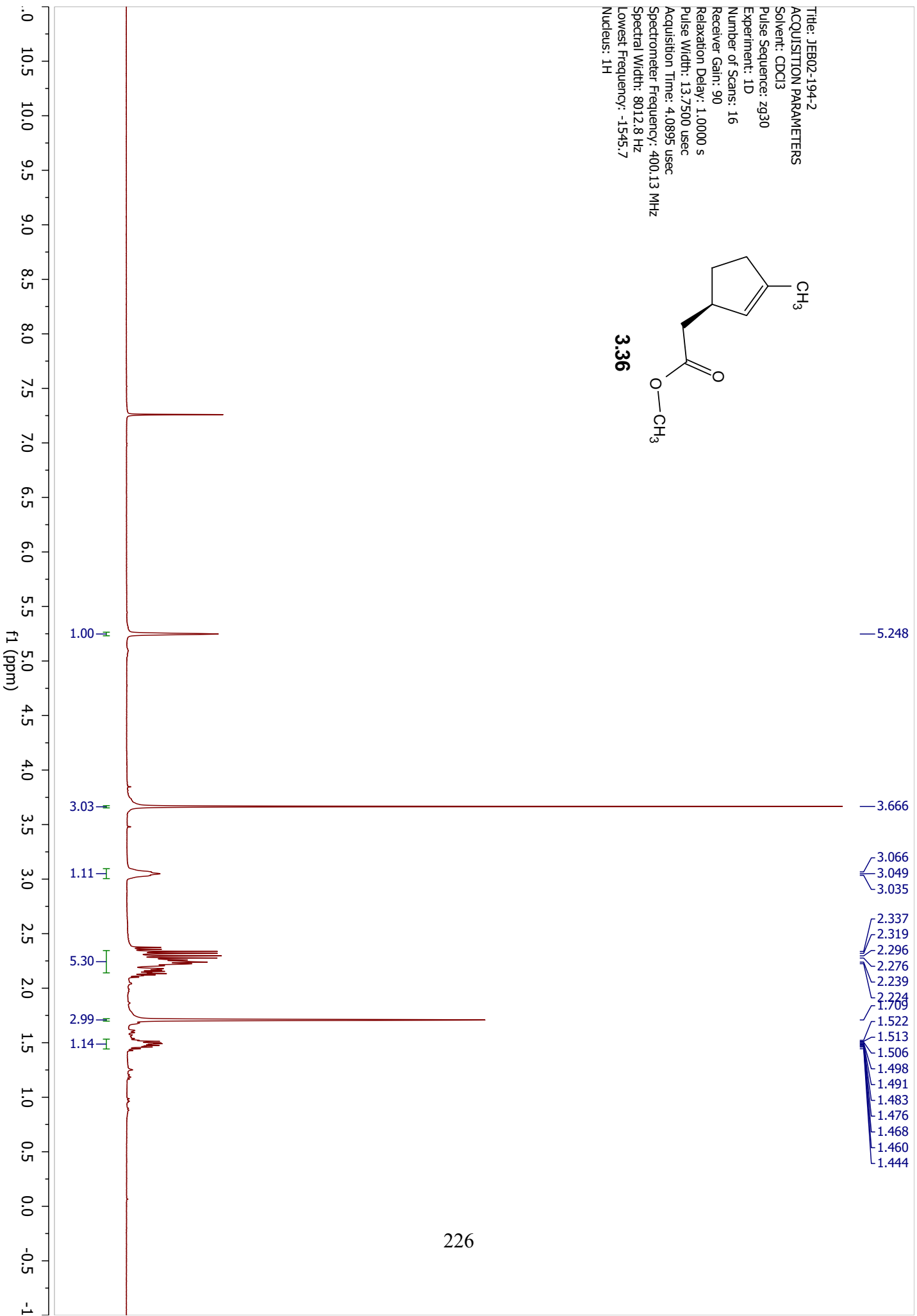
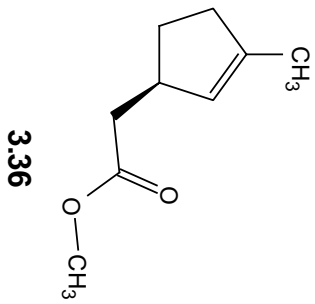
2.61



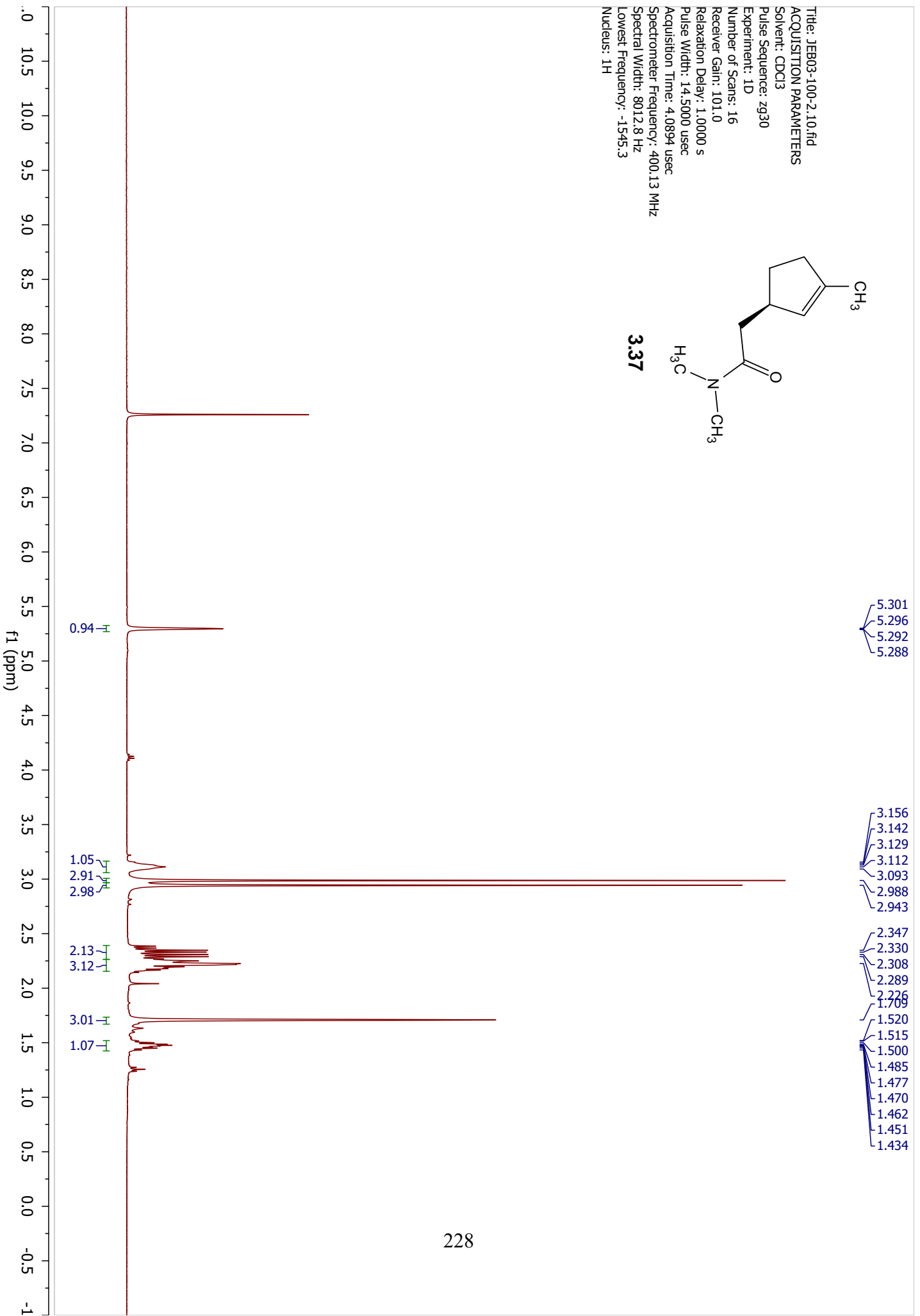
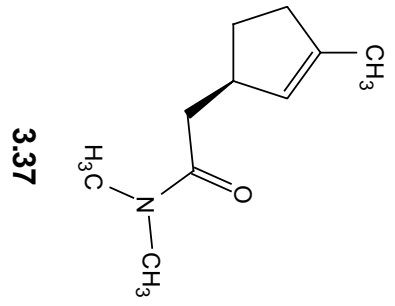
Title: JEB04-006-1
ACQUISITION PARAMETERS
Solvent: CDCl3
Pulse Sequence: zpgp30
Experiment: 1D
Number of Scans: 2048
Receiver Gain: 203
Relaxation Delay: 2.0000 s
Pulse Width: 10.0000 usec
Acquisition Time: 1.3631 usec
Spectrometer Frequency: 100.61 MHz
Spectral Width: 24038.5 Hz
Lowest Frequency: -1945.6
Nucleus: 13C



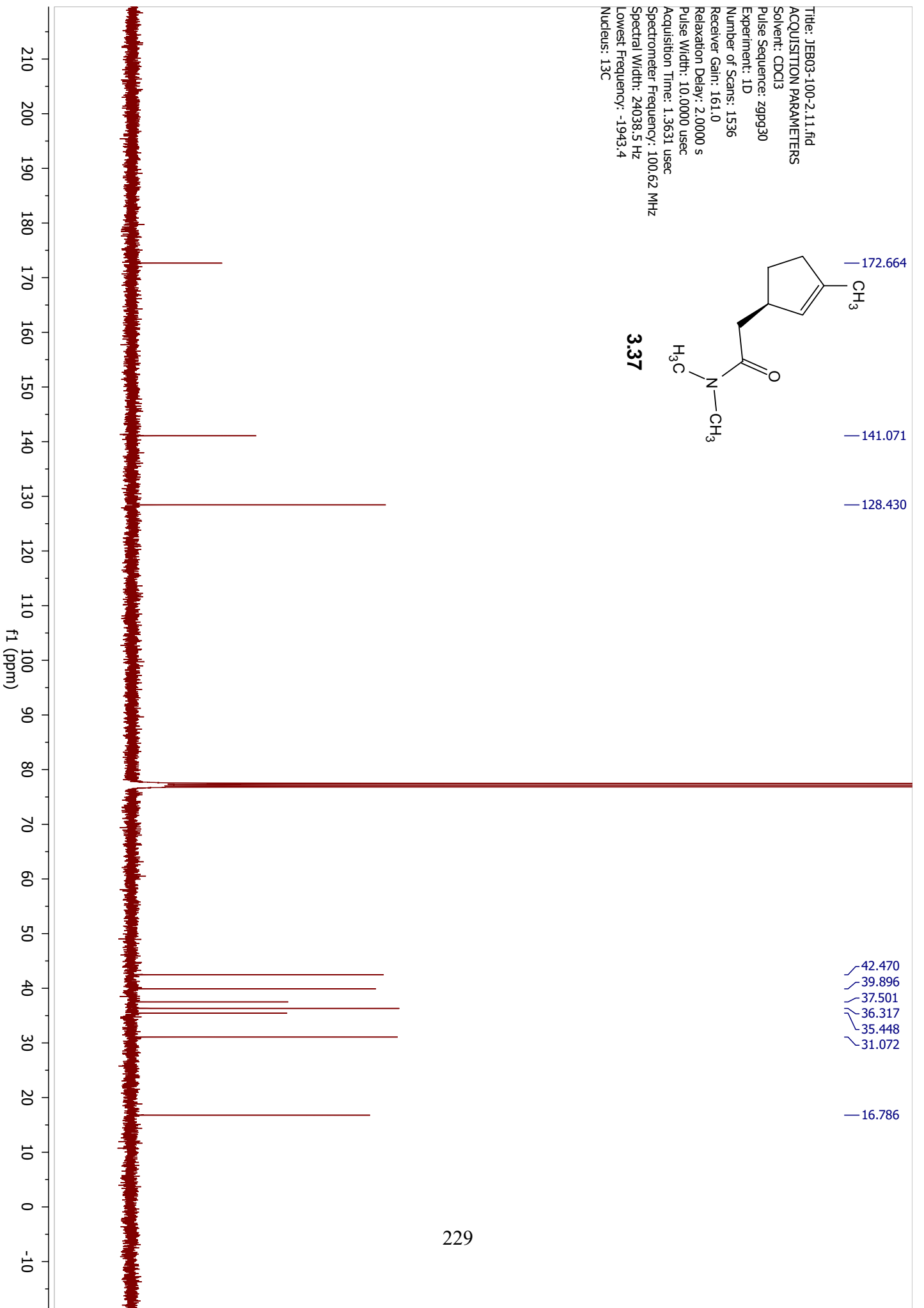
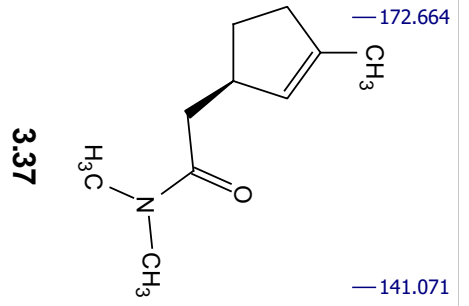
Title: JEB02-194-2
ACQUISITION PARAMETERS
Solvent: CDCl3
Pulse Sequence: zg30
Experiment: 1D
Number of Scans: 16
Receiver Gain: 90
Relaxation Delay: 1.0000 s
Pulse Width: 13.7500 usec
Acquisition Time: 4.0895 usec
Spectrometer Frequency: 400.13 MHz
Spectral Width: 8012.8 Hz
Lowest Frequency: -1545.7
Nucleus: 1H



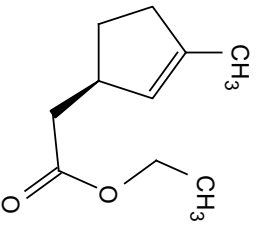
Title: JEB03-100-2.10.fid
ACQUISITION PARAMETERS
Solvent: CDCl3
Pulse Sequence: zg30
Experiment: 1D
Number of Scans: 16
Receiver Gain: 101.0
Relaxation Delay: 1.0000 s
Pulse Width: 14.5000 usec
Acquisition Time: 4.0894 usec
Spectrometer Frequency: 400.13 MHz
Spectral Width: 8012.8 Hz
Lowest Frequency: -1545.3
Nucleus: 1H



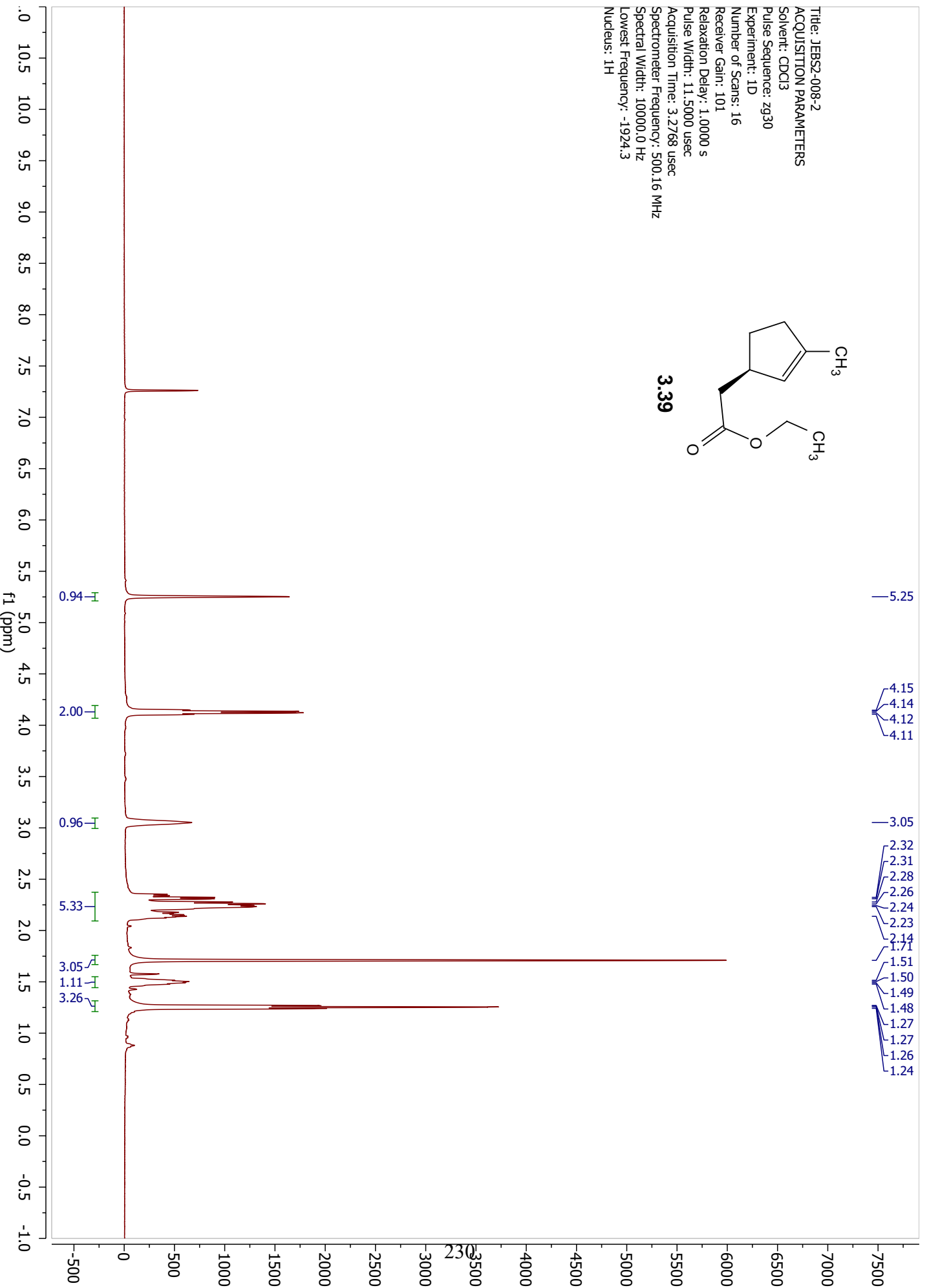
Title: JEB03-100-2.11.fid
ACQUISITION PARAMETERS
Solvent: CDCl3
Pulse Sequence: zpgp30
Experiment: 1D
Number of Scans: 1536
Receiver Gain: 161.0
Relaxation Delay: 2.0000 s
Pulse Width: 10.0000 usec
Acquisition Time: 1.3631 usec
Spectrometer Frequency: 100.62 MHz
Spectral Width: 24038.5 Hz
Lowest Frequency: -1943.4
Nucleus: 13C



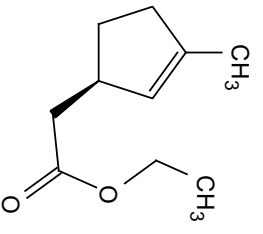
Title: JEBSS2-008-2
ACQUISITION PARAMETERS
Solvent: CDCl3
Pulse Sequence: zg30
Experiment: 1D
Number of Scans: 16
Receiver Gain: 101
Relaxation Delay: 1.0000 s
Pulse Width: 11.5000 usec
Acquisition Time: 3.2768 usec
Spectrometer Frequency: 500.16 MHz
Spectral Width: 10000.0 Hz
Lowest Frequency: -1924.3
Nucleus: 1H



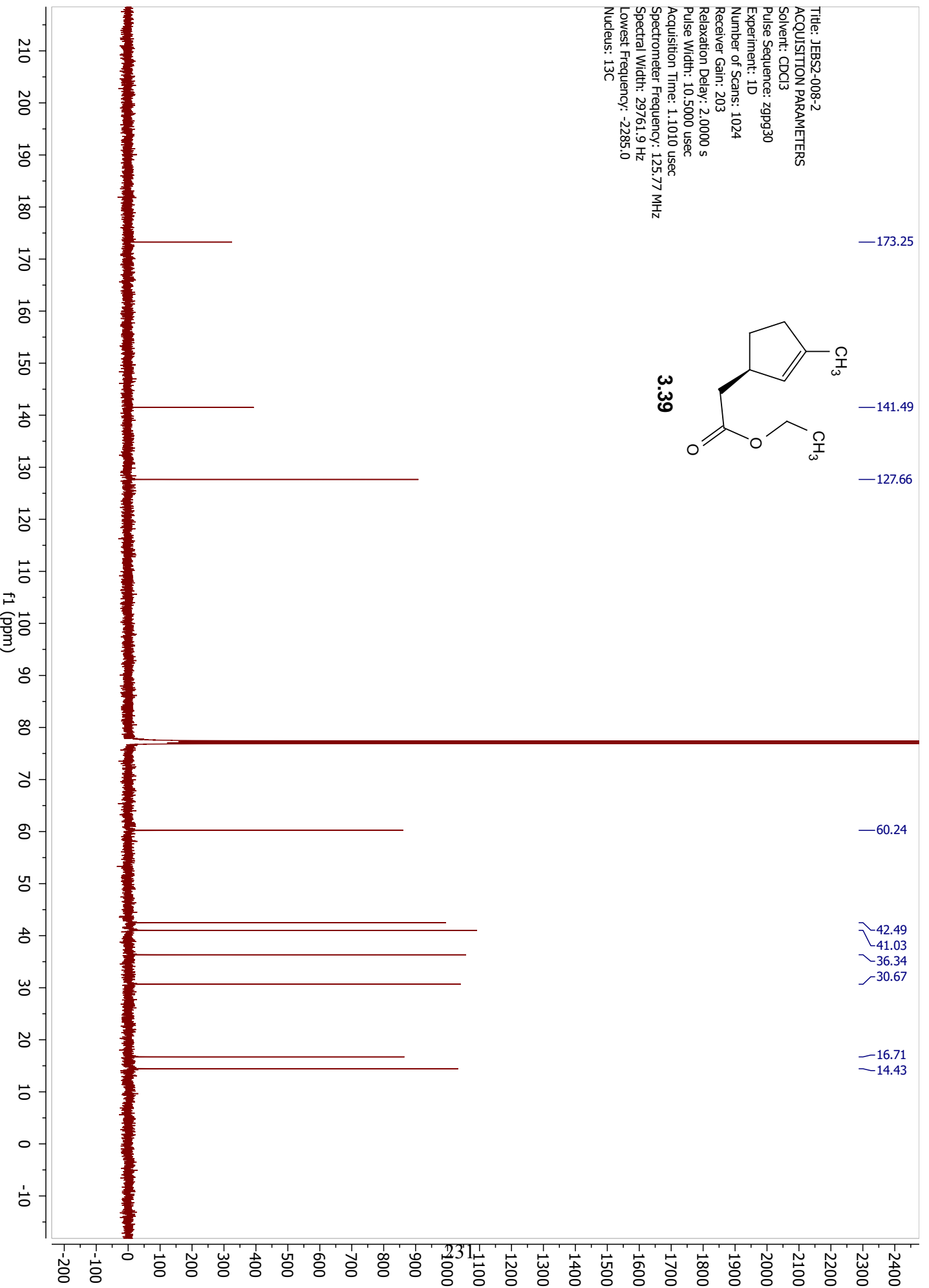
3.39



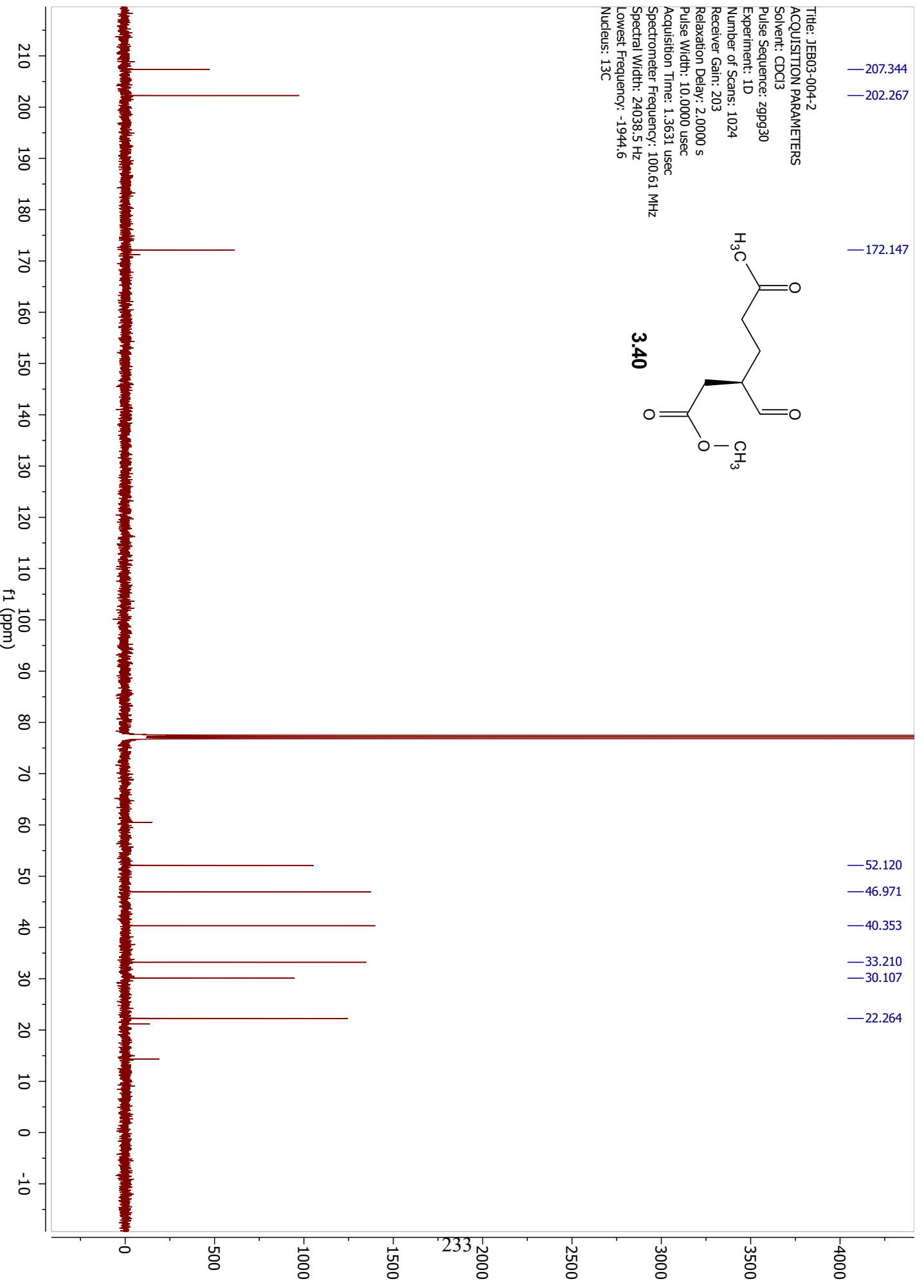
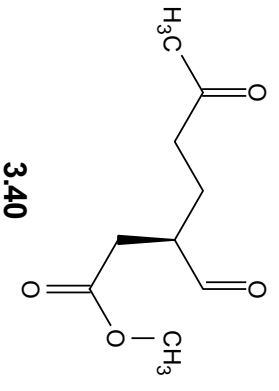
Title: JEBS2-008-2
ACQUISITION PARAMETERS
Solvent: CDCl3
Pulse Sequence: zpgp30
Experiment: 1D
Number of Scans: 1024
Receiver Gain: 203
Relaxation Delay: 2.0000 s
Pulse Width: 10.5000 usec
Acquisition Time: 1.1010 usec
Spectrometer Frequency: 125.77 MHz
Spectral Width: 29761.9 Hz
Lowest Frequency: -2285.0
Nucleus: 13C



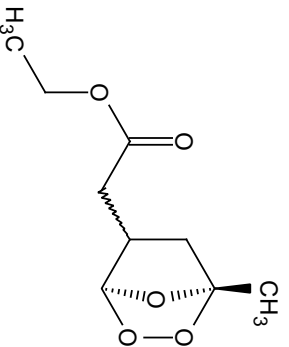
3.39



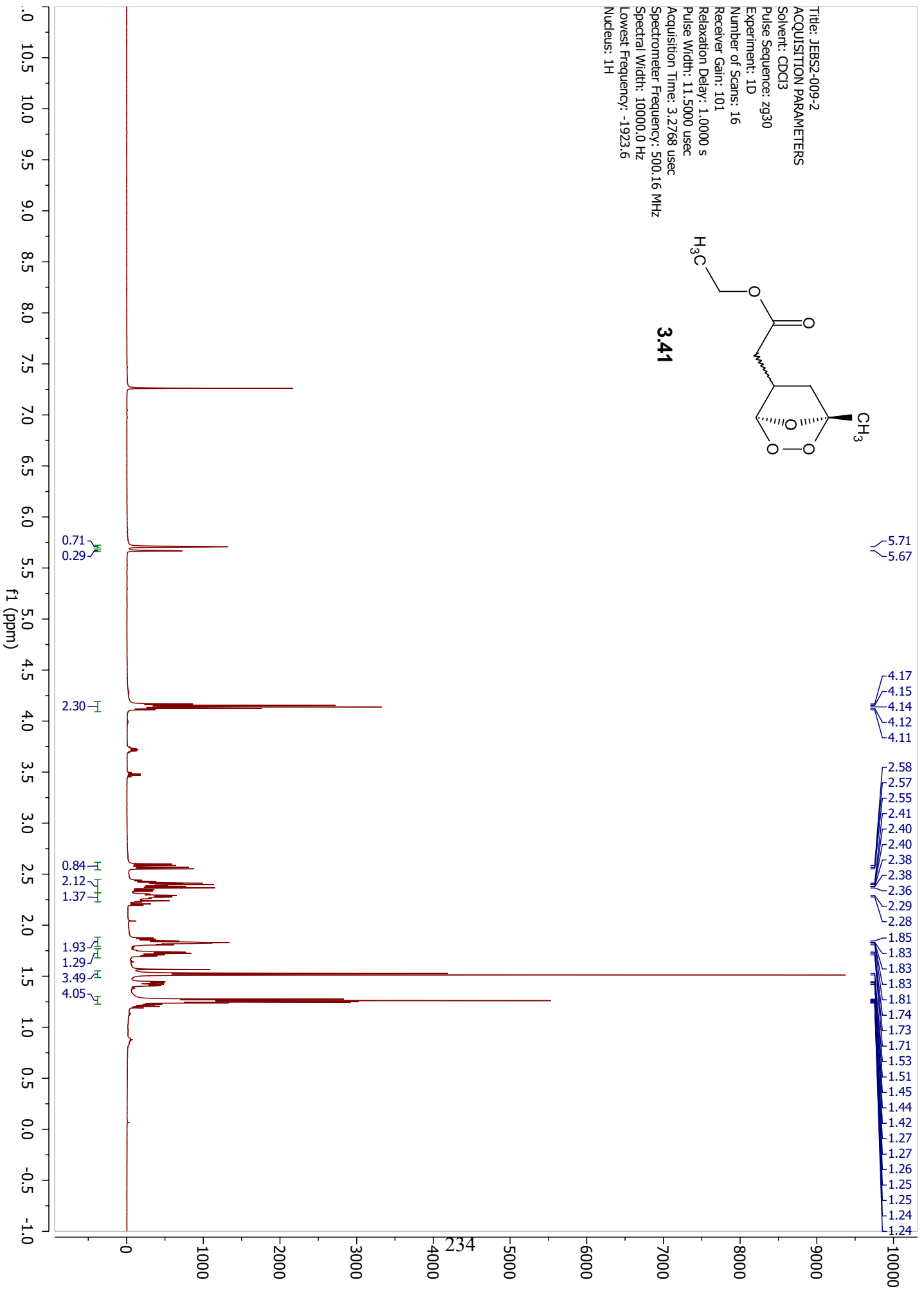
Title: JEB03-004-2
ACQUISITION PARAMETERS
Solvent: CDCl3
Pulse Sequence: zppg30
Experiment: 1D
Number of Scans: 1024
Receiver Gain: 203
Relaxation Delay: 2.0000 s
Pulse Width: 10.0000 usec
Acquisition Time: 1.3631 usec
Spectrometer Frequency: 100.61 MHz
Spectral Width: 24038.5 Hz
Lowest Frequency: -1944.6
Nucleus: 13C



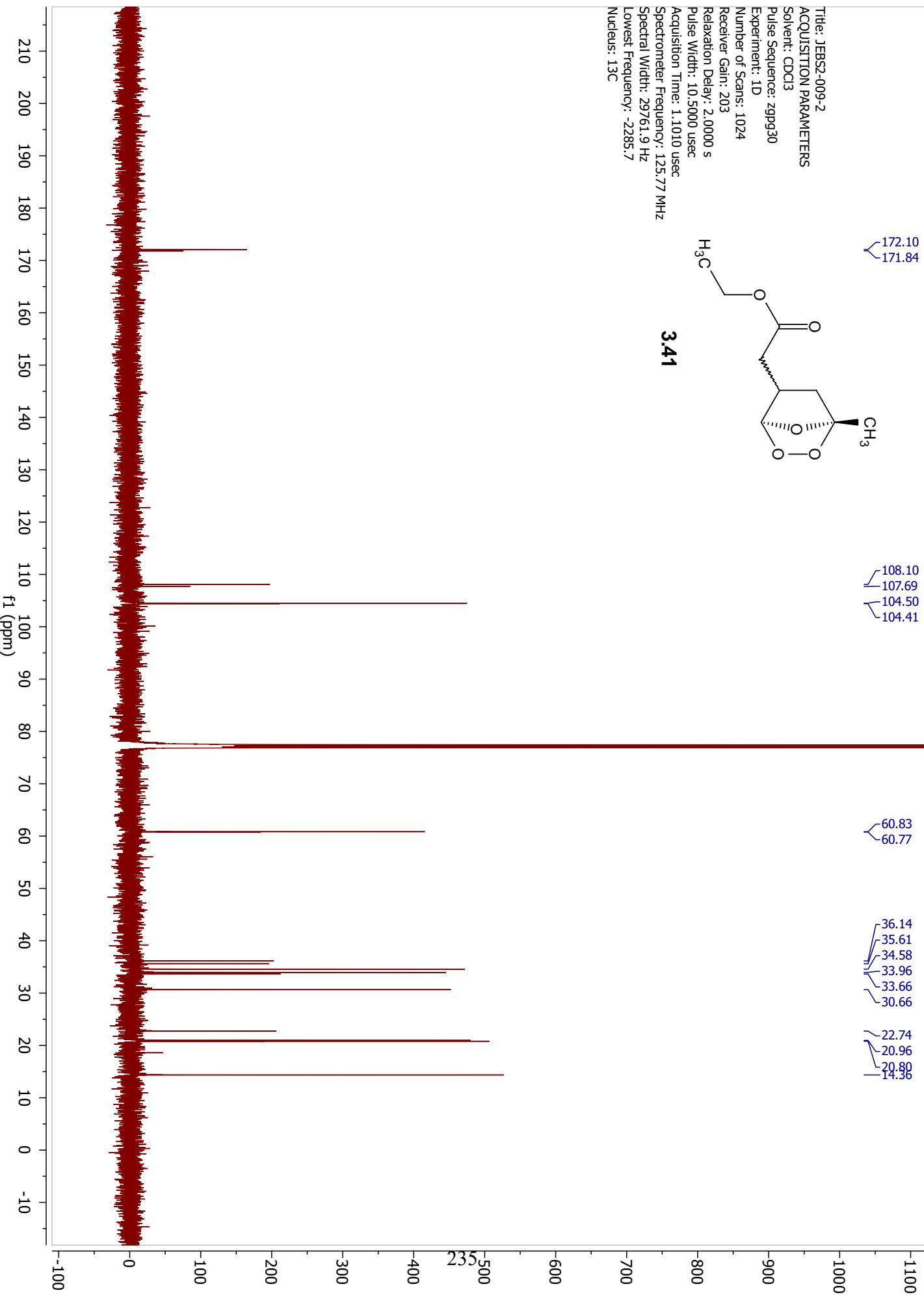
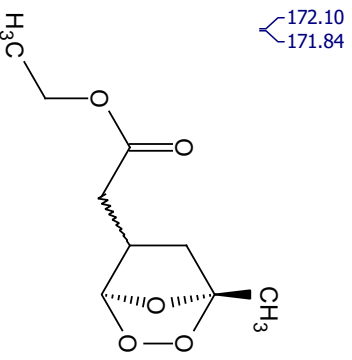
Title: JEBS2-009-2
ACQUISITION PARAMETERS
Solvent: CDCl3
Pulse Sequence: zg30
Experiment: 1D
Number of Scans: 16
Receiver Gain: 101
Relaxation Delay: 1.0000 s
Pulse Width: 11.5000 usec
Acquisition Time: 3.2768 usec
Spectrometer Frequency: 500.16 MHz
Spectral Width: 10000.0 Hz
Lowest Frequency: -1923.6
Nucleus: 1H



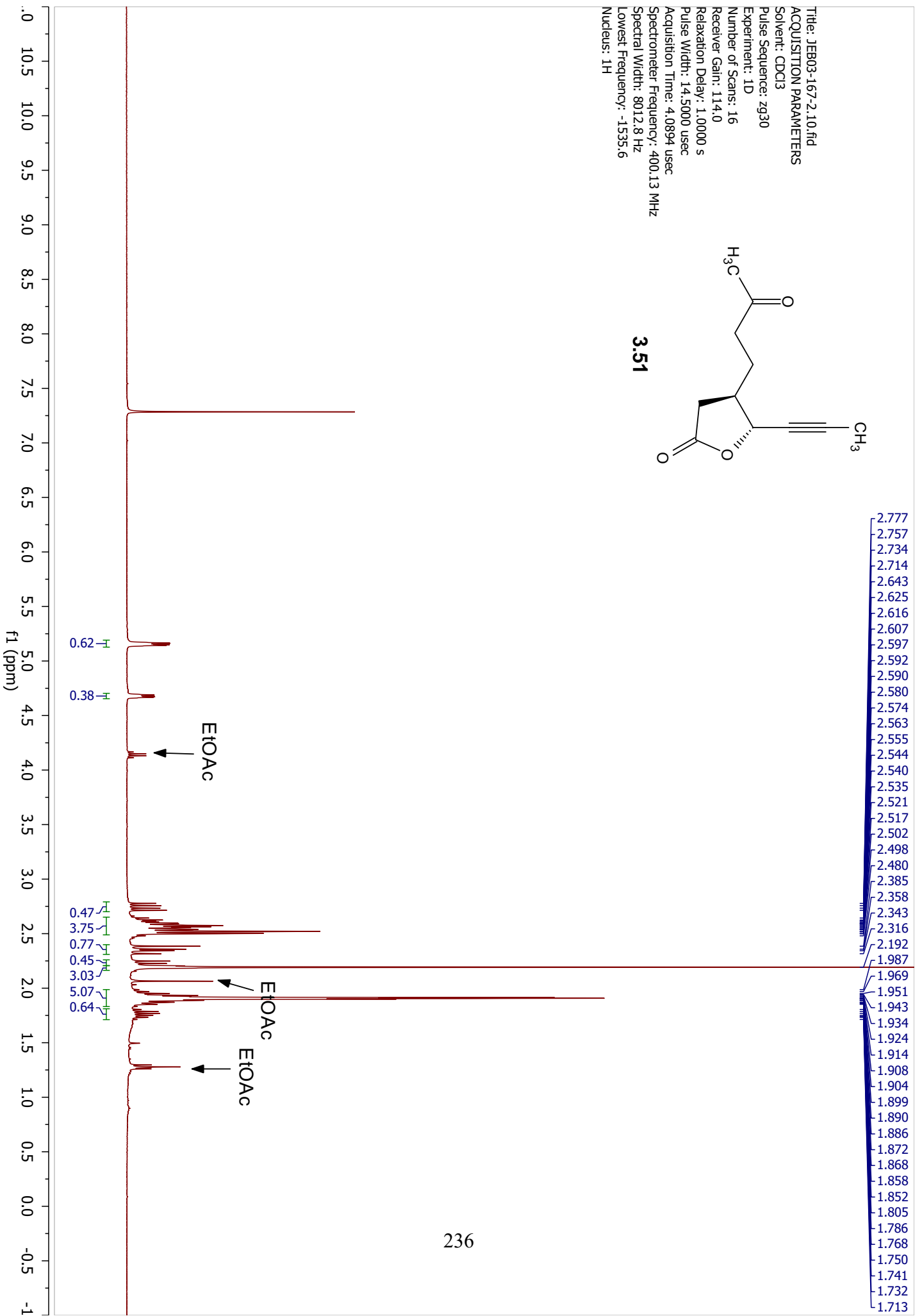
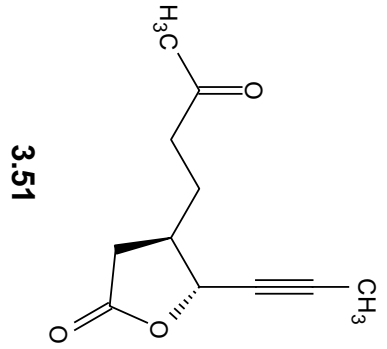
3.41



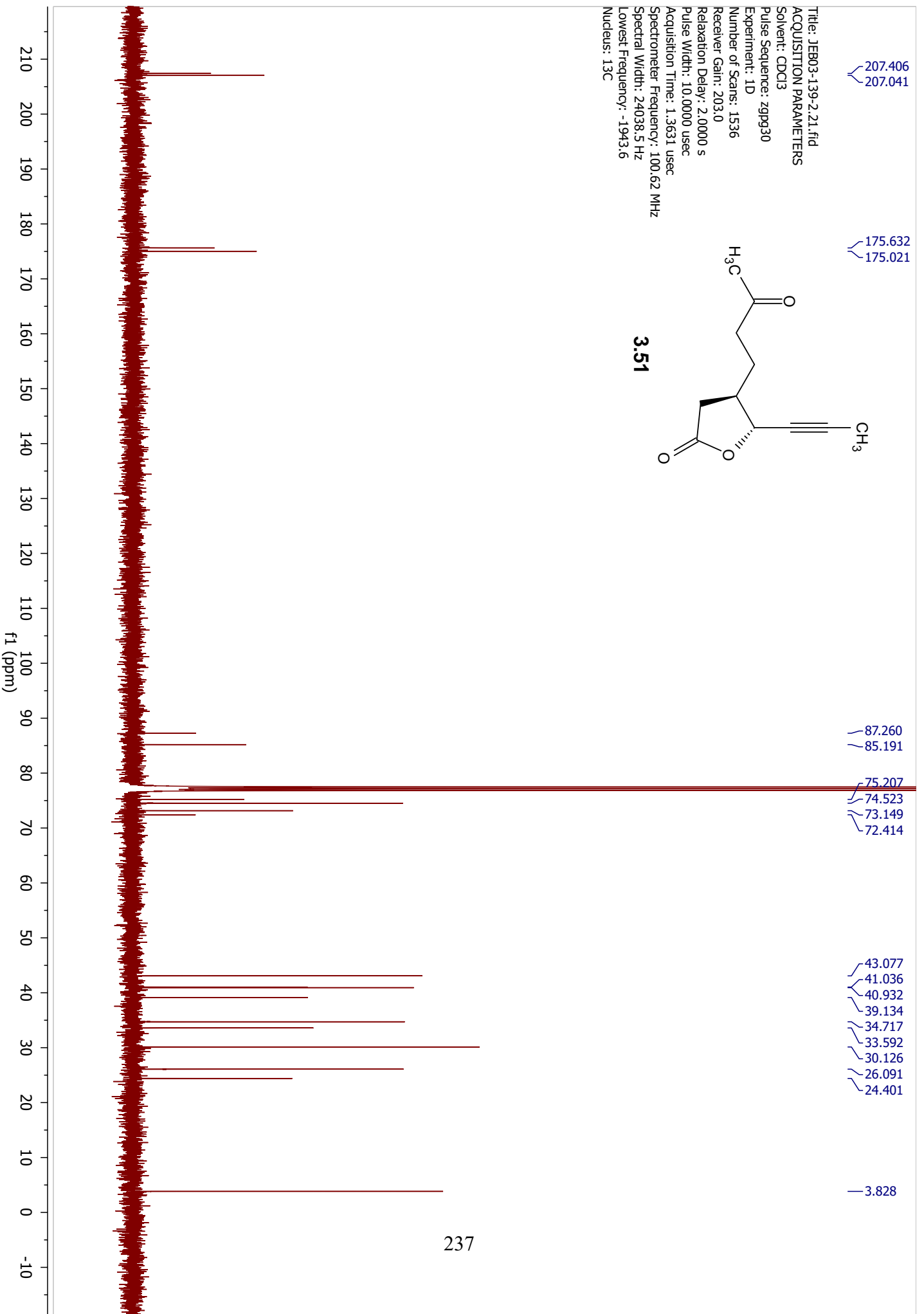
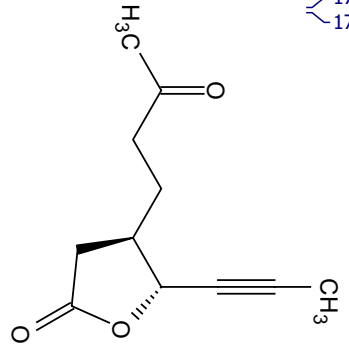
Title: JEBSS2-009-2
ACQUISITION PARAMETERS
Solvent: CDCl3
Pulse Sequence: zpgp30
Experiment: 1D
Number of Scans: 1024
Receiver Gain: 203
Relaxation Delay: 2.0000 s
Pulse Width: 10.5000 usec
Acquisition Time: 1.1010 usec
Spectrometer Frequency: 125.77 MHz
Spectral Width: 29761.9 Hz
Lowest Frequency: -2285.7
Nucleus: 13C



Title: JEB03-167-2.10.fid
ACQUISITION PARAMETERS
Solvent: CDCl3
Pulse Sequence: zg30
Experiment: 1D
Number of Scans: 16
Receiver Gain: 114.0
Relaxation Delay: 1.0000 s
Pulse Width: 14.5000 usec
Acquisition Time: 4.0894 usec
Spectrometer Frequency: 400.13 MHz
Spectral Width: 8012.8 Hz
Lowest Frequency: -1535.6
Nucleus: 1H

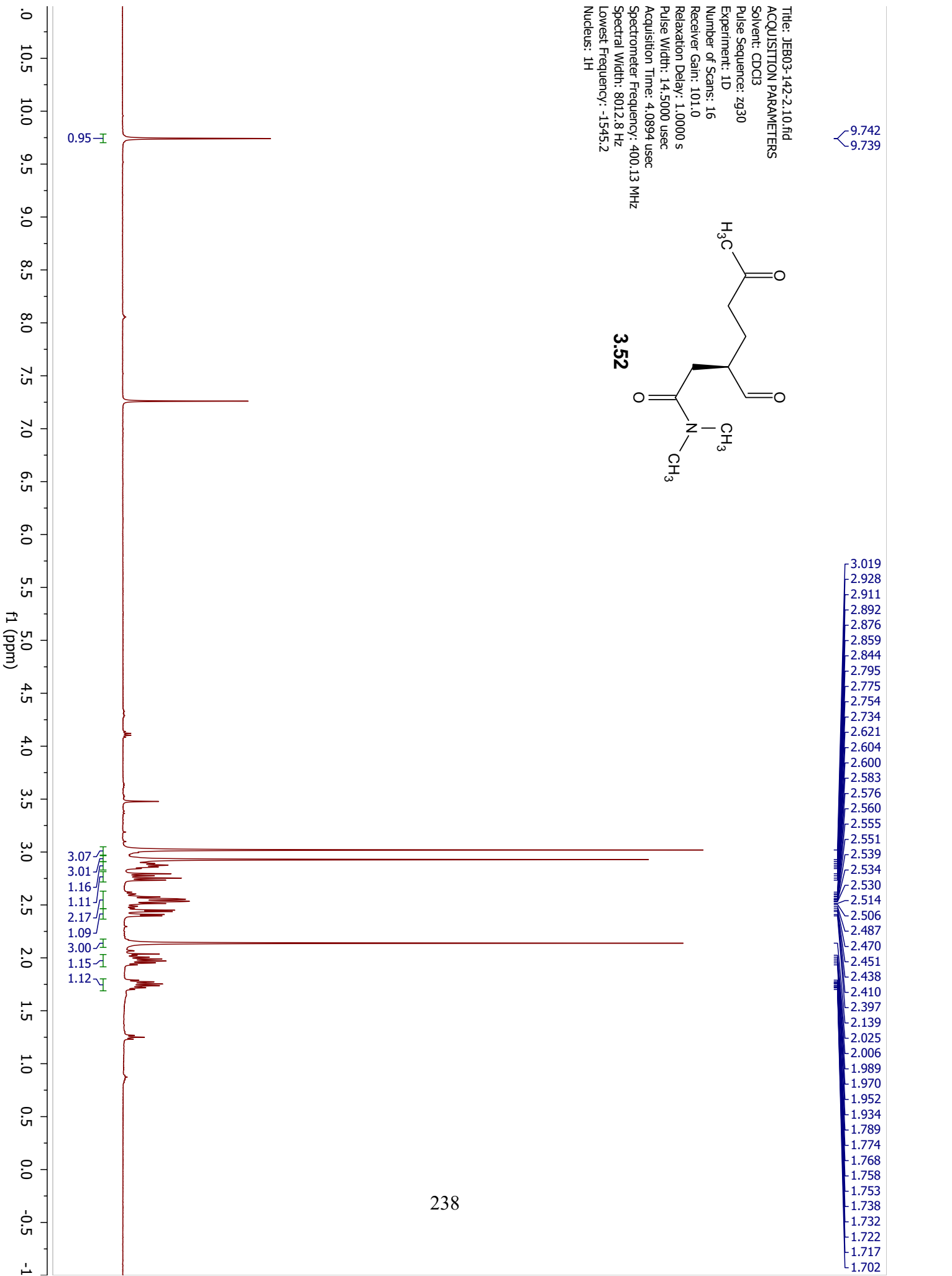
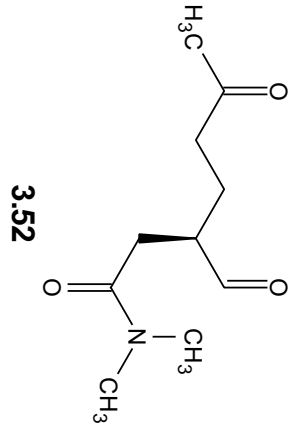


Title: JEB03-139-2.21.fid
ACQUISITION PARAMETERS
Solvent: CDCl3
Pulse Sequence: zgpg30
Experiment: 1D
Number of Scans: 1536
Receiver Gain: 203.0
Relaxation Delay: 2.0000 s
Pulse Width: 10.0000 usec
Acquisition Time: 1.3631 usec
Spectrometer Frequency: 100.62 MHz
Spectral Width: 24038.5 Hz
Lowest Frequency: -1943.6
Nucleus: 13C

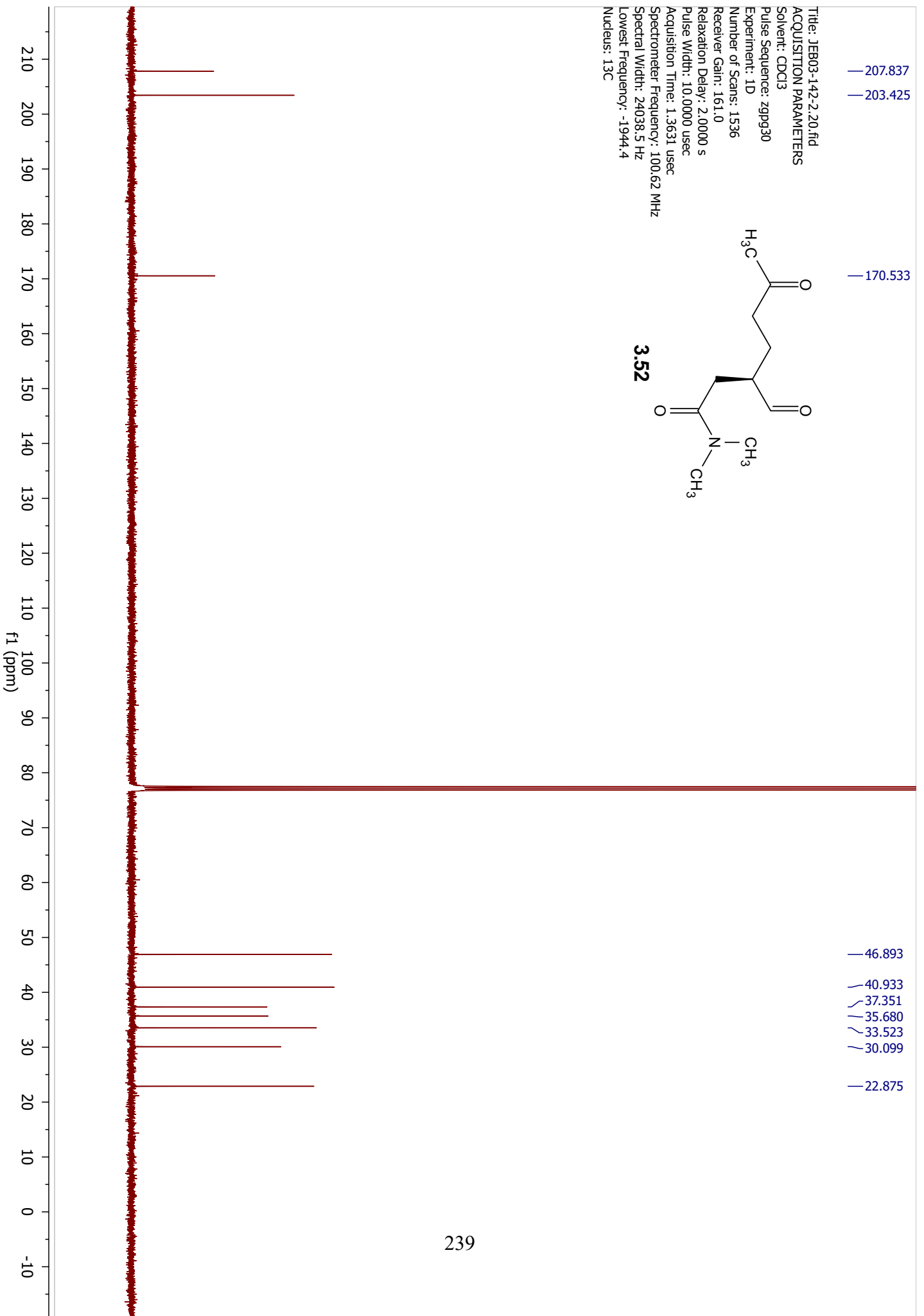
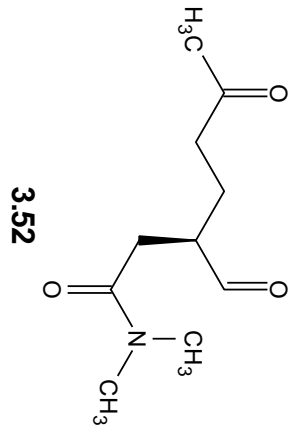


9.742
9.739

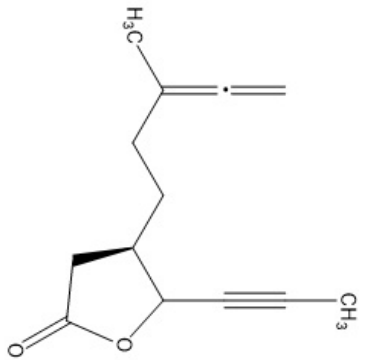
Title: JEB03-142-2.10.fid
ACQUISITION PARAMETERS
Solvent: CDCl3
Pulse Sequence: zg30
Experiment: 1D
Number of Scans: 16
Receiver Gain: 101.0
Relaxation Delay: 1.0000 s
Pulse Width: 14.5000 usec
Acquisition Time: 4.0894 usec
Spectrometer Frequency: 400.13 MHz
Spectral Width: 8012.8 Hz
Lowest Frequency: -1545.2
Nucleus: 1H



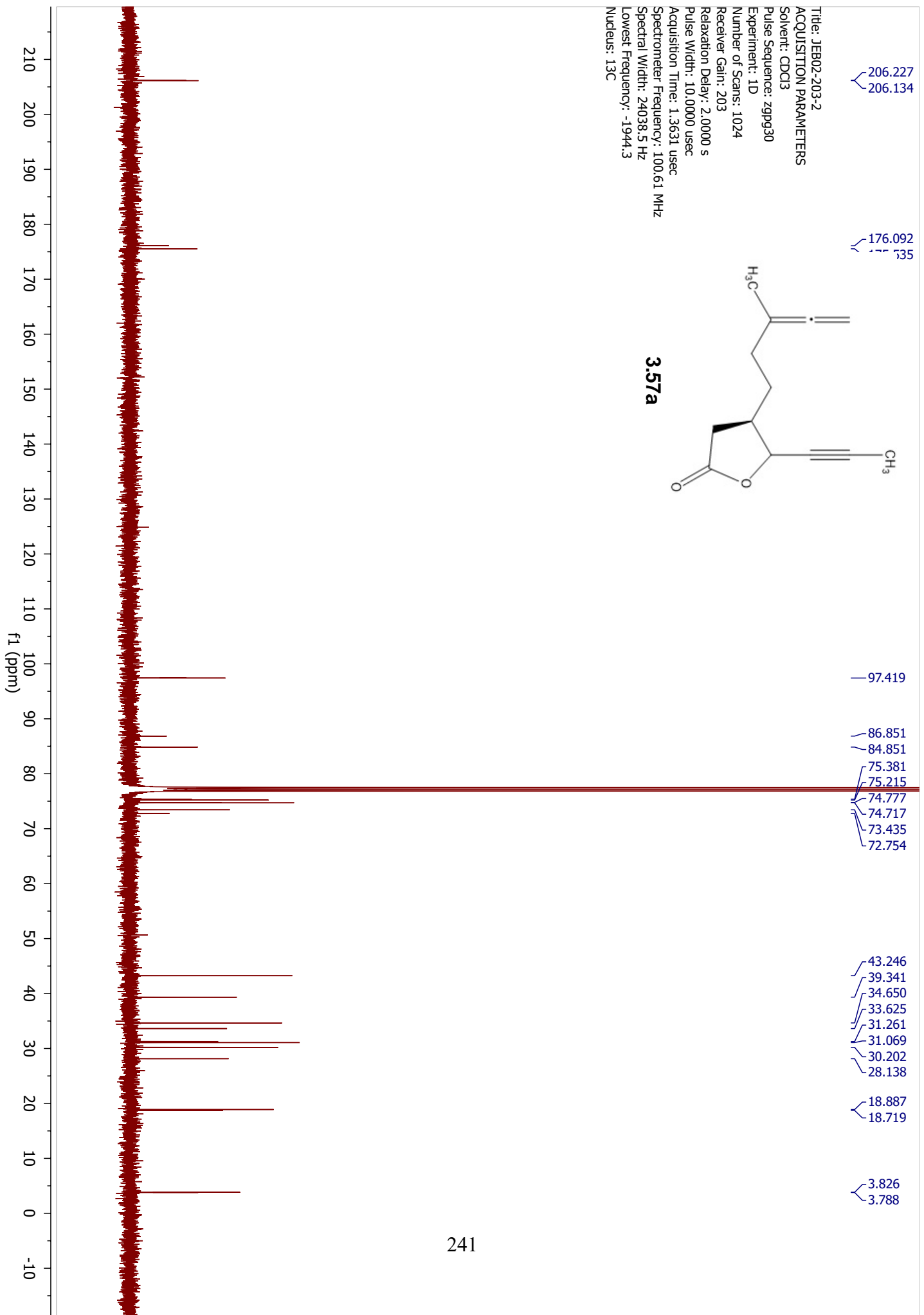
Title: JEB03-142-2.20.fid
ACQUISITION PARAMETERS
Solvent: CDCl3
Pulse Sequence: zppg30
Experiment: 1D
Number of Scans: 1536
Receiver Gain: 161.0
Relaxation Delay: 2.0000 s
Pulse Width: 10.0000 usec
Acquisition Time: 1.3631 usec
Spectrometer Frequency: 100.62 MHz
Spectral Width: 24038.5 Hz
Lowest Frequency: -1944.4
Nucleus: 13C



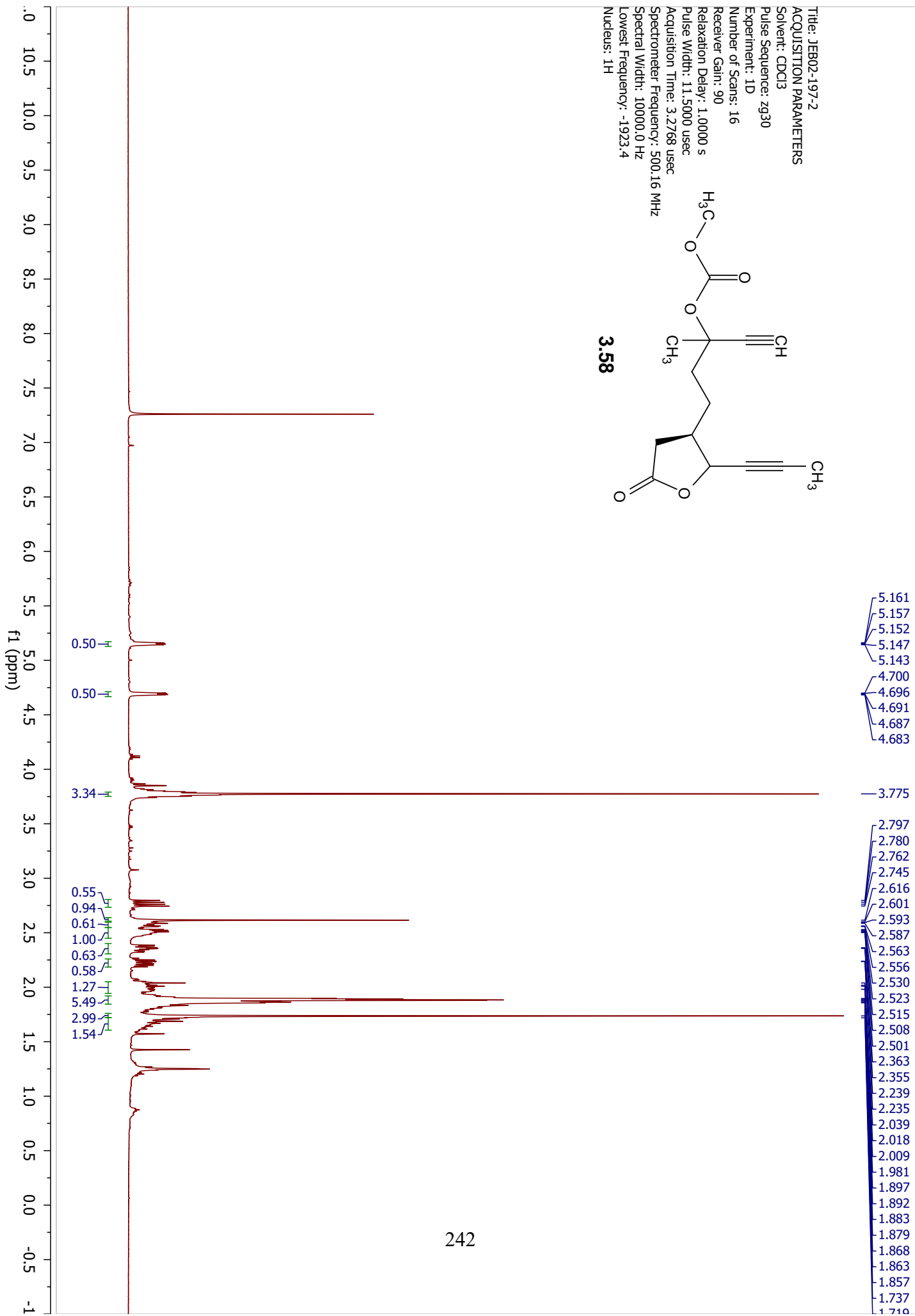
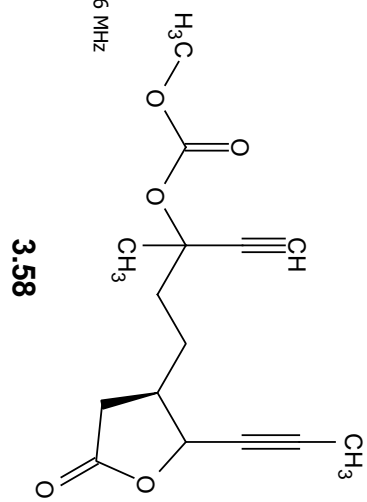
Title: JEB02-203-2
ACQUISITION PARAMETERS
Solvent: CDCl3
Pulse Sequence: zpgp30
Experiment: 1D
Number of Scans: 1024
Receiver Gain: 203
Relaxation Delay: 2.0000 s
Pulse Width: 10.0000 usec
Acquisition Time: 1.3631 usec
Spectrometer Frequency: 100.61 MHz
Spectral Width: 24038.5 Hz
Lowest Frequency: -1944.3
Nucleus: 13C



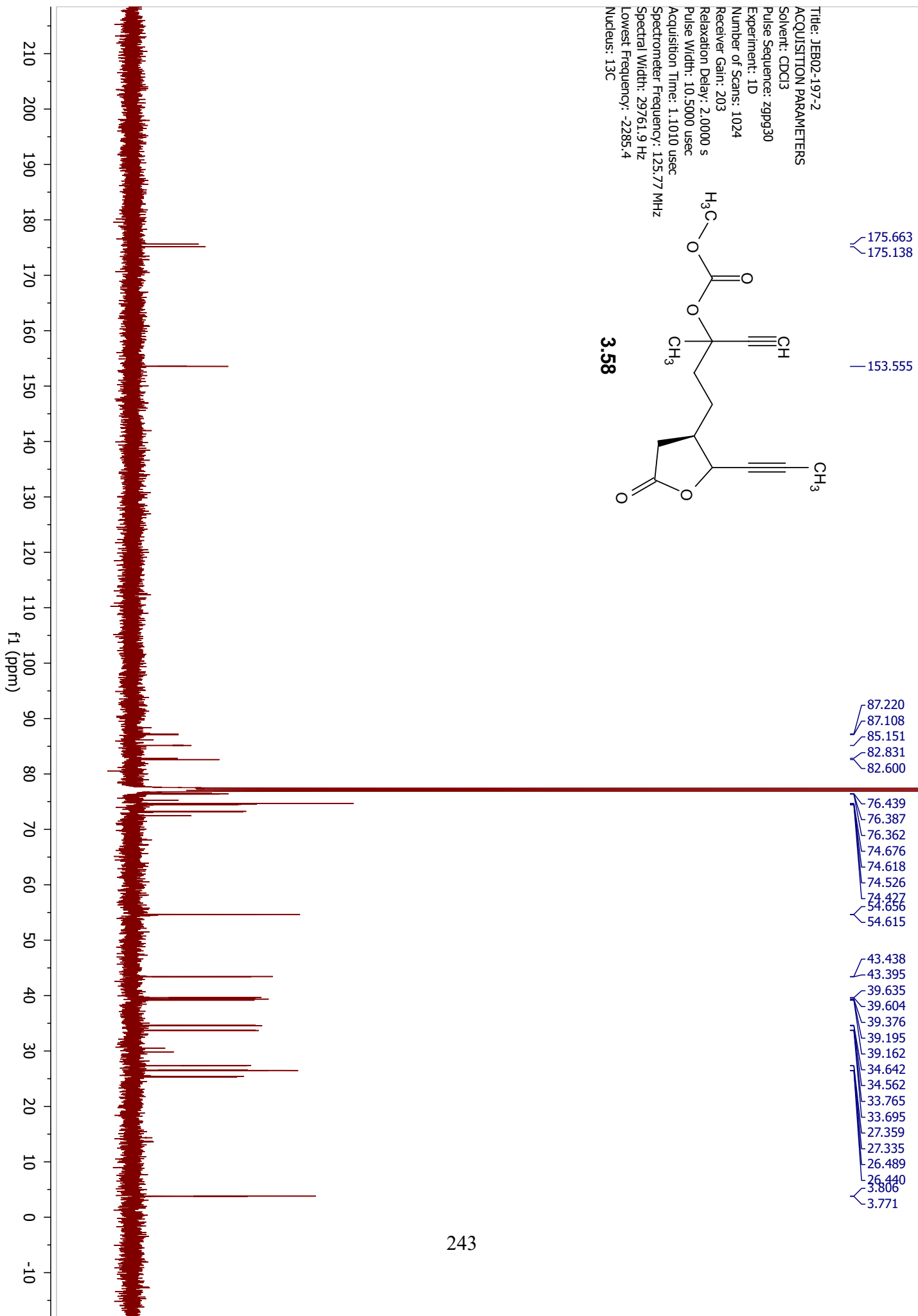
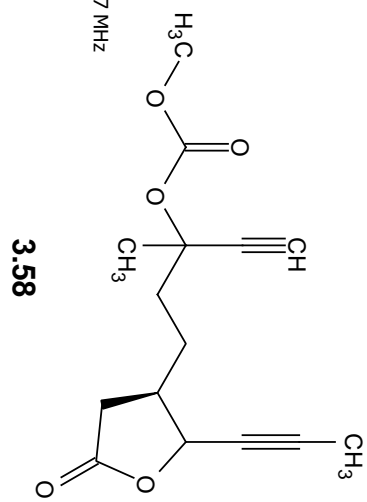
3.57a



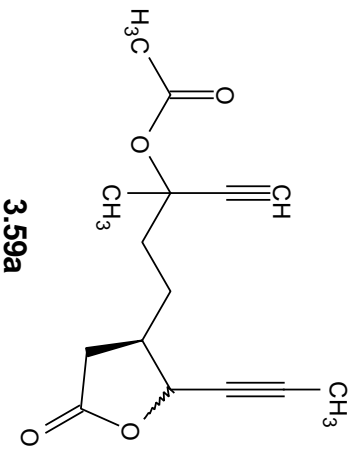
Title: JEB02-197-2
 ACQUISITION PARAMETERS
 Solvent: CDCl3
 Pulse Sequence: zg30
 Experiment: 1D
 Number of Scans: 16
 Receiver Gain: 90
 Relaxation Delay: 1.0000 s
 Pulse Width: 11.5000 usec
 Acquisition Time: 3.2768 usec
 Spectrometer Frequency: 500.16 MHz
 Spectral Width: 10000.0 Hz
 Lowest Frequency: -1923.4
 Nucleus: 1H



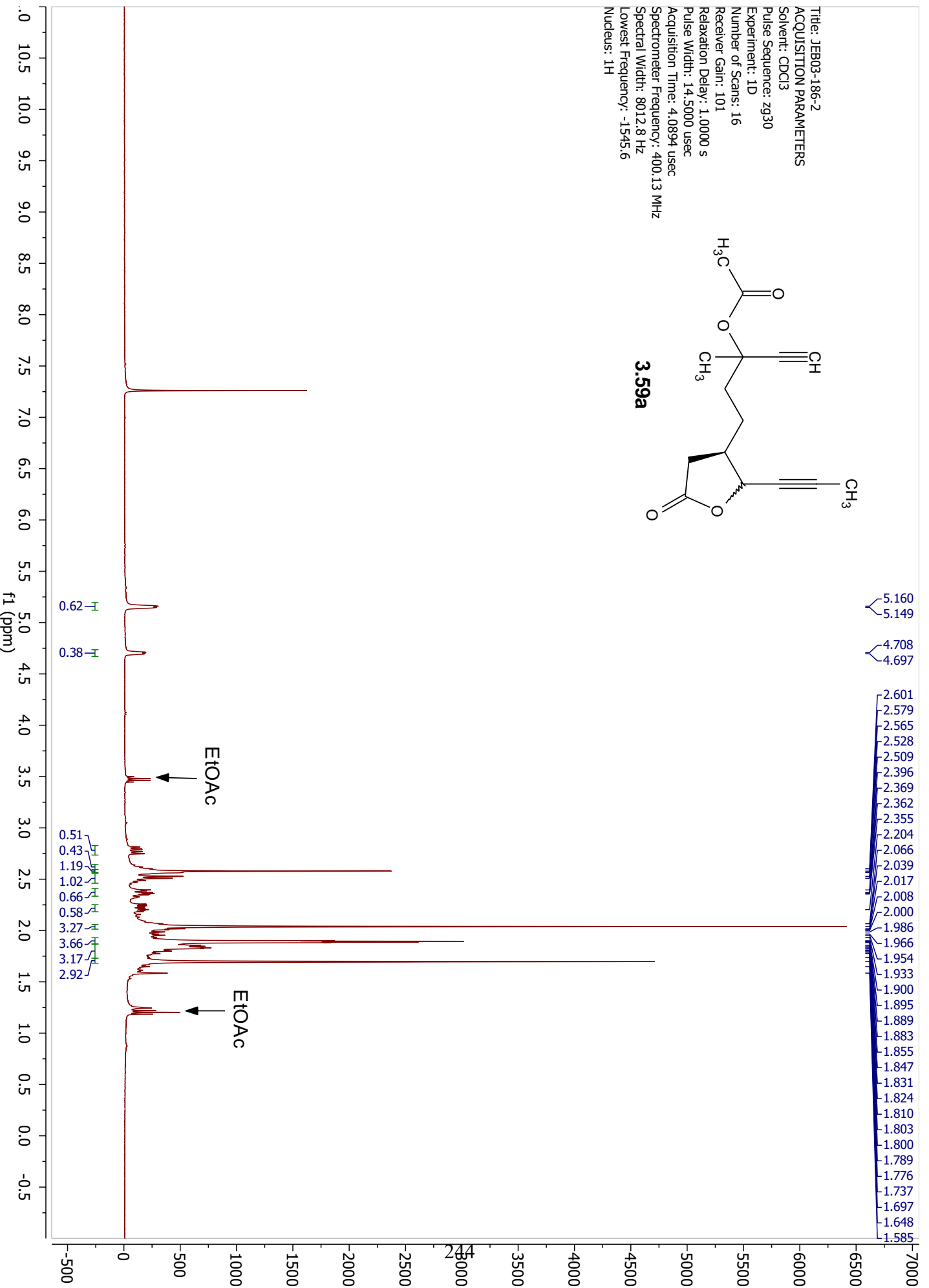
Title: JEB02-197-2
ACQUISITION PARAMETERS
Solvent: CDCl3
Pulse Sequence: zppg30
Experiment: 1D
Number of Scans: 1024
Receiver Gain: 203
Relaxation Delay: 2.0000 s
Pulse Width: 10.5000 usec
Acquisition Time: 1.1010 usec
Spectrometer Frequency: 125.77 MHz
Spectral Width: 29761.9 Hz
Lowest Frequency: -2285.4
Nucleus: 13C



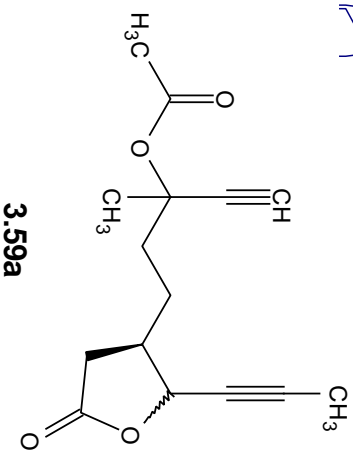
Title: JEB03-186-2
 ACQUISITION PARAMETERS
 Solvent: CDCl3
 Pulse Sequence: zg30
 Experiment: 1D
 Number of Scans: 16
 Receiver Gain: 101
 Relaxation Delay: 1.0000 s
 Pulse Width: 14.5000 usec
 Acquisition Time: 4.0894 usec
 Spectrometer Frequency: 400.13 MHz
 Spectral Width: 8012.8 Hz
 Lowest Frequency: -1545.6
 Nucleus: 1H



3.59a



Title: JEB03-186-2
ACQUISITION PARAMETERS
Solvent: CDCl3
Pulse Sequence: zpgp30
Experiment: 1D
Number of Scans: 2048
Receiver Gain: 203
Relaxation Delay: 2.0000 s
Pulse Width: 10.0000 usec
Acquisition Time: 1.3631 usec
Spectrometer Frequency: 100.61 MHz
Spectral Width: 24038.5 Hz
Lowest Frequency: -1944.8
Nucleus: 13C



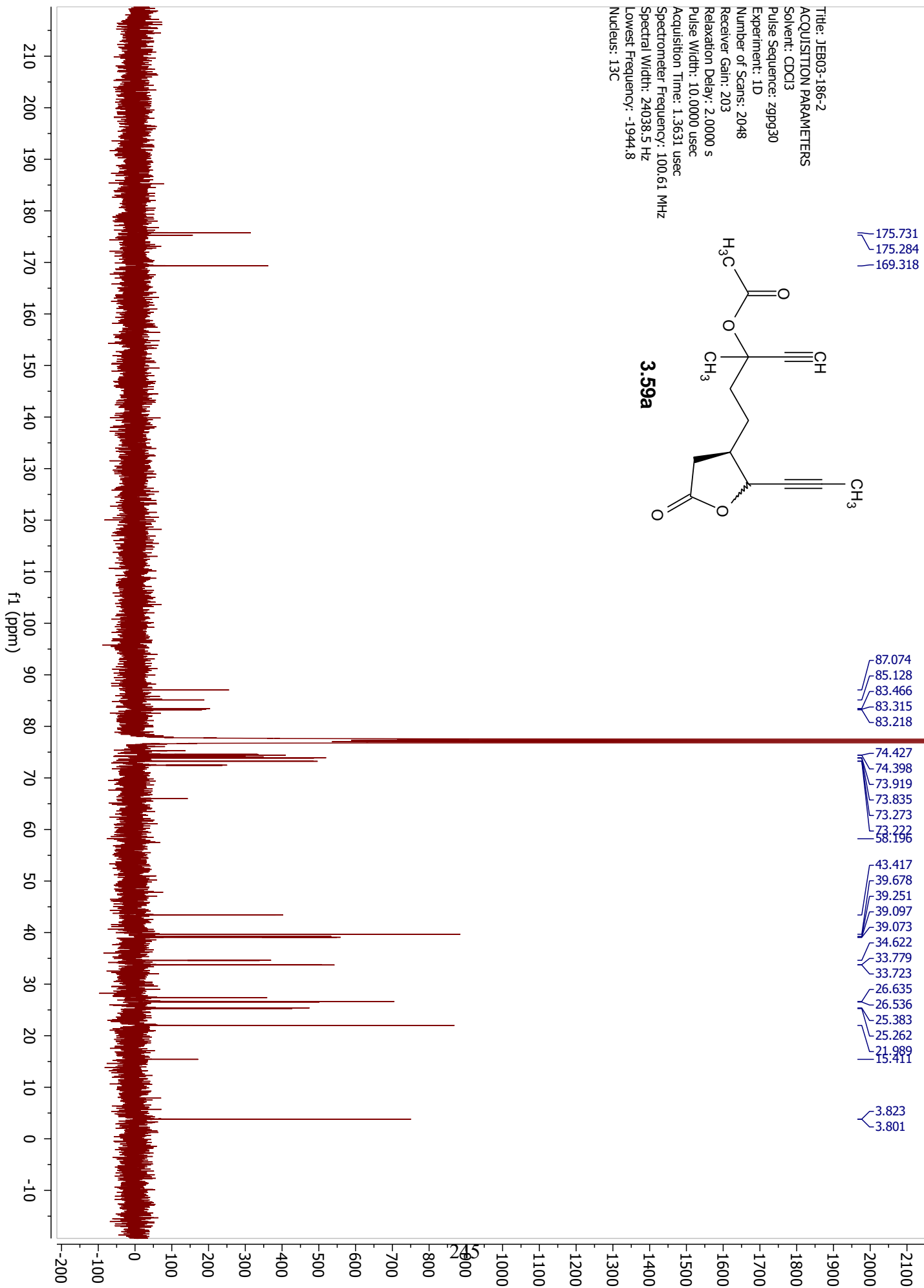
175.731
175.284
169.318

87.074
85.128
83.466
83.315
83.218

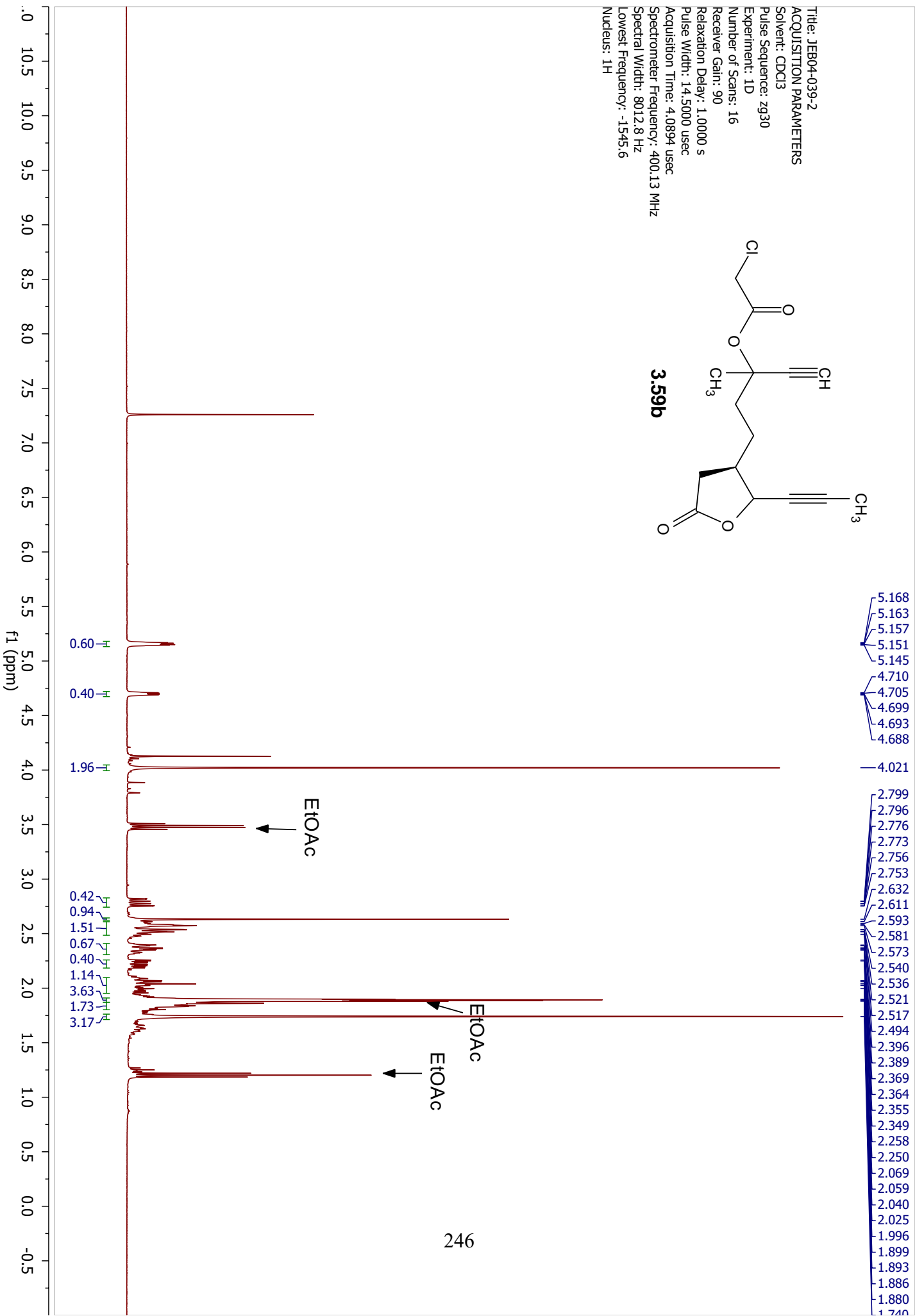
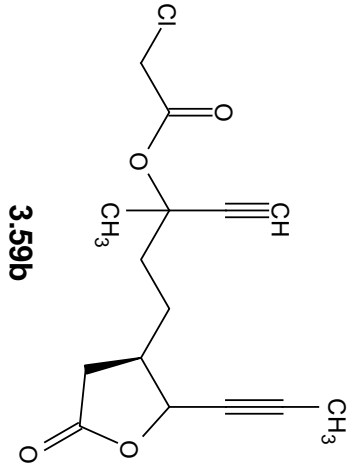
74.427
74.398
73.919
73.835
73.273
73.222
58.196

43.417
39.678
39.251
39.097
39.073
34.622
33.779
33.723
26.635
26.536
25.383
25.262
21.989
15.411

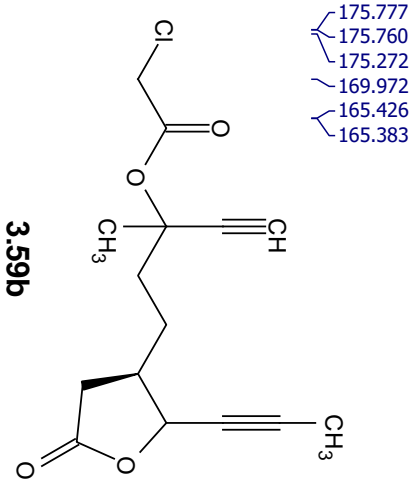
3.823
3.801



Title: JEB04-039-2
 ACQUISITION PARAMETERS
 Solvent: CDCl3
 Pulse Sequence: zg30
 Experiment: 1D
 Number of Scans: 16
 Receiver Gain: 90
 Relaxation Delay: 1.0000 s
 Pulse Width: 14.5000 usec
 Acquisition Time: 4.0894 usec
 Spectrometer Frequency: 400.13 MHz
 Spectral Width: 8012.8 Hz
 Lowest Frequency: -1545.6
 Nucleus: 1H



Title: JEB04-039-2
ACQUISITION PARAMETERS
Solvent: CDCl3
Pulse Sequence: zpgp30
Experiment: 1D
Number of Scans: 2048
Receiver Gain: 144
Relaxation Delay: 2.0000 s
Pulse Width: 10.0000 usec
Acquisition Time: 1.3631 usec
Spectrometer Frequency: 100.61 MHz
Spectral Width: 24038.5 Hz
Lowest Frequency: -1946.5
Nucleus: 13C



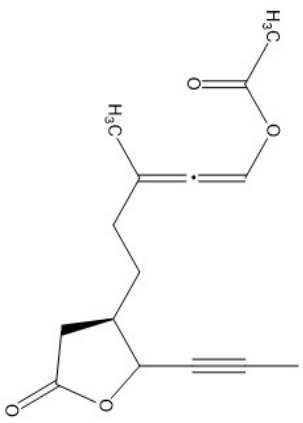
175.777
175.760
175.272
169.972
165.426
165.383

87.260
87.217
85.272
82.393
82.240
82.112
76.721
76.594
75.150
75.129
75.090
74.940
74.862
74.577
74.508
73.231
73.183
72.329

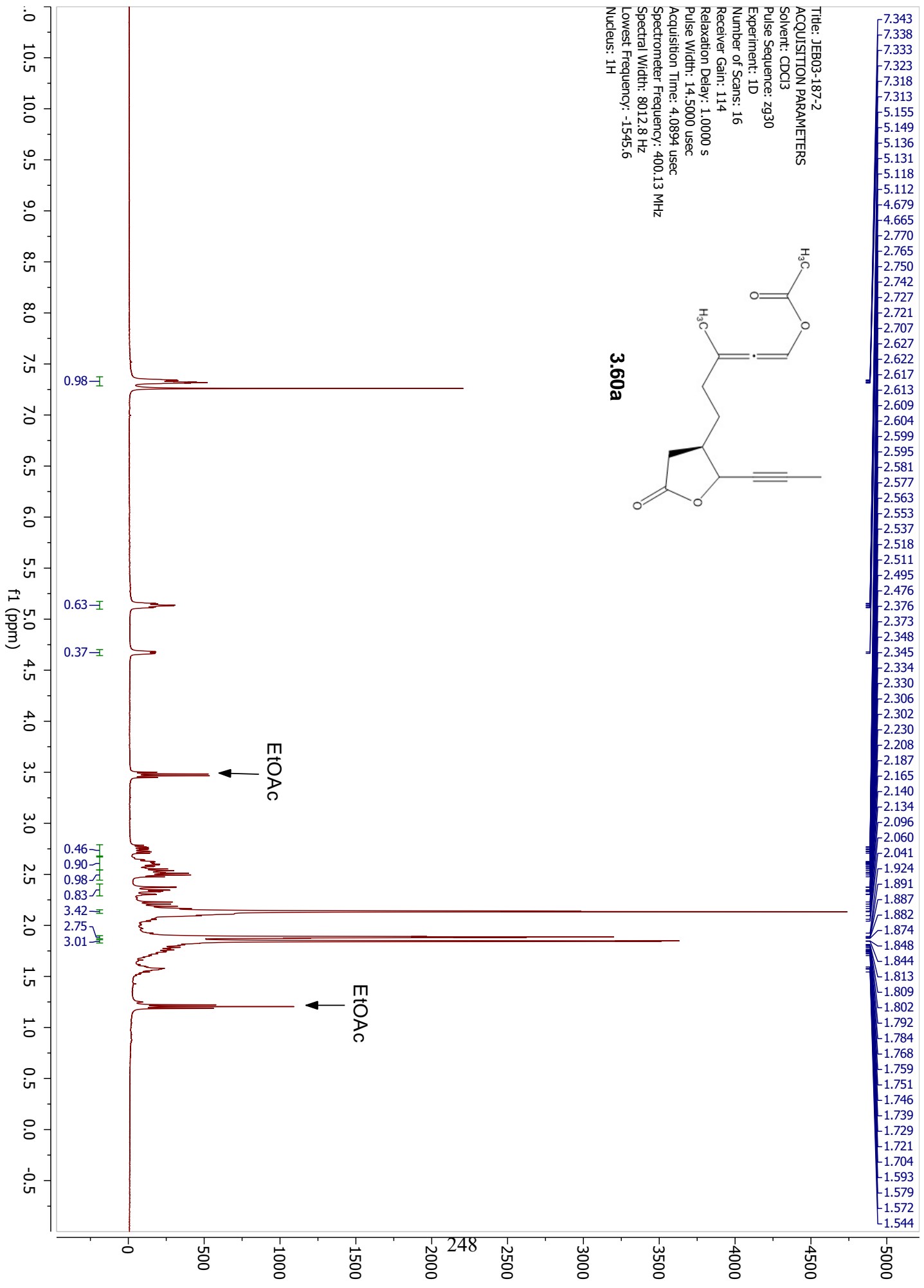
43.346
43.319
41.406
39.567
39.548
38.987
38.972
33.733
33.694
27.281
27.255
26.516
26.487
26.411
25.308
25.198



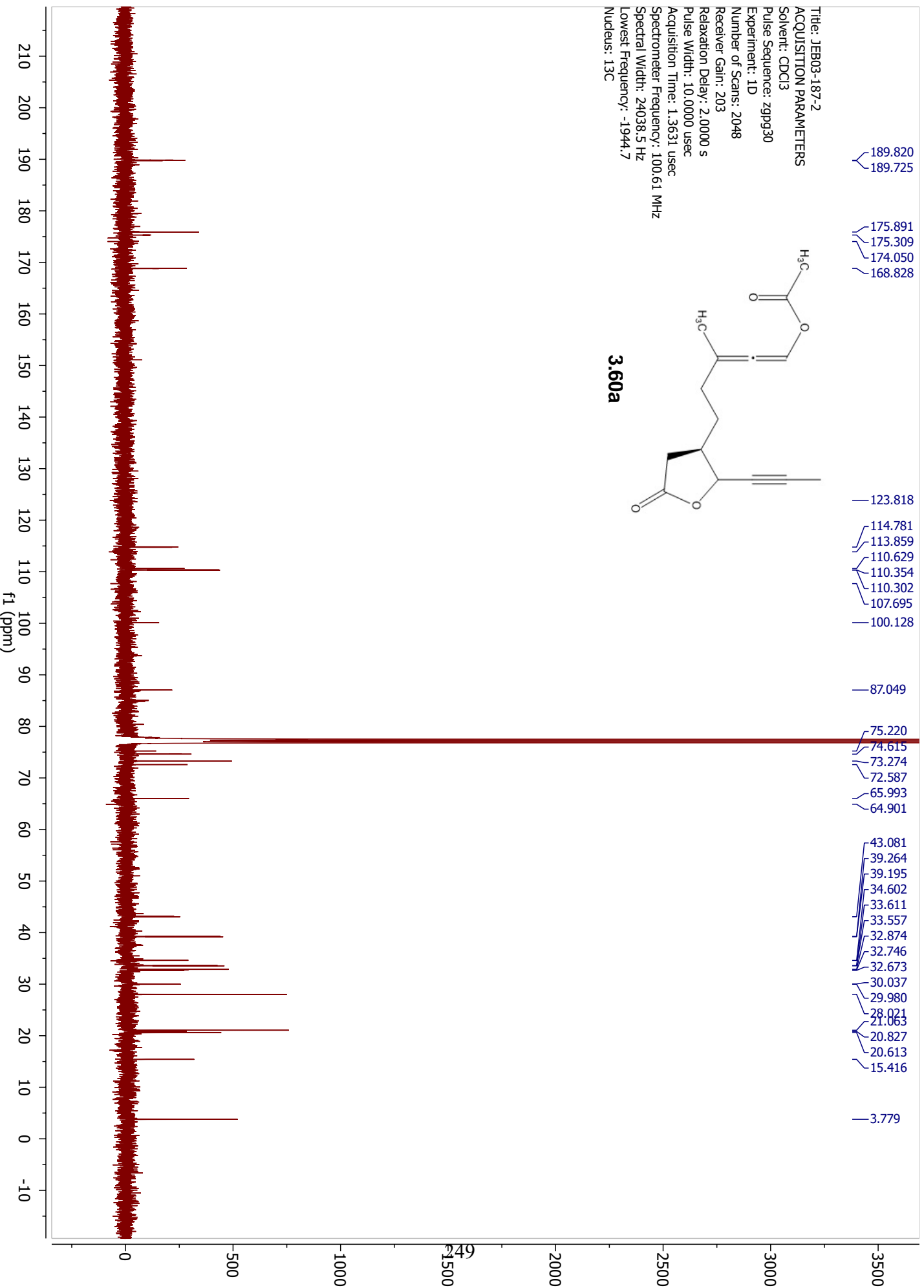
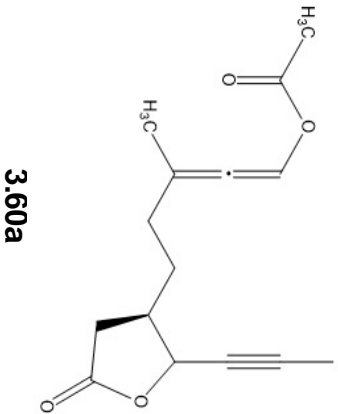
Title: JEB03-187-2
ACQUISITION PARAMETERS
Solvent: CDCl3
Pulse Sequence: zg30
Experiment: 1D
Number of Scans: 16
Receiver Gain: 114
Relaxation Delay: 1.0000 s
Pulse Width: 14.5000 usec
Acquisition Time: 4.0894 usec
Spectrometer Frequency: 400.13 MHz
Spectral Width: 8012.8 Hz
Lowest Frequency: -1545.6
Nucleus: 1H



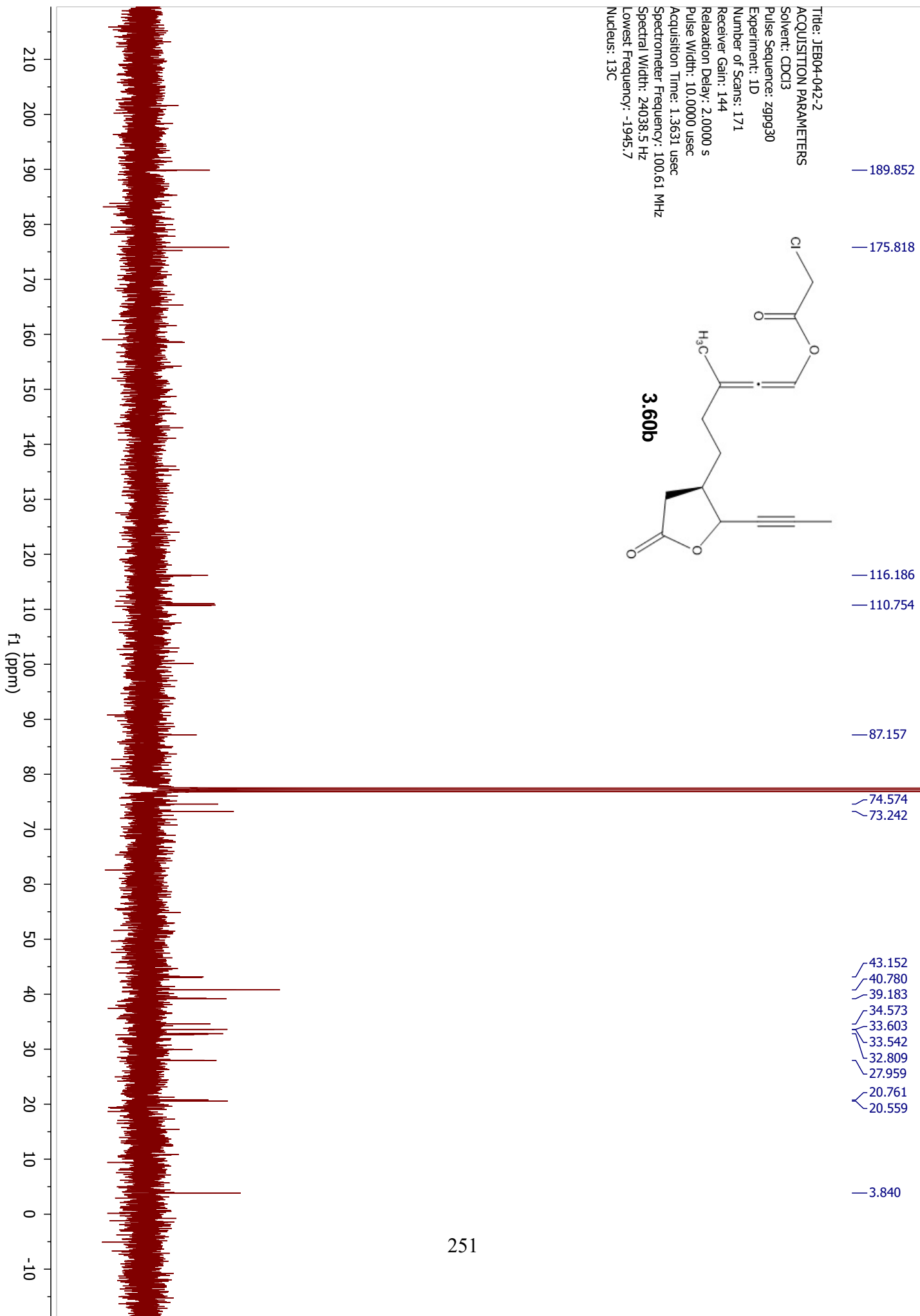
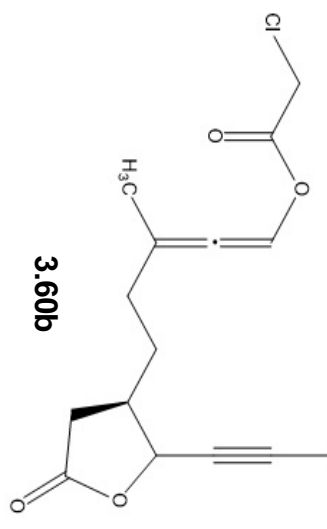
3.60a



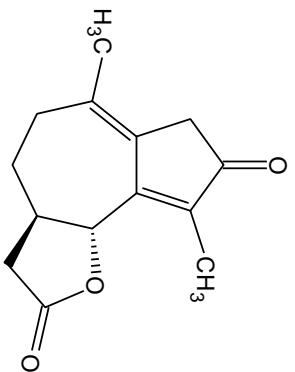
Title: JEB03-187-2
ACQUISITION PARAMETERS
Solvent: CDCl3
Pulse Sequence: zpgp30
Experiment: 1D
Number of Scans: 2048
Receiver Gain: 203
Relaxation Delay: 2.0000 s
Pulse Width: 10.0000 usec
Acquisition Time: 1.3631 usec
Spectrometer Frequency: 100.61 MHz
Spectral Width: 24038.5 Hz
Lowest Frequency: -1944.7
Nucleus: 13C



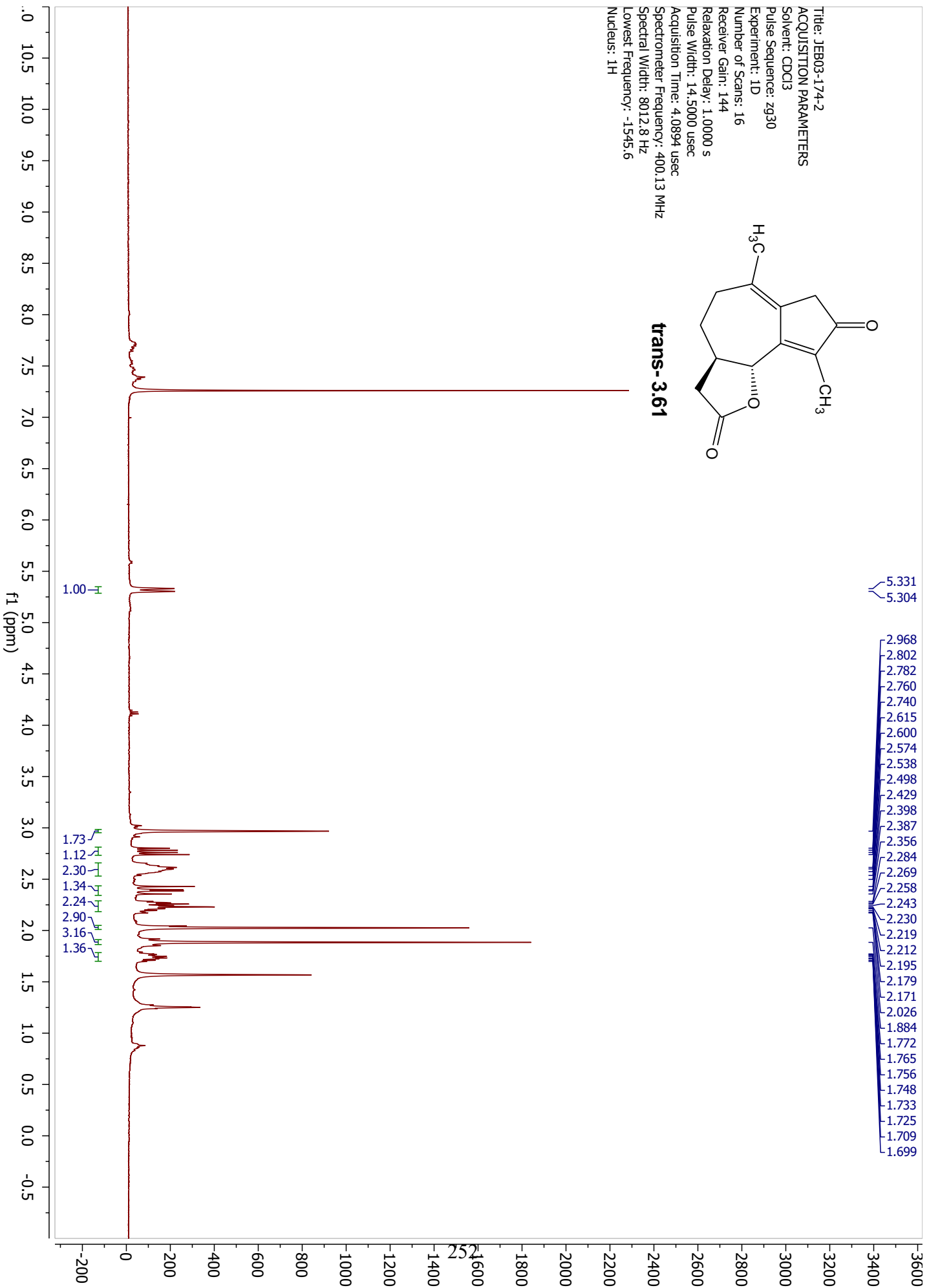
Title: JEB04-042-2
ACQUISITION PARAMETERS
Solvent: CDCl3
Pulse Sequence: zpgp30
Experiment: 1D
Number of Scans: 171
Receiver Gain: 144
Relaxation Delay: 2.0000 s
Pulse Width: 10.0000 usec
Acquisition Time: 1.3631 usec
Spectrometer Frequency: 100.61 MHz
Spectral Width: 24038.5 Hz
Lowest Frequency: -1945.7
Nucleus: 13C



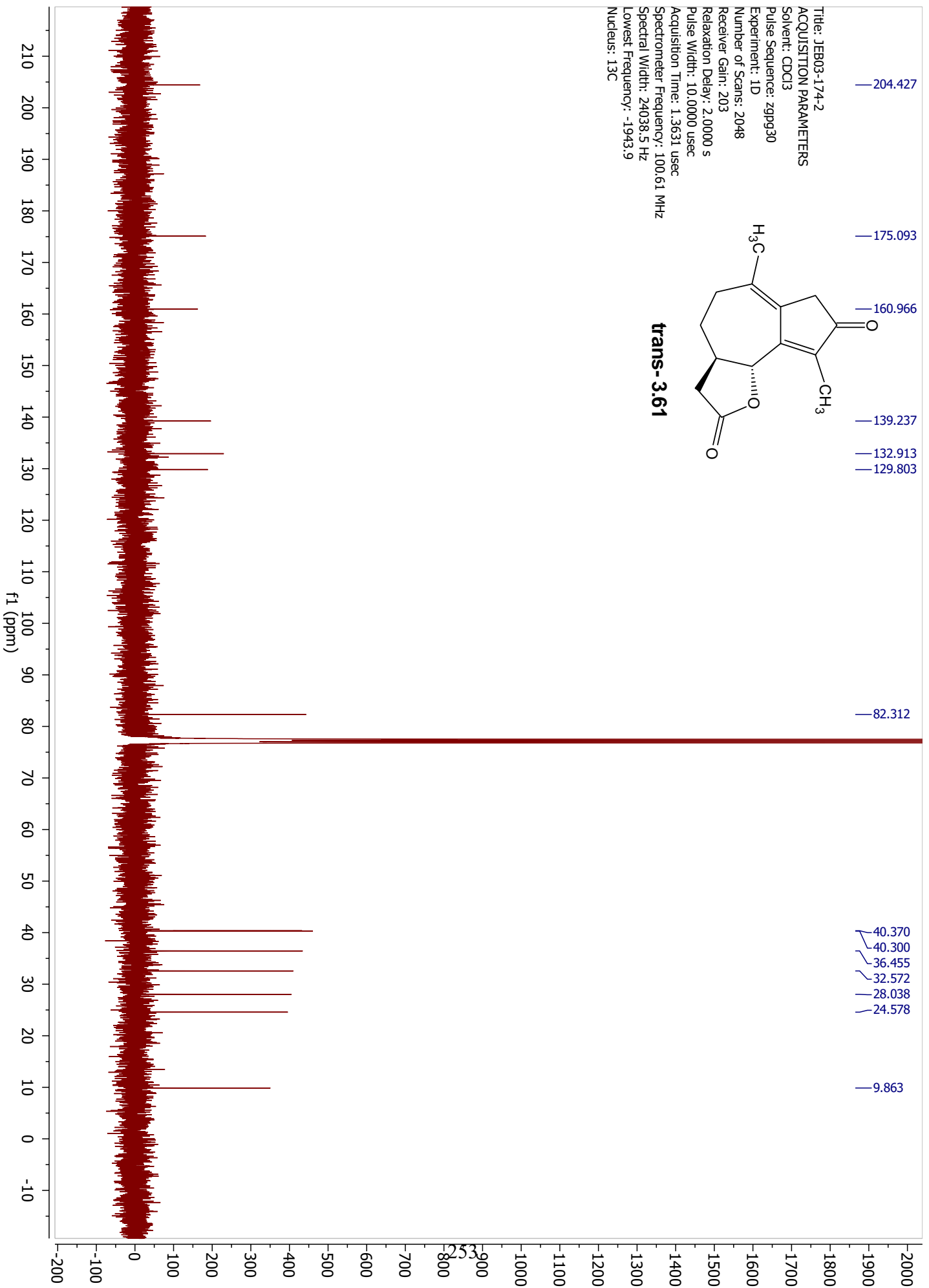
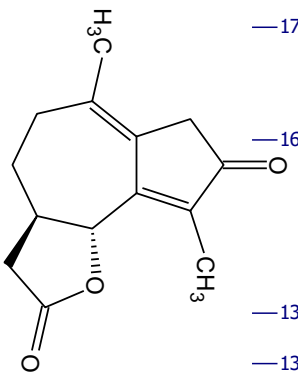
Title: JEB03-174-2
ACQUISITION PARAMETERS
Solvent: CDCl3
Pulse Sequence: zg30
Experiment: 1D
Number of Scans: 16
Receiver Gain: 144
Relaxation Delay: 1.0000 s
Pulse Width: 14.5000 usec
Acquisition Time: 4.0894 usec
Spectrometer Frequency: 400.13 MHz
Spectral Width: 8012.8 Hz
Lowest Frequency: -1545.6
Nucleus: 1H



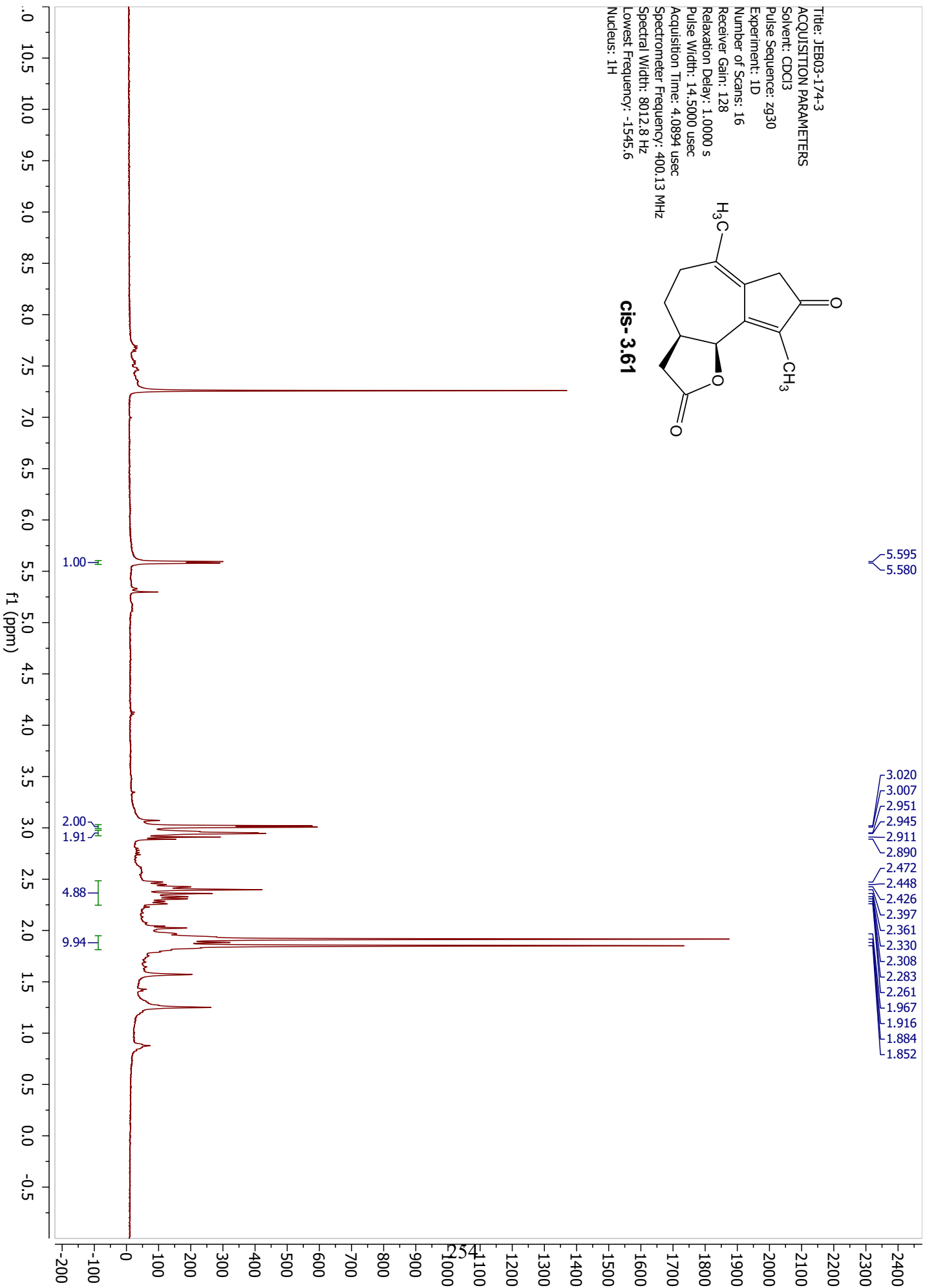
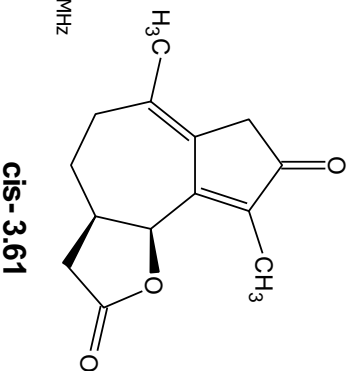
trans-3,6,1



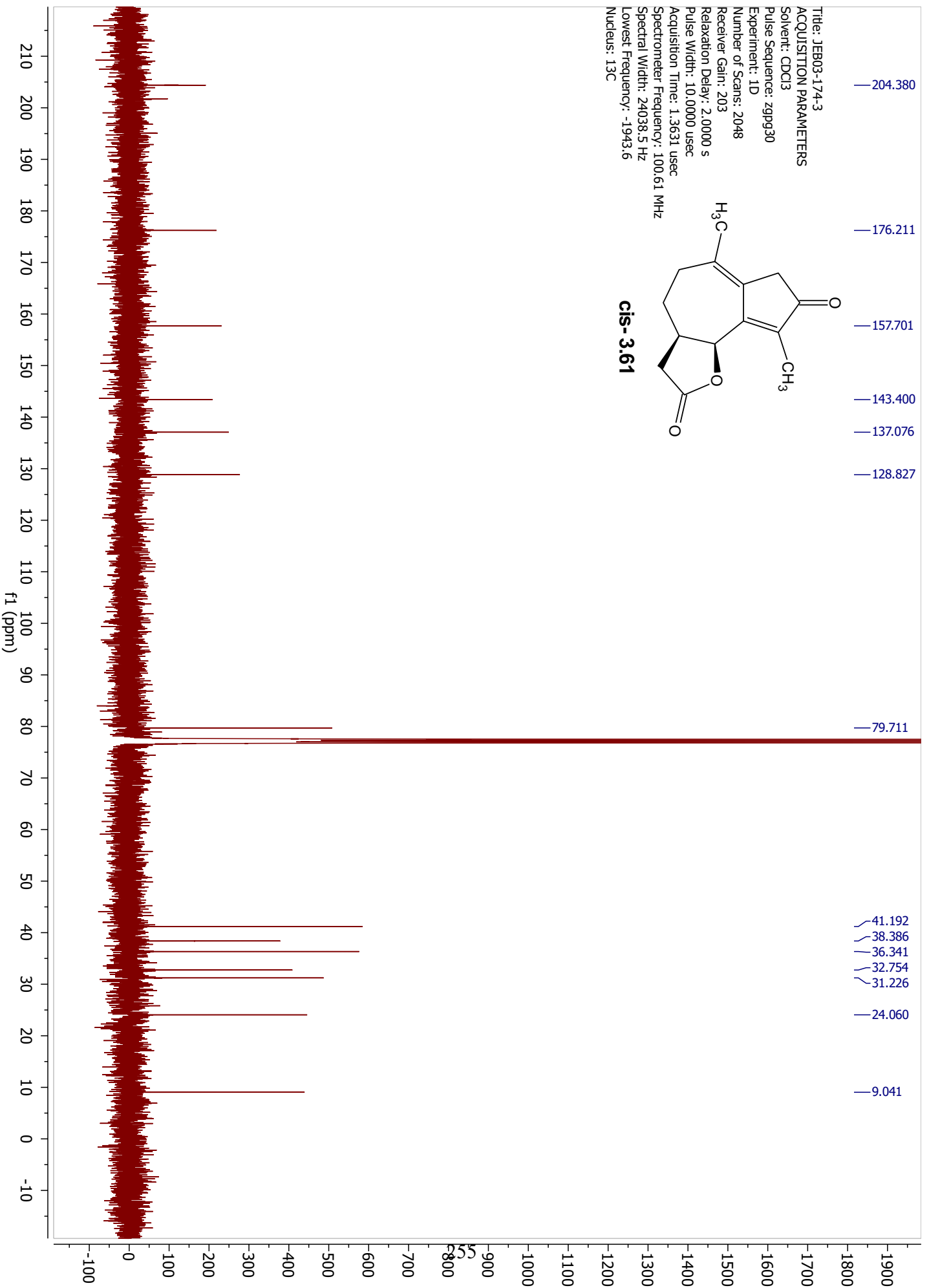
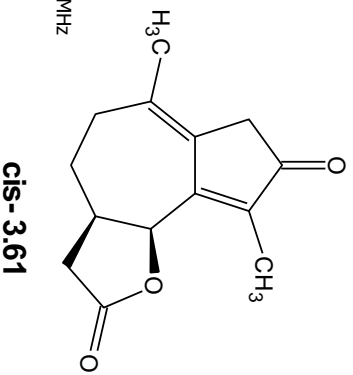
Title: JEB03-174-2
ACQUISITION PARAMETERS
Solvent: CDCl3
Pulse Sequence: zppg30
Experiment: 1D
Number of Scans: 2048
Receiver Gain: 203
Relaxation Delay: 2.0000 s
Pulse Width: 10.0000 usec
Acquisition Time: 1.3631 usec
Spectrometer Frequency: 100.61 MHz
Spectral Width: 24038.5 Hz
Lowest Frequency: -1943.9
Nucleus: 13C



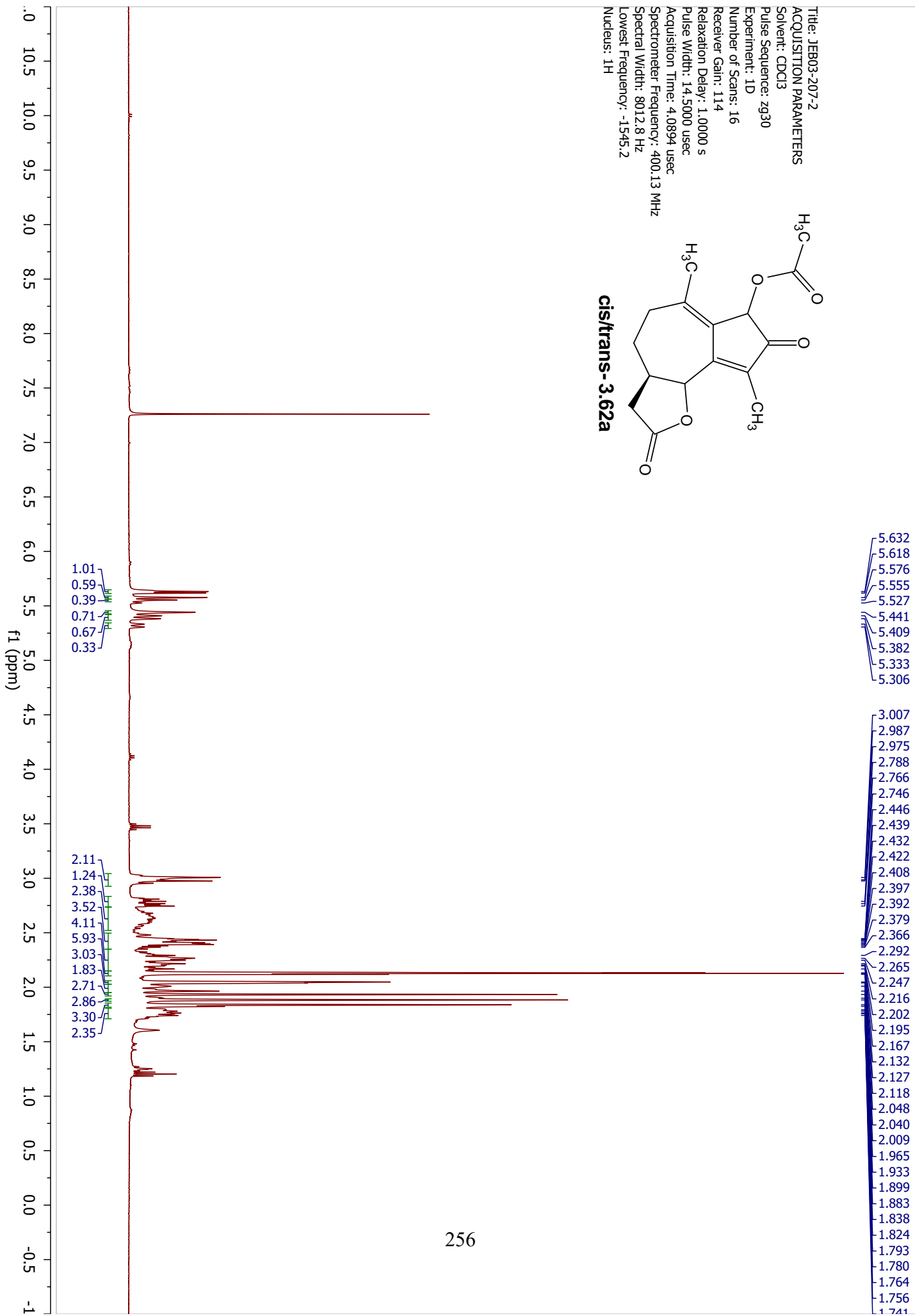
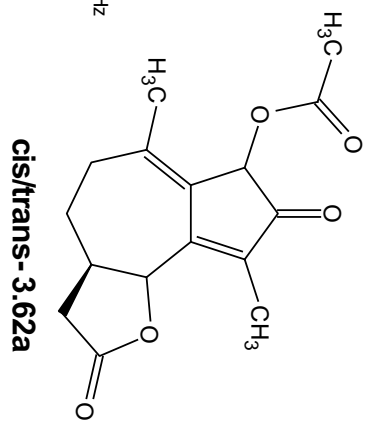
Title: JEB03-174-3
ACQUISITION PARAMETERS
Solvent: CDCl3
Pulse Sequence: zg30
Experiment: 1D
Number of Scans: 16
Relaxation Delay: 1.0000 s
Pulse Width: 14.5000 usec
Acquisition Time: 4.0894 usec
Spectrometer Frequency: 400.13 MHz
Spectral Width: 8012.8 Hz
Lowest Frequency: -1545.6
Nucleus: 1H



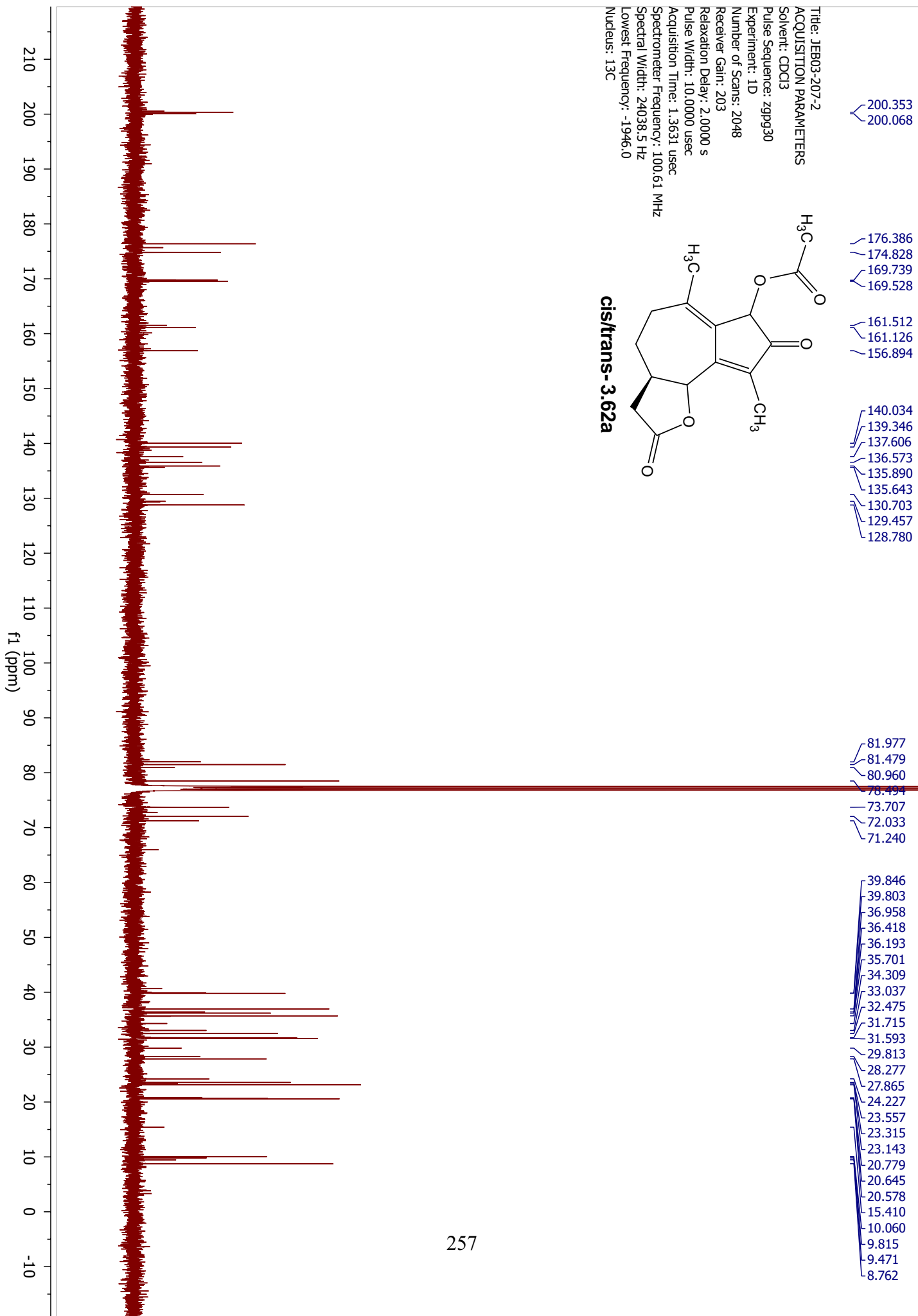
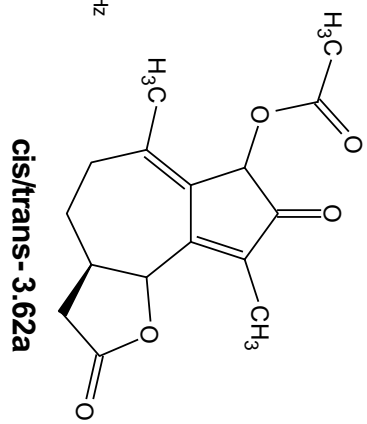
Title: JEB03-174-3
ACQUISITION PARAMETERS
Solvent: CDCl3
Pulse Sequence: zppg30
Experiment: 1D
Number of Scans: 2048
Receiver Gain: 203
Relaxation Delay: 2.0000 s
Pulse Width: 10.0000 usec
Acquisition Time: 1.3631 usec
Spectrometer Frequency: 100.61 MHz
Spectral Width: 24038.5 Hz
Lowest Frequency: -1943.6
Nucleus: 13C



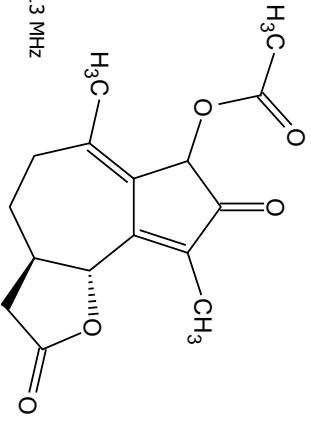
Title: JEB03-207-2
ACQUISITION PARAMETERS
Solvent: CDCl3
Pulse Sequence: zg30
Experiment: 1D
Number of Scans: 16
Receiver Gain: 114
Relaxation Delay: 1.0000 s
Pulse Width: 14.5000 usec
Acquisition Time: 4.0894 usec
Spectrometer Frequency: 400.13 MHz
Spectral Width: 8012.8 Hz
Lowest Frequency: -1545.2
Nucleus: 1H



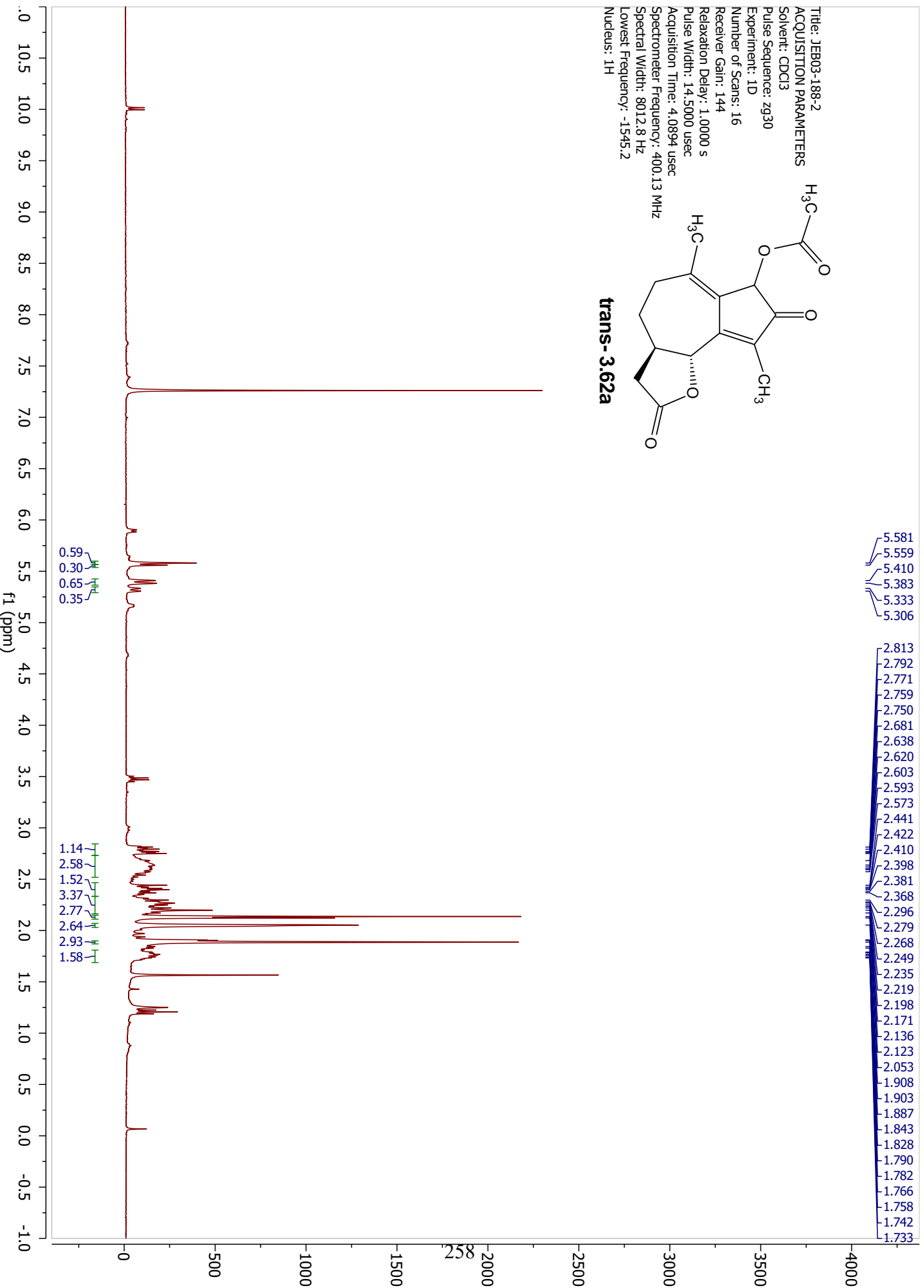
Title: JEB03-207-2
ACQUISITION PARAMETERS
Solvent: CDCl3
Pulse Sequence: zppg30
Experiment: 1D
Number of Scans: 2048
Receiver Gain: 203
Relaxation Delay: 2.0000 s
Pulse Width: 10.0000 usec
Acquisition Time: 1.3631 usec
Spectrometer Frequency: 100.61 MHz
Spectral Width: 24038.5 Hz
Lowest Frequency: -1946.0
Nucleus: 13C



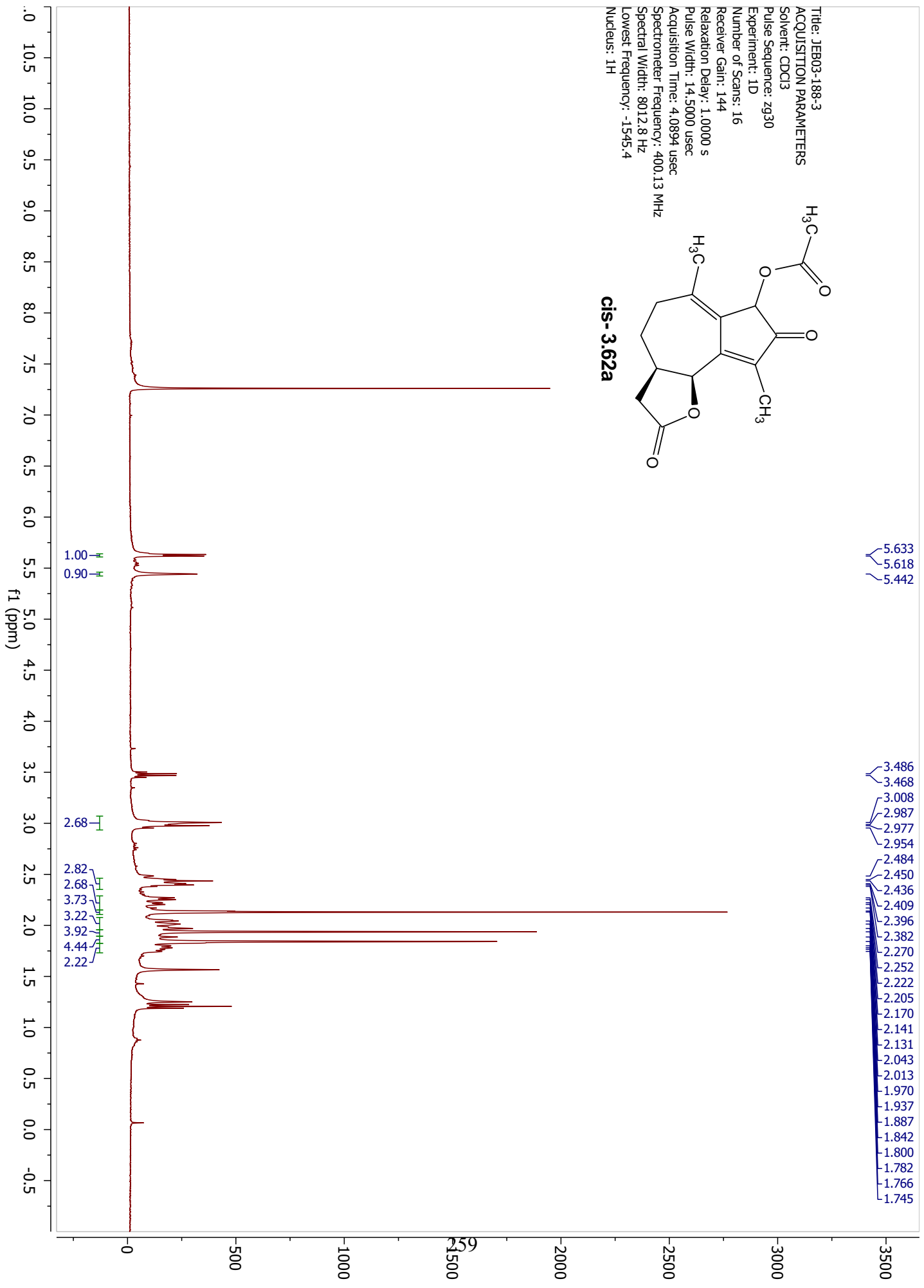
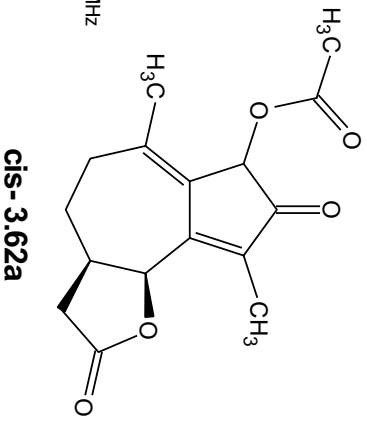
Title: JEB03-188-2
ACQUISITION PARAMETERS
Solvent: CDCl3
Pulse Sequence: zg30
Experiment: 1D
Number of Scans: 16
Receiver Gain: 144
Relaxation Delay: 1.0000 s
Pulse Width: 14.5000 usec
Acquisition Time: 4.0894 usec
Spectrometer Frequency: 400.13 MHz
Spectral Width: 8012.8 Hz
Lowest Frequency: -1545.2
Nucleus: 1H



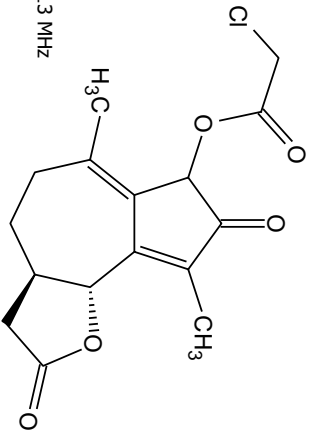
trans-3.62a



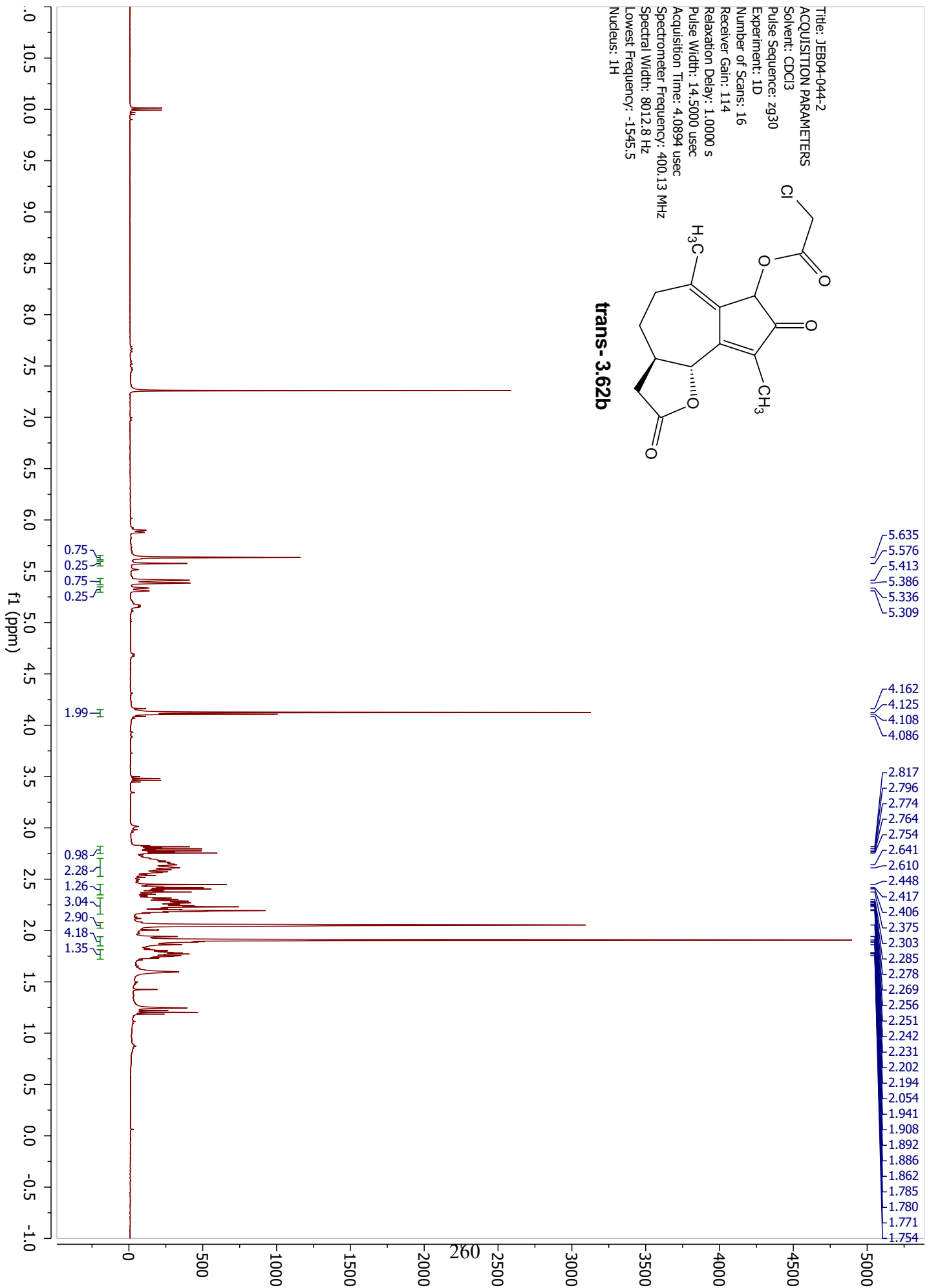
Title: JEB03-188-3
ACQUISITION PARAMETERS
Solvent: CDCl3
Pulse Sequence: zg30
Experiment: 1D
Number of Scans: 16
Receiver Gain: 144
Relaxation Delay: 1.0000 s
Pulse Width: 14.5000 usec
Acquisition Time: 4.0894 usec
Spectrometer Frequency: 400.13 MHz
Spectral Width: 8012.8 Hz
Lowest Frequency: -1545.4
Nucleus: 1H



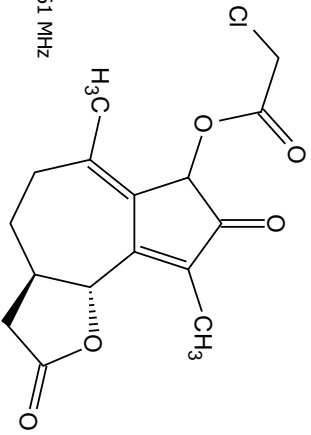
Title: JEB04-044-2
ACQUISITION PARAMETERS
Solvent: CDCl3
Pulse Sequence: zg30
Experiment: 1D
Number of Scans: 16
Receiver Gain: 114
Relaxation Delay: 1.0000 s
Pulse Width: 14.5000 usec
Acquisition Time: 4.0894 usec
Spectrometer Frequency: 400.13 MHz
Spectral Width: 8012.8 Hz
Lowest Frequency: -1545.5
Nucleus: 1H



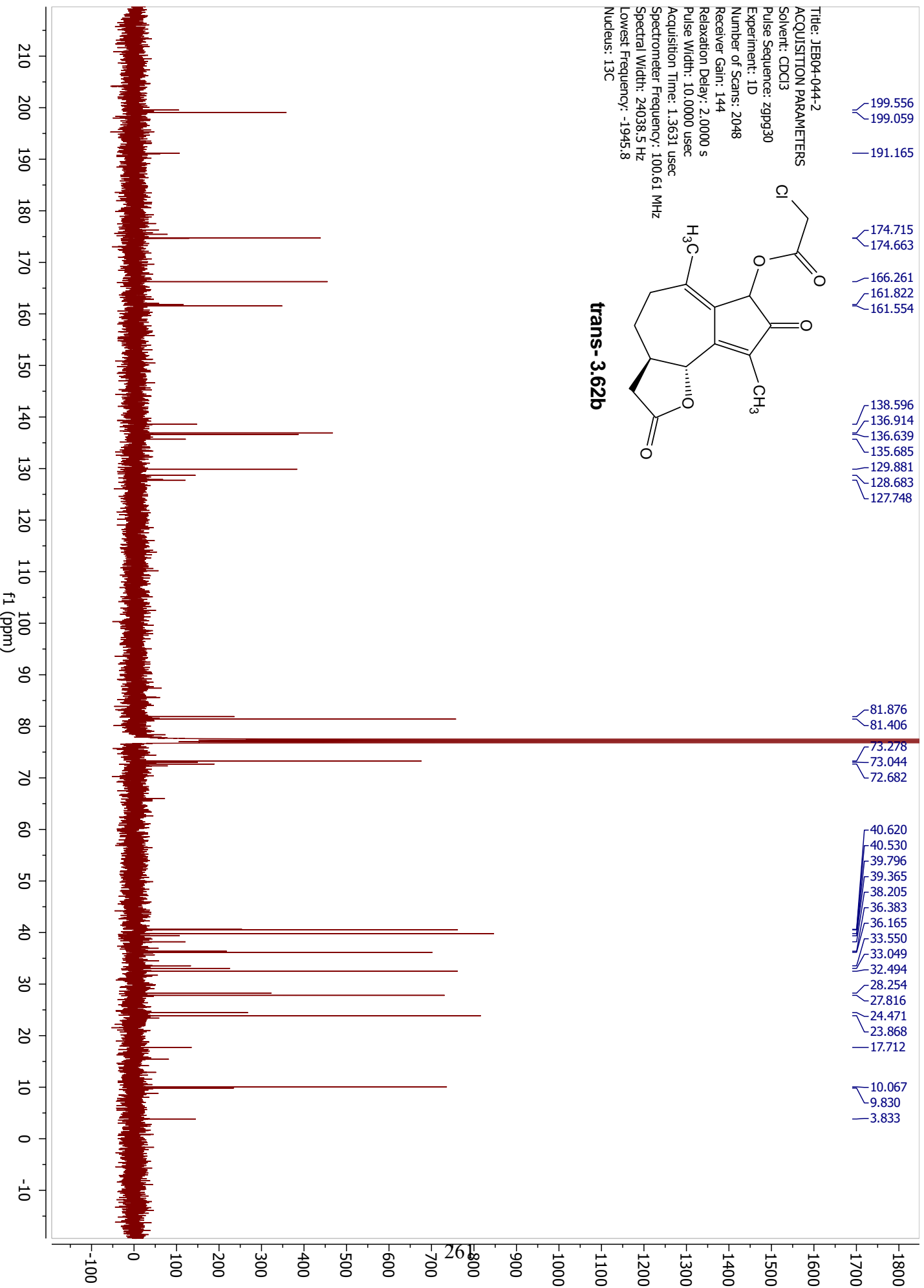
trans-3.62b



Title: JEB04-044-2
ACQUISITION PARAMETERS
Solvent: CDCl3
Pulse Sequence: zgpg30
Experiment: 1D
Number of Scans: 2048
Receiver Gain: 144
Relaxation Delay: 2.0000 s
Pulse Width: 10.0000 usec
Acquisition Time: 1.3631 usec
Spectrometer Frequency: 100.61 MHz
Spectral Width: 24038.5 Hz
Lowest Frequency: -1945.8
Nucleus: 13C

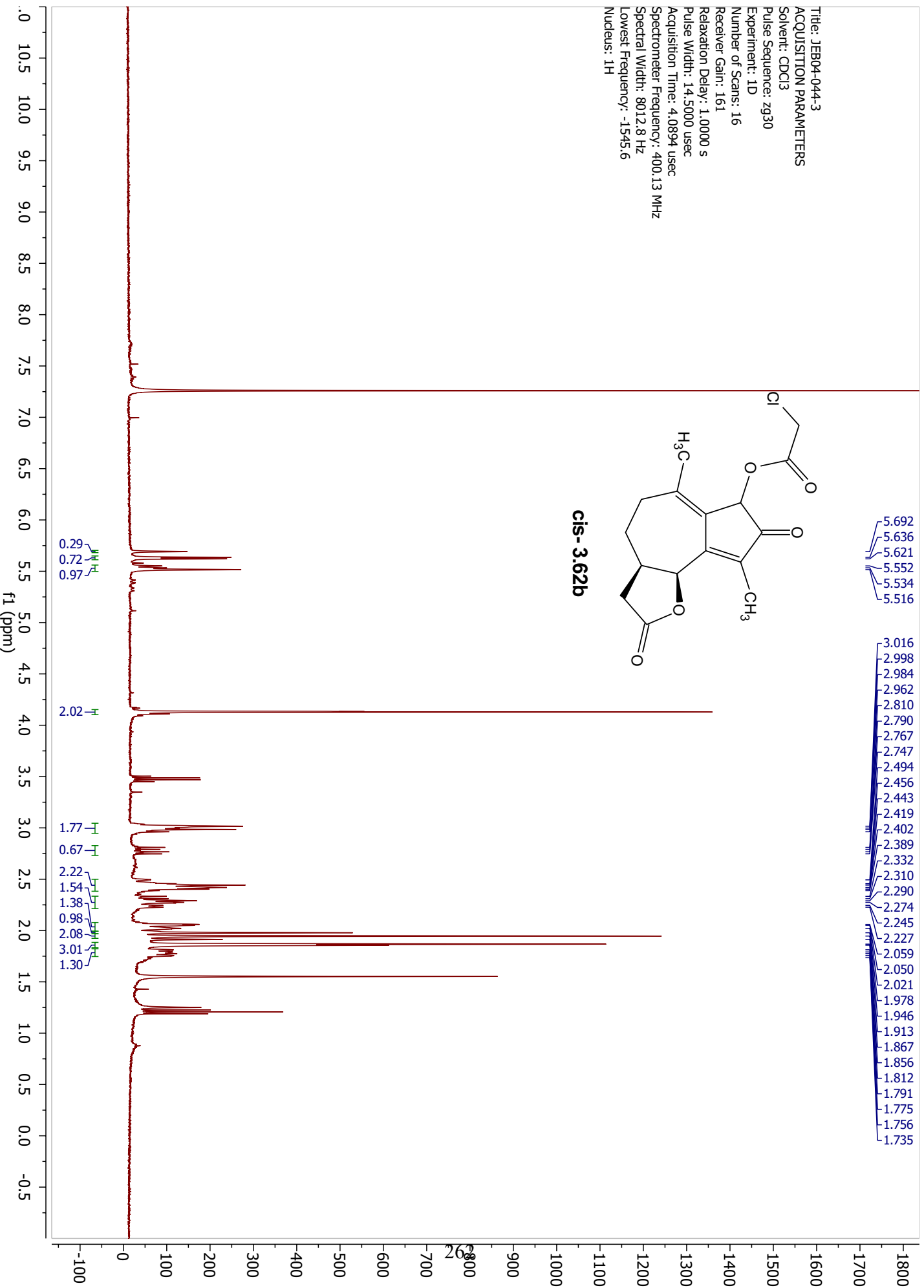
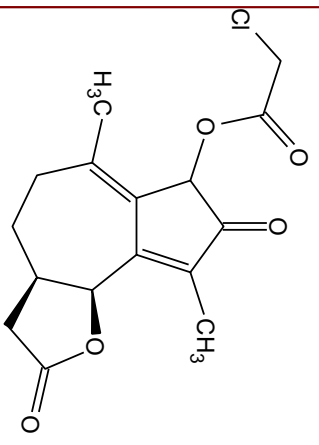


trans-3.62b

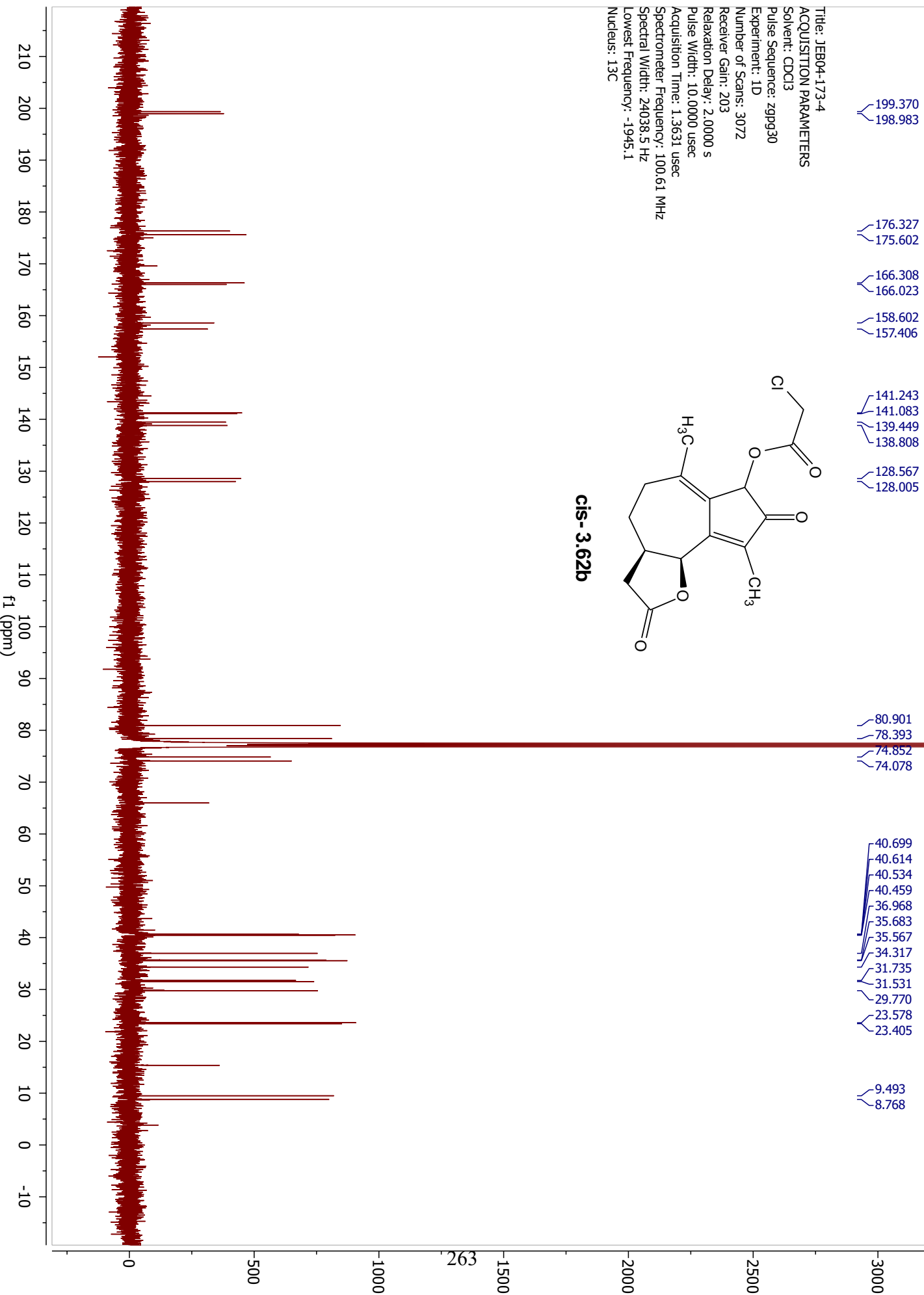
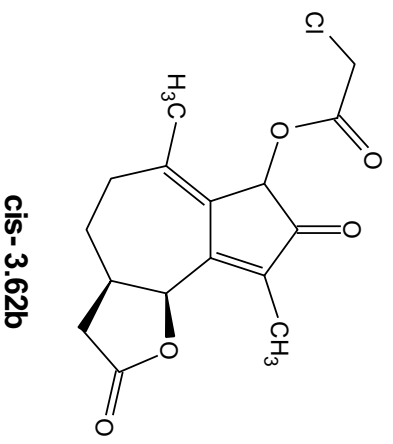


Title: JEB04-044-3
ACQUISITION PARAMETERS
Solvent: CDCl3
Pulse Sequence: zg30
Experiment: 1D
Number of Scans: 16
Receiver Gain: 161
Relaxation Delay: 1.0000 s
Pulse Width: 14.5000 usec
Acquisition Time: 4.0894 usec
Spectrometer Frequency: 400.13 MHz
Spectral Width: 8012.8 Hz
Lowest Frequency: -1545.6
Nucleus: 1H

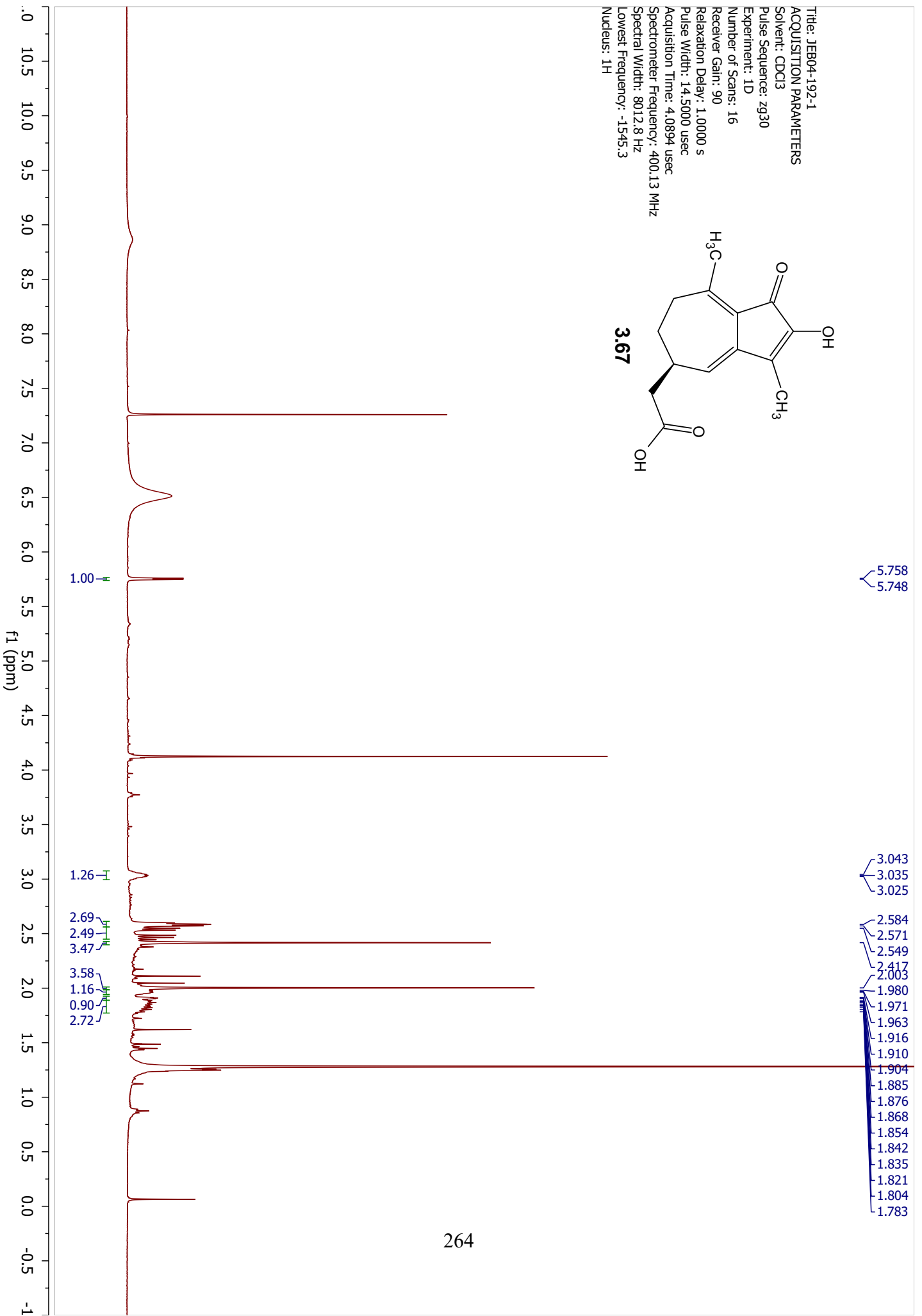
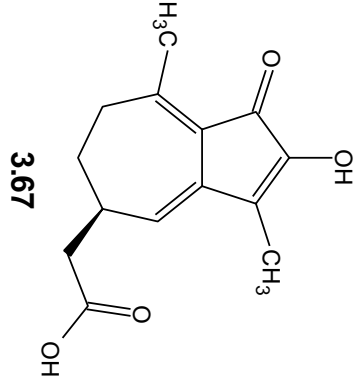
cis-3.62b



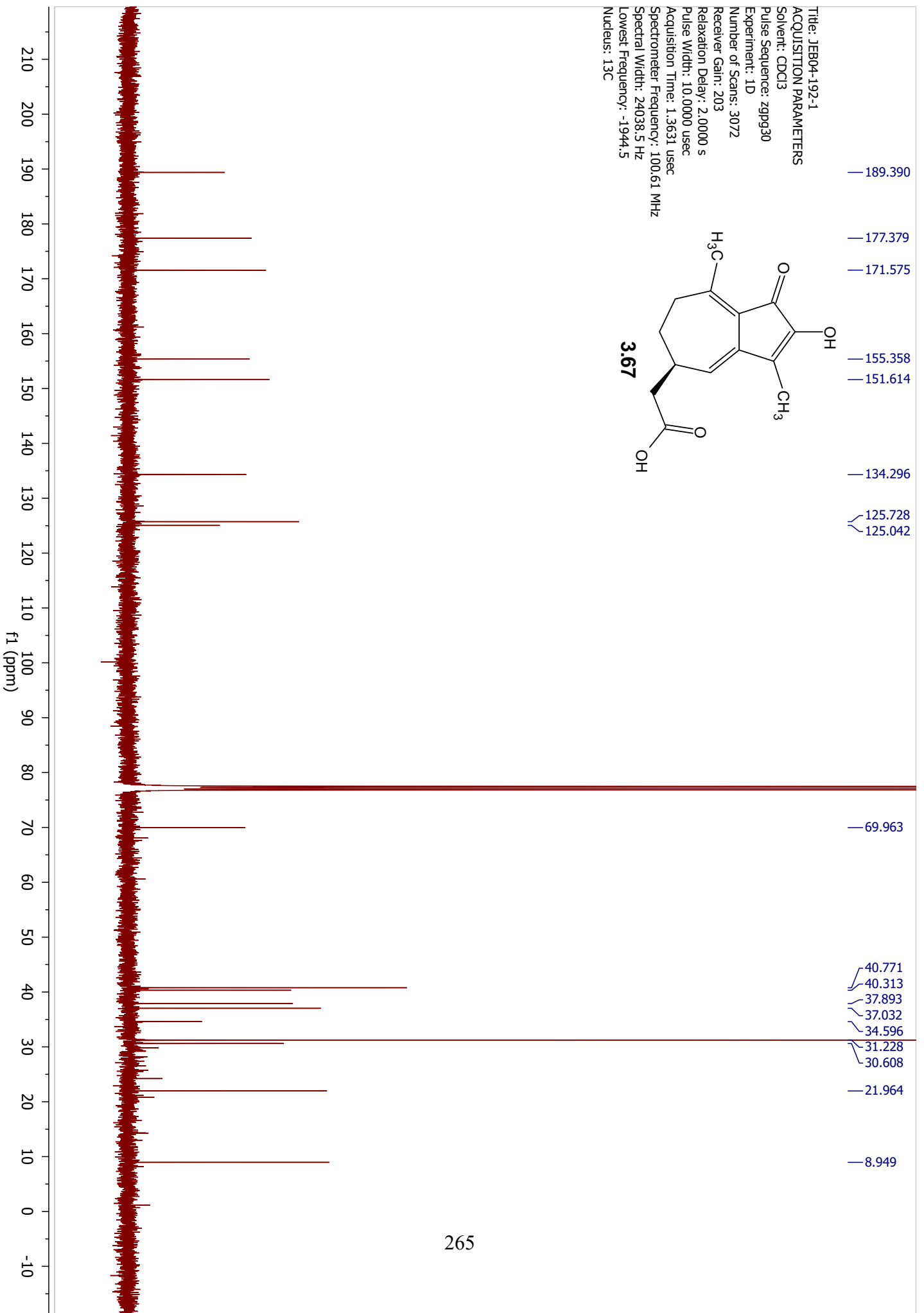
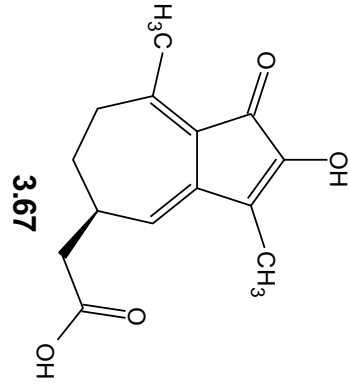
Title: JEB04-173-4
ACQUISITION PARAMETERS
Solvent: CDCl3
Pulse Sequence: zpgp30
Experiment: 1D
Number of Scans: 3072
Receiver Gain: 203
Relaxation Delay: 2.0000 s
Pulse Width: 10.0000 usec
Acquisition Time: 1.3631 usec
Spectrometer Frequency: 100.61 MHz
Spectral Width: 24038.5 Hz
Lowest Frequency: -1945.1
Nucleus: 13C



Title: JEB04-192-1
ACQUISITION PARAMETERS
Solvent: CDCl3
Pulse Sequence: zg30
Experiment: 1D
Number of Scans: 16
Receiver Gain: 90
Relaxation Delay: 1.0000 s
Pulse Width: 14.5000 usec
Acquisition Time: 4.0894 usec
Spectrometer Frequency: 400.13 MHz
Spectral Width: 8012.8 Hz
Lowest Frequency: -1545.3
Nucleus: 1H



Title: JEB04-192-1
ACQUISITION PARAMETERS
Solvent: CDCl3
Pulse Sequence: zgpg30
Experiment: 1D
Number of Scans: 3072
Receiver Gain: 203
Relaxation Delay: 2.0000 s
Pulse Width: 10.0000 usec
Acquisition Time: 1.3631 usec
Spectrometer Frequency: 100.61 MHz
Spectral Width: 24038.5 Hz
Lowest Frequency: -1944.5
Nucleus: 13C



Bibliography

- (1) Santana, A.; Molinillo, J. M. G.; Macías, F. A. Trends in the Synthesis and Functionalization of Guaianolides. *European Journal of Organic Chemistry* **2015**, *2015* (10), 2093–2110. <https://doi.org/10.1002/ejoc.201403244>.
- (2) Foley, D. A.; Maguire, A. R. Synthetic Approaches to Bicyclo[5.3.0]Decane Sesquiterpenes. *Tetrahedron* **2010**, *66* (6), 1131–1175. <https://doi.org/10.1016/j.tet.2009.11.045>.
- (3) Zhuzbaev, B. T.; Adekenov, S. M.; Veselovskii, V. V. Approaches to the Total Synthesis of Sesquiterpenoids of the Guaiane Series. *Russian Chemical Reviews* **1995**, *64* (2), 187–120.
- (4) Macías, F. A.; Santana, A.; Yamahata, A.; Varela, R. M.; Fronczek, F. R.; Molinillo, J. M. G. Facile Preparation of Bioactive Seco -Guaianolides and Guaianolides from *Artemisia Gorgonum* and Evaluation of Their Phytotoxicity. *J Nat Prod* **2012**, *75* (11), 1967–1973. <https://doi.org/10.1021/np300639b>.
- (5) Sakipova, Z.; Wong, N. S. H.; Bekezhanova, T.; Sadykova; Shukirbekova, A.; Boylan, F. Quantification of Santonin in Eight Species of *Artemisia* from Kazakhstan by Means of HPLC-UV: Method Development and Validation. *Plos One* **2017**, *12* (3), e0173714. <https://doi.org/10.1371/journal.pone.0173714>.
- (6) Chu, H.; Smith, J. M.; Felding, J.; Baran, P. S. Scalable Synthesis of (–)-Thapsigargin. *ACS Central Science* **2017**, *3* (1), 47–51. <https://doi.org/10.1021/acscentsci.6b00313>.
- (7) Hullaert, J.; Laplace, D. R.; Winne, J. M. A Three-Step Synthesis of the Guaianolide Ring System. *European Journal of Organic Chemistry* **2014**, *2014* (15), 3097–3100. <https://doi.org/10.1002/ejoc.201402170>.
- (8) Valot, G.; Garcia, J.; Duplan, V.; Serba, C.; Barluenga, S.; Winssinger, N. Diversity-Oriented Synthesis of Diverse Polycyclic Scaffolds Inspired by the Logic of Sesquiterpene Lactones Biosynthesis. *Angewandte Chemie Int Ed* **2012**, *51* (22), 5391–5394. <https://doi.org/10.1002/anie.201201157>.
- (9) Devreese, A. A.; Demuynck, M.; Clercq, P. J. D.; Vandewalle, M. Guaianolides 1. Perhydroazulenic Lactones as Intermediates for Total Synthesis. *Tetrahedron* **1983**, *39* (19), 3039–3048. [https://doi.org/10.1016/s0040-4020\(01\)91543-1](https://doi.org/10.1016/s0040-4020(01)91543-1).
- (10) Grillet, F.; Huang, C.; Brummond, K. M. An Allenic Pauson–Khand Approach to 6,12-Guaianolides. *Org Lett* **2011**, *13* (23), 6304–6307. <https://doi.org/10.1021/ol2028515>.

- (11) Wen, B.; Hexum, J. K.; Widen, J. C.; Harki, D. A.; Brummond, K. M. A Redox Economical Synthesis of Bioactive 6,12-Guaianolides. *Org Lett* **2013**, *15* (11), 2644–2647. <https://doi.org/10.1021/ol400904y>.
- (12) Khand, I. U.; Knox, G. R.; Pauson, P. L.; Watts, W. E. A Cobalt Induced Cleavage Reaction and a New Series of Arenecobalt Carbonyl Complexes. *Journal of the Chemical Society D: Chemical Communications* **1971**, No. 1, 36a–361. <https://doi.org/10.1039/c2971000036a>.
- (13) Ricker, J. D. Recent Advances in the Pauson–Khand Reaction. *Topics in Catalysis* **2017**, *60* (8), 609–619. <https://doi.org/10.1007/s11244-017-0741-0>.
- (14) Shibata, T. Recent Advances in the Catalytic Pauson–Khand-Type Reaction. *Advanced Synthesis & Catalysis* **2006**, *348* (16–17), 2328–2336. <https://doi.org/10.1002/adsc.200600328>.
- (15) Gibson, S. E.; Mainolfi, N. The Intermolecular Pauson-Khand Reaction. *Angewandte Chemie International Edition* **2005**, *44* (20), 3022–3037. <https://doi.org/10.1002/anie.200462235>.
- (16) Blanco-Urgoiti, J.; Añorbe, L.; Pérez-Serrano, L.; Domínguez, G.; Pérez-Castells, J. The Pauson–Khand Reaction, a Powerful Synthetic Tool for the Synthesis of Complex Molecules. *Chemical Society Reviews* **2004**, *33* (1), 32–42. <https://doi.org/10.1039/b300976a>.
- (17) Thomas, S. E. G. née; Stevenazzi, A. The Pauson–Khand Reaction: The Catalytic Age Is Here! *Angewandte Chemie International Edition* **2003**, *42* (16), 1800–1810. <https://doi.org/10.1002/anie.200200547>.
- (18) Rivero, M. R.; Adrio, J.; Carretero, J. C. Pauson-Khand Reactions of Electron-Deficient Alkenes. *European Journal of Organic Chemistry* **2002**, 2881–2889.
- (19) Sugihara, T.; Yamaguchi, M.; Nishizawa, M. Advances in the Pauson-Khand Reaction: Development of Reactive Cobalt Complexes. *Chemistry - A European Journal* **2001**, *7* (8), 1589–1595.
- (20) Brummond, K. M.; Kent, J. L. Recent Advances in the Pauson-Khand Reaction and Related [2+2+1] Cycloadditions. *Tetrahedron* **2000**, *56*, 3263–3283.
- (21) Narasaka, K.; Shibata, T. Conversion of 1-(w-Alkynyl)-1,2-Propadienyl Sulfides to Bicyclic Dienones by the Use of Iron Carbonyl Complex. *Chemistry Letters* **1994**, 315–318.
- (22) Brummond, K. M.; Kent, J. L.; Wan, H. A New Allenic Pauson-Khand Cycloaddition for the Preparation of α -Methylene Cyclopentenones. *Tetrahedron Letters* **1995**, *36* (14), 2407–2410.
- (23) Brummond, K. M.; Chen, H.; Fisher, K. D.; Kerekes, A. D.; Rickards, B.; Sill, P. C.; Geib, S. J. An Allenic Pauson–Khand-Type Reaction: A Reversal in π -Bond Selectivity and the

Formation of Seven-Membered Rings. *Org Lett* **2002**, *4* (11), 1931–1934. <https://doi.org/10.1021/ol025955w>.

(24) Bayden, A. S.; Brummond, K. M.; Jordan, K. D. Computational Insight Concerning Catalytic Decision Points of the Transition Metal Catalyzed [2 + 2 + 1] Cyclocarbonylation Reaction of Allenes. *Organometallics* **2006**, *25* (22), 5204–5206. <https://doi.org/10.1021/om0607503>.

(25) McKerrall, S. J.; Jørgensen, L.; Kuttruff, C. A.; Ungeheuer, F.; Baran, P. S. Development of a Concise Synthesis of (+)-Ingenol. *J Am Chem Soc* **2014**, *136* (15), 5799–5810. <https://doi.org/10.1021/ja501881p>.

(26) Kawamura, S.; Chu, H.; Felding, J.; Baran, P. S. Nineteen-Step Total Synthesis of (+)-Phorbol. *Nature* **2016**, *532* (7597), 90–93. <https://doi.org/10.1038/nature17153>.

(27) Jørgensen, L.; McKerrall, S. J.; Kuttruff, C. A.; Ungeheuer, F.; Felding, J.; Baran, P. S. 14-Step Synthesis of (+)-Ingenol from (+)-3-Carene. *Science* **2013**, *341* (6148), 878–882. <https://doi.org/10.1126/science.1241606>.

(28) Hirose, T.; Miyakoshi, N.; Mukai, C. Total Synthesis of (+)-Achalensolide Based on the Rh(I)-Catalyzed Allenic Pauson–Khand-Type Reaction. *J Org Chem* **2008**, *73* (3), 1061–1066. <https://doi.org/10.1021/jo702330y>.

(29) Hayashi, Y.; Ogawa, K.; Inagaki, F.; Mukai, C. First Total Synthesis of (+)-Indicanone. *Org Biomol Chem* **2012**, *10* (24), 4747–4751. <https://doi.org/10.1039/c2ob25500f>.

(30) Williams, D. R.; Shah, A. A. Total Synthesis of (+)-Ileabethoxazole via an Iron-Mediated Pauson–Khand [2 + 2 + 1] Carbocyclization. *J Am Chem Soc* **2014**, *136* (24), 8829–8836. <https://doi.org/10.1021/ja5043462>.

(31) Heinz, C.; Cramer, N. Synthesis of Fijiolide A via an Atropselective Paracyclophane Formation. *J Am Chem Soc* **2015**, *137* (35), 11278–11281. <https://doi.org/10.1021/jacs.5b07964>.

(32) Brummond, K. M.; Sill, P. C.; Chen, H. The First Total Synthesis of 15-Deoxy- Δ 12,14 - Prostaglandin J 2 and the Unambiguous Assignment of the C 14 Stereochemistry. *Org Lett* **2004**, *6* (2), 149–152. <https://doi.org/10.1021/ol035590v>.

(33) Tap, A.; Lecourt, C.; Dhambri, S.; Arnould, M.; Galvani, G.; Buu, O. N. V.; Jouanneau, M.; Férézou, J.-P.; Ardisson, J.; Lannou, M.-I.; Sorin, G. Alkoxyallene-Ynes: Selective Preparation of Bicyclo[5.3.0] Ring Systems Including a δ -Alkoxy Cyclopentadienone. *Chemistry - A European Journal* **2016**, *22* (14), 4938–4944. <https://doi.org/10.1002/chem.201504753>.

(34) Aburano, D.; Inagaki, F.; Tomonaga, S.; Mukai, C. Synthesis of a Core Carbon Framework of Cyanosporasides A and B. *J Org Chem* **2009**, *74* (15), 5590–5594. <https://doi.org/10.1021/jo901141t>.

- (35) Jin, Y.; Yeh, C.; Kuttruff, C. A.; Jørgensen, L.; Dünstl, G.; Felding, J.; Natarajan, S. R.; Baran, P. S. C H Oxidation of Ingenanes Enables Potent and Selective Protein Kinase C Isoform Activation. *Angewandte Chemie Int Ed* **2015**, *54* (47), 14044–14048. <https://doi.org/10.1002/anie.201507977>.
- (36) Cacchi, S.; Morera, E.; Ortar, G. Palladium-Catalyzed Reduction of Enol Triflates to Alkenes. **1984**, *25* (42), 4821–4824.
- (37) Hirose, T.; Miyakoshi, N.; Mukai, C. Total Synthesis of (+)-Achalensolide Based on the Rh(I)-Catalyzed Allenic Pauson–Khand-Type Reaction. *The Journal of Organic Chemistry* **2008**, *73* (3), 1061–1066. <https://doi.org/10.1021/jo702330y>.
- (38) Bourhis, R.; Frainnet, E.; Moulines, F. Action Du Triethylsilane Sur Des Aldehydes α -Ethyl-Eniques En Presence de Catalyseurs Au Nickel Ou Au Palladium. *J Organomet Chem* **1977**, *141* (2), 157–171. [https://doi.org/10.1016/s0022-328x\(00\)92269-1](https://doi.org/10.1016/s0022-328x(00)92269-1).
- (39) Barlow, A. P.; Boag, N. M.; Stone, F. G. A. Hydrosilylation of α,β -Unsaturated Aldehydes and Ketones by Trans-DI- μ -Hydrido-Bis(Silyl)Bis-(Trialkylphosphine)Diplatinum Complexes. *J Organomet Chem* **1980**, *191* (1), 39–47. [https://doi.org/10.1016/s0022-328x\(00\)88553-8](https://doi.org/10.1016/s0022-328x(00)88553-8).
- (40) Ojima, I.; Kogure, T. Reduction of Carbonyl Compounds via Hydrosilylation. 4. Highly Regioselective Reductions of α,β -Unsaturated Carbonyl Compounds. *Organometallics* **1982**, *1* (10), 1390–1399. <https://doi.org/10.1021/om00070a024>.
- (41) Johnson, C. R.; Raheja, R. K. Hydrosilylation of Enones: Platinum Divinyltetramethyldisiloxane Complex in the Preparation of Triisopropylsilyl and Triphenylsilyl Enol Ethers. *J Org Chem* **1994**, *59* (9), 2287–2288. <https://doi.org/10.1021/jo00088a006>.
- (42) Hutchins, R. O.; Milewski, C. A.; Maryanoff, B. E. Selective Deoxygenation of Ketones and Aldehydes Including Hindered Systems with Sodium Cyanoborohydride. *Journal of the American Chemical Society* **1973**, *95* (11), 3662–3668. <https://doi.org/10.1021/ja00792a033>.
- (43) Kabalka, G. W.; Baker, J. D. New Mild Conversion of Ketones to the Corresponding Methylene Derivatives. *The Journal of Organic Chemistry* **1975**, *40* (12), 1834–1835. <https://doi.org/10.1021/jo00900a033>.
- (44) Kabalka, G. W.; Yang, D. T. C.; Baker, J. D. Deoxygenation of α,β -Unsaturated Aldehydes and Ketones via the Catecholborane Reduction of the Corresponding Tosylhydrazones. *The Journal of Organic Chemistry* **1976**, *41* (3), 574–575. <https://doi.org/10.1021/jo00865a043>.
- (45) Greene, A. E. Highly Stereoselective Total Syntheses of (+)-Pachydietylol A and (-)-Dictyolene, Novel Marine Diterpenes from Brown Seaweeds of the Family Dictyotaceae. *Journal of the American Chemical Society* **1980**, *102* (16), 5337–5343. <https://doi.org/10.1021/ja00536a036>.

- (46) Chu, M.; Coates, R. M. Partial Synthesis of 9,10-Syn-Diterpenes via Tosylhydrazone Reduction: (-)-(9.Beta.)-Pimara-7,15-Diene and (-)-(9.Beta.)-Isopimaradiene. *The Journal of Organic Chemistry* **1992**, *57* (17), 4590–4597. <https://doi.org/10.1021/jo00043a013>.
- (47) Chai, Y.; Vicic, D. A.; McIntosh, M. C. Cycloaldol Approach to the Isobenzofuran Core of Eunicellin Diterpenes. *Organic Letters* **2003**, *5* (7), 1039–1042. <https://doi.org/10.1021/ol034052f>.
- (48) Trost, B. M.; Fleming, I. *Comprehensive Organic Synthesis*; Pergamon: Oxford, 1991; Vol. 1.13-1.14, pp 307, 327.
- (49) Snider, B. B.; Kirk, T. C. New Route to Functionalized Trans-Hydrindenones. *Journal of the American Chemical Society* **1983**, *105* (8), 2364–2368.
- (50) Jammi, S.; Maury, J.; Suppo, J.-S.; Bertrand, M. P.; Feray, L. Intramolecular Trapping of Allenylzincs by Carbonyl Groups. *The Journal of Organic Chemistry* **2013**, *78* (24), 12566–12576. <https://doi.org/10.1021/jo4022293>.
- (51) Shono, T.; Ito, K.; Tsubouchi, A.; Takeda, T. Titanocene(Ii)-Promoted Carbonyl Allenation Utilizing 1,1-Dichloroalk-1-Enes. *Organic & Biomolecular Chemistry* **2005**, *3* (16), 2914–3. <https://doi.org/10.1039/b508820h>.
- (52) Tsuji, J.; Sugiura, T.; Minami, I. Preparation of 1,2-Dienes by the Palladium-Catalyzed Hydrogenolysis of 3-Methoxycarbonyloxy-1-Alkynes with Ammonium Formate. *Synthesis* **1987**, No. 7, 603–606.
- (53) Imamoto, T.; Takiyama, N.; Nakamura, K.; Hatajima, T.; Kamiya, Y. Reactions of Carbonyl Compounds with Grignard Reagents in the Presence of Cerium Chloride. *J Am Chem Soc* **1989**, *111* (12), 4392–4398. <https://doi.org/10.1021/ja00194a037>.
- (54) Mandai, T.; Tsujiguchi, Y.; Matsuoka, S.; Tsuji, J. Preparation of Conjugated Enynes by the Palladium-Catalyzed Elimination Reaction of Propargylic Carbonates. *Tetrahedron Lett* **1993**, *34* (47), 7615–7618. [https://doi.org/10.1016/s0040-4039\(00\)60414-8](https://doi.org/10.1016/s0040-4039(00)60414-8).
- (55) Wells, S. M.; Brummond, K. M. Conditions for a Rh(I)-Catalyzed [2+2+1] Cycloaddition Reaction with Methyl Substituted Allenes and Alkynes. *Tetrahedron Letters* **2015**, *56*, 3546–3549. <https://doi.org/10.1016/j.tetlet.2015.01.075>.
- (56) Burrows, L. C.; Jesikiewicz, L. T.; Lu, G.; Geib, S. J.; Liu, P.; Brummond, K. M. Computationally Guided Catalyst Design in the Type I Dynamic Kinetic Asymmetric Pauson–Khand Reaction of Allenyl Acetates. *J Am Chem Soc* **2017**, *139* (42), 15022–15032. <https://doi.org/10.1021/jacs.7b07121>.
- (57) Kabalka, G. W.; Jr, J. D. B.; Neal, G. W. Catecholborane (1,3,2-Benzodioxaborole). A Versatile Reducing Agent. *The Journal of Organic Chemistry* **1977**, *42* (3), 512–517.

- (58) Yang, D. T. C.; Kabalka, G. W. An Improved Synthesis of 5 β -Cholest-3-Ene. *Org Prep Proced Int* **1977**, 9 (2), 85–87. <https://doi.org/10.1080/00304947709355667>.
- (59) Shrestha, M. L.; Qi, W.; McIntosh, M. C. Acyclic 1,4-Stereocontrol via the Allylic Diazene Rearrangement: Development, Applications, and the Essential Role of Kinetic EStereoselectivity in Tosylhydrazone Formation. *The Journal of Organic Chemistry* **2017**, 82 (16), 8359–8370. <https://doi.org/10.1021/acs.joc.7b00428>.
- (60) Greene, A. E.; Edgar, M. T. Synthesis of Oxoisodehydroleucodin: A Novel Guaianolide from *Montanoa Imbricata*. *J Org Chem* **1989**, 54 (6), 1468–1470. <https://doi.org/10.1021/jo00267a049>.
- (61) Tanaka, T.; Maeda, K.; Mikamiyama, H.; Funakoshi, Y.; Uenaka, K.; Iwata, C. Synthetic Studies on the Aromadendrane-Type Compounds. Stereoselective Total Syntheses of (+)-Aromadendrene and (-)-Alloaromadendrene. *Tetrahedron* **1996**, 52 (12), 4257–4268.
- (62) Blay, G.; García, B.; Molina, E.; Pedro, J. R. Syntheses of (+)-Alismoxide and (+)-4- e Pi -Alismoxide. *J Org Chem* **2006**, 71 (20), 7866–7869. <https://doi.org/10.1021/jo061278y>.
- (63) Wang, X.; Sun, W.-B.; Zou, J.-P.; Lin, G.-Q.; Sun, B.-F. Asymmetric Total Synthesis of Hedyosumin E Aglycon, 7,10-Epoxyhedyosminolide and Ent -Zedolactone A. *Org Biomol Chem* **2016**, 14 (45), 10581–10584. <https://doi.org/10.1039/c6ob02179d>.
- (64) Taylor, E. J.; Djerassi, C. Mechanism of the Sodium Cyanoborohydride Reduction of .Alpha..Beta.-Unsaturated Tosylhydrazones. *J Am Chem Soc* **1976**, 98 (8), 2275–2281. <https://doi.org/10.1021/ja00424a046>.
- (65) Kabalka, G. W.; Summers, S. T. A Mild and Convenient Conversion of Ketones to the Corresponding Methylene Derivatives via Reduction of Tosylhydrazones by Bis(Benzoyloxy)Borane. *The Journal of Organic Chemistry* **1981**, 46, 1217–1218.
- (66) Wang, K. K.; Brown, H. C. Hydroboration Kinetics. 6. 1 Hydroboration of Alkenes with 9-Borabicyclo[3.3.1]Nonane Dimer and 9-Borabicyclo[3.3.1]Nonane-Lewis Base Complexes in Various Solvents: An Interpretation of the Catalytic Effect of Ether Solvents on the Hydroboration Reaction. *J Am Chem Soc* **1982**, 104 (25), 7148–7155. <https://doi.org/10.1021/ja00389a043>.
- (67) Jabbari, A.; Sorensen, E. J.; Houk, K. N. Transition States of the Retro-Ene Reactions of Allylic Diazenes. *Organic Letters* **2006**, 8 (14), 3105–3107. <https://doi.org/10.1021/ol0612049>.
- (68) Myers, A. G.; Movassaghi, M.; Zheng, B. Mechanistic Studies of the Free-Radical Fragmentation of Monoalkyl Diazenes. *Tetrahedron Letters* **1997**, 38 (37), 6569–6572.
- (69) Kosower, E. M. Monosubstituted Diazenes (Diimides). Surprising Intermediates. *Accounts of Chemical Research* **1971**, 4 (6), 193–198. <https://doi.org/10.1021/ar50042a001>.

- (70) Yoshida, K.; Kubota, T. Studies on A-Norsteroids - IV The C-1,2 Isomeric Ketols in 17b-Hydroxy-a-nor-5b-Androstane Series. *Tetrahedron* **1965**, *21*, 759–770.
- (71) Ireland, R. E.; Grand, P. S.; Dickerson, R. E.; Bordner, J.; Rydjeski, D. R. Total Synthesis of Terpenes. XIV. Interpretation of the Transmogrification of 4.Beta., 7a.Alpha.-Dimethyl-1.Alpha.-Hydroxy-4.Alpha.-Phenyl-4,5,6,7-Tetrahydro-2-Indanone by Base. *The Journal of Organic Chemistry* **1970**, *35* (3), 570–584. <https://doi.org/10.1021/jo00828a007>.
- (72) Chang, Y.; Shi, L.; Huang, J.; Shi, L.; Zhang, Z.; Hao, H.-D.; Gong, J.; Yang, Z. Stereoselective Total Synthesis of (\pm)-5-Epi-Cyanthiwigin I via an Intramolecular Pauson–Khand Reaction as the Key Step. *Organic Letters* **2018**, *20* (10), 2876–2879. <https://doi.org/10.1021/acs.orglett.8b00903>.
- (73) McCabe, J. M. Applications of Rhodium(I)-Catalysis to Natural Product Synthesis: Routes to Ovalicin and Guanacastepene A. **2AD**, University of Pittsburgh.
- (74) Burrows, L. C.; Jesikiewicz, L. T.; Lu, G.; Geib, S. J.; Liu, P.; Brummond, K. M. Computationally Guided Catalyst Design in the Type I Dynamic Kinetic Asymmetric Pauson–Khand Reaction of Allenyl Acetates. *J Am Chem Soc* **2017**, *139* (42), 15022–15032. <https://doi.org/10.1021/jacs.7b07121>.
- (75) Reese, C. B.; Stewart, J. C. M.; Boom, J. H. van; Leeuw, H. P. M. de; Nagel, J.; Rooy, J. F. M. de. The Synthesis of Oligoribonucleotides. Part XI. Preparation of Ribonucleoside 2'-Acetal 3'-Esters by Selective Deacylation. *J Chem Soc Perkin Transactions 1* **1975**, *0* (10), 934–942. <https://doi.org/10.1039/p19750000934>.
- (76) Mouriès-Mansuy, V.; Fensterbank, L. Gold-Catalyzed Migration of Propargyl Acetate as an Entry into the Total Synthesis of Natural Products. *Israel J Chem* **2018**, *58* (5), 586–595. <https://doi.org/10.1002/ijch.201700074>.
- (77) Zhou, Q.-M.; Chen, M.-H.; Li, X.-H.; Peng, C.; Lin, D.-S.; Li, X.-N.; He, Y.; Xiong, L. Absolute Configurations and Bioactivities of Guaiane-Type Sesquiterpenoids Isolated from Pogostemon Cablin. *J Nat Prod* **2018**, *81* (9), 1919–1927. <https://doi.org/10.1021/acs.jnatprod.7b00690>.
- (78) Jing, C.; Guo, J.; Yang, B.; Fan, S.; Wang, Y.; Chen, D.; Hao, X. Stelleraguaianone B and C, Two New Sesquiterpenoids from Stelleria Chamaejasme L. *Fitoterapia* **2019**, *134*, 443–446. <https://doi.org/10.1016/j.fitote.2019.03.024>.
- (79) Hoveyda, A. H.; Evans, D. A.; Fu, G. C. Substrate-Directable Chemical Reactions. *Chem Rev* **1993**, *93* (4), 1307–1370. <https://doi.org/10.1021/cr00020a002>.
- (80) Sawano, T.; Yamamoto, H. Regio- and Enantioselective Substrate-Directed Epoxidation. *Eur J Org Chem* **2020**. <https://doi.org/10.1002/ejoc.201901656>.

- (81) Kočovský, P. Stereochemistry of Epoxidation of Allylic and Homoallylic Cyclohexene Alcohols. *J Chem Soc Perkin Transactions 1* **1994**, 0 (13), 1759–1763. <https://doi.org/10.1039/p19940001759>.
- (82) Itoh, T.; Jitsukawa, K.; Kaneda, K.; Teranishi, S. Vanadium-Catalyzed Epoxidation of Cyclic Allylic Alcohols. Stereoselectivity and Stereocontrol Mechanism. *J Am Chem Soc* **1979**, *101* (1), 159–169. <https://doi.org/10.1021/ja00495a027>.
- (83) Distler, H. The Chemistry of Bunte Salts. *Angewandte Chemie Int Ed Engl* **1967**, *6* (6), 544–553. <https://doi.org/10.1002/anie.196705441>.
- (84) Tap, A.; Jouanneau, M.; Galvani, G.; Sorin, G.; Lannou, M.-I.; Férézou, J.-P.; Ardisson, J. Asymmetric Synthesis of a Highly Functionalized Enantioenriched System Close to Thapsigargin Framework. *Organic & Biomolecular Chemistry* **2012**, *10* (40), 8140–8147. <https://doi.org/10.1039/c2ob26194d>.
- (85) Wen, B.; Hexum, J. K.; Widen, J. C.; Harki, D. A.; Brummond, K. M. A Redox Economical Synthesis of Bioactive 6,12-Guaianolides. *Organic Letters* **2013**, *15* (11), 2644–2647. <https://doi.org/10.1021/ol400904y>.
- (86) Grillet, F.; Huang, C.; Brummond, K. M. An Allenic Pauson–Khand Approach to 6,12-Guaianolides. *Organic Letters* **2011**, *13* (23), 6304–6307. <https://doi.org/10.1021/ol2028515>.
- (87) Hayashi, Y.; Ogawa, K.; Inagaki, F.; Mukai, C. First Total Synthesis of (+)-Indicanone. *Organic & Biomolecular Chemistry* **2012**, *10* (24), 4747–5. <https://doi.org/10.1039/c2ob25500f>.
- (88) Bohlmann, F.; Zdero, C. Zwei Neue Sesquiterpen-Lactone Aus *Lidbeckia Pectinata* Berg. Und *Pentzia Elegans* DC. *Tetrahedron Lett* **1972**, *13* (7), 621–624. [https://doi.org/10.1016/s0040-4039\(01\)84393-8](https://doi.org/10.1016/s0040-4039(01)84393-8).
- (89) Bailon-Moscoso, N.; González-Arévalo, G.; Velásquez-Rojas, G.; Malagón, O.; Vidari, G.; Zentella-Dehesa, A.; Ratovitski, E. A.; Ostrosky-Wegman, P. Phytometabolite Dehydroleucodine Induces Cell Cycle Arrest, Apoptosis, and DNA Damage in Human Astrocytoma Cells through P73/P53 Regulation. *PLOS ONE* **2015**, *10* (8), e0136527-18. <https://doi.org/10.1371/journal.pone.0136527>.
- (90) Ordóñez, P. E.; Sharma, K. K.; Bystrom, L. M.; Alas, M. A.; Enriquez, R. G.; Malagón, O.; Jones, D. E.; Guzman, M. L.; Compadre, C. M. Dehydroleucodine, a Sesquiterpene Lactone from *Gynoxys Verrucosa*, Demonstrates Cytotoxic Activity against Human Leukemia Cells. *Journal of Natural Products* **2016**, *79* (4), 691–696. <https://doi.org/10.1021/acs.jnatprod.5b00383>.
- (91) Ratovitski, E. A. Dehydroleucodine Induces a TP73-Dependent Transcriptional Regulation of Multiple Cell Death Target Genes in Human Glioblastoma Cells. *Anti-Cancer Agents in Medicinal Chemistry* **2017**, *17* (6), 1–13. <https://doi.org/10.2174/1871520616666160923105546>.

- (92) Galvis, A.; Marcano, A.; Stefancin, C.; Villaverde, N.; Priestap, H. A.; Tonn, C. E.; Lopez, L. A.; Barbieri, M. A. The Effect of Dehydroleucodine in Adipocyte Differentiation. *European Journal of Pharmacology* **2011**, *671* (1–3), 18–25. <https://doi.org/10.1016/j.ejphar.2011.09.033>.
- (93) Brummond, K. M.; Davis, M. M.; Huang, C. Rh(I)-Catalyzed Cyclocarbonylation of Allenol Esters To Prepare Acetoxy 4-Alkylidenecyclopent-3-En-2-Ones. *The Journal of Organic Chemistry* **2009**, *74* (21), 8314–8320. <https://doi.org/10.1021/jo901459t>.
- (94) Reissig, H.-U.; Angert, H. Ester Groups as Effective Ligands in Chelate-Controlled Additions of Cuprates and Grignard Reagents to Chiral B-Formyl Esters. *The Journal of Organic Chemistry* **1993**, *58*, 6280–6285.
- (95) Reetz, M. T.; Kyung, S. H.; Hullmann, M. CH₃Li/TiCl₄: A Non-Basic and Highly Selective Grignard Analogue. *Tetrahedron* **1986**, *42* (11), 2931–2935.
- (96) Kunz, T.; Reissig, H.-U. A New Path to Trans-Substituted Gamma-Lactones. *Angewandte Chemie* **1988**, *100*, 297–298.
- (97) Nino, A. D.; Maiuolo, L.; Merino, P.; Nardi, M.; Procopio, A.; pez, D. R.-L.; Russo, B.; Algieri, V. Efficient Organocatalyst Supported on a Simple Ionic Liquid as a Recoverable System for the Asymmetric Diels-Alder Reaction in the Presence of Water. *ChemCatChem* **2015**, *7* (5), 830–835. <https://doi.org/10.1002/cctc.201402973>.
- (98) Chi, Y.; Gellman, S. H. Diphenylprolinol Methyl Ether: A Highly Enantioselective Catalyst for Michael Addition of Aldehydes to Simple Enones. *Organic Letters* **2005**, *7* (19), 4253–4256. <https://doi.org/10.1021/ol0517729>.
- (99) Peelen, T. J.; Chi, Y.; Gellman, S. H. Enantioselective Organocatalytic Michael Additions of Aldehydes to Enones with Imidazolidinones: Cocatalyst Effects and Evidence for an Enamine Intermediate. *Journal of the American Chemical Society* **2005**, *127* (33), 11598–11599. <https://doi.org/10.1021/ja0532584>.
- (100) Kolb, A.; Zuo, W.; Siewert, J.; Harms, K.; Zezschwitz, P. von. Improved Synthesis of Cyclic Tertiary Allylic Alcohols by Asymmetric 1,2-Addition of AlMe₃ to Enones. *Chemistry - A European Journal* **2013**, *19* (48), 16366–16373. <https://doi.org/10.1002/chem.201303061>.
- (101) Meylemans, H. A.; Quintana, R. L.; Goldsmith, B. R.; Harvey, B. G. Solvent-Free Conversion of Linalool to Methylcyclopentadiene Dimers: A Route To Renewable High-Density Fuels. *ChemSusChem* **2011**, *4* (4), 465–469. <https://doi.org/10.1002/cssc.201100017>.
- (102) Wu, Z.; Madduri, A. V. R.; Harutyunyan, S. R.; Minnaard, A. J. Catalytic Asymmetric Synthesis of Dihydrofurans and Cyclopentenols with Tertiary Stereocenters. *Eur J Org Chem* **2014**, *2014* (3), 575–582. <https://doi.org/10.1002/ejoc.201301476>.

- (103) Chakor, J. N.; Merlini, L.; Dallavalle, S. Enantioselective Total Synthesis and Absolute Configuration of the Alleged Structure of Crassinervic Acid. *Tetrahedron* **2011**, *67* (34), 6300–6307. <https://doi.org/10.1016/j.tet.2011.06.015>.
- (104) Sparling, B. A.; Moebius, D. C.; Shair, M. D. Enantioselective Total Synthesis of Hyperforin. *Journal of the American Chemical Society* **2012**, *135* (2), 644–647. <https://doi.org/10.1021/ja312150d>.
- (105) Wu, Y.-K.; Liu, H.-J.; Zhu, J.-L. An Efficient Procedure for the 1,3-Transposition of Allylic Alcohols Based on Lithium Naphthalenide Induced Reductive Elimination of Epoxy Mesylates. *Synlett* **2008**, *2008* (04), 621–623. <https://doi.org/10.1055/s-2008-1032092>.
- (106) Mehl, F.; Bombarda, I.; Franklin, C.; Gaydou, E. M. Optimization of the Microwave-Assisted Ortho Ester Claisen Rearrangement: Application to Monoterpenols. *Synthetic Commun* **2010**, *40* (3), 462–468. <https://doi.org/10.1080/00397910902985515>.
- (107) margo. Synthetic Studies towards the Anti-Inflammatory Agent, Oleocanthal using a Johnson–Claisen (Orthoester) Rearrangement Strategy. **2009**, 1–14.
- (108) Piemontesi, C.; Wang, Q.; Zhu, J. Enantioselective Synthesis of (+)-Peganumine A. *Journal of the American Chemical Society* **2016**, *138* (35), 11148–11151. <https://doi.org/10.1021/jacs.6b07846>.
- (109) Imanishi, T.; Matsui, M.; Yamashita, M.; Iwata, C. A Novel Construction of Octahydro-3a,7-Ethano-3aH-Indene Skeleton from a Tricyclo[3.3.0.0^{2,8}]Octane: A Total Synthesis of (±)-Descarboxyquadrone. *Tetrahedron Lett* **2000**, *27* (27), 3161–3164. [https://doi.org/10.1016/s0040-4039\(00\)84743-7](https://doi.org/10.1016/s0040-4039(00)84743-7).
- (110) Selig, P.; Herdtweck, E.; Bach, T. Total Synthesis of Meloscine by a [2+2]-Photocycloaddition/Ring-Expansion Route. *Chemistry - A European Journal* **2009**, *15* (14), 3509–3525. <https://doi.org/10.1002/chem.200802383>.
- (111) Takada, A.; Fujiwara, H.; Sugimoto, K.; Ueda, H.; Tokuyama, H. Total Synthesis of (–)-Isoschizogamine. *Chemistry - A European Journal* **2015**, *21* (46), 16400–16403. <https://doi.org/10.1002/chem.201503606>.
- (112) Liptak, M. D.; Gross, K. C.; Seybold, P. G.; Feldgus, S.; Shields, G. C. Absolute p K a Determinations for Substituted Phenols. *J Am Chem Soc* **2002**, *124* (22), 6421–6427. <https://doi.org/10.1021/ja012474j>.
- (113) Wick, A. E.; Felix, D.; Steen, K.; Eschenmoser, A. CLAISEN'sche Umlagerungen Bei Allyl- Und Benzylalkoholen Mit Hilfe von Acetalen Des N, N-Dimethylacetamids. Vorläufige Mitteilung. *Helv Chim Acta* **1964**, *47* (8), 2425–2429. <https://doi.org/10.1002/hlca.19640470835>.

- (114) Felix, D.; Gschwend-Steen, K.; Wick, A. E.; Eschenmoser, A. CLAISEN'sche Umlagerungen Bei Allyl- Und Benzylalkoholen Mit 1-Dimethylamino-1-methoxy-äthen. *Helv Chim Acta* **1969**, 52 (4), 1030–1042. <https://doi.org/10.1002/hlca.19690520418>.
- (115) BOBBITT, J. M.; SCOLA, D. A. Synthesis of Isoquinoline Alkaloids. II. The Synthesis and Reactions of 4-Methyl-3-Pyridinecarboxaldehyde and Other 4-Methyl-3-Substituted Pyridines 1,2. *J Org Chem* **1960**, 25 (4), 560–564. <https://doi.org/10.1021/jo01074a018>.
- (116) Kiessling, A. J.; McClure, C. K. The Conversion of Amides to Esters with Meerwein's Reagent. Application to the Synthesis of a Carfentanil Precursor. *Synthetic Commun* **1997**, 27 (5), 923–937. <https://doi.org/10.1080/00397919708004212>.
- (117) Charette, A. B.; Chua, P. A New Mild Method for the Cleavage of the Amide Bond: Conversion of Secondary and Tertiary Amides to Esters. *Synlett* **1998**, 2, 163–165.
- (118) Fisher, T. J.; Dussault, P. H. Alkene Ozonolysis. *Tetrahedron* **2017**, 73 (30), 4233–4258. <https://doi.org/10.1016/j.tet.2017.03.039>.
- (119) Bunnelle, W. H. Preparation, Properties, and Reactions of Carbonyl Oxides. *Chem Rev* **1991**, 91 (3), 335–362. <https://doi.org/10.1021/cr00003a003>.
- (120) Chi, Y.; Peelen, T. J.; Gellman, S. H. A Rapid ¹H NMR Assay for Enantiomeric Excess of α -Substituted Aldehydes. *Organic Letters* **2005**, 7 (16), 3469–3472. <https://doi.org/10.1021/ol051174u>.
- (121) Nicolaou, K. C.; Adsool, V. A.; Hale, C. R. H. An Expedient Procedure for the Oxidative Cleavage of Olefinic Bonds with PhI(OAc)₂, NMO, and Catalytic OsO₄. *Organic Letters* **2010**, 12 (7), 1552–1555. <https://doi.org/10.1021/ol100290a>.
- (122) Jiang, X.; Fu, C.; Ma, S. A Concise Synthesis of (-)- and (+)- Trans-Whisky Lactones. *European Journal of Organic Chemistry* **2010**, 2010 (4), 687–693. <https://doi.org/10.1002/ejoc.200901058>.
- (123) Kamigaito, M.; Sawamoto, M.; Higashimura, T. Alkoxy-Substituted Titanium(IV) Chlorides as Lewis Acid Activators for Living Cationic Polymerization of Isobutyl Vinyl Ether: Control of Lewis Acidity in the Design of Initiating Systems. *Macromolecules* **1995**, 28 (16), 5671–5675. <https://doi.org/10.1021/ma00120a037>.
- (124) GENERATION OF 1-PROPYNYL LITHIUM FROM (Z/E)-1-BROMO-1-PROPENE: 6-PHENYLHEX-2-YN-5-EN-4-OL. *Organic Syntheses* **1999**, 76, 214–216. <https://doi.org/10.15227/orgsyn.076.0214>.
- (125) Cahiez, G.; Bernard, D.; Normant, J. F. Reactivity of Organomanganese(II) Reagents; II. A New, Convenient Preparation of Alkyl, Alkenyl, and Alkynyl Ketones via Organomanganese(II) Iodides. *Synthesis* **1977**, 130–133.

- (126) Cahiez, G.; Alami, M. Organomanganese(II) Reagents XV. Conjugate Addition of Organomanganese Reagents to Alkylidenemalononic Esters and Related Compounds. *Tetrahedron* **1989**, *45* (13), 4163–4176.
- (127) Cahiez, G.; Duplais, C.; Buendia, J. Chemistry of Organomanganese(II) Compounds. *Chemical Reviews* **2009**, *109* (3), 1434–1476. <https://doi.org/10.1021/cr800341a>.
- (128) Friour, G.; Cahiez, G.; Normant, J. F. Organomanganous Reagents; IX. Preparation of Various Halogenated, Alkoxyated, Aryloxyated, and Arylsulfonylated Ketones from Correspondingly Functionalized Carboxylic Acid Chlorides or Anhydrides. *Synthesis* **1984**, 37–40.
- (129) Kajiro, H.; Mitamura, S.; Mori, A.; Hiyama, T. Scandium Trifluoromethanesulfonate-Catalyzed Cleavage of Esters Bearing a Coordinative Group at a Vicinal Position. *Bulletin of the Chemical Society of Japan* **1999**, 1553–1560.
- (130) Barton, D. H. R.; Narayanan, C. R. 194. Sesquiterpenoids. Part X. The Constitution of Lactucin. *J Chem Soc Resumed* **1958**, *0* (0), 963–971. <https://doi.org/10.1039/jr9580000963>.